

Visualizing Parkinson's disease brain signatures using advanced MRI techniques

Citation for published version (APA):

Wolters, A. F. (2024). Visualizing Parkinson's disease brain signatures using advanced MRI techniques. [Doctoral Thesis, Maastricht University]. Maastricht University. <https://doi.org/10.26481/dis.20240110aw>

Document status and date:

Published: 01/01/2024

DOI:

[10.26481/dis.20240110aw](https://doi.org/10.26481/dis.20240110aw)

Document Version:

Publisher's PDF, also known as Version of record

Please check the document version of this publication:

- A submitted manuscript is the version of the article upon submission and before peer-review. There can be important differences between the submitted version and the official published version of record. People interested in the research are advised to contact the author for the final version of the publication, or visit the DOI to the publisher's website.
- The final author version and the galley proof are versions of the publication after peer review.
- The final published version features the final layout of the paper including the volume, issue and page numbers.

[Link to publication](#)

General rights

Copyright and moral rights for the publications made accessible in the public portal are retained by the authors and/or other copyright owners and it is a condition of accessing publications that users recognise and abide by the legal requirements associated with these rights.

- Users may download and print one copy of any publication from the public portal for the purpose of private study or research.
- You may not further distribute the material or use it for any profit-making activity or commercial gain
- You may freely distribute the URL identifying the publication in the public portal.

If the publication is distributed under the terms of Article 25fa of the Dutch Copyright Act, indicated by the "Taverne" license above, please follow below link for the End User Agreement:

www.umlib.nl/taverne-license

Take down policy

If you believe that this document breaches copyright please contact us at:

repository@maastrichtuniversity.nl

providing details and we will investigate your claim.

Amée Wolters

Visualizing Parkinson's
disease brain signatures using
advanced MRI techniques



Visualizing Parkinson's disease brain signatures using advanced MRI techniques

Amée Wolters

© Amée Wolters, Maastricht 2023

Cover design: Simone Golob | sgiv.nl

Lay-out and printing by: ProefschriftMaken | proefschriftmaken.nl

ISBN: 978-94-6469-636-3

All rights reserved. No part of this thesis may be reproduced, stored in a retrieval system of any nature, or transmitted in any form or by any means, electronic, mechanical, photocopying, recording, or otherwise, without permission of the author.

Visualizing Parkinson's disease brain signatures using advanced MRI techniques

PROEFSCHRIFT

Ter verkrijging van de graad van doctor
aan de Universiteit Maastricht,
op gezag van de Rector Magnificus, Prof. dr. Pamela Habibović
volgens het besluit van het College van Decanen,
in het openbaar te verdedigen op woensdag
10 januari 2024 om 16.00 uur

door

Amée Fleur Wolters

Promotores

Prof. dr. Yasin Temel

Prof. dr. Albert F.G. Leentjens

Copromotor

Dr. Mark L. Kuijf

Beoordelingscommissie

Prof. dr. David E.J. Linden (voorzitter)

Prof. dr. Volker A. Coenen (University Hospital Freiburg)

Dr. Rick C.G. Helmich (Radboudumc)

Prof. dr. Sonja A. Kotz

The research described in this thesis was performed at the School for Mental Health and Neuroscience, Department of Neurosurgery, Maastricht University, Maastricht, The Netherlands.

The research described in this thesis was sponsored by Stichting De Weijerhorst. Printing of this thesis was kindly supported by Maastricht University.

Contents

Chapter 1	General introduction	7
PART I	VISUALIZING COGNITIVE IMPAIRMENT IN PARKINSON'S DISEASE	23
Chapter 2	Resting-state fMRI in Parkinson's disease patients with cognitive impairment: A meta-analysis	25
Chapter 3	Brain network characteristics and cognitive performance in motor subtypes of Parkinson's disease: A resting state fMRI study	67
Chapter 4	Grey matter abnormalities are associated only with severe cognitive decline in early stages of Parkinson's disease	89
PART II	ULTRA-HIGH FIELD IMAGING AS A BIOMARKER IN PARKINSON'S DISEASE	117
Chapter 5	The TRACK-PD study: protocol of a longitudinal ultra-high field imaging study in Parkinson's disease	119
Chapter 6	Neuromelanin related ultra-high field signal intensity of the locus coeruleus differs between Parkinson's disease and controls	141
Chapter 7	Comparison of olfactory tract diffusion measures between early stage Parkinson's disease patients and healthy controls using ultra-high field MRI	167
Chapter 8	General discussion	185
ADDENDUM	Summary	205
	Nederlandse samenvatting	209
	Impact paragraph	213
	Dankwoord	219
	Curriculum Vitae	223
	List of publications	224

CHAPTER 1



General introduction

Parkinson's disease (PD), a neurodegenerative disorder that was first described by Dr. James Parkinson in the year 1817, is characterized by rigidity, rest tremor and bradykinesia (1). In less than two centuries it has become a common disorder, affecting 6.2 million people worldwide in 2015 (2). Moreover, in about 20 years the PD population is expected to reach more than 12 million patients globally (3). This is also why more and more people refer to it as the Parkinson pandemic (3) and urgent calls are made to search for ways to prevent and treat PD.

The pathophysiology of PD is still not completely understood, and we as yet have no treatment options to cure PD or to delay disease progression (4). Symptoms can be partly controlled with medication, but only limited progression in treatment options has been made as the most effective pharmacological treatment option (levodopa) is already fifty years old. In the non-pharmacological field, the most important therapeutic milestone was the introduction of deep brain stimulation of the subthalamic nucleus as a treatment for motor disability in the 1990s (5).

While PD is primarily recognized as a motor disorder, a broad spectrum of non-motor symptoms can occur, such as cognitive decline, depression, anxiety, sleep disturbances and autonomic dysfunction. Up to 80% of the patients eventually develop Parkinson's disease dementia in the advanced stages of the disease (6). These non-motor features often have a greater impact on patient's quality of life than the motor manifestations (7). However, the pathophysiology of these non-motor symptoms is not very well understood (8) and a considerable number of research questions are therefore still unanswered.

New and improved magnetic resonance imaging (MRI) techniques create the opportunity to search for anatomical and functional substrates for PD. MRI could potentially aid in the elucidation of the PD pathophysiology and in the discovery of radiological biomarkers which could be used to evaluate future therapies.

This thesis aims to contribute to the understanding of the PD pathophysiology and to the search for MRI biomarkers in PD. In part I we mainly focus on cognitive impairment in PD. We evaluate the existing literature related to functional MRI and investigate both structural changes and brain network connectivity in relation to cognitive performance in PD. We also explore cognitive performance in different PD motor subtypes and the role of grey matter changes. In part II we focus on ultra-high field 7T MRI in PD. We explain the TRACK-PD study protocol and investigate the use of 7T MRI as a PD biomarker, specifically focused on neuromelanin (NM) related signal changes in the substantia nigra (SN) and locus coeruleus (LC) and on diffusion measures in the olfactory tract.

The next paragraphs of this introduction provide a brief overview of PD, its implications for clinicians and patients and the MRI techniques that are used in this thesis.

1. Parkinson's disease

PD is a progressive neurodegenerative disorder which increases in incidence with age (9). The number of people with PD is rapidly increasing and is expected to exceed 12 million worldwide in 2040 (10). Due to its long-lasting nature and wide range of symptoms, PD puts an enormous burden on both patients and caregivers. It is a heterogeneous whole-body disease consisting of motor and non-motor symptoms. The pathogenesis is thought to be determined by a combination of multiple factors, such as genetic predisposition, environmental and behavioral factors (11, 12). In some epidemiologic studies pesticides, air pollution and heavy metal exposures are linked to an increased PD risk (13). Others suggest a prion-like mechanism (14) or hypothesize that infectious etiologies influencing neuronal pathways lead to the development of PD (15). However, the exact role of these factors remains unclear and the cause of PD is still unknown.

1.1. Pathophysiology

The PD pathophysiology is characterized by accumulation of alpha-synuclein aggregates leading to the formation of Lewy bodies and Lewy neurites. These Lewy bodies lead to cell loss in the SN and other brain regions and cause striatal dopaminergic depletion. Braak and colleagues have proposed a bottom-up progression of disease theory, suggesting that the Lewy body pathology starts in the medulla oblongata and olfactory bulb (stages 1 and 2) and gradually progresses upwards to the midbrain regions (stages 3 and 4) and eventually to the neocortex (stages 5 and 6) (16). It remains uncertain if this pattern of disease progression applies to all patients (17). Additionally, it is hypothesized that factors initiating alpha-synuclein pathology enter the body via the gut and spread through the vagus nerve to the medulla by a prion-like cell-to-cell transmission (8, 18). Early PD symptoms, such as hyposmia and rapid eye movement sleep behavior disorder (RBD) are thought to reflect the first stages of disease. It is only until the Lewy body pathology progresses towards the SN and other midbrain and basal forebrain structures that the characteristic PD motor symptoms become manifest. Normally, dopaminergic stimulation of the direct and indirect basal ganglia pathway eventually results in an excitatory signal from the thalamus to the motor cortex. In contrast, loss of dopaminergic cells in the SN causes thalamic inhibition, which explains the paucity of movement characteristic for PD (19) (Figure 1). In advanced disease stages, when pathology also affects the cerebral cortices, symptoms like hallucinations and dementia occur (16).

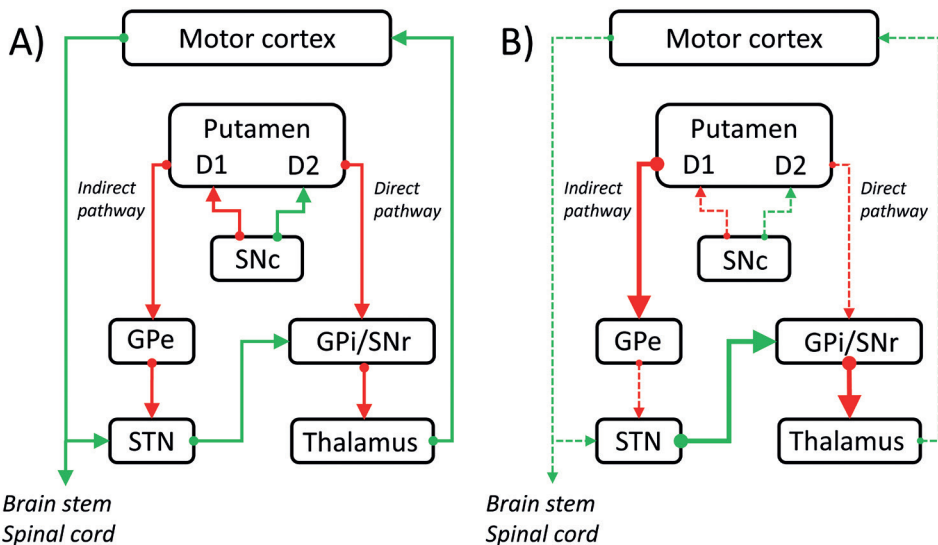


Figure 1. Schematic representation of the basal ganglia circuitry. A: Normal situation, B: Parkinson's disease. Red arrows indicate inhibitory projections and green arrows represent excitatory projections. The thickness of the arrows indicates the degree of activation.

Besides the well-known dopaminergic dysfunction, cholinergic, serotonergic and noradrenergic neurotransmitter systems are also involved in PD. These others systems are implicated in several of the non-motor symptoms (8). For example, noradrenergic neurons in the LC serve an important role in cognition and autonomic function in the general population (20). In PD, there is some evidence that noradrenergic dysfunction is associated with cognitive impairment, RBD and orthostatic hypotension (21, 22). Furthermore, PD dementia is associated with a reduction of cortical cholinergic markers (23). However, the exact pathophysiology of non-motor symptoms remains largely undefined (8).

1.2. Motor symptoms

The diagnostic criteria for PD are based on the characteristic motor symptoms and defined as bradykinesia with rigidity, rest tremor, or both (24). Bradykinesia means slowness of movement. In the limbs this manifests as a rapid decrement in amplitude and speed during repetitive movements (also termed motor decrement) (25). Rigidity is defined as an increased resistance during passive mobilization of an extremity (26). Rest tremor is the most well-known symptom in the general population. It typically displays as a low frequency (4-6 Hz) tremor in rest and is most prominent in the distal upper limbs, but resting tremor onset in the lower limbs can also occur (9). PD symptoms typically commence unilateral and progress towards both body sides during the disease

course. However, asymmetry often persists with one body side continuing to be most affected. Bradykinesia and rigidity typically show dramatic improvement after the start of dopaminergic medication, which is also one of the supportive criteria for PD (24). During the course of the disease patients usually also develop other motor problems, such as gait difficulties, postural instability, dysphagia and dysarthria (9). A typical manifestation of gait difficulties is freezing of gait. This is defined by motor blocks during walking or turning, with a sudden and transient inability to move (9).

1.3. Non-motor symptoms

Besides the well-recognized motor symptoms of PD, a broad spectrum of non-motor symptoms can occur. This includes hyposmia, sleep disturbances, neuropsychiatric symptoms, autonomic failure, pain and cognitive impairment. Some of these non-motor features develop in the course of the disease, but others (e.g. RBD, hyposmia, depression and constipation) are often the presenting symptom and can manifest itself years before the development of motor symptoms.

Non-motor symptoms in PD can be subdivided into several categories. Sensory symptoms comprise of hyposmia, visual disturbances, pain and somatosensory disturbances (8). Autonomic failure leads to constipation, orthostatic hypotension and urinary dysfunction. Neuropsychiatric features include anxiety, depression, apathy and fatigue (8). Psychosis in PD occurs in up to 40% of the patients in late stages of the diseases (8). Furthermore, already in the earliest phases of the disease mild cognitive impairment can be found in up to 42.5% of the PD patients (27). In the advanced stages of the disease 80% of the patients eventually develop Parkinson's disease dementia (PDD) (6). The burden of non-motor symptoms in PD increases with disease progression (8).

The importance of non-motor symptoms is underlined by the fact that these features have a greater impact on the quality of life than motor manifestations (7). In addition, non-motor symptoms are the most important factor in the overall cost of care in PD (28). However, very few therapeutic studies focus on non-motor aspects of PD and evidence on how to manage these symptoms is scarce (29). It is therefore essential to improve our knowledge about these symptoms, in order to create momentum for the development of more effective management options.

1.4. Diagnosis

PD is a clinical diagnosis, based on clinical symptoms and their course over time. However, due to its heterogeneous presentation and the fact that symptoms can be mild at presentation, PD is often not immediately recognized. Many patients have visited multiple healthcare providers such as an orthopedic surgeon, rheumatologist

or psychiatrist, before getting diagnosed with PD. Moreover, clinico-pathological research demonstrates that about a quarter of the clinical diagnoses of PD is incorrect (30). However, receiving a correct diagnosis and clear education about PD is extremely important. This is apparent from the fact that patient satisfaction with the explanation of the condition at diagnosis has a long-lasting impact on the health-related quality of life of PD patients (31). Delay of diagnosis and the involvement of more than one additional healthcare provider has been associated with patient dissatisfaction related to the diagnostic pathway (32). This underlines the importance of communication and education regarding the diagnosis of PD and indicates that the diagnostic process is actually the first treatment step and the beginning of the coping process. Imaging studies searching for early diagnostic signs could facilitate the diagnostic process in PD.

In addition, one of the most burning questions a patient often expresses at the time of diagnosis is “What is my prognosis?” or “What does the future look like for me?”. At this moment it is virtually impossible to offer patients a detailed prediction of their disease course, due to the significant disease variability between individuals. Longitudinal studies, following large patients groups over a longer time course, could assist in the discovery of predictive factors which can improve patient counseling.

1.5. Atypical parkinsonism

In addition to what we call idiopathic PD, there are a number of conditions which share some aspects of PD, but also display other symptoms that tend to progress faster and benefit less from medication. These conditions are called atypical parkinsonisms. In the early stages of the disease it might be hard to distinguish between these conditions and idiopathic PD. However the diagnosis often becomes apparent within the first three to five years of the disease course (24). Examples of atypical parkinsonism are multiple system atrophy, dementia with Lewy bodies, progressive supranuclear palsy and corticobasal degeneration. While idiopathic PD patients often show a dramatic improvement after the start of dopaminergic medication, the medication effect in atypical parkinsonisms is often very limited. Treatment therefore mainly consists of supportive therapy (33). In recent years several MRI characteristics have been linked to different kinds of clinically established atypical parkinsonisms. But so far there are no radiological biomarkers that enable clinicians to predict which patients will develop atypical parkinsonism (34).

1.6. Parkinson disease subtypes

As demonstrated by the information above, idiopathic PD is a heterogenous disorder consisting of a variable collection of symptoms that manifest to different extents in individual patients. This is also why some suggest that PD might actually be an umbrella diagnosis, which encompasses several different disease entities (35). Although the

involvement of different neuronal pathways and neurotransmitter systems are implied, the underlying etiology of the clinical heterogeneity in PD is not well understood (36). Different subtypes in PD might be influenced by distinct environmental and genetic factors and might therefore need personalized treatment approaches.

Several attempts have been made to define different PD subtypes. Most often based on motor features, subdividing individuals with PD into a tremor-dominant (TD) and postural instability and gait disorder (PIGD) subtype (37). However, since PD involves a wide range of both motor and non-motor symptoms, subtyping based on solely motor symptoms might be too simplistic. These difficulties in defining PD subtypes were recently the focus of a Movement Disorders Society (MDS) task force, which concluded that subtyping in PD has substantial methodological shortcomings and questionable clinical applicability (38). In line with this, the National Institutes of Health (NIH) pointed out that obtaining more insight in PD subtypes is one of the research priorities in PD (39).

2. Magnetic resonance imaging

MRI enables the creation of detailed brain images by using the body's natural magnetic properties. Because of its abundance in the human body (water and fat) hydrogen atoms are used to generate these images. Hydrogen protons can be imagined as small spherical magnets with a north-south pole. Normally these protons spin around in the body with an arbitrary axis position, but when the body is placed into an MRI scanner, the scanner's strong magnetic field aligns all hydrogen protons in the same direction of that magnetic field (B_0). This creates a magnetic vector. Although the atoms are now positioned in the same axis direction, they are not yet rotating synchronously. Radiofrequency (RF) waves added to the magnetic field are able to alter the direction of the magnetic vector (B_1) and to cause all hydrogen protons to rotate in sync (Figure 2). The extent to which the direction of the magnetic vector is altered (also called the flip angle) depends on the strength and length of the RF waves. The RF energy that gets absorbed by the hydrogen protons induces a voltage that can be detected by the MRI coil. Between each RF wave there is a short relaxation time in which the system returns to an equilibrium before the next RF wave is applied. In this way series of RF waves produce multiple magnetic signal changes, which are detected by the MRI scanner and are eventually averaged into a MR image (40, 41)

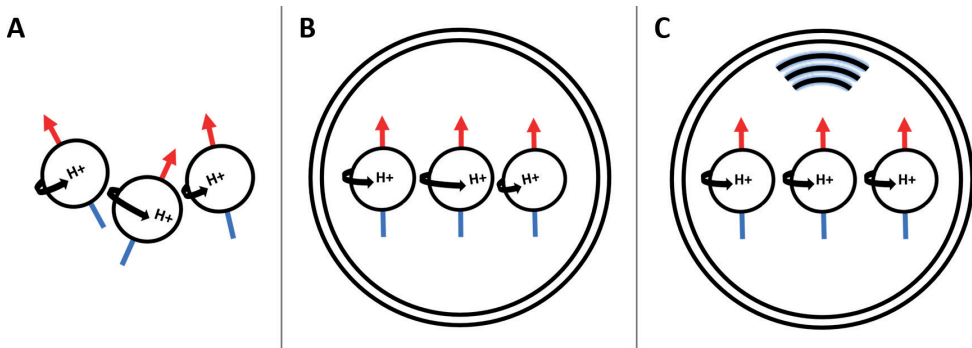


Figure 2. Hydrogen protons in A) Neutral position; B) Within the MRI-scanner; C) Within the MRI-scanner after adding radiofrequency waves to the magnetic field.

MRI is a non-invasive, safe imaging technique in which no harmful X-rays are used. However, patients should be screened for incompatible metallic devices in the body (e.g. pacemakers, metal valves), since MRI can potentially cause movement or heating of these devices (40).

2.1. Structural magnetic resonance imaging

Whether and how well a certain brain structure is visible on MRI depends on the contrast that is created between this brain structure and the surrounding area. Each MR image is made up of two types of relaxation signals of the hydrogen protons, relaxation in the longitudinal and transverse direction. This corresponds with the T1 and the T2 component respectively (42). However, with the current MRI techniques it is possible to largely eliminate one of these two components and to create so called T1 or T2-weighted images.

MRI contrast is largely determined by the difference in T1 relaxation time between fat and water. Fat has a relatively short T1 relaxation time (260 ms) and therefore appears bright on MRI. In contrast, water and cerebrospinal fluid have a dark MRI appearance due to their long T1 time (3000-5000 ms) (42). T1-weighted imaging provides the best anatomical information and is used for visualizing normal anatomical structures.

The transverse relaxation on which T2-weighted imaging is based, is mostly determined by the rotating component of the hydrogen protons. Transverse relaxation arises from dephasing of the spin component of these protons after the RF wave (42). T2-weighted imaging is characterized by the bright appearance of water. Since cerebral pathology is often accompanied by edema or fluid, T2-weighted imaging is particularly useful for the assessment of brain pathology.

2.2. Diffusion-weighted imaging

Diffusion-weighted imaging (DWI) is a technique which allows for the measurement of water molecule movement. When unconstrained, water molecules move equally into all directions (isotropic movements). But inside the brain movement of water molecules is restricted by structural boundaries such as white matter tracts. In this situation, water molecules tend to move in parallel direction with the white matter tracts (anisotropic movements) (43). The direction of movement of the molecules in the x, y and z plane and the correlation between these directions are mathematically combined into the so-called diffusion tensor. Based on the diffusion tensor of multiple consecutive voxels the dominant direction of the water molecules diffusion can be plotted. Since the diffusion of these paths is likely to represent the white matter tracts, this is also called tractography (44).

2.3. Neuromelanin sensitive imaging

One very specific imaging technique that has been developed in the recent years is neuromelanin (NM) sensitive MRI. NM is an insoluble pigment that arises as a by-product of the oxidative metabolism of dopamine and noradrenalin. It is most abundant in the SN and LC (45). One of these techniques, called magnetization transfer (MT)-weighted imaging proved to be able to visualize NM related signal. This method is based on the detection of MT contrast between pools of protons bound in surrounding macromolecules and pools of protons in free water, reflecting the contrast between regions with lots of NM and surrounding brain tissue. To create this contrast, protons in the bound pool are saturated by off-resonance RF waves. Subsequently this magnetization transfers to the surrounding free pool at a tissue specific rate, producing a contrast detectable by the MRI scanner (46).

2.4. Functional MRI

In contrast to structural imaging, functional MRI (fMRI) can assess cerebral activity. fMRI detects localized brain activity by measuring blood oxygen level-dependent (BOLD) signal fluctuations. An increase in neural activity in a certain area of the cortex attracts a higher amount of blood in order to meet the increased oxygen demand. These changes in blood oxygenation lead to altered magnetic properties and a stronger MRI signal in these regions. fMRI records these small BOLD signal increases (47). This enables us to investigate which brain areas are most active in certain tasks (task-based fMRI) or which areas or networks have the same brain activity in rest (resting-state fMRI).

2.5. Magnetic field strength

The magnetic field strength of a MRI scanner is expressed in Tesla (T). Most clinical MRI scanners have a field strength of 1.5 or 3 T. In recent years, the emergence of ultra-high-field scanners (7 T and above) enables us to potentially obtain an even higher

degree of anatomic detail. 7T MRI scanners proved an increased spatial resolution and a higher signal-to-noise ratio compared to 3 T MRI (48). It might be particularly useful for the visualization of small nuclei in the brainstem and basal ganglia and is therefore an attractive imaging technique in PD research. However, there are also some challenges. For instance, ultra-high field imaging techniques are more sensitive to image artifacts and there is an increased risks of RF tissue heating (49).

3. Magnetic resonance imaging in Parkinson's disease

Currently a lot of effort is put into biomarker investigations for PD. In order to develop and evaluate disease modifying therapies for PD, accurate diagnostic markers and monitoring indicators are necessary (44). In clinical practice MRI is now only used as a method to exclude other potential causes of PD symptoms. To date, it is impossible to diagnose PD based on MRI characteristics. However, over the past years substantial development in MRI methodology has taken place and MRI is now regarded a promising method in the diagnostic work-up of PD (48). Early indicators such as signal loss of the nigrosome-1 area on iron-sensitive MR images and reduced volume and signal intensity of the SN on NM sensitive MRI account for the most promising radiological biomarkers in PD (50-52). Alterations on fMRI have also been described in relation to different PD symptoms (53). There is however a need for further validation, reliability assessment and capturing of the longitudinal progression of these markers. Much more work is needed to establish reliable PD biomarkers that can be used in clinical practice.

4. Problem statements and outline of this thesis

From the previous paragraphs, it has become clear that accurate diagnostic markers and monitoring indicators are highly necessary for the development of an improved therapeutic arsenal for PD (54). Specifically for non-motor symptoms our knowledge of the underlying disease process is still very limited (8). In addition, better knowledge about PD subtypes is required to develop personalized treatment approaches and to enable clinicians to reliably educate patients about their diagnosis and prognosis. In this thesis we aim to contribute to the elucidation of the PD pathophysiology and to search for MRI biomarkers.

In part I we mainly focus on cognitive impairment in PD. Chapter 2 reports a meta-analysis in which we review the existing literature related to resting-state fMRI in PD patients with cognitive impairment. In Chapter 3 we investigate functional brain network characteristics and cognitive performance in different motor subtypes of PD.

In Chapter 4 grey matter alterations are compared between clusters of PD patients with mild, moderate and severe stages of cognitive impairment. In part II we focus on ultra-high field imaging, using 7T MRI in PD and investigate its potential use as a PD biomarker. Chapter 5 provides the detailed protocol of the TRACK-PD study, which is the first and largest longitudinal ultra-high field 7T MRI study in PD patients to date. Chapter 6 describes an ultra-high field imaging study comparing NM related signal intensity in the SN and LC between early-stage PD patients and HC. In chapter 7 we visualized the olfactory tract with DWI techniques on ultra-high field MRI and evaluated if previous findings showing different diffusion measures of the olfactory tract between PD and HC could be replicated on 7T MRI. Chapter 8 provides a general discussion in which the most relevant findings of this thesis will be discussed and put into perspective. Also, potential future directions for research will be discussed.

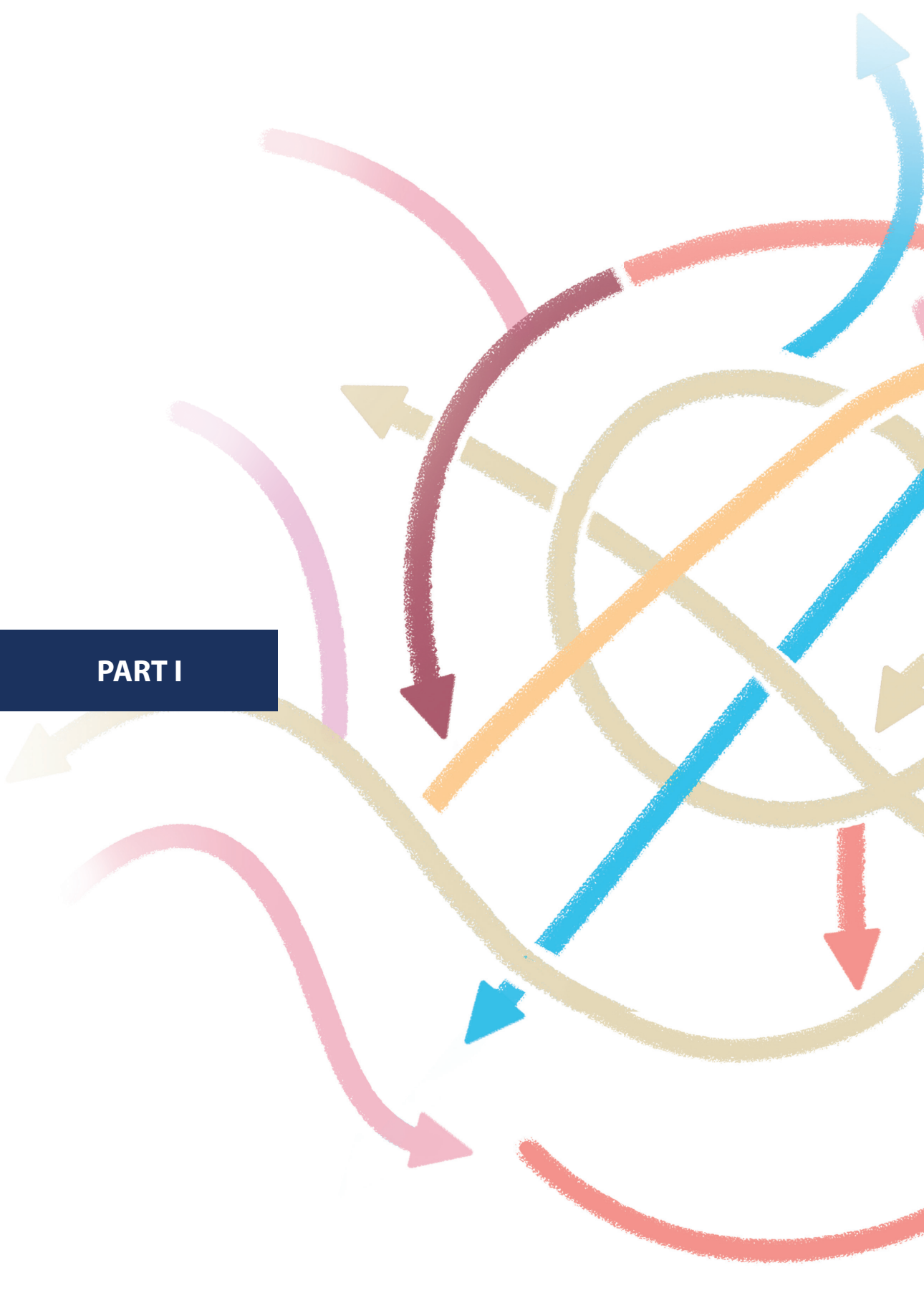
5. References


1. Parkinson J. An essay on the shaking palsy. 1817. *J Neuropsychiatry Clin Neurosci.* 2002;14(2):223-36; discussion 2.
2. Global Burden of Disease Study C. Global, regional, and national incidence, prevalence, and years lived with disability for 301 acute and chronic diseases and injuries in 188 countries, 1990-2013: a systematic analysis for the Global Burden of Disease Study 2013. *Lancet.* 2015;386(9995):743-800.
3. Dorsey ER, Bloem BR. The Parkinson Pandemic-A Call to Action. *JAMA Neurol.* 2018;75(1):9-10.
4. Fox SH, Katzenschlager R, Lim SY, Barton B, de Bie RMA, Seppi K, et al. International Parkinson and movement disorder society evidence-based medicine review: Update on treatments for the motor symptoms of Parkinson's disease. *Mov Disord.* 2018;33(8):1248-66.
5. Limousin P, Pollak P, Benazzouz A, Hoffmann D, Broussolle E, Perret JE, et al. Bilateral subthalamic nucleus stimulation for severe Parkinson's disease. *Mov Disord.* 1995;10(5):672-4.
6. Hely MA, Reid WG, Adena MA, Halliday GM, Morris JG. The Sydney multicenter study of Parkinson's disease: the inevitability of dementia at 20 years. *Mov Disord.* 2008;23(6):837-44.
7. Santos-Garcia D, de la Fuente-Fernandez R. Impact of non-motor symptoms on the quality of life of patients with Parkinson's disease: some questions beyond research findings. *J Neurol Sci.* 2013;335(1-2):239.
8. Schapira AHV, Chaudhuri KR, Jenner P. Non-motor features of Parkinson disease. *Nat Rev Neurosci.* 2017;18(8):509.
9. Jankovic J. Parkinson's disease: clinical features and diagnosis. *J Neurol Neurosurg Psychiatry.* 2008;79(4):368-76.
10. Dorsey ER, Sherer T, Okun MS, Bloem BR. The Emerging Evidence of the Parkinson Pandemic. *J Parkinsons Dis.* 2018;8(s1):S3-S8.
11. Collaborators GBDN. Global, regional, and national burden of neurological disorders, 1990-2016: a systematic analysis for the Global Burden of Disease Study 2016. *Lancet Neurol.* 2019;18(5):459-80.
12. Blauwendraat C, Nalls MA, Singleton AB. The genetic architecture of Parkinson's disease. *Lancet Neurol.* 2020;19(2):170-8.
13. Kouli A, Torsney KM, Kuan WL. Parkinson's Disease: Etiology, Neuropathology, and Pathogenesis. In: Stoker TB, Greenland JC, editors. *Parkinson's Disease: Pathogenesis and Clinical Aspects.* Brisbane (AU)2018.
14. Ma J, Gao J, Wang J, Xie A. Prion-Like Mechanisms in Parkinson's Disease. *Frontiers in neuroscience.* 2019;13:552.
15. Limphaibool N, Iwanowski P, Holstad MJV, Kobylarek D, Kozubski W. Infectious Etiologies of Parkinsonism: Pathomechanisms and Clinical Implications. *Front Neurol.* 2019;10:652.
16. Braak H, Del Tredici K, Bratzke H, Hamm-Clement J, Sandmann-Keil D, Rub U. Staging of the intracerebral inclusion body pathology associated with idiopathic Parkinson's disease (preclinical and clinical stages). *J Neurol.* 2002;249 Suppl 3:III/1-5.
17. Rietdijk CD, Perez-Pardo P, Garssen J, van Wezel RJ, Kraneveld AD. Exploring Braak's Hypothesis of Parkinson's Disease. *Front Neurol.* 2017;8:37.
18. Steiner JA, Quansah E, Brundin P. The concept of alpha-synuclein as a prion-like protein: ten years after. *Cell Tissue Res.* 2018;373(1):161-73.
19. Blumenfeld H. *Neuroanatomy through clinical cases.* 2nd ed. Sunderland, Mass: Sinauer Associates; 2010. xxiii, 1006 pages : illustrations (some color) p.

20. Mather M, Harley CW. The Locus Coeruleus: Essential for Maintaining Cognitive Function and the Aging Brain. *Trends Cogn Sci*. 2016;20(3):214-26.
21. Sommerauer M, Fedorova TD, Hansen AK, Knudsen K, Otto M, Jeppesen J, et al. Evaluation of the noradrenergic system in Parkinson's disease: an 11C-MeNER PET and neuromelanin MRI study. *Brain*. 2018;141(2):496-504.
22. Chan-Palay V, Asan E. Alterations in catecholamine neurons of the locus coeruleus in senile dementia of the Alzheimer type and in Parkinson's disease with and without dementia and depression. *J Comp Neurol*. 1989;287(3):373-92.
23. Emre M, Ford PJ, Bilgic B, Uc EY. Cognitive impairment and dementia in Parkinson's disease: practical issues and management. *Mov Disord*. 2014;29(5):663-72.
24. Postuma RB, Berg D, Stern M, Poewe W, Olanow CW, Oertel W, et al. MDS clinical diagnostic criteria for Parkinson's disease. *Mov Disord*. 2015;30(12):1591-601.
25. Berardelli A, Rothwell JC, Thompson PD, Hallett M. Pathophysiology of bradykinesia in Parkinson's disease. *Brain*. 2001;124(Pt 11):2131-46.
26. Delwaide PJ. Parkinsonian rigidity. *Funct Neurol*. 2001;16(2):147-56.
27. Yarnall AJ, Breen DP, Duncan GW, Khoo TK, Coleman SY, Firbank MJ, et al. Characterizing mild cognitive impairment in incident Parkinson disease: the ICICLE-PD study. *Neurology*. 2014;82(4):308-16.
28. Tolosa E, Garrido A, Scholz SW, Poewe W. Challenges in the diagnosis of Parkinson's disease. *Lancet Neurol*. 2021;20(5):385-97.
29. Barone P, Erro R, Picillo M. Quality of Life and Nonmotor Symptoms in Parkinson's Disease. *Int Rev Neurobiol*. 2017;133:499-516.
30. Joutsa J, Gardberg M, Røyttä M, Kaasinen V. Diagnostic accuracy of parkinsonism syndromes by general neurologists. *Parkinsonism Relat Disord*. 2014;20(8):840-4.
31. Global Parkinson's Disease Survey Steering C. Factors impacting on quality of life in Parkinson's disease: results from an international survey. *Mov Disord*. 2002;17(1):60-7.
32. Plouvier AOA, Olde Hartman TC, de Bont OA, Maandag S, Bloem BR, van Weel C, et al. The diagnostic pathway of Parkinson's disease: a cross-sectional survey study of factors influencing patient dissatisfaction. *BMC Fam Pract*. 2017;18(1):83.
33. Keener AM, Bordelon YM. Parkinsonism. *Semin Neurol*. 2016;36(4):330-4.
34. Aludin S, Schmill LA. MRI Signs of Parkinson's Disease and Atypical Parkinsonism. *Rof*. 2021;193(12):1403-10.
35. Titova N, Padmakumar C, Lewis SJG, Chaudhuri KR. Parkinson's: a syndrome rather than a disease? *J Neural Transm (Vienna)*. 2017;124(8):907-14.
36. Thenganatt MA, Jankovic J. Parkinson disease subtypes. *JAMA Neurol*. 2014;71(4):499-504.
37. Stebbins GT, Goetz CG, Burn DJ, Jankovic J, Khoo TK, Tilley BC. How to identify tremor dominant and postural instability/gait difficulty groups with the movement disorder society unified Parkinson's disease rating scale: comparison with the unified Parkinson's disease rating scale. *Mov Disord*. 2013;28(5):668-70.
38. Mestre TA, Ferestehnejad SM, Berg D, Bohnen NI, Dujardin K, Erro R, et al. Parkinson's Disease Subtypes: Critical Appraisal and Recommendations. *J Parkinsons Dis*. 2021;11(2):395-404.
39. Sieber BA, Landis S, Koroshetz W, Bateman R, Siderowf A, Galpern WR, et al. Prioritized research recommendations from the National Institute of Neurological Disorders and Stroke Parkinson's Disease 2014 conference. *Ann Neurol*. 2014;76(4):469-72.
40. Berger A. Magnetic resonance imaging. *BMJ*. 2002;324(7328):35.

41. Grover VP, Tognarelli JM, Crossey MM, Cox IJ, Taylor-Robinson SD, McPhail MJ. Magnetic Resonance Imaging: Principles and Techniques: Lessons for Clinicians. *J Clin Exp Hepatol*. 2015;5(3):246-55.
42. Westbrook C, Roth CK, Talbot J, Ebscohost. *MRI in practice*. Fourth edition ed. Chichester, West Sussex ; Malden, MA: Wiley-Blackwell; 2011.
43. Le Bihan D. Looking into the functional architecture of the brain with diffusion MRI. *Nat Rev Neurosci*. 2003;4(6):469-80.
44. Basser PJ, Jones DK. Diffusion-tensor MRI: theory, experimental design and data analysis - a technical review. *NMR Biomed*. 2002;15(7-8):456-67.
45. Prange S, Metereau E, Thobois S. Structural Imaging in Parkinson's Disease: New Developments. *Curr Neurol Neurosci Rep*. 2019;19(8):50.
46. Priovoulos N, Jacobs HIL, Ivanov D, Uludag K, Verhey FRJ, Poser BA. High-resolution in vivo imaging of human locus coeruleus by magnetization transfer MRI at 3T and 7T. *Neuroimage*. 2018;168:427-36.
47. Gore JC. Principles and practice of functional MRI of the human brain. *J Clin Invest*. 2003;112(1):4-9.
48. Lehericy S, Vaillancourt DE, Seppi K, Monchi O, Rektorova I, Antonini A, et al. The role of high-field magnetic resonance imaging in parkinsonian disorders: Pushing the boundaries forward. *Mov Disord*. 2017;32(4):510-25.
49. Duyn JH. The future of ultra-high field MRI and fMRI for study of the human brain. *Neuroimage*. 2012;62(2):1241-8.
50. Bae YJ, Kim JM, Kim E, Lee KM, Kang SY, Park HS, et al. Loss of Nigral Hyperintensity on 3 Tesla MRI of Parkinsonism: Comparison With (123) I-FP-CIT SPECT. *Mov Disord*. 2016;31(5):684-92.
51. Schwarz ST, Afzal M, Morgan PS, Bajaj N, Gowland PA, Auer DP. The 'swallow tail' appearance of the healthy nigrosome - a new accurate test of Parkinson's disease: a case-control and retrospective cross-sectional MRI study at 3T. *PLoS One*. 2014;9(4):e93814.
52. Castellanos G, Fernandez-Seara MA, Lorenzo-Betancor O, Ortega-Cubero S, Puigvert M, Uranga J, et al. Automated neuromelanin imaging as a diagnostic biomarker for Parkinson's disease. *Mov Disord*. 2015;30(7):945-52.
53. Filippi M, Elisabetta S, Piramide N, Agosta F. Functional MRI in Idiopathic Parkinson's Disease. *Int Rev Neurobiol*. 2018;141:439-67.
54. Ryman SG, Poston KL. MRI biomarkers of motor and non-motor symptoms in Parkinson's disease. *Parkinsonism Relat Disord*. 2020;73:85-93.

PART I





Visualizing cognitive impairment in Parkinson's disease

CHAPTER 2



Resting-state fMRI in Parkinson's disease patients with cognitive impairment: A meta-analysis

Wolters AF, van de Weijer SCF, Leentjens AFG, Duits AA, Jacobs HIL, Kuijf ML

Abstract

Background: Cognitive impairment is a common non-motor symptom in Parkinson's disease. So far, the underlying pathophysiology remains unclear. Several alterations in functional network connectivity have been described in Parkinson's disease patients with cognitive impairment which are probably the result of the heterogenous pathophysiology underlying this cognitive decline, including dopaminergic and cholinergic deficits. Accordingly, the reported resting-state connectivity patterns vary greatly among studies.

Objective: To evaluate the localization and magnitude of functional connectivity patterns in resting-state brain networks in Parkinson's disease patients with cognitive impairment by pooling data from available studies.

Methods: We searched PubMed, the Cochrane Library, MEDLINE, Embase and PsycINFO to identify functional MRI studies in Parkinson's disease patients with cognitive impairment. A voxel-based meta-analysis combined with quality statistics was performed, using the anisotropic effect-size version of the signed differential mapping method.

Results: Seventeen studies with cognitively impaired Parkinson's disease patients were included consisting of 222 Parkinson's disease patients with mild cognitive impairment, 68 patients with Parkinson's disease dementia, 289 cognitively unimpaired Parkinson's disease patients and 353 healthy controls. Parkinson's disease patients with cognitive impairment predominantly showed a reduced connectivity in specific brain regions that are part of the default mode network.

Conclusion: Cognitive impairment in Parkinson's disease is associated with reduced connectivity in networks relevant to cognition, most prominently the default mode network. Specific alterations in functional connectivity may contribute to cognitive decline in Parkinson patients and may be a promising future biomarker.

1. Introduction

Parkinson's disease (PD) is the second most common neurodegenerative disorder after Alzheimer's disease and is characterized by motor symptoms such as bradykinesia, rigidity and tremor (1, 2, 3). Moreover, patients with PD also experience a broad spectrum of non-motor symptoms such as neuropsychiatric disturbances and autonomic dysfunction. Already in the earliest phases of the disease, cognitive impairment (CI) can be found in up to 42.5% of the PD patients (4). Furthermore, up to 80% of the patients eventually develop Parkinson's Disease Dementia (PDD) in the advanced stages of the disease (5, 6). Patients with PD experiencing mild cognitive impairment (MCI) are at a higher risk of subsequently developing PDD (7).

The pathophysiological mechanism of cognitive impairment in Parkinson's disease patients has not yet been elucidated and no valid biomarkers have been identified (8). Research in this field has focused on the formation of protein aggregates, neurotransmitter system dysfunction as well as genetic risk factors and underlying pathways. Lewy-body depositions, formed by neuronal alpha-synuclein aggregates, cause the loss of mesencephalic dopaminergic neurons and result in the typical dopaminergic deficit in the basal ganglia of PD with CI (9, 10, 11, 12). In addition, differences in cerebral levels of A β -amyloid depositions as shown in PET-studies suggest a differential role in cognitive deterioration and development of dementia in PD patients (13). A previous study of Compta et al. (2011) suggested that it is the combination of cortical amyloid deposits and cortical Lewy bodies that has the most predictive value for the development of CI in PD (14). The spatial distribution of neuronal dysfunction also plays a role in the "dual syndrome hypothesis" (15). This suggests that (1) dopaminergic dysfunction in the fronto-striatal regions is more involved in a subgroup of PD patients with MCI and predominantly deficits in planning, working memory and executive functions, whereas (2) cholinergic dysfunction within the posterior cortical and temporal lobes is more involved in early deficits in visuo-spatial function and semantic fluency and a more rapid cognitive decline to dementia (15). Indeed, several lines of research indicate that besides dopaminergic dysfunction the noradrenergic, serotonergic and cholinergic systems are also affected in PD patients. Dysfunctional neurotransmitter synaptic activity within the locus coeruleus (16, 17, 18), dorsal raphe nuclei (19, 20), and cholinergic brainstem nuclei (21) respectively have all been associated with degeneration within these structures in PD. However, as suggested by the dopaminergic overdosing theory, dysfunction of the relatively less effected ventral cortico-striatal circuits, involved in reward processing and learning, may also arise due to an overdose of dopamine in these areas. (15, 22, 23, 24, 25). From another perspective, several genotypes, such as APOE ϵ 4, MAPT, H1 haplotypes and GBA mutation (26, 27, 28, 29, 30) are increasingly recognized as potential risk factors for dementia in PD and may shed new light in pathophysiological

mechanisms of PD-MCI (31, 32, 33, 34). This also points to the direction that there may be several mechanisms involved in CI and the development of dementia in PD (8).

Of interest, several neuroimaging techniques are able to characterize the pathological substrates of PD and other neurodegenerative disorders (35). One promising method is resting-state functional MRI, which has shown the ability to explore the functional activity in different brain networks in a reliable and reproducible way (36, 37). It has been reported that alterations in several neurotransmitter systems influence the functional brain activity measured with fMRI (38, 39, 40, 41, 42). Additionally, a correlation was reported between the loss of dopaminergic neurons and alterations in functional brain network activity in PD (43). Since the basal ganglia are part of neuronal networks involving the entire cortex, one can expect that reductions in dopaminergic release will affect the functioning of many large-scale cerebral networks relevant for cognitive processing (44). Furthermore, it has been suggested that an abnormal alpha-synuclein level in the cerebrospinal fluid influences both sensorimotor and non-motor functional connectivity networks in PD (45). Based on these results, there has been growing interest in using functional magnetic resonance imaging (fMRI) to investigate the neural basis for CI in PD. By measuring intrinsic blood oxygen level-dependent (BOLD) low-frequency signal fluctuations, fMRI can be used to detect interregional correlations in specific brain networks during rest (46, 47).

Various studies have investigated the resting-state networks in PD-MCI and PDD and disruptions are predominantly described in the default mode network and the fronto-parietal network (37, 48, 49, 50, 51, 52, 53, 54). The default mode network is thought to serve an important role in several higher order cognitive functions, such as autobiographical memory and imagining the future, while the fronto-parietal network is predominantly involved in attention and cognitive control (37, 55). Unfortunately, results between studies vary greatly and most fMRI studies consist of small samples.

In this study, we pool functional connectivity data in resting-state brain networks of PD patients with CI by means of a voxel-based meta-analysis. The aim of this study is to obtain a better understanding of the functional connectivity networks involved in PD with CI and to provide evidence as to whether fMRI results could serve as a biomarker for PD with CI. Based on previous studies, we hypothesize that PD patients with CI show reduced resting-state brain connectivity compared to healthy controls and PD patients without CI. We specifically expect to observe these alterations most prominently in the default mode network and fronto-parietal network.

2. Methods

2.1 Search strategies and study selection

A literature search in PubMed, Medline, Embase, PsycINFO and the Cochrane Library was performed. For this search, the following search terms were used: ((Parkinson's disease) OR (Parkinson)) AND ((Mild cognitive impairment) OR (MCI) OR (Parkinson's disease dementia) OR (Dementia) OR (Cognitive impairment)) AND ((fMRI) OR (functional MRI)). Afterwards, the reference lists of the included articles were searched for additional eligible publications. The final search was conducted on the 30th of April 2018 and resulted in a total of 1122 articles.

For this meta-analysis, we included resting-state fMRI studies comparing a group of cognitively impaired PD patients (PD-CI) with either a sample of healthy controls (HC) or a sample of PD patients without CI. Studies comparing the functional connectivity patterns of HC or PD with dementia with Lewy bodies were not included. Furthermore, only studies applying a whole-brain analysis, independent component analysis or seed-based analysis, with a correlation of the seeds to voxels encompassing the entire brain, were included in this meta-analysis. To prevent the results from being biased towards certain region of interest, studies performing a region of interest analysis were excluded. Other exclusion criteria were: 1. Undefined PD with CI study groups or not enough information provided to determine whether CI was present; 2. No resting-state fMRI; 3. Review articles reporting no original data; or 4. Conference proceedings without full report publication. Three manuscripts had to be excluded because they focused on global connectivity and network topological parameters and did not report specific changes on a regional or voxel-level (56, 57, 58).

First, duplicates were removed from the search results, followed by screening of the abstracts independently by two researchers (AW, SW). When any discrepancies existed between the included articles, this was resolved in a consensus meeting. When no consensus was reached, a third specialist was consulted (MK). The following information was extracted from each included study: first author, year of publication, published journal, sample size, MRI type, definition of CI, statistical analysis technique and patient characteristics (UPDRS score, age, dopaminergic medication, LEDD, and MMSE or MoCA-score). Peak coordinates and effect size measures of the regions with a significant difference in functional connectivity were also collected. Some publications did not report peak coordinates and therefore the relevant authors were contacted by e-mail to request this information.

2.2 Quality assessment

To our knowledge, there are no official guidelines for assessing the quality of fMRI studies. Therefore for the overall quality assessment of the reports in this meta-analysis, we derived our own criteria from the guidelines for reporting fMRI studies as described by Poldrack et al. (2009) (59). This resulted in nine quality criteria, which comprise of the following domains: (1) Inclusion and exclusion procedure and patient demographics; (2) fMRI procedure and patient instructions; (3) Spatial normalization method; (4) Determination of the regions of interest; (5) Reproducibility of the analysis; (6) Statistical tests used to substantiate the results; (7) Correction for the multiple testing problem; (8) Figures and tables; (9) Quality control measures. Studies could score 0, 0.5 or 1 point for each item. An overall score of ≥ 7.5 was considered as good, 4-7.5 as fair and ≤ 4 as poor quality. See supplementary data S1 for further specification of the criteria. Quality assessment was performed by two researchers (AW, SW) and discrepancies were discussed until consensus was reached. If no consensus could be reached, a third specialist was consulted (HJ).

2.3 Data analysis

This meta-analysis was carried out using the anisotropic effect size version of signed differential mapping (AES-SDM) (60, 61). This validated voxel-based meta-analysis approach has been used in meta-analysis of several other neuropsychiatric studies (62-67). AES-SDM is specifically designed to combine neuroimaging studies with studies reporting solely peak coordinates in coordinate systems (e.g. MNI, Talairach). The peak coordinates and their statistical values are used to recreate a statistical parametric map for each study. This map is created by using the effect sizes of the differences between patients and controls. Subsequently, a random-effects variance-weighted image-based meta-analysis is conducted in each voxel. In this meta-analysis, we applied the default AES-SDM kernel size and thresholds (FWHM = 20mm, voxel $p = 0.005$, peak height SDM-Z = 1, cluster extent = 10 voxels). The SDM-Z score represents a probability measure. In the random-effects analysis the results are thresholded to this given probability, to detect if more studies report functional connectivity changes near a certain voxel than would be expected by chance (61, 62, 68).

To assess the residual heterogeneity of the results, examination of the funnel plots of the peaks coordinates was carried out. This allowed us to check whether the results were driven by one or very few studies and to detect gross differences in study results. These funnel plots were statistically tested with Egger's regression test. To further assess the robustness of the results, we performed a jack-knife analysis within AES-SDM, in which the meta-analysis is systematically repeated as many times as studies have been included, subsequently removing one different study at a time.

After performing the statistical analysis, the spatial layout of these results was compared with the intrinsic connectivity network templates as described by Smith et al. (2009) (69). These templates were obtained from the BrainMap database (70, 71, 72). We performed a spatial correlation analysis in FSL to determine the degree of spatial overlap between our map with peak coordinate clusters and these well-defined functional networks. This also includes a calculation of the number of voxels of our peak coordinate clusters inside the resting-state network templates as a percentage of the total number of voxels in the clusters. Afterwards we visually inspected these images to identify which peak coordinates led to the corresponding spatial correlation value.

3. Results

3.1 Demographic data and quality assessment

Seventeen studies met the in- and exclusion criteria and were included in this meta-analysis (48, 49, 52, 73-86). Among these, fifteen studies compared PD-CI with healthy controls (HC) and nine studies compared PD-CI patients to PD patients who were cognitively unimpaired (PD-CU). Two studies, from Madhyastha et al. (2015) and Canu et al. (2015), reported results for the comparison of HC to a group of PD patients comprising of both CU patients and patients with MCI (48, 76). Both studies were included because, firstly, the sample size of PD contained more MCI than PD-CU patients and, secondly, the PD group as a whole scored considerably worse on the neuropsychological assessment compared to the control group. The complete in- and exclusion procedure is displayed in figure 1. Altogether, these studies included 932 participants of which 353 HC, 289 PD-CU, 222 PD-MCI and 68 patients with PDD. Basic demographics of the participants per group are summarized in table 1. Baseline characteristics showed a higher mean age for PDD (71.5) and PD MCI (66.9) when compared to PD CU (63.6) and HC (64.5). Additionally, as expected the PD MCI and PDD groups showed worse results regarding the global cognition scores. Moreover, higher mean LEDD and UPDRS-III scores were found in the PD-MCI and PDD subgroup, indicating more advanced stages of the disease.

The fMRI characteristics and statistical details of the included studies are described in table 2. Eight of the studies performed a seed-based analysis (49, 52, 78-80, 83, 85, 86), six studies performed an independent component analysis (48, 73, 75, 76, 81, 84) and the three remaining studies adopted different whole brain methodologies (74, 77, 82). Atrophy correction was applied in only six studies (52, 75, 77, 79, 80, 83). Twelve studies did not enter the subjects gray matter volume maps as a voxel-wise regressor in the group comparison (48, 49, 73, 74, 76, 78, 81, 82, 84-86). However, three of these twelve studies conducted a voxel-based morphometry analysis (73, 76, 86), which did not show

a significant difference between HC and PD-CI. Another study of Bezdicsek et al. (2018) has also performed a voxel-based morphometry which did not show significant differences between PD-MCI and PD-CU, but the analysis did express significant differences in brain atrophy between HC and PD-MCI for which the results were not corrected (82).

Based on our quality assessment, all included studies reached a score of either 'Good' or 'Fair'. Three studies were classified as fair (49, 83, 85). The main reasons for this were the lack of motion or atrophy correction, inadequate normalization methods, or the fact that the in- and exclusion criteria and patient instructions for the resting-state fMRI were not clearly reported. All other studies had a total score above 7 and were therefore considered as being of good quality. Further specification of the quality assessment can be found in the supplementary data S1.

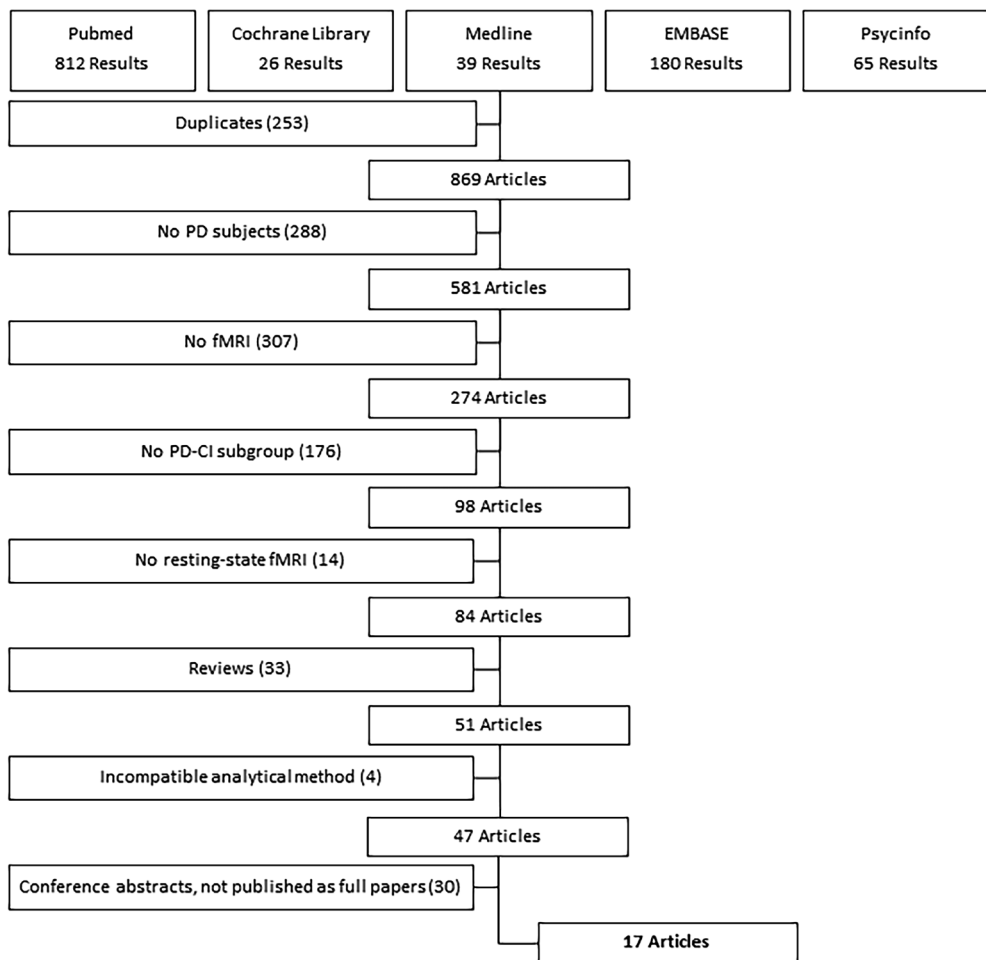


Figure 1. Flowchart of the study selection procedure, performed according to the PRISMA 2009 guidelines.

Table 1. Demographic characteristics of the included studies

Study	Sample Size			Age ¹			Medication ON/OFF			MMSE ² /MoCA ³			LEDD ¹			UPDRS-III ¹		
	HC	PD	CU	HC	PD	CU	HC	PD	CU	HC	PD	CU	HC	PD	CU	HC	PD	CU
Amboni et al. 2015 [73]	20	21	21	-	61.9 ±9.2	65.8 ±6.5	65.2 ±8.7	ON	28.7 ±0.9*	28.7 ±1.4*	26.7 ±1.8*	530.9 ±299.4	453.1 ±307.4	-	13.1 ±5.3	14.3 ±8.5	-	-
Baggio et al. 2015 [75]	36	43	22	-	63.4 ±10.5	64.0 ±9.8	66.1 ±12.2	ON	29.7 ±0.5*	29.4 ±0.9*	28.5 ±1.2*	646.7 ±419.2	951.9 ±498.2	-	14.1 ±7.5	18.2 ±8.7	-	-
Bezdzicek et al. 2018 [82]	30	15	16	-	63.6 ±8.1	64.8 ±7.9	64.7 ±7.9	ON	27.0 ±2.2*	26.4 ±1.9*	25.3 ±2.6*	1447.2 ±768.4	1305.8 ±561.1	-	13.3 ±6.4	15.1 ±8.2	-	-
Borroni et al. 2015 [77]	10	11	-	10	62.2 ±8.0	66.3 ±3.8	-	ON	NR (≥28*)	NR	27.8 ±1.8*	504.5 ±336.4	-	714.2 ±348.1	10.7 ±5.4	-	27.9 ±10.5	-
Canu et al. 2015 [76]	35	10	13	-	67.7 ±7.6	66.9 ±8.0	-	UPDRSON fMRI/OFF	29.1 ±1.0*	27.7 ±1.8*	-	937.0 ±435.9	-	-	25.4 ±9.2	-	-	-
Chen et al. 2015 [78]	21	19	-	11	61.1 ±8.3	59.5 ±8.8	-	OFF	28.2 ±1.2*	25.8 ±2.8*	-	NR	NR	NR	14.7 ±6.3	-	18.6 ±5.2	-
Chen et al. 2017 [83]	21	11	21	-	61.1 ±8.3	59.2 ±5.1	63.6 ±11.2	NR	28.3 ±1.1*	27.1 ±2.2*	22.6 ±2.3*	NR	NR	-	16.0 ±7.1	16.9 ±5.4	-	-
Diez-Cirarda et al. 2018 [84]	26	12	23	-	68.3 ±7.5	65.2 ±8.3	69.2 ±4.5	ON	28.9 ±1.3*	28.7 ±1.3*	26.9 ±2.1*	548.9 ±459.6	904.52 ±518.5	-	18.5 ±6.9	22.7 ±11.1	-	-
Gorges et al. 2015 [52]	22	14	11	6	68 (65-73)	70 (65-77)	72 (64-74)	ON	30 (30-30)*	29 (28-30)*	27 (26-28)*	475 (205-880)	360 (231-620)	10 (5-13)	12 (9-18)	-	-	-
Hou et al. 2016 [80]	22	18	14	-	52.6 ±6.7	53.6 ±8.7	54.9 ±8.1	OFF	NR	27.6 ±2.2*	22.4 ±2.6*	0	0	-	15.4 ±5.6	17.8 ±8.5	-	-
Madhyashta et al. 2015 [48]	21	11	13	-	61.9 ±10.00	66.1 ±10.3	-	ON	27.3 ±2.0*	26.4 ±2.2*	-	NR	NR	-	23.1 ±8.61	-	-	-
Peraza et al. 2015 [79]	17	-	-	12	76.9 ±5.8	-	-	ON	29.1 ±0.9*	-	22.5 ±5.2*	-	-	857 (125-1580)	-	-	26.4 ±9.0	-
Peraza et al. 2017 [81]	30	62	37	-	64.1 ±7.9	62.8 ±10.8	70.4 ±9.1	ON	29.4 ±0.88*	29.0 ±0.9*	28.2 ±1.5*	147.1 ±112.0	201.6 ±155.8	-	24.6 ±10.4	28.9 ±11.0	-	-
Possin et al. 2013 [74]	15	-	6	6	72.9 ±5.2	-	73.9 ±5.9	UPDRSOFF fMRI/ON	NR	-	23.0 ±4.8*	-	665 ±343	-	-	30.8 ±14.5	-	-

Table 1. Continued

Study	Sample Size			Age ¹			Medication ON/OFF			MMSE ² /MoCA ³			LEDD ⁴			UPDRS-III ⁵		
	HC	PD	CU	HC	PD	CU	HC	PD	CU	HC	PD	CU	HC	PD	CU	HC	PD	CU
Rektorova et al. 2012 [49]	18	18	-	60.9 ±6.7	63.5 ±9.1	72.4 ±5.9	ON	29.5 ±0.7*	29.6 ±0.8*	-	23.2 ±2.6*	696 ±430.4	-	925.5 ±412.0	NR	-	-	NR
Shin et al. 2016 [86]	-	15	16	-	65.7 ±6.4	-	NR	-	28.6 ±1.2	26.3 ±1.5	-	0.0 (0-0)	0.0 (0-360)	-	19.1 ±8.3	25.4 ±8.8	-	-
Zhan et al. 2018 [85]	9	9	9	70.0 ±5.9	68.4 ±7.8	74.0 ±5.1	UPDRS ON	26.7 ±1.2	27.0 ±0.9°	21.9 ±2.4°	14.1 ±3.1°	630 ±270	718 ±372	721 ±182	28.9 ±10.5	33.1 ±11.6	37.0 ±12.1	-
Total sample	353	289	222	64.5	63.6	71.5	28.7	28.3	26.1	21.2	468.3	564.9	716.9	18.0	21.6	25.7	-	-

UPDRS-III: Unified Parkinson's disease rating scale part III. LEDD: Levodopa equivalent daily dose. MMSE: Mini-mental state examination. MoCA: Montreal cognitive assessment. NR: Not reported. ¹Values are mean ± standard deviation (SD), except for Gorges et al. (2015); mean (IQ range) and LEDD data from Shin et al. (2016) and Peraza et al. (2015); median (range).

Table 2. Experimental design of the included studies

	fMRI	Criteria for PD-MCI	Criteria for PDD	Number of foci		Analysis	GSR	Software	AC
				Contrast HC vs. PD-CI	Contrast PD-CU vs. PD-CI				
Amboni et al. 2015 [73]	3T	MDS Task Force criteria, Level I [126]	-	4	-	ICA	Yes	Brain-Voyager QX	No ¹
Baggio et al. 2015 [75]	3T	MDS Task Force criteria, Level I [126]	-	6	3	ICA	No	FSL, AFNI	Yes
Bezdicek et al. 2018 [82]	3T	MDS Task Force criteria, Level II [126]	-	3	2	WBA	No	SPM12, ECM	No ²
Borroni et al. 2015 [77]	1.5T	-	MDS Task Force criteria [127]	1	-	WBA	No	REST, SPM8	Yes
Canu et al. 2015 [76]	3T	MDS Task Force criteria, Level II [126]	-	13	-	ICA	No	FSL	No ¹
Chen et al. 2015 [78]	3T	-	MDS Task Force criteria [128]	4	4	SBA	Yes	REST, SPM8	No
Chen et al. 2017 [83]	3T	MDS Task Force criteria, Level I [126]	-	5	6	SBA	No	REST, SPM8	Yes
Díez-Cirarda et al. 2018 [84]	3T	MDS Task Force criteria, Level III [126]	-	11	-	ICA	No	CONN, GIFT, BCT	No
Gorges et al. 2015 [52]	3T	MDS Task Force criteria, Level I [126]	NR	13	34	SBA	No	TIFTSP, MATLAB	Yes
Hou et al. 2016 [80]	3T	MDS Task Force criteria, Level III [126]	-	22	2	SBA	No	REST, SPM8	Yes
Madhyastha et al. 2015 [48]	3T	Estimated decline from premorbid abilities.	-	4	-	ICA	No	FSL, AFNI, FreeSurfer	No
Peraza et al. 2015 [79]	3T	-	MDS Task Force criteria [127]	44	-	SBA	No	FSL 5.0, SPM8	Yes

Table 2. Continued

	fMRI	Criteria for PD-MCI	Criteria for PDD	Number of foci	Analysis	GSR	Software	AC
				Contrast HC vs. PD-CI	Contrast PD-CU vs. PD-CI			
Peraza et al. 2017 [81]	3T	MDS Task Force criteria, Level III [126]	-	3	19	No	FSL, REST	No
Possin et al. 2013 [74]	3T	NR	NR	48	-	No	SPM8, REST	No
Rektorova et al. 2012 [49]	1.5T	-	NR	2	-	No	SPM5	No
Shin et al. 2016 [86]	3T	MDS Task Force criteria, Level I [126]	-	-	35	Yes	REST, SPM8	No ¹
Zhan et al. 2018 [85]	3T	MDS Task Force criteria, Level I [126]	MDS Task Force criteria [127]	-	3	No	SPM8, REST	No
Total				183	108			

² A voxel-based morphometry showed no significant differences between PD-MCI and PD-CU. However, significant differences were found comparing HC with PD-MCI.

ACE-R: The Addenbrooke's Cognitive Examination Revised, NA: Not applicable, GSR: Global signal regression, AC: Atrophy correction, ICA: Independent component analysis, WBA: Whole brain analysis, SBA: Seed-based analysis, NR: Not reported.

¹ Instead of entering the subjects' GM volume maps as a voxel-wise regressor in intergroup comparison, a voxel-based morphometry was conducted and no significant differences were found between HC and PD-CI.

3.2 Regional changes in resting-state connectivity

The meta-analysis showed reduced functional brain connectivity in several brain regions in patients with PD-CI as compared to HC. More specifically, our meta-analysis demonstrated a reduced connectivity in PD-CI in the right Rolandic operculum, left inferior parietal gyri, right angular gyrus, left parahippocampal gyrus, right calcarine fissure, right superior frontal gyrus and right precentral gyrus as compared to the HC (see table 3, figure 2A). An increased functional connectivity in PD-CI was found in the right supramarginal gyrus when compared to the HC group.

For the contrast PD-CU vs. PD-CI, lower connectivity was detected in PD-CI patients in the left precuneus, right median cingulate gyrus, left superior frontal gyrus and right precentral gyrus. In addition, increased functional connectivity of the right cerebellum (hemispheric lobule VI) was found in the PD-CI group as compared to PD-CU (see table 3, figure 2B).

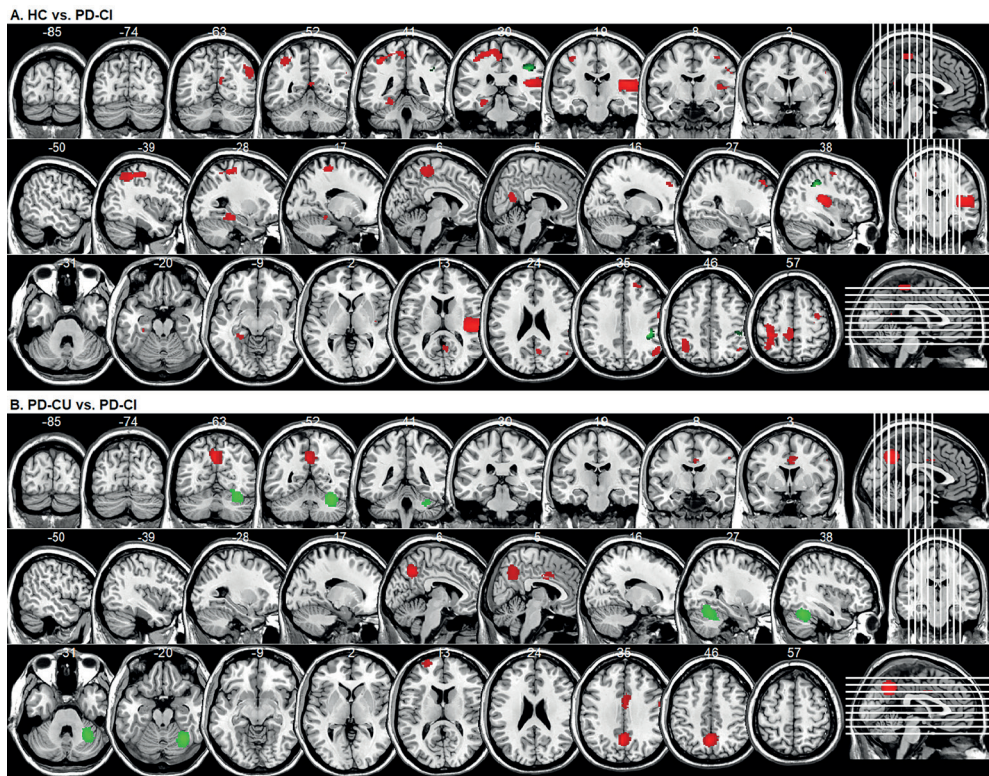


Figure 2. Statistically significant effects of voxel-based meta-analysis for HC vs. PD-CI [A] and PD-CU vs. PD-CI [B]. Decreased functional connectivity in PD-CI is indicated in red and increased connectivity in PD-CI is indicated in green for all contrasts. Voxel threshold $p < 0.005$, peak height threshold: peak SDM-Z > 1.000 , extent threshold: cluster size ≥ 10 voxels. x,y,z-coordinates of axial, sagittal and coronal slices are indicated in white.

Table 3. Clusters of voxels with significant intergroup functional connectivity differences

Contrast	Neural region	Side	MNI coordinates			Voxels	P-value	SDM-Z
			X	Y	Z			
HC > PD-CI	Rolandic operculum, BA 48	Right	44	-24	16	1363	0.00002	-2.705
	Inferior parietal gyri, BA 40	Left	-38	-42	52	1400	0.00004	-2.565
	Angular gyrus, BA 39	Right	48	-58	42	327	0.00089	-2.159
	Parahippocampal gyrus, BA 37	Left	-28	-34	-14	260	0.00025	-2.328
	Calcarine fissure / surrounding cortex, BA 23	Right	6	-60	16	161	0.00056	-2.221
	Superior frontal gyrus, dorsolateral, BA 9	Right	24	38	40	104	0.00056	-2.220
	Precentral gyrus, BA 4	Right	54	-2	36	67	0.00124	-2.114
	Precentral gyrus, BA 6	Right	38	-8	56	63	0.00143	-2.093
	PD-CI > HC	Supramarginal gyrus, BA 40	Right	38	-32	38	277	~0
PD CU > PD-CI	Precuneus, BA 7	Left	-4	-60	42	931	~0	-2.312
	Median cingulate/paracingulate gyrus, BA 24	Right	4	2	34	261	0.00051	-1.820
	Superior frontal gyrus, dorsolateral, BA 10	Left	-22	64	14	191	0.00022	-1.939
	Precentral gyrus, BA 4	Right	56	-2	38	53	0.00214	-1.620
PD-CI > PD CU	Cerebellum, hemispheric lobule VI, BA 37	Right	30	-58	-20	1083	0.00029	1.371

Voxel threshold $p < 0.005$, peak height threshold: peak SDM-Z > 1.000, extent threshold: cluster size ≥ 10 voxels.

3.3 Robustness analysis

The robustness analysis was performed with the Egger's linear regression method and visual inspection of the jack-knife analysis. See supplementary data S2 for further specification of the funnel plots and this analysis. The Egger's test showed a significant asymmetry regarding the funnel plot of the right Rolandic operculum, with a p-value smaller than 0.1. None of the other reported peak coordinates in this study showed an intercept that significantly differed from zero ($P > 0.1$). Visual inspection of the jack-knife analysis for the contrast of HC vs. PD-CI, exhibited a poor reproducibility of the peak coordinate in the right precentral gyrus (BA 6). With respect to the comparison of PD-CU with PD-CI patients, the right cerebellar region (BA 37) showed a somewhat lower reproducibility.

3.4 Network localization

We performed a spatial correlation analysis in which we compared the total brain map of our reported peak coordinates with the intrinsic connectivity network templates

as described by Smith et al. (2009) to detect in which resting-state networks the peak coordinates are situated. With this analysis, a spatial correlation was found between our reported peak coordinates and several resting-state networks. For all associated networks, we have displayed both the spatial correlation coefficient (r) and the percentage of voxels of our peak coordinate clusters inside the resting-state networks as a fraction of the total number of voxels of our peak coordinate clusters. Regarding the contrast of HC vs. PD-CI, our analysis displayed a correlation between the total map of peak coordinates with a decreased connectivity in PD-CI and the auditory network ($r = 0.13$; 28,5%), the sensorimotor network ($r = 0.13$; 30,6%). Spatial correlation was also found to a lesser extent, in the right fronto-parietal network ($r = 0.07$; 14,4%) and default mode network ($r = 0.07$; 17,2%). Upon visual inspection, the spatial correlation with the auditory network appeared to be driven by the peak coordinate of the right Rolandic operculum and right precentral gyrus (BA 4). The observed spatial correlation with the sensorimotor network seemed to be based on the peak coordinate of the left inferior parietal gyri and precentral gyrus (BA 6). Moreover, predominantly the peak coordinate in the right Rolandic operculum explains the spatial correlation with the right fronto-parietal network. And finally, the peak coordinates of the right calcarine fissure and right angular gyrus were mainly associated with the default mode network. The peak coordinate in the right supramarginal gyrus, which showed an increased connectivity in PD-CI showed a correlation with the sensorimotor network ($r = 0.05$; 90,6%) and the right fronto-parietal network ($r = 0.05$; 36,1%).

For our second contrast, PD-CI vs PD-CU, we observed a decreased connectivity in PD-CI which correlated spatially specifically with the default mode network ($r = 0.24$; 66,2%). After visual inspection we noticed that the spatial correlation with the default mode network could be attributed to the peak coordinates in the left precuneus, right precentral gyrus and the right median cingulate gyrus. The peak coordinate in the right cerebellum, which displayed an increased functional connectivity for PD-CI as compared to PD-CU, did primarily show a notable spatial correlation with the cerebellar network ($r = 0.19$; 99,7%). For further specification of the spatial correlation analysis, see supplementary data S3.

4. Discussion

In this study, we aimed to evaluate the hypothesis that reduced functional connectivity changes in PD patients with CI can be detected in specific resting-state networks, as the disease induced dopaminergic deficits can have widespread repercussions on brain function. As expected, the found spatial correlation coefficients (r) with specific resting-state networks are rather low. The reason for this is that the results from our

meta-analysis contain far fewer voxels than the large functional resting-state networks. The correlation analysis measures overlap and since our peak coordinates overlap only a small part of these networks, there are many voxels in the network not included. To provide more insight into the meaning of the spatial correlation results, we have therefore also provided the number of voxels of our peak coordinate clusters inside the network as a percentage of the total number of voxels of the clusters. Within our analysis, a reduced connectivity was found in the default mode network, auditory network and right fronto-parietal network when PD patients with CI were compared with HC. Furthermore, when comparing PD-CI with HC, we also noted a spatial correlation with the sensorimotor network, which could be related to the motor symptoms of patients with PD. For the comparison of PD-CU with PD-CI, we detected a reduced connectivity specifically in the default mode network. After varying results in previous studies, our findings provide a more definite step in the differentiation of network disruptions associated with cognitive impairment in PD.

The default mode network is believed to serve an important role in various cognitive functions. It includes the medial parietal, bilateral inferior-lateral-parietal and ventromedial frontal cortex (69). In healthy populations, reduced default mode network connectivity is associated with decreased memory performance, but also slower processing speed and decreased executive function (87, 88, 89). In addition, alterations of the default mode network have been described in several other neurodegenerative disorders such as Alzheimer's disease, Huntington's disease and frontotemporal dementia (90-93). Also in Parkinson's disease, changes in default mode network connectivity have been previously reported by several studies (94-96). A recent meta-analysis of Tahmasian et al. (2017) investigated the resting-state functional connectivity in Parkinson's disease patients which were not selected specifically on the basis of cognitive performance. They similarly found an alteration in regions connected to the default mode network (97). The authors concluded that this could be related to dysfunction of perception and executive functions in the PD patients. This supports our finding that the default mode network seems to be involved in cognitive decline in PD.

Besides the default mode network, we also found a notable decrease of functional connectivity in the auditory network of PD-CI when compared to HC. This network consists of the superior temporal gyrus, Heschl's gyrus and the posterior insular region (69). The auditory network is not as well studied as the default mode network in PD. So far, only one study has reported functional connectivity changes in this network in PD patients (98). It has also been described that, compared to age matched controls, PD patients show greater difficulty in hearing spoken words (99). Furthermore, a correlation between CI and changes in auditory evoked potentials in PD has been reported by Nojszewska et al. (2009). The authors conclude that evaluation of the auditory evoked

potentials may even serve as an indicator for CI in PD (100). Thus, although disruption of this network may not necessarily cause CI, these changes in the auditory network could point to hearing-loss as a potential risk factor for CI in PD as has been suggested for dementia in the aging population (101). However, only few studies have reported results about this network and in our meta-analysis this outcome was not preserved within the contrast of PD-CU with PD-CI. Therefore this outcome should be interpreted carefully. Based on our results it is also possible that disturbances in the auditory network are related to Parkinson's disease, but not specifically to cognitive impairment.

With respect to the fronto-parietal network, several studies have reported disruptions in the fronto-parietal network in PD patients with CI (53, 102, 103). The fronto-parietal network seems to serve an important role in attention control (104). While we hypothesized to find differences in functional connectivity of this network in PD-CI as compared to HC and PD-CU, our meta-analysis did not show this as convincingly as expected. Only for the peak coordinates of the contrast HC vs. PD-CI, a weak spatial correlation was found with this network. Since this association was not found for the PD-CU vs. PD-CI contrast, while the connection with the default mode network became more explicit in this second comparison, a more significant role for the default mode network in cognitive impairment in PD is implicated.

Interestingly, the AES-SDM analysis also revealed patterns of increased functional connectivity when comparing PD-CI patients with HC, in particular in the right supramarginal gyrus. Furthermore, an increased connectivity was also found in the right cerebellum for the contrast of PD-CI vs. PD-CU. It has been postulated that higher cortical functional connectivity in PD patients in the early stages of the disease, may reflect a compensatory mechanism to counteract slowly progressing CI (105). The ability of brain areas to display compensatory overactivation was first suggested by Reuter-Lorenz et al. (2008) (106). Based upon PET CT observations, several studies have also reported such compensatory mechanisms in PD patients (107, 108). It has also been described that loss of compensatory hyperactivation is associated with a worse performance on cognitive tasks (109). This hypothesis may form an explanation for the observed increased functional connectivity in this meta-analysis. However, it is important to note that our robustness analysis indicated that the peak coordinate in the right supramarginal gyrus was driven by the studies of Chen et al. (2017) and Madhyastha et al. (2015), while the increased connectivity in the right cerebellar area was based solely on the study of Chen et al. (2015) and Chen et al. (2017). Because both peak coordinates were driven by only two studies these results must be interpreted cautiously.

Given the consistent involvement of the default mode network, our results suggest this network may hold promise as a biomarker for CI in PD patients, though further research

is warranted. PD is thought to be a complex and heterogenic disease, probably with several different subtypes and changes over time (110, 111). For example, as stated in the introduction section, the dual syndrome hypothesis suggests that there are at least two PD subtypes, which among other things display a different profile of cognitive characteristics and a dissimilar degree of cognitive deterioration. (15). This makes it more complex to determine a specific pattern of functional connectivity alterations in PD with CI (112). Therefore, deep phenotyping in longitudinal cohort studies, combining fMRI with other biomarkers such as structural imaging, genetic and clinical characteristics and cerebrospinal fluid biomarkers, would allow to further define specific fMRI correlates underlying the various phenotypes of the disease (113). A number of studies performing multivariate analysis combining multi-modal neuroimaging techniques support the idea that Parkinson's disease is caused by a network-spread pathophysiology affecting several networks, including the default mode network, that correlate with cognitive deficits in PD (114-116). Moreover, Long and colleagues (2012) developed a method which discriminated PD patients from HC with a power of 86.96% based on the combination of both structural and functional MRI characteristics (117). The results of these studies support the promising future role of fMRI as a biomarker for PD.

As implicated by the multi-variate analysis described above, a relationship seems to exist between age-related brain atrophy in the healthy population and functional MRI activity of the brain (118). For this reason, the application of brain atrophy corrections in fMRI studies in the PD population is important to avoid misleading results. However, in a considerable number of the studies included in our meta-analysis brain atrophy was not taken into account. Since our PD groups with cognitive decline showed a higher mean age when compared to the HC and PD-CU group, it cannot be ruled out that this might have influenced the meta-analysis to some extent.

This study has several other limitations. First, the study is limited by the small to moderate amount of studies and a certain level of heterogeneity in study characteristics. As demonstrated in table 2, a variety of statistical or imaging methods, software packages and threshold settings were used in the included studies, which may have influenced our study results (119). Specifically the inclusion of studies with different types of analytical methods (e.g. region of interest versus whole brain, or seed-based versus ICA) may introduce a bias in study results towards specific regions of interests. A meta-analysis using only studies applying a whole-brain analysis would give more conclusive results. Our analysis could therefore be seen as an exploratory study, which provides an indication of the results, while waiting for more conclusive results in the future. We suggest the validation of our findings in future studies consisting of an independent, methodologically homogeneous data set. Furthermore, sleeping during the acquisition

has been shown to potentially increase functional connectivity in resting-state fMRI (120). Unfortunately, only three of the included studies verified whether the subjects remained awake during the acquisition of the resting-state fMRI. Another major point of concern is that the fMRI was performed in 'ON' medication state as well as and in 'OFF' medication states among the studies included in the meta-analysis. Eleven studies completed the MRI procedure while patients were 'ON' medication, three studies performed the fMRI in 'OFF' status and three studies did not report if the patients were 'ON' or 'OFF' dopaminergic medication during the scanning procedure. Although most studies acquired the fMRI data after patients took their dopaminergic medication, this heterogeneity can still lead to misleading results, since dopaminergic medication influences brain connectivity patterns both in a linear and non-linear way (42, 121). More specifically, this effect has also been described in the default mode network (122, 123). Although these effects are particularly relevant for intra-individual differences we cannot rule out that the meta-analysis is influenced by this dissimilarity in study characteristics. For this reason, further studies with homogeneity regarding the dopaminergic status of the PD patients are necessary to validate our results. Finally, diversity in the definition of MCI is another concern and although agreement on the diagnostic criteria has been formulated (124-128) there is no consensus yet and the cut-off scores for mild cognitive impairment are still ranging between -1 SD and -2 SD. In this meta-analysis, different criteria were allowed for MCI in the included studies (Table 2). Unfortunately, due to the limited number of included articles, we were not able to perform further subgroup analysis.

In conclusion, this meta-analysis reveals specific resting-state network disruptions in PD patients with CI, especially in the default mode network. Quantification of these network connectivity changes could serve as a biomarker for CI in PD and as such may be helpful in unravelling its pathophysiology. However, future studies with methodologically homogenous data sets, preferably combining different biomarkers in larger samples are necessary to confirm these outcomes and to further explore the potential role of fMRI as a biomarker for CI.

5. References

1. Jankovic J. Parkinson's disease: clinical features and diagnosis. *J Neurol Neurosurg Psychiatry*. 2008;79(4):368-76.
2. Al-Radaideh AM, Rababah EM. The role of magnetic resonance imaging in the diagnosis of Parkinson's disease: a review. *Clinical imaging*. 2016;40(5):987-96.
3. Postuma RB, Berg D, Stern M, Poewe W, Olanow CW, Oertel W, et al. MDS clinical diagnostic criteria for Parkinson's disease. *Mov Disord*. 2015;30(12):1591-601.
4. Yarnall AJ, Breen DP, Duncan GW, Khoo TK, Coleman SY, Firbank MJ, et al. Characterizing mild cognitive impairment in incident Parkinson disease: the ICICLE-PD study. *Neurology*. 2014;82(4):308-16.
5. Svenningsson P, Westman E, Ballard C, Aarsland D. Cognitive impairment in patients with Parkinson's disease: diagnosis, biomarkers, and treatment. *The Lancet Neurology*. 2012;11(8):697-707.
6. Hely MA, Reid WG, Adena MA, Halliday GM, Morris JG. The Sydney multicenter study of Parkinson's disease: the inevitability of dementia at 20 years. *Movement disorders : official journal of the Movement Disorder Society*. 2008;23(6):837-44.
7. Janvin CC, Larsen JP, Aarsland D, Hugdahl K. Subtypes of mild cognitive impairment in Parkinson's disease: progression to dementia. *Movement disorders : official journal of the Movement Disorder Society*. 2006;21(9):1343-9.
8. Delgado-Alvarado M, Gago B, Navalpotro-Gomez I, Jimenez-Urbieta H, Rodriguez-Oroz MC. Biomarkers for dementia and mild cognitive impairment in Parkinson's disease. *Movement disorders : official journal of the Movement Disorder Society*. 2016.
9. Spillantini MG, Schmidt ML, Lee VM, Trojanowski JQ, Jakes R, Goedert M. Alpha-synuclein in Lewy bodies. *Nature*. 1997;388(6645):839-40.
10. Skogseth RE, Bronnick K, Pereira JB, Mollenhauer B, Weintraub D, Fladby T, et al. Associations between Cerebrospinal Fluid Biomarkers and Cognition in Early Untreated Parkinson's Disease. *Journal of Parkinson's disease*. 2015;5(4):783-92.
11. Aarsland D, Perry R, Brown A, Larsen JP, Ballard C. Neuropathology of dementia in Parkinson's disease: a prospective, community-based study. *Annals of neurology*. 2005;58(5):773-6.
12. Halliday GM, Leverenz JB, Schneider JS, Adler CH. The neurobiological basis of cognitive impairment in Parkinson's disease. *Movement disorders : official journal of the Movement Disorder Society*. 2014;29(5):634-50.
13. Petrou M, Bohnen NI, Muller ML, Koeppe RA, Albin RL, Frey KA. Abeta-amyloid deposition in patients with Parkinson disease at risk for development of dementia. *Neurology*. 2012;79(11):1161-7.
14. Compta Y, Parkkinen L, O'Sullivan SS, Vandrovцова J, Holton JL, Collins C, et al. Lewy- and Alzheimer-type pathologies in Parkinson's disease dementia: which is more important? *Brain : a journal of neurology*. 2011;134(Pt 5):1493-505.
15. Kehagia AA, Barker RA, Robbins TW. Cognitive impairment in Parkinson's disease: the dual syndrome hypothesis. *Neurodegener Dis*. 2013;11(2):79-92.
16. Cash R, Dennis T, L'Heureux R, Raisman R, Javoy-Agid F, Scatton B. Parkinson's disease and dementia: norepinephrine and dopamine in locus ceruleus. *Neurology*. 1987;37(1):42-6.
17. Chan-Palay V, Asan E. Alterations in catecholamine neurons of the locus coeruleus in senile dementia of the Alzheimer type and in Parkinson's disease with and without dementia and depression. *J Comp Neurol*. 1989;287(3):373-92.

18. Zarow C, Lyness SA, Mortimer JA, Chui HC. Neuronal loss is greater in the locus coeruleus than nucleus basalis and substantia nigra in Alzheimer and Parkinson diseases. *Archives of neurology*. 2003;60(3):337-41.
19. Brooks DJ, Piccini P. Imaging in Parkinson's disease: the role of monoamines in behavior. *Biol Psychiatry*. 2006;59(10):908-18.
20. Scatton B, Javoy-Agid F, Rouquier L, Dubois B, Agid Y. Reduction of cortical dopamine, noradrenaline, serotonin and their metabolites in Parkinson's disease. *Brain research*. 1983;275(2):321-8.
21. Jellinger KA. Pathology of Parkinson's disease. Changes other than the nigrostriatal pathway. *Mol Chem Neuropathol*. 1991;14(3):153-97.
22. Gotham AM, Brown RG, Marsden CD. 'Frontal' cognitive function in patients with Parkinson's disease 'on' and 'off' levodopa. *Brain : a journal of neurology*. 1988;111 (Pt 2):299-321.
23. Cools R, Barker RA, Sahakian BJ, Robbins TW. Enhanced or impaired cognitive function in Parkinson's disease as a function of dopaminergic medication and task demands. *Cerebral cortex (New York, NY : 1991)*. 2001;11(12):1136-43.
24. Cools R, Barker RA, Sahakian BJ, Robbins TW. L-Dopa medication remediates cognitive inflexibility, but increases impulsivity in patients with Parkinson's disease. *Neuropsychologia*. 2003;41(11):1431-41.
25. Swainson R, Rogers RD, Sahakian BJ, Summers BA, Polkey CE, Robbins TW. Probabilistic learning and reversal deficits in patients with Parkinson's disease or frontal or temporal lobe lesions: possible adverse effects of dopaminergic medication. *Neuropsychologia*. 2000;38(5):596-612.
26. Williams-Gray CH, Goris A, Saiki M, Foltynie T, Compston DA, Sawcer SJ, et al. Apolipoprotein E genotype as a risk factor for susceptibility to and dementia in Parkinson's disease. *Journal of neurology*. 2009;256(3):493-8.
27. Morley JF, Xie SX, Hurtig HI, Stern MB, Colcher A, Horn S, et al. Genetic influences on cognitive decline in Parkinson's disease. *Movement disorders : official journal of the Movement Disorder Society*. 2012;27(4):512-8.
28. Harhangi BS, de Rijk MC, van Duijn CM, Van Broeckhoven C, Hofman A, Breteler MM. APOE and the risk of PD with or without dementia in a population-based study. *Neurology*. 2000;54(6):1272-6.
29. de Lau LM, Schipper CM, Hofman A, Koudstaal PJ, Breteler MM. Prognosis of Parkinson disease: risk of dementia and mortality: the Rotterdam Study. *Archives of neurology*. 2005;62(8):1265-9.
30. Williams-Gray CH, Evans JR, Goris A, Foltynie T, Ban M, Robbins TW, et al. The distinct cognitive syndromes of Parkinson's disease: 5 year follow-up of the CamPaIGN cohort. *Brain*. 2009;132(Pt 11):2958-69.
31. Seto-Salvia N, Pagonabarraga J, Houlden H, Pascual-Sedano B, Dols-Icardo O, Tucci A, et al. Glucocerebrosidase mutations confer a greater risk of dementia during Parkinson's disease course. *Movement disorders : official journal of the Movement Disorder Society*. 2012;27(3):393-9.
32. Alcalay RN, Caccappolo E, Mejia-Santana H, Tang M, Rosado L, Orbe Reilly M, et al. Cognitive performance of GBA mutation carriers with early-onset PD: the CORE-PD study. *Neurology*. 2012;78(18):1434-40.
33. Brockmann K, Srulijes K, Pfliederer S, Hauser AK, Schulte C, Maetzler W, et al. GBA-associated Parkinson's disease: reduced survival and more rapid progression in a prospective

- longitudinal study. *Movement disorders : official journal of the Movement Disorder Society*. 2015;30(3):407-11.
34. Winder-Rhodes SE, Hampshire A, Rowe JB, Peelle JE, Robbins TW, Owen AM, et al. Association between MAPT haplotype and memory function in patients with Parkinson's disease and healthy aging individuals. *Neurobiology of aging*. 2015;36(3):1519-28.
 35. Pievani M, de Haan W, Wu T, Seeley WW, Frisoni GB. Functional network disruption in the degenerative dementias. *The Lancet Neurology*. 2011;10(9):829-43.
 36. Biswal BB, Mennes M, Zuo XN, Gohel S, Kelly C, Smith SM, et al. Toward discovery science of human brain function. *Proceedings of the National Academy of Sciences of the United States of America*. 2010;107(10):4734-9.
 37. van den Heuvel MP, Hulshoff Pol HE. Exploring the brain network: a review on resting-state fMRI functional connectivity. *European neuropsychopharmacology : the journal of the European College of Neuropsychopharmacology*. 2010;20(8):519-34.
 38. Pa J, Berry AS, Compagnone M, Boccanfuso J, Greenhouse I, Rubens MT, et al. Cholinergic enhancement of functional networks in older adults with mild cognitive impairment. *Annals of neurology*. 2013;73(6):762-73.
 39. Shah D, Blockx I, Guns PJ, De Deyn PP, Van Dam D, Jonckers E, et al. Acute modulation of the cholinergic system in the mouse brain detected by pharmacological resting-state functional MRI. *NeuroImage*. 2015;109:151-9.
 40. Zheng H, Onoda K, Wada Y, Mitaki S, Nabika T, Yamaguchi S. Serotonin-1A receptor C-1019G polymorphism affects brain functional networks. *Sci Rep*. 2017;7(1):12536.
 41. Klaassens BL, van Gorsel HC, Khalili-Mahani N, van der Grond J, Wyman BT, Whitcher B, et al. Single-dose serotonergic stimulation shows widespread effects on functional brain connectivity. *NeuroImage*. 2015;122:440-50.
 42. Cole DM, Beckmann CF, Oei NY, Both S, van Gerven JM, Rombouts SA. Differential and distributed effects of dopamine neuromodulations on resting-state network connectivity. *Neuroimage*. 2013;78:59-67.
 43. Lin WC, Chen HL, Hsu TW, Hsu CC, Huang YC, Tsai NW, et al. Correlation between Dopamine Transporter Degradation and Striatocortical Network Alteration in Parkinson's Disease. *Front Neurol*. 2017;8:323.
 44. Dagher A, Nagano-Saito A. Functional and anatomical magnetic resonance imaging in Parkinson's disease. *Molecular Imaging and Biology*. 2007;9(4):234-42.
 45. Campbell MC, Koller JM, Snyder AZ, Buddhala C, Kotzbauer PT, Perlmutter JS. CSF proteins and resting-state functional connectivity in Parkinson disease. *Neurology*. 2015;84(24):2413-21.
 46. Biswal B, Yetkin FZ, Haughton VM, Hyde JS. Functional connectivity in the motor cortex of resting human brain using echo-planar MRI. *Magnetic resonance in medicine*. 1995;34(4):537-41.
 47. Gusnard DA, Raichle ME, Raichle ME. Searching for a baseline: functional imaging and the resting human brain. *Nature reviews Neuroscience*. 2001;2(10):685-94.
 48. Madhyastha TM, Askren MK, Zhang J, Leverenz JB, Montine TJ, Grabowski TJ. Group comparison of spatiotemporal dynamics of intrinsic networks in Parkinson's disease. *Brain: a journal of neurology*. 2015;138(Pt 9):2672-86.
 49. Rektorova I, Krajcovicova L, Marecek R, Mikl M. Default mode network and extrastriate visual resting state network in patients with Parkinson's disease dementia. *Neuro-degenerative diseases*. 2012;10(1-4):232-7.

50. van Eimeren T, Monchi O, Ballanger B, Strafella AP. Dysfunction of the default mode network in Parkinson disease: a functional magnetic resonance imaging study. *Archives of neurology*. 2009;66(7):877-83.
51. Tinaz S, Schendan HE, Stern CE. Fronto-striatal deficit in Parkinson's disease during semantic event sequencing. *Neurobiology of aging*. 2008;29(3):397-407.
52. Gorges M, Muller HP, Lule D, Pinkhardt EH, Ludolph AC, Kassubek J. To rise and to fall: functional connectivity in cognitively normal and cognitively impaired patients with Parkinson's disease. *Neurobiology of aging*. 2015;36(4):1727-35.
53. Lebedev AV, Westman E, Simmons A, Lebedeva A, Siepel FJ, Pereira JB, et al. Large-scale resting state network correlates of cognitive impairment in Parkinson's disease and related dopaminergic deficits. *Frontiers in systems neuroscience*. 2014;8:45.
54. Rektorova I, Krajcovicova L, Marecek R, Mikl M. Effective connectivity of the default mode network in parkinson's disease and parkinson's disease dementia. *Clinical Neurophysiology*. 2014;125:S126-S7.
55. Laird AR, Fox PM, Eickhoff SB, Turner JA, Ray KL, McKay DR, et al. Behavioral interpretations of intrinsic connectivity networks. *Journal of cognitive neuroscience*. 2011;23(12):4022-37.
56. Abos A, Baggio HC, Segura B, Garcia-Diaz AI, Compta Y, Marti MJ, et al. Discriminating cognitive status in Parkinson's disease through functional connectomics and machine learning. *Sci Rep*. 2017;7:45347.
57. Mijalkov M, Kakaei E, Pereira JB, Westman E, Volpe G, Alzheimer's Disease Neuroimaging I. BRAPH: A graph theory software for the analysis of brain connectivity. *PloS one*. 2017;12(8):e0178798.
58. Baggio HC, Sala-Llonch R, Segura B, Marti MJ, Valldeoriola F, Compta Y, et al. Functional brain networks and cognitive deficits in Parkinson's disease. *Human brain mapping*. 2014;35(9):4620-34.
59. Poldrack RA, Fletcher PC, Henson RN, Worsley KJ, Brett M, Nichols TE. Guidelines for reporting an fMRI study. *NeuroImage*. 2008;40(2):409-14.
60. Radua J, Mataix-Cols D, Phillips ML, El-Hage W, Kronhaus DM, Cardoner N, et al. A new meta-analytic method for neuroimaging studies that combines reported peak coordinates and statistical parametric maps. *European psychiatry : the journal of the Association of European Psychiatrists*. 2012;27(8):605-11.
61. Radua J, Mataix-Cols D. Meta-analytic methods for neuroimaging data explained. *Biology of mood & anxiety disorders*. 2012;2:6.
62. Jacobs HI, Radua J, Luckmann HC, Sack AT. Meta-analysis of functional network alterations in Alzheimer's disease: toward a network biomarker. *Neuroscience and biobehavioral reviews*. 2013;37(5):753-65.
63. Cooper D, Barker V, Radua J, Fusar-Poli P, Lawrie SM. Multimodal voxel-based meta-analysis of structural and functional magnetic resonance imaging studies in those at elevated genetic risk of developing schizophrenia. *Psychiatry research*. 2014;221(1):69-77.
64. Hart H, Radua J, Nakao T, Mataix-Cols D, Rubia K. Meta-analysis of functional magnetic resonance imaging studies of inhibition and attention in attention-deficit/hyperactivity disorder: exploring task-specific, stimulant medication, and age effects. *JAMA psychiatry*. 2013;70(2):185-98.
65. Meng YJ, Deng W, Wang HY, Guo WJ, Li T, Lam C, et al. Reward pathway dysfunction in gambling disorder: A meta-analysis of functional magnetic resonance imaging studies. *Behavioural brain research*. 2014;275:243-51.

66. Shen D, Cui L, Fang J, Cui B, Li D, Tai H. Voxel-Wise Meta-Analysis of Gray Matter Changes in Amyotrophic Lateral Sclerosis. *Frontiers in aging neuroscience*. 2016;8:64.
67. Yang X, Tian F, Zhang H, Zeng J, Chen T, Wang S, et al. Cortical and subcortical gray matter shrinkage in alcohol-use disorders: a voxel-based meta-analysis. *Neuroscience and biobehavioral reviews*. 2016;66:92-103.
68. Radua J, Mataix-Cols D. Voxel-wise meta-analysis of grey matter changes in obsessive-compulsive disorder. *The British journal of psychiatry : the journal of mental science*. 2009;195(5):393-402.
69. Smith SM, Fox PT, Miller KL, Glahn DC, Fox PM, Mackay CE, et al. Correspondence of the brain's functional architecture during activation and rest. *Proceedings of the National Academy of Sciences of the United States of America*. 2009;106(31):13040-5.
70. Fox PT, Lancaster JL. Opinion: Mapping context and content: the BrainMap model. *Nature reviews Neuroscience*. 2002;3(4):319-21.
71. Fox PT, Laird AR, Fox SP, Fox PM, Uecker AM, Crank M, et al. BrainMap taxonomy of experimental design: description and evaluation. *Human brain mapping*. 2005;25(1):185-98.
72. Laird AR, Lancaster JL, Fox PT. BrainMap: the social evolution of a human brain mapping database. *Neuroinformatics*. 2005;3(1):65-78.
73. Amboni M, Tessitore A, Esposito F, Santangelo G, Picillo M, Vitale C, et al. Resting-state functional connectivity associated with mild cognitive impairment in Parkinson's disease. *Journal of neurology*. 2015;262(2):425-34.
74. Possin KL, Kang GA, Guo C, Fine EM, Trujillo AJ, Racine CA, et al. Rivastigmine is associated with restoration of left frontal brain activity in Parkinson's disease. *Movement disorders : official journal of the Movement Disorder Society*. 2013;28(10):1384-90.
75. Baggio HC, Segura B, Sala-Llonch R, Marti MJ, Valldeoriola F, Compta Y, et al. Cognitive impairment and resting-state network connectivity in Parkinson's disease. *Human brain mapping*. 2015;36(1):199-212.
76. Canu E, Agosta F, Sarasso E, Volonte MA, Sarro L, Galantucci S, et al. Brain structural and functional abnormalities in Parkinson's disease patients with freezing of gait. *European journal of neurology*. 2015;22:295.
77. Borroni B, Premi E, Formenti A, Turrone R, Alberici A, Cottini E, et al. Structural and functional imaging study in dementia with Lewy bodies and Parkinson's disease dementia. *Parkinsonism & related disorders*. 2015;21(9):1049-55.
78. Chen B, Fan GG, Liu H, Wang S. Changes in anatomical and functional connectivity of Parkinson's disease patients according to cognitive status. *European journal of radiology*. 2015;84(7):1318-24.
79. Peraza LR, Colloby SJ, Firbank MJ, Greasy GS, McKeith IG, Kaiser M, et al. Resting state in Parkinson's disease dementia and dementia with Lewy bodies: commonalities and differences. *International journal of geriatric psychiatry*. 2015;30(11):1135-46.
80. Hou Y, Yang J, Luo C, Song W, Ou R, Liu W, et al. Dysfunction of the Default Mode Network in Drug-Naive Parkinson's Disease with Mild Cognitive Impairments: A Resting-State fMRI Study. *Frontiers in aging neuroscience*. 2016;8:247.
81. Peraza LR, Nesbitt D, Lawson RA, Duncan GW, Yarnall AJ, Khoo TK, et al. Intra- and inter-network functional alterations in Parkinson's disease with mild cognitive impairment. *Human brain mapping*. 2017;38(3):1702-15.

82. Bezdicek O, Ballarini T, Ruzicka F, Roth J, Mueller K, Jech R, et al. Mild cognitive impairment disrupts attention network connectivity in Parkinson's disease: A combined multimodal MRI and meta-analytical study. *Neuropsychologia*. 2018;112:105-15.
83. Chen B, Wang S, Sun W, Shang X, Liu H, Liu G, et al. Functional and structural changes in gray matter of parkinson's disease patients with mild cognitive impairment. *European journal of radiology*. 2017;93:16-23.
84. Diez-Cirarda M, Strafella AP, Kim J, Pena J, Ojeda N, Cabrera-Zubizarreta A, et al. Dynamic functional connectivity in Parkinson's disease patients with mild cognitive impairment and normal cognition. *NeuroImage Clinical*. 2018;17:847-55.
85. Zhan ZW, Lin LZ, Yu EH, Xin JW, Lin L, Lin HL, et al. Abnormal resting-state functional connectivity in posterior cingulate cortex of Parkinson's disease with mild cognitive impairment and dementia. *CNS neuroscience & therapeutics*. 2018.
86. Shin NY, Shin YS, Lee PH, Yoon U, Han S, Kim DJ, et al. Different Functional and Microstructural Changes Depending on Duration of Mild Cognitive Impairment in Parkinson Disease. *AJNR American journal of neuroradiology*. 2016;37(5):897-903.
87. Vidal-Pineiro D, Valls-Pedret C, Fernandez-Cabello S, Arenaza-Urquijo EM, Sala-Llonch R, Solana E, et al. Decreased Default Mode Network connectivity correlates with age-associated structural and cognitive changes. *Frontiers in aging neuroscience*. 2014;6:256.
88. Andrews-Hanna JR, Snyder AZ, Vincent JL, Lustig C, Head D, Raichle ME, et al. Disruption of large-scale brain systems in advanced aging. *Neuron*. 2007;56(5):924-35.
89. Damoiseaux JS, Beckmann CF, Arigita EJ, Barkhof F, Scheltens P, Stam CJ, et al. Reduced resting-state brain activity in the "default network" in normal aging. *Cerebral cortex (New York, NY : 1991)*. 2008;18(8):1856-64.
90. Toussaint PJ, Maiz S, Coynel D, Doyon J, Messe A, de Souza LC, et al. Characteristics of the default mode functional connectivity in normal ageing and Alzheimer's disease using resting state fMRI with a combined approach of entropy-based and graph theoretical measurements. *NeuroImage*. 2014;101:778-86.
91. Balthazar ML, de Campos BM, Franco AR, Damasceno BP, Cendes F. Whole cortical and default mode network mean functional connectivity as potential biomarkers for mild Alzheimer's disease. *Psychiatry research*. 2014;221(1):37-42.
92. Zhou J, Greicius MD, Gennatas ED, Growdon ME, Jang JY, Rabinovici GD, et al. Divergent network connectivity changes in behavioural variant frontotemporal dementia and Alzheimer's disease. *Brain : a journal of neurology*. 2010;133(Pt 5):1352-67.
93. Wolf RC, Sambataro F, Vasic N, Wolf ND, Thomann PA, Saft C, et al. Default-mode network changes in preclinical Huntington's disease. *Experimental neurology*. 2012;237(1):191-8.
94. Tessitore A, Esposito F, Vitale C, Santangelo G, Amboni M, Russo A, et al. Default-mode network connectivity in cognitively unimpaired patients with Parkinson disease. *Neurology*. 2012;79(23):2226-32.
95. Yao N, Shek-Kwan Chang R, Cheung C, Pang S, Lau KK, Suckling J, et al. The default mode network is disrupted in Parkinson's disease with visual hallucinations. *Human brain mapping*. 2014;35(11):5658-66.
96. Disbrow EA, Carmichael O, He J, Lanni KE, Dressler EM, Zhang L, et al. Resting state functional connectivity is associated with cognitive dysfunction in non-demented people with Parkinson's disease. *Journal of Parkinson's disease*. 2014;4(3):453-65.
97. Tahmasian M, Eickhoff SB, Giehl K, Schwartz F, Herz DM, Drzezga A, et al. Resting-state functional reorganization in Parkinson's disease: An activation likelihood estimation meta-analysis. *Cortex*. 2017;92:119-38.

98. Berman BD, Smucny J, Wylie KP, Shelton E, Kronberg E, Leehey M, et al. Levodopa modulates small-world architecture of functional brain networks in Parkinson's disease. *Movement disorders : official journal of the Movement Disorder Society*. 2016;31(11):1676-84.
99. Folmer RL, Vachhani JJ, Theodoroff SM, Ellinger R, Riggins A. Auditory Processing Abilities of Parkinson's Disease Patients. *BioMed research international*. 2017;2017:2618587.
100. Nojszewska M, Pilczuk B, Zakrzewska-Pniewska B, Rowinska-Marcinska K. The auditory system involvement in Parkinson disease: electrophysiological and neuropsychological correlations. *Journal of clinical neurophysiology : official publication of the American Electroencephalographic Society*. 2009;26(6):430-7.
101. Hardy CJ, Marshall CR, Golden HL, Clark CN, Mummery CJ, Griffiths TD, et al. Hearing and dementia. *Journal of neurology*. 2016;263(11):2339-54.
102. Lewis SJG, Dove A, Robbins TW, Barker RA, Owen AM. Cognitive impairments in early Parkinson's disease are accompanied by reductions in activity in frontostriatal neural circuitry. *Journal of Neuroscience*. 2003;23(15):6351-6.
103. Caminiti SP, Siri C, Guidi L, Antonini A, Perani D. The neural correlates of spatial and object working memory in elderly and Parkinson's disease subjects. *Behavioural neurology*. 2015;2015:123636.
104. Japee S, Holiday K, Satyshur MD, Mukai I, Ungerleider LG. A role of right middle frontal gyrus in reorienting of attention: a case study. *Frontiers in systems neuroscience*. 2015;9:23.
105. Manza P, Zhang S, Li CS, Leung HC. Resting-state functional connectivity of the striatum in early-stage Parkinson's disease: Cognitive decline and motor symptomatology. *Human brain mapping*. 2016;37(2):648-62.
106. Reuter-Lorenz PA, Cappell KA. Neurocognitive Aging and the Compensation Hypothesis. *Current Directions in Psychological Science*. 2008;17(3):177-82.
107. Samuel M, Ceballos-Baumann AO, Blin J, Uema T, Boecker H, Passingham RE, et al. Evidence for lateral premotor and parietal overactivity in Parkinson's disease during sequential and bimanual movements. A PET study. *Brain : a journal of neurology*. 1997;120 (Pt 6):963-76.
108. Dagher A, Owen AM, Boecker H, Brooks DJ. The role of the striatum and hippocampus in planning: a PET activation study in Parkinson's disease. *Brain : a journal of neurology*. 2001;124(Pt 5):1020-32.
109. Poston KL, YorkWilliams S, Zhang K, Cai W, Everling D, Tayim FM, et al. Compensatory neural mechanisms in cognitively unimpaired Parkinson disease. *Annals of neurology*. 2016;79(3):448-63.
110. Rektorova I. Resting-state networks in Alzheimer's disease and Parkinson's disease. *Neurodegenerative diseases*. 2014;13(2-3):186-8.
111. Lopes R, Delmaire C, Defebvre L, Moonen AJ, Duits AA, Hofman P, et al. Cognitive phenotypes in parkinson's disease differ in terms of brain-network organization and connectivity. *Hum Brain Mapp*. 2017;38(3):1604-21.
112. Duncan GW, Firbank MJ, O'Brien JT, Burn DJ. Magnetic resonance imaging: a biomarker for cognitive impairment in Parkinson's disease? *Movement disorders : official journal of the Movement Disorder Society*. 2013;28(4):425-38.
113. Marks W, Evers L, Faber M, Verbeek M, De Vries N, Bloem B. Study design for a multi-modal approach to understanding parkinson's disease: The personalized parkinson project. *Movement Disorders*. 2017;32 (Supplement 2):948.
114. Chen Y, Yang W, Long J, Zhang Y, Feng J, Li Y, et al. Discriminative analysis of Parkinson's disease based on whole-brain functional connectivity. *PloS one*. 2015;10(4):e0124153.

115. Vo A, Sako W, Fujita K, Peng S, Mattis PJ, Skidmore FM, et al. Parkinson's disease-related network topographies characterized with resting state functional MRI. *Human brain mapping*. 2017;38(2):617-30.
116. Zeighami Y, Ulla M, Iturria-Medina Y, Dadar M, Zhang Y, Larcher KM, et al. Network structure of brain atrophy in de novo Parkinson's disease. *Elife*. 2015;4.
117. Long D, Wang J, Xuan M, Gu Q, Xu X, Kong D, et al. Automatic classification of early Parkinson's disease with multi-modal MR imaging. *PloS one*. 2012;7(11):e47714.
118. Kalpouzos G, Persson J, Nyberg L. Local brain atrophy accounts for functional activity differences in normal aging. *Neurobiology of aging*. 2012;33(3):623 e1- e13.
119. Rajagopalan V, Yue GH, Piro EP. Do preprocessing algorithms and statistical models influence voxel-based morphometry (VBM) results in amyotrophic lateral sclerosis patients? A systematic comparison of popular VBM analytical methods. *Journal of magnetic resonance imaging : JMRI*. 2014;40(3):662-7.
120. Zhurakovskaya E, Paasonen J, Shatillo A, Lipponen A, Salo R, Aliev R, et al. Global Functional Connectivity Differences between Sleep-Like States in Urethane Anesthetized Rats Measured by fMRI. *PloS one*. 2016;11(5):e0155343.
121. Dang LC, O'Neil JP, Jagust WJ. Dopamine supports coupling of attention-related networks. *J Neurosci*. 2012;32(28):9582-7.
122. Krajcovicova L, Mikl M, Marecek R, Rektorova I. The default mode network integrity in patients with Parkinson's disease is levodopa equivalent dose-dependent. *Journal of neural transmission (Vienna, Austria : 1996)*. 2012;119(4):443-54.
123. Delaveau P, Salgado-Pineda P, Fossati P, Witjas T, Azulay JP, Blin O. Dopaminergic modulation of the default mode network in Parkinson's disease. *European neuropsychopharmacology : the journal of the European College of Neuropsychopharmacology*. 2010;20(11):784-92.
124. Litvan I, Aarsland D, Adler CH, Goldman JG, Kulisevsky J, Mollenhauer B, et al. MDS Task Force on mild cognitive impairment in Parkinson's disease: critical review of PD-MCI. *Movement disorders : official journal of the Movement Disorder Society*. 2011;26(10):1814-24.
125. Litvan I, Goldman JG, Troster AI, Schmand BA, Weintraub D, Petersen RC, et al. Diagnostic criteria for mild cognitive impairment in Parkinson's disease: Movement Disorder Society Task Force guidelines. *Movement disorders : official journal of the Movement Disorder Society*. 2012;27(3):349-56.
126. Emre M, Aarsland D, Brown R, Burn DJ, Duyckaerts C, Mizuno Y, et al. Clinical diagnostic criteria for dementia associated with Parkinson's disease. *Mov Disord*. 2007;22(12):1689-707; quiz 837.
127. Dubois B, Burn D, Goetz C, Aarsland D, Brown RG, Broe GA, et al. Diagnostic procedures for Parkinson's disease dementia: recommendations from the movement disorder society task force. *Movement disorders : official journal of the Movement Disorder Society*. 2007;22(16):2314-24.
128. Dujardin K, Moonen AJ, Behal H, Defebvre L, Duhamel A, Duits AA, et al. Cognitive disorders in Parkinson's disease: Confirmation of a spectrum of severity. *Parkinsonism Relat Disord*. 2015;21(11):1299-305.

Supporting data (S1): Quality assessment

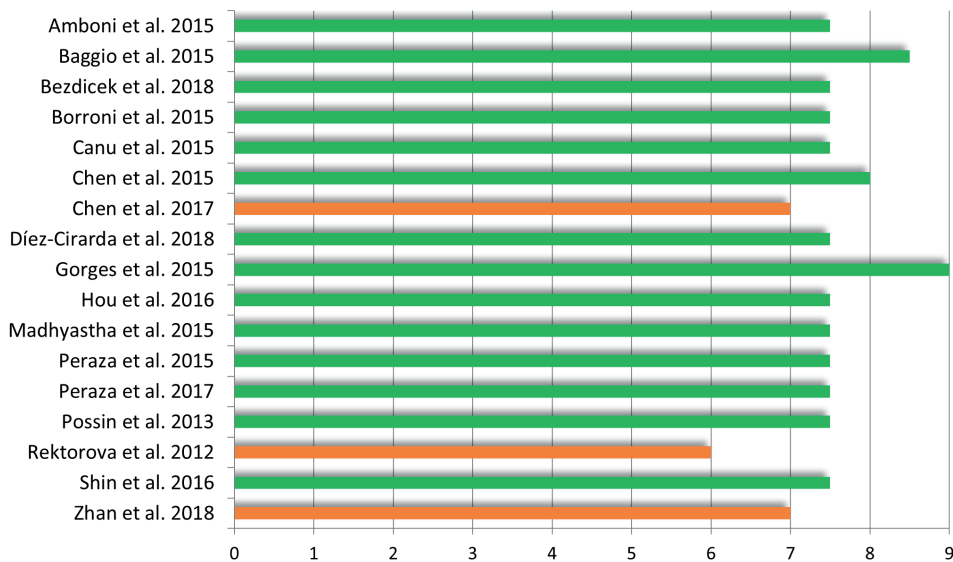


Figure 1. Quality assessment derived from the guidelines of Poldrack et al. [28]. Total score was based on 9 criteria. For each item 0, 0.5 or 1 point could be scored. An overall score of ≥ 7.5 was considered as good (green), 4-7.5 as fair (orange) and ≤ 4 as poor (red) quality.

Table 1. Amboni et al. (2015)

	+	+/-	-	Other (CD, NR,NA)*
1. Did they give a full description of the study participants?	V			
2. Did they give a full description of the psychological task used in fMRI?	V			
3. Did they specify the spatial normalization procedure, including the atlas or template which is used to match the images to?	V			
4. Did they specify how the regions of interest were determined?		V		
5. Did they provide enough detail to reproduce the analysis?	V			
6. Are all the empirical claims supported by a specific statistical test?	V			
7. Did they describe and account for the multiple testing problem?	V			
8. Do the figures and tables stand on their own?		V		
9. Are the quality control measures documented?		V		
Quality Rating (Good, Fair or Poor) (See guidance)			7.5 (Good)	
Rater #1 initials:			AW	
Rater #2 initials:			SW	

Additional Comments (If POOR, please state why):

4: The regions of interest are not clearly defined; no sphere coordinates or voxel sizes are given.

8: No voxel sizes in table 3, no slice coordinates given for figure 1.

9: Mask applied for within three-group comparison, although not clearly described which voxels were included.

*CD, cannot determine; NA, not applicable; NR, not reported

Table 2. Gorges et al. (2015)

	+	+/-	-	Other (CD, NR,NA)*
1. Did they give a full description of the study participants?	V			
2. Did they give a full description of the psychological task used in fMRI?	V			
3. Did they specify the spatial normalization procedure, including the atlas or template which is used to match the images to?	V			
4. Did they specify how the regions of interest were determined?	V			
5. Did they provide enough detail to reproduce the analysis?	V			
6. Are all the empirical claims supported by a specific statistical test?	V			
7. Did they describe and account for the multiple testing problem?	V			
8. Do the figures and tables stand on their own?	V			
9. Are the quality control measures documented?	V			
Quality Rating (Good, Fair or Poor) (See guidance)			9 (Good)	
Rater #1 initials:			AW	
Rater #2 initials:			SW	

Additional Comments (If POOR, please state why):

1: In- and exclusion criteria are described in Balzer-Geldsetzer et al. (2011).

5: The iFCMRI algorithms have been described previously in Gorges et al. (2014).

*CD, cannot determine: NA, not applicable: NR, not reported

Table 3. Madhyastha et al. (2015)

	+	+/-	-	Other (CD, NR,NA)*
1. Did they give a full description of the study participants?		V		
2. Did they give a full description of the psychological task used in fMRI?	V			
3. Did they specify the spatial normalization procedure, including the atlas or template which is used to match the images to?		V		
4. Did they specify how the regions of interest were determined?	V			
5. Did they provide enough detail to reproduce the analysis?	V			
6. Are all the empirical claims supported by a specific statistical test?	V			
7. Did they describe and account for the multiple testing problem?	V			
8. Do the figures and tables stand on their own?		V		
9. Are the quality control measures documented?	V			
Quality Rating (Good, Fair or Poor) (See guidance)			7.5 (Good)	
Rater #1 initials:			AW	
Rater #2 initials:			SW	

Additional Comments (If POOR, please state why):

1: Exclusion criteria are described in Madhyastha et al. (2014). Inclusion criteria not clearly described.

3: No details of spatial normalization method are given.

8: No slice coordinates are given in figure 3.

*CD, cannot determine: NA, not applicable: NR, not reported

Table 4. Possin et al. (2013)

	+	+/-	-	Other (CD, NR,NA)*
1. Did they give a full description of the study participants?		V		
2. Did they give a full description of the psychological task used in fMRI?	V			
3. Did they specify the spatial normalization procedure, including the atlas or template which is used to match the images to?			V	NR
4. Did they specify how the regions of interest were determined?				NA
5. Did they provide enough detail to reproduce the analysis?	V			
6. Are all the empirical claims supported by a specific statistical test?	V			
7. Did they describe and account for the multiple testing problem?	V			
8. Do the figures and tables stand on their own?	V			
9. Are the quality control measures documented?	V			
Quality Rating (Good, Fair or Poor) (See guidance)			7.5 (Good)	
Rater #1 initials:			AW	
Rater #2 initials:			SW	

Additional Comments (If POOR, please state why):

1: Inclusion criteria not clearly described.

3: Atlas or template not specified (we have contacted the author for this information).

*CD, cannot determine: NA, not applicable: NR, not reported

Table 5. Baggio et al. (2015)

	+	+/-	-	Other (CD, NR,NA)*
1. Did they give a full description of the study participants?	V			
2. Did they give a full description of the psychological task used in fMRI?	V			
3. Did they specify the spatial normalization procedure, including the atlas or template which is used to match the images to?	V			
4. Did they specify how the regions of interest were determined?	V			
5. Did they provide enough detail to reproduce the analysis?	V			
6. Are all the empirical claims supported by a specific statistical test?	V			
7. Did they describe and account for the multiple testing problem?	V			
8. Do the figures and tables stand on their own?		V		
9. Are the quality control measures documented?	V			
Quality Rating (Good, Fair or Poor) (See guidance)			8.5 (Good)	
Rater #1 initials:			AW	
Rater #2 initials:			SW	

Additional Comments (If POOR, please state why):

2: Described in Baggio et al. (2014)

8: No slice coordinates are given in figure 1.

*CD, cannot determine: NA, not applicable: NR, not reported

Table 6. Borroni et al. (2015)

	+	+/-	-	Other (CD, NR,NA)*
1. Did they give a full description of the study participants?		V		
2. Did they give a full description of the psychological task used in fMRI?	V			
3. Did they specify the spatial normalization procedure, including the atlas or template which is used to match the images to?		V		
4. Did they specify how the regions of interest were determined?				NA
5. Did they provide enough detail to reproduce the analysis?	V			
6. Are all the empirical claims supported by a specific statistical test?	V			
7. Did they describe and account for the multiple testing problem?		V		
8. Do the figures and tables stand on their own?		V		
9. Are the quality control measures documented?		V		
Quality Rating (Good, Fair or Poor) (See guidance)			7.5 (Good)	
Rater #1 initials:			AW	
Rater #2 initials:			SW	

Additional Comments (If POOR, please state why):

1: *Subjects who had a maximum displacement in any direction larger than 1.5mm, or a maximum rotation larger than 1.5° were excluded. However, they did not report if and how many patients had to be excluded for this reason.*

7: *No correction for the multiple testing problem applied, however they have set a statistical threshold at $p < 0.005$ voxel-level with a voxel threshold of 200 voxels.*

8: *Figure 1 & 2 contain no description of the highlighted areas (no coordinates or anatomical names)*

*CD, cannot determine: NA, not applicable: NR, not reported

Table 7. Chen et al. (2015)

	+	+/-	-	Other (CD, NR,NA)*
1. Did they give a full description of the study participants?		V		
2. Did they give a full description of the psychological task used in fMRI?	V			
3. Did they specify the spatial normalization procedure, including the atlas or template which is used to match the images to?		V		
4. Did they specify how the regions of interest were determined?	V			
5. Did they provide enough detail to reproduce the analysis?	V			
6. Are all the empirical claims supported by a specific statistical test?	V			
7. Did they describe and account for the multiple testing problem?	V			
8. Do the figures and tables stand on their own?		V		
9. Are the quality control measures documented?		V		
Quality Rating (Good, Fair or Poor) (See guidance)			8 (Good)	
Rater #1 initials:			AW	
Rater #2 initials:			SW	

Additional Comments (If POOR, please state why):

1: *In- and exclusion criteria can be partly derived from the text, but are not clearly described.*

8: *Location of activation in stereotactic space (x,y,z, coordinates) is not provided. We have contacted the author to request this information.*

*CD, cannot determine: NA, not applicable: NR, not reported

Table 8. Canu et al. (2015)

	+	+/-	-	Other (CD, NR,NA)*
1. Did they give a full description of the study participants?		V		
2. Did they give a full description of the psychological task used in fMRI?	V			
3. Did they specify the spatial normalization procedure, including the atlas or template which is used to match the images to?	V			
4. Did they specify how the regions of interest were determined?	V			
5. Did they provide enough detail to reproduce the analysis?	V			
6. Are all the empirical claims supported by a specific statistical test?	V			
7. Did they describe and account for the multiple testing problem?	V			
8. Do the figures and tables stand on their own?		V		
9. Are the quality control measures documented?		V		
Quality Rating (Good, Fair or Poor) (See guidance)			7.5 (Good)	
Rater #1 initials:			AW	
Rater #2 initials:			SW	

Additional Comments (If POOR, please state why):

1: It seems like one HC subject was excluded during the study. However, this is not described in the text and no explanation is given.

8: No slice coordinates are given in figure 3.

9: No voxel sizes described for the applied mask. No covariates described.

*CD, cannot determine: NA, not applicable: NR, not reported

Table 9. Rektorova et al. (2012)

	+	+/-	-	Other (CD, NR,NA)*
1. Did they give a full description of the study participants?			V	
2. Did they give a full description of the psychological task used in fMRI?			V	
3. Did they specify the spatial normalization procedure, including the atlas or template which is used to match the images to?	V			
4. Did they specify how the regions of interest were determined?	V			
5. Did they provide enough detail to reproduce the analysis?	V			
6. Are all the empirical claims supported by a specific statistical test?	V			
7. Did they describe and account for the multiple testing problem?	V			
8. Do the figures and tables stand on their own?		V		
9. Are the quality control measures documented?		V		
Quality Rating (Good, Fair or Poor) (See guidance)			6 (Fair)	
Rater #1 initials:			AW	
Rater #2 initials:			SW	

Additional Comments (If POOR, please state why):

1: No in- and exclusion criteria are described.

2: No instructions for the resting-state functional measurement are described.

8: No slice coordinates/coordinates are given in figure 3&4. Contrast not clearly described in figure 4.

9: No motion correction described.

*CD, cannot determine: NA, not applicable: NR, not reported

Table 10. Peraza et al. (2015)

	+	+/-	-	Other (CD, NR,NA)*
1. Did they give a full description of the study participants?			V	
2. Did they give a full description of the psychological task used in fMRI?		V		
3. Did they specify the spatial normalization procedure, including the atlas or template which is used to match the images to?	V			
4. Did they specify how the regions of interest were determined?	V			
5. Did they provide enough detail to reproduce the analysis?	V			
6. Are all the empirical claims supported by a specific statistical test?	V			
7. Did they describe and account for the multiple testing problem?	V			
8. Do the figures and tables stand on their own?	V			
9. Are the quality control measures documented?	V			
Quality Rating (Good, Fair or Poor) (See guidance)			7.5 (Good)	
Rater #1 initials:			AW	
Rater #2 initials:			SW	

Additional Comments (If POOR, please state why):

1: In- and exclusion criteria and recruitment method of subjects not clearly described.

2: Patient instruction for resting-state fMRI acquisition not clearly described.

*CD, cannot determine: NA, not applicable: NR, not reported

Table 11. Hou et al. (2016)

	+	+/-	-	Other (CD, NR,NA)*
1. Did they give a full description of the study participants?	V			
2. Did they give a full description of the psychological task used in fMRI?	V			
3. Did they specify the spatial normalization procedure, including the atlas or template which is used to match the images to?			V	
4. Did they specify how the regions of interest were determined?	V			
5. Did they provide enough detail to reproduce the analysis?	V			
6. Are all the empirical claims supported by a specific statistical test?	V			
7. Did they describe and account for the multiple testing problem?	V			
8. Do the figures and tables stand on their own?		V		
9. Are the quality control measures documented?	V			
Quality Rating (Good, Fair or Poor) (See guidance)			7.5 (Good)	
Rater #1 initials:			AW	
Rater #2 initials:			SW	

Additional Comments (If POOR, please state why):

3. The fMRI images are resampled to voxel size 3x3x3mm, while they were obtained at a voxel size of 3.75x3.75x5mm.

8. No exact Z-scores are presented in figure 1.

*CD, cannot determine: NA, not applicable: NR, not reported

Table 12. Shin et al. (2016)

	+	+/-	-	Other (CD, NR,NA)*
1. Did they give a full description of the study participants?	V			
2. Did they give a full description of the psychological task used in fMRI?	V			
3. Did they specify the spatial normalization procedure, including the atlas or template which is used to match the images to?		V		
4. Did they specify how the regions of interest were determined?	V			
5. Did they provide enough detail to reproduce the analysis?	V			
6. Are all the empirical claims supported by a specific statistical test?	V			
7. Did they describe and account for the multiple testing problem?	V			
8. Do the figures and tables stand on their own?			V	
9. Are the quality control measures documented?	V			
Quality Rating (Good, Fair or Poor) (See guidance)			7.5 (Good)	
Rater #1 initials:			AW	
Rater #2 initials:			SW	

Additional Comments (If POOR, please state why):

3. The atlas is only specified in the supplementary data.

8. Coordinates and atlas are missing in some of the figures.

*CD, cannot determine: NA, not applicable: NR, not reported

Table 13. Peraza et al. (2017)

	+	+/-	-	Other (CD, NR,NA)*
1. Did they give a full description of the study participants?	V			
2. Did they give a full description of the psychological task used in fMRI?	V			
3. Did they specify the spatial normalization procedure, including the atlas or template which is used to match the images to?	V			
4. Did they specify how the regions of interest were determined?		V		
5. Did they provide enough detail to reproduce the analysis?	V			
6. Are all the empirical claims supported by a specific statistical test?	V			
7. Did they describe and account for the multiple testing problem?	V			
8. Do the figures and tables stand on their own?		V		
9. Are the quality control measures documented?		V		
Quality Rating (Good, Fair or Poor) (See guidance)			7.5 (Good)	
Rater #1 initials:			AW	
Rater #2 initials:			SW	

Additional Comments (If POOR, please state why):

4. No voxel sizes or specific coordinates are given for the used resting state networks.

8. The intensity thresholds/scale are not presented in figure 2.

9. No gray matter/atrophy correction applied (However, they substantiated their considerations).

*CD, cannot determine: NA, not applicable: NR, not reported

Table 14. Bezdicek et al. (2018)

	+	+/-	-	Other (CD, NR,NA)*
1. Did they give a full description of the study participants?	V			
2. Did they give a full description of the psychological task used in fMRI?	V			
3. Did they specify the spatial normalization procedure, including the atlas or template which is used to match the images to?		V		
4. Did they specify how the regions of interest were determined?				NA
5. Did they provide enough detail to reproduce the analysis?	V			
6. Are all the empirical claims supported by a specific statistical test?	V			
7. Did they describe and account for the multiple testing problem?	V			
8. Do the figures and tables stand on their own?			V	
9. Are the quality control measures documented?	V			
Quality Rating (Good, Fair or Poor) (See guidance)			7.5 (Good)	
Rater #1 initials:			AW	
Rater #2 initials:			SW	

Additional Comments (If POOR, please state why):

3. The atlas used to match the images to, is not clearly specified.
 8. No slice coordinates are given in figure 2, 4 and 5. Furthermore, also non-significant results are displayed.
 *CD, cannot determine: NA, not applicable: NR, not reported

Table 15. Chen et al. (2017)

	+	+/-	-	Other (CD, NR,NA)*
1. Did they give a full description of the study participants?			V	
2. Did they give a full description of the psychological task used in fMRI?	V			
3. Did they specify the spatial normalization procedure, including the atlas or template which is used to match the images to?	V			
4. Did they specify how the regions of interest were determined?	V			
5. Did they provide enough detail to reproduce the analysis?	V			
6. Are all the empirical claims supported by a specific statistical test?		V		
7. Did they describe and account for the multiple testing problem?	V			
8. Do the figures and tables stand on their own?		V		
9. Are the quality control measures documented?	V			
Quality Rating (Good, Fair or Poor) (See guidance)			7 (Fair)	
Rater #1 initials:			AW	
Rater #2 initials:			SW	

Additional Comments (If POOR, please state why):

2. In- and exclusion criteria can be largely derived from the text, but are not specifically described. Also, the use of dopaminergic medication is not reported.
 6. The text does not explicitly state that the results are significant.
 8. No intensity thresholds are given in figure 1 and 2.

*CD, cannot determine: NA, not applicable: NR, not reported

Table 16. Díez-Cirarda et al. (2018)

	+	+/-	-	Other (CD, NR,NA)*
1. Did they give a full description of the study participants?	V			
2. Did they give a full description of the psychological task used in fMRI?	V			
3. Did they specify the spatial normalization procedure, including the atlas or template which is used to match the images to?	V			
4. Did they specify how the regions of interest were determined?				NA
5. Did they provide enough detail to reproduce the analysis?	V			
6. Are all the empirical claims supported by a specific statistical test?	V			
7. Did they describe and account for the multiple testing problem?	V			
8. Do the figures and tables stand on their own?		V		
9. Are the quality control measures documented?			V	
Quality Rating (Good, Fair or Poor) (See guidance)			7.5 (Good)	
Rater #1 initials:			AW	
Rater #2 initials:			SW	

Additional Comments (If POOR, please state why):

8. No x,y,z coordinates are given in table 3.

9. No gray matter/atrophy correction applied.

*CD, cannot determine: NA, not applicable: NR, not reported

Table 17. Zhan et al. (2018)

	+	+/-	-	Other (CD, NR,NA)*
1. Did they give a full description of the study participants?	V			
2. Did they give a full description of the psychological task used in fMRI?	V			
3. Did they specify the spatial normalization procedure, including the atlas or template which is used to match the images to?			V	
4. Did they specify how the regions of interest were determined?	V			
5. Did they provide enough detail to reproduce the analysis?	V			
6. Are all the empirical claims supported by a specific statistical test?	V			
7. Did they describe and account for the multiple testing problem?	V			
8. Do the figures and tables stand on their own?	V			
9. Are the quality control measures documented?			V	
Quality Rating (Good, Fair or Poor) (See guidance)			7 (Fair)	
Rater #1 initials:			AW	
Rater #2 initials:			SW	

Additional Comments (If POOR, please state why):

3. The fMRI images are resampled to voxel size 3x3x3mm, while they were obtained with a 5-mm slice thickness.

9. No gray matter/atrophy correction applied.

*CD, cannot determine: NA, not applicable: NR, not reported

Supporting data (S2): Robustness analysis

I. Contrast HC vs. PD-CI

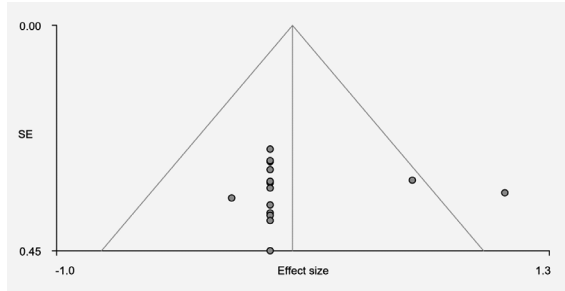


Figure 1. Right Supramarginal gyrus, BA 40, Bias: 0.25, t : 0.14, df : 13, p : 0.887

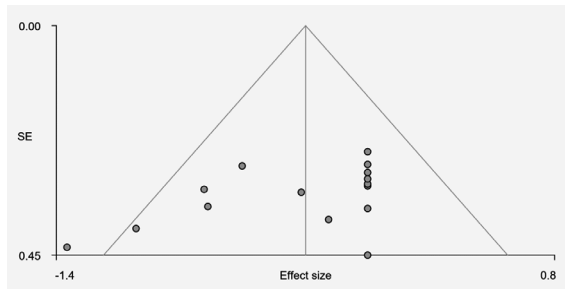


Figure 2. Right Rolandic operculum (BA 48), Bias: -3.39, t : -1.97, df : 13, p : 0.070

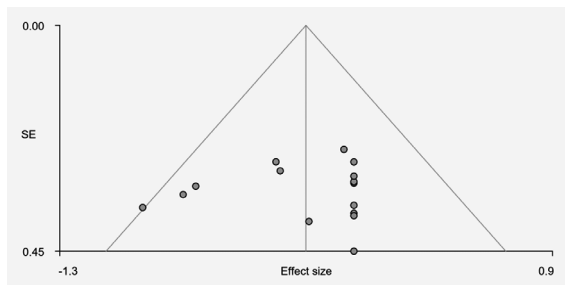


Figure 3. Left inferior parietal gyri (BA 40), Bias: -0.65, t : -0.39, df : 13, p : 0.701

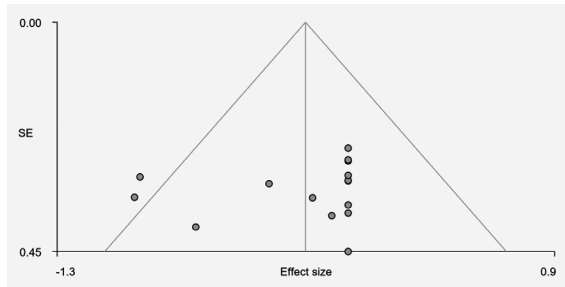


Figure 4. Right angular gyrus (BA 39), Bias: -1.43, t : -0.79, df : 13, p : 0.442

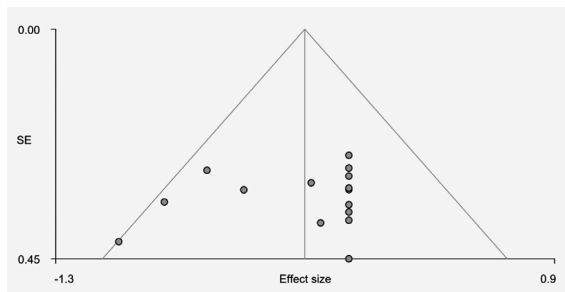


Figure 5. Left parahippocampal gyrus (BA 37), Bias: -1.20, t : -0.72, df : 13, p : 0.485

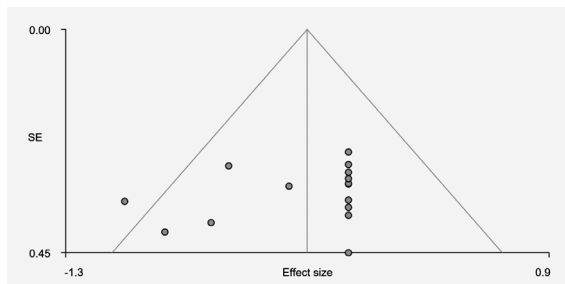


Figure 6. Right calcarine fissure/surrounding cortex (BA 23), Bias: -1.94, t : -1.16, df : 13, p : 0.267

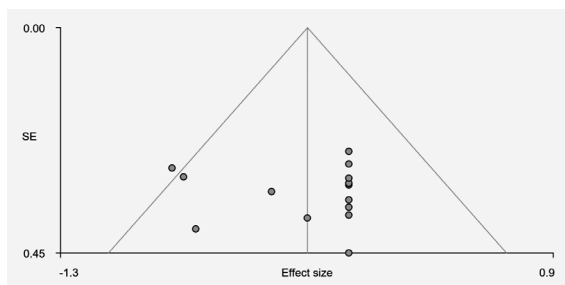


Figure 7. Right superior frontal gyrus, dorsolateral (BA 9), Bias: 0.11, t : 0.06, df : 13, p : 0.952

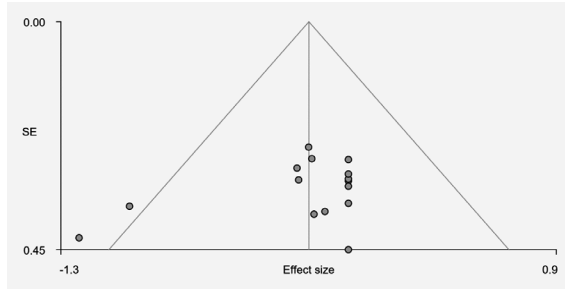


Figure 8. Right precentral gyrus (BA 4), Bias: -2.11, t : -1.44, df : 13, p : 0.174

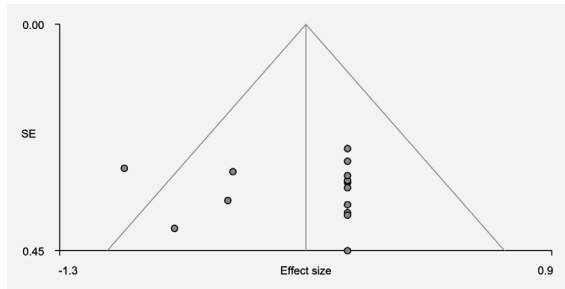


Figure 9. Right precentral gyrus (BA 6), Bias: -0.14, t : -0.08, df : 13, p : 0.940

II. Contrast PD-CI vs. PD CU

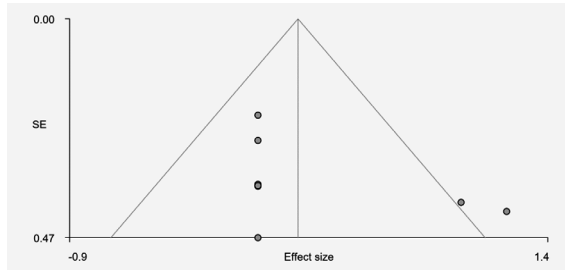


Figure 10. Right cerebellum, hemispheric lobule VI (BA 37), Bias: 2.15, t : 1.35, df : 7, p : 0.221

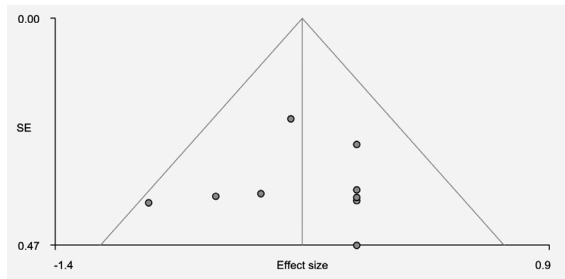


Figure 11. Left precuneus, Bias: -0.27, t : -0.20, df : 7, p : 0.849

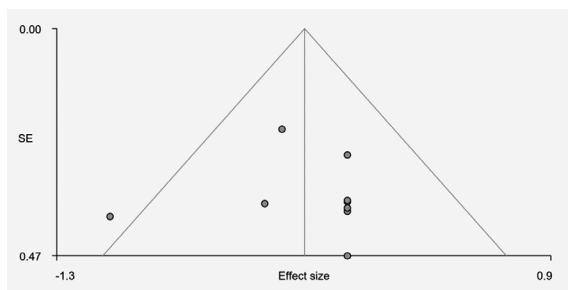


Figure 12. Right median cingulate / paracingulate gyri (BA 24), Bias: 0.06, t: 0.04, df: 7, p: 0.967

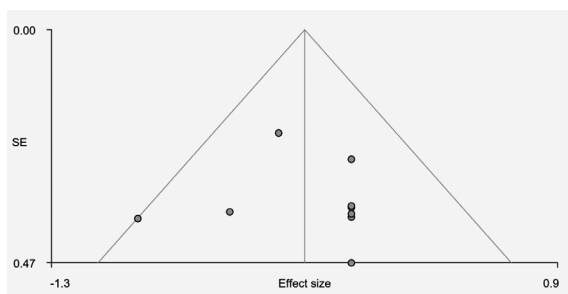


Figure 13. Left superior frontal gyrus, dorsolateral (BA 10), Bias: 0.21, t: 0.15, df: 7, p: 0.882

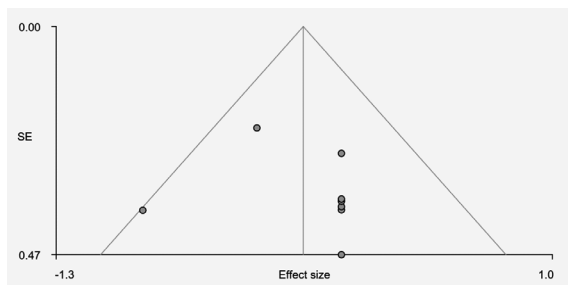


Figure 14. Right precentral gyrus (BA 4), Bias: 0.93, t: 0.74, df: 7, p: 0.486

Supporting data (S3): Spatial correlation analysis

Table 1. FSL correlation analysis between AES-SDM peak coordinates and resting-state networks.

Resting-state networks	HC > PD-CI	HC < PD-CI	PD-CU > PD-CI	PD-CU < PD-CI
Smith et al. (2009)				
Medial visual network	0.03	0.02	0.03	0.04
Occipital visual network	0.01	0.01	0.01	0.04
Lateral visual network	0.00	0.03	0.02	0.05
Default mode network	0.07	0.01	0.24	0.02
Cerebellum	0.01	0.00	0.02	0.19
Sensorimotor network	0.13	0.05	0.00	0.01
Auditory network	0.13	0.01	0.02	0.04
Executive control network	0.03	0.01	0.02	0.00
Right frontoparietal network	0.07	0.05	0.04	0.03
Left frontoparietal network	0.00	0.01	0.01	0.00

Spatial correlation values (r) are given for each network. All images in MNI-space, with a voxel size of 2x2mm.

CHAPTER 3

3

Brain network characteristics and cognitive performance in motor subtypes of Parkinson's disease: A resting state fMRI study

Wolters AF, Michielse S, Kuijf ML, Defebvre L, Lopes R, Dujardin K, Leentjens AFG.

Abstract

Introduction: Parkinson's disease (PD) is a heterogeneous disorder with great variability in motor and non-motor manifestations. It is hypothesized that different motor subtypes are characterized by different neuropsychiatric and cognitive symptoms, but the underlying correlates in cerebral connectivity remain unknown. Our aim is to compare brain network connectivity between the postural instability and gait disorder (PIGD) and tremor-dominant (TD) subtypes, using both a within- and between-network analysis.

Methods: This cross-sectional resting-state fMRI study includes 81 PD patients, 54 belonging to the PIGD and 27 to the TD subgroup. Group-level spatial maps were created using independent component analysis. Differences in functional connectivity were investigated using dual regression analysis and inter-network connectivity analysis. An additional voxel-based morphometry analysis was performed to examine if results were influenced by grey matter atrophy.

Results: The PIGD subgroup scored worse than the TD subgroup on all cognitive domains. Resting-state fMRI network analyses suggested that the connection between the visual and sensorimotor network is a potential differentiator between PIGD and TD subgroups. However, after correcting for dopaminergic medication use these results were not significant anymore. There was no between-group difference in grey matter volume.

Conclusion: Despite clear motor and cognitive differences between the PIGD and TD subtypes, no significant differences were found in network connectivity. Methodological challenges, substantial symptom heterogeneity and many involved variables make analyses and hypothesis building around PD subtypes highly complex. More sensitive visualisation methods combined with machine learning approaches may be required in the search for characteristic underpinnings of PD subtypes.

1. Introduction

Parkinson's disease (PD) is a heterogeneous neurodegenerative disorder, that shows a rapid increase in worldwide incidence and prevalence over the past two decades (1). A great variability in presentation exists, not only in motor manifestations, but also in cognitive functioning, autonomic symptoms, prognosis, and treatment response (2). This is why the National Institutes of Health state that obtaining more insight in the heterogenous nature and defining different subtypes of PD, is one of the top three research priorities in PD (3). Although the scientific validity of PD subtypes is questioned (4), in clinical practice, the subdivision of patients into a tremor-dominant (TD) and postural instability and gait disorder (PIGD) subtype is often used to describe the main motor phenotypes (5, 6).

The different clinical presentations of PD may be related to the involvement of different neuronal pathways and alterations in neurotransmitter activities. Bradykinesia and rigidity are thought to be mainly related to dopaminergic deficits, whereas it has been suggested that serotonin plays an important role in tremor. In addition, cholinergic modulations seem to influence gait disorders in PD (7). This suggests that different pathophysiological processes and various functional brain networks may be involved in different PD subtypes. However, results vary greatly between studies. For example, one study showed an increased functional connectivity density in the cerebellum and a decreased functional connectivity density in the frontal lobes of TD patients compared to PIGD PD patients (8), whereas others have reported an increased connectivity between the basal ganglia and the ventral somatomotor network in TD subjects and a decreased connectivity between the basal ganglia and the fronto-parietal network in non-TD subjects (9). Moreover, cerebral activity within the default mode network has been described as distinctive between TD and akinetic-rigid PD patients (10). Most studies have focused on specific regions of interest while, in order to elucidate the underlying pathophysiology of PD motor subtypes, it might be more relevant to study complex whole-brain interactions and functional brain organization at a global network level (11). Advances in functional magnetic resonance imaging (fMRI) analysis offer the possibility to study the overall resting-state function of brain networks using both within- and between-network analysis. This may open the perspective of modelling the pathways of pathology spreading in PD, which might precede structural damage, and to characterize the most vulnerable networks (11). Furthermore, knowledge of the pathophysiology of distinct PD subtypes might eventually lead towards more specific and reliable clinical biomarkers and personalized medicine in the future.

The main aim of the present study was to compare brain network organization between PIGD and TD subtypes using resting-state fMRI. Furthermore, our secondary aim is to

associate potential significant differences in cerebral connectivity with alterations in cognitive performance. Based on previous studies, we expect the PIGD subtype to show altered connections in brain regions that are part of the default mode network, while the TD subtype is expected to show alterations mainly in the fronto-parietal network (11). In addition, we expect the PIGD subtype to be more prone to develop cognitive decline in general, particularly in visuospatial, executive and memory domains (7).

2. Materials and methods

The present study is based on a previous published cross-sectional observational resting-state fMRI study, in which cognitive phenotypes of PD were investigated. This study is extensively described elsewhere (12, 13).

2.1 Participants

The study consisted of 156 PD patients. All patients met the United Kingdom Brain Bank criteria for idiopathic PD (14). We excluded patients with a diagnosis of a neurological disease other than PD, moderate and severe dementia (defined as a score >1 on the Clinical Dementia Rating (15) and according to the Movement Disorders criteria (16)) and an age older than 80 years. Participants were recruited among the outpatients of two European movement disorder centres, in Lille, France and Maastricht, the Netherlands. All participants gave informed consent prior to participation in the study. The study was approved by the local institutional review boards (CPP Nord-Ouest IV, 2012- A 01317-36 and METC AZM/UM 12-3-064 and registered at clinicalTrials.gov: NCT01792843) and performed in accordance with the principles of the Declaration of Helsinki (Fortaleza, Brazil, 2013).

Detailed demographic and disease related variables were documented, including the antiparkinsonian medication and levodopa equivalent daily dose (LEDD) (17). All participants were assessed after having received their usual anti-parkinsonian medication ("ON" state). Severity of motor symptoms was assessed by the score on the Movement Disorders Society - Unified Parkinson Disease Rating Scale (MDS-UPDRS III) and disease stage by the Hoehn & Yahr score (H&Y) (18).

Based on a numerical ratio derived from the mean tremor score and mean-PIGD score at the MDS-UPDRS III, two subgroups were defined, namely a TD and PIGD subgroup. This classification is based on a previously described method (6), in which the tremor score is determined by assessing 11 items, derived from the MDS-UPDRS (Item 2.10, 3.15a, 3.15b, 3.16a, 3.16b, 3.17a, 3.17b, 3.17c, 3.17d, 3.17e and 3.18). The mean of these items is divided by the mean of the five items that are used to assess the PIGD score

(item 2.12, 2.13, 3.10, 3.11, 3.12). Participants with a ratio ≤ 0.9 were classified as a PIGD subtype, while patients with a ratio ≥ 1.15 were classified as TD subtype. Patients with a ratio between 0.90 and 1.15, were classified as indeterminate. Only PD patients with a PIGD or TD subtype classification were included in the present analysis.

The cognitive assessment battery that was performed in this study was extensively described elsewhere (12). Overall cognitive function was assessed with the Mattis Dementia Rating Scale (Mattis DRS). Additionally, a comprehensive neuropsychological assessment was performed evaluating five cognitive domains: 1) attention and working memory (Digit span forward and backward Symbol Digit Modalities Test), 2) executive functions (Trail Making Test B/A ratio, the interference index and the number of errors in the interference condition of a 50-item version of the Stroop word colour test and a 1-minute phonemic word generation task performed in single and alternating conditions), 3) verbal episodic memory (Hopkins verbal learning test), 4) language (the 15-item short form of the Boston naming test and animal names generation task in 1 minute), 5) visuospatial functions (the short version of the judgment of line orientation test).

2.2 MRI acquisition

Patients were scanned at two sites (Maastricht and Lille) using 3T Philips Achieva MRI scanners with matching software versions and MR sequences. All participants were scanned in medication ON state. 3D T1-weighted images were acquired with a magnetization-prepared gradient echo sequence (voxel size: $1 \times 1 \times 1 \text{ mm}^3$; repetition time (TR): 7.2 ms; echo time (TE): 3.3 ms; matrix size: $176 \times 256 \times 256$ voxels, flip angle: 9°). Resting-state fMRI was performed with a T2*-weighted echo-planar imaging (EPI) sequence lasting 10 minutes (Maastricht: Voxel size: $3 \times 3 \times 3 \text{ mm}^3$; TR: 2400 ms; TE: 30 ms; matrix size: $80 \times 80 \times 40$ voxels; flip angle: 90° / Lille: Voxel size: $3 \times 3 \times 3 \text{ mm}^3$; TR: 2400 ms; TE: 30 ms; matrix size: $64 \times 64 \times 40$ voxels; flip angle: 90°). Patients were instructed to close their eyes, remain quiet and stay awake. All images were visually inspected and incomplete or disturbed brain images, with largely incomplete brain coverage, ghosting or large motion artefacts (defined as $\geq 3 \text{ mm}$ displacement in any of the translation parameters), were excluded.

2.3 MRI pre-processing

After conversion from raw data to nifti format, structural T1-weighted images were pre-processed using Freesurfer v7.1.0 software (<http://surfer.nmr.mgh.harvard.edu/>). This included the processing steps of non-uniform signal correction, signal and spatial normalizations, skull stripping and brain tissues segmentation.

fMRI images were pre-processed with FSL software v6 (fsl.fmrib.ox.ac.uk/fsl). First, the first three image volumes were removed to avoid T1 equilibration effects. Motion was corrected using `mcfliirt` function with the middle volume as the reference volume (19). Furthermore, a noise filter was applied at level 0.66 and with noise AR (auto-correlation) at 0.34, as well as high-pass temporal filtering to reduce nuisance related to respiratory and pulsation processes. After this, slice-timing correction and spatial smoothing with 6 mm full width at half maximum (FWHM) were performed.

fMRI images were registered to the anatomical T1 data by using non-linear and boundary-based registration (BBR) in FSL (20). Both fMRI images and anatomical T1-images were normalised to standard MNI space, with a resampling resolution of 3 mm³.

134 participants had an MRI scan. Based on severe head motion (defined as ≥ 3 mm displacement in any of the translation parameters), 17 datasets were excluded from analysis. In addition, participants were excluded because of an incomplete MRI acquisition (2 participants), poor quality of the anatomical images (5 participants) or ischemic cerebral lesions (5 participants). This resulted in 105 participants for the current study.

2.4 Analysis of resting-state data

Group-level spatial maps, called resting-state networks, were created by performing MELODIC group independent component analysis (ICA). In advance, ICA's were performed for each participant on a single subject level using automatic dimensionality. These typically displayed 50 to 70 components per individual subject. Therefore, the group ICA was performed with a dimensionality of 75. All 75 spatial maps were visually inspected and classified as either displaying resting-state activity or noise components, in accordance with the guidelines for ICA component classification (21). Eventually, 51 components were discarded as noise components (movement artifacts, MRI artifacts, white matter, physiological noise) and 24 were classified as resting-state activity. A dual-regression analysis was performed to derive subject-specific time series for each of these spatial maps (22). First, for each subject, the group-average set of spatial maps was regressed (as spatial regressors in a multiple regression) into the subject's 4D space-time dataset. This resulted in a set of subject-specific timeseries, one per group-level spatial map. Next, those timeseries were regressed (as temporal regressors, again in a multiple regression) into the same 4D dataset, resulting in a set of subject-specific spatial maps, one per group-level spatial map. We then tested for group differences using FSL's randomise permutation-testing tool. Between-group effects were considered significant if they reached two-tailed p-values of < 0.001 (family-wise error (FWE) corrected at the voxel level with Threshold-Free Cluster Enhancement (TFCE) and Bonferroni-corrected for two-sided testing in 24 spatial maps).

The subject-specific time series from each component of interest were used as input for FSLnets v0.6, in order to study inter-network connectivity. FSLnets is a network modelling tool in which the brain is represented as a network consisting of a collection of nodes and edges. The resting-state network components of interest are indicated as nodes, while the connections between these nodes are called edges. A correlation matrix was calculated, demonstrating the correlation strength between all components of interest. Partial correlations (Ridge Regression, $\rho = 0.1$), representing direct connections between different components, were calculated. The resulting correlation r -values were transformed into Z-scores with Fishers's transformation for further analysis. Subsequently, a group-level analysis was performed to assess group differences in inter-network connectivity. For this, FSL-randomize was used with 5000 permutations, in order to FWE (family-wise error) correct for multiple comparisons across all edges. Results were considered significant when demonstrating a FWE-corrected p -value < 0.05 . Outcomes were corrected for demographic characteristics that significantly differed between study centres (years of formal education, PD side of onset and sex). Although LEDD values did not significantly differ between groups, dopaminergic medication is known to influence cerebral network connectivity (23). For this reason, a correction was also applied for the use of dopaminergic medication by adding the LEDD as a co-variate.

2.5 Voxel-based morphometry

In order to investigate voxel-wise differences in grey matter volume the anatomical T1-weighted images were analysed with FSL-VBM, an optimised voxel-based morphometry (VBM) protocol carried out with FSL tools (24). First, structural images were brain-extracted and grey matter-segmented before being registered to the MNI 152 standard space using non-linear registration (25). The resulting images were averaged and flipped along the x -axis to create a left-right symmetric, study-specific grey matter template. Second, all native grey matter images were non-linearly registered to this study-specific template and "modulated" to correct for local expansion (or contraction) due to the non-linear component of the spatial transformation. The modulated grey matter images were then smoothed with an isotropic Gaussian kernel with a sigma of 8 mm. Finally, voxel wise general linear model (GLM) was applied using permutation-based testing, correcting for multiple comparisons across space by threshold-free cluster enhancement at $p < 0.05$.

2.6 Statistical analysis

Demographic variables were analysed using IBM SPSS version 25 (IBM Corp. Released 2017. IBM SPSS Statistics for Windows, Version 25.0. Armonk, NY: IBM Corp). Demographic and disease-related variables were compared with Pearson's chi-squared test for categorical variables (non-parametric test), the Mann-Whitney U Test for ordinal variables and non-normally distributed continuous variables and the student's t -test

for normally distributed continuous variables. The Kolmogorov-Smirnov test was used to assess the normality of the data. An analysis of covariance (ANCOVA) with LEDD and HAM-D (Hamilton depression rating scale) total score as covariates, was performed to compare both groups on cognitive performance. The statistical significance threshold was set to $p < 0.05$.

3. Results

3.1 Demographic, Clinical and Neuropsychological Characteristics

Initially, 105 participants were included in the current analysis. After assessing the motor subtype based on the numerical ratio of the MDS-UPDRS score, 24 participants were classified as indeterminate subtype and were excluded from analysis. Therefore, 81 PD patients were included in the study. This involved 54 PIGD patients and 27 TD patients. Details regarding the demographic and clinical features can be found in Table 1. The Hoehn & Yahr stage of the PIGD subgroup (mean 2.2 ± 0.6) was significantly higher, compared to the TD subgroup (mean 2.0 ± 0.3 , $p = 0.024$). Furthermore, the distribution of PIGD and TD differed significantly between centres, in Lille there were less TD patients than in Maastricht ($p < 0.001$). No significant differences in other demographic variables were found between the two groups. When comparing the TD and PIGD subgroups between the two centres, it appeared that the between-centre difference was largely driven by three variables, namely years of formal education, PD side of onset and sex. However, for the PIGD subgroup there was also a significant difference for the MDS-UPDRS III and Mattis DRS scores (Supplementary data, Table 1 and 2).

Table 1. Demographic and clinical features

n = 81	PIGD	TD	P-value
n (%)	54 (67)	27 (33)	
TD/PIGD ratio	0.3 (0.2)	2.5 (1.4)	
Centre (Lille/Maastricht)	35/19	6/21	<0.001*
Sex (% male)	59.26	77.78	0.099
Age (years)	65.9 (8.1)	63.2 (8.5)	0.178
Handedness (% right)	85.2	85.2	0.368
Formal education (years)	11.7 (3.4)	12.7 (4.0)	0.266
Disease duration (years)	9.7 (6.3)	8.2 (5.9)	0.234
MDS UPDRS III score	26.8 (12.4)	31.6 (10.9)	0.095
Hoehn & Yahr stage	2.2 (0.6)	2.0 (0.3)	0.024*
Side of onset (% right)	50	44	0.969
LEDD (mg/day)	941.4 (422.4)	687.2 (832.6)	0.145
HAM-D	6.7 (5.0)	5.3 (3.4)	0.433

PIGD = postural instability and gait disorder; TD = tremor-dominant; MDS UPDRS III = Movement Disorders Society sponsored revision of the Unified Parkinson's disease Rating Scale-Part III (severity of motor symptoms); LEDD = Levodopa Equivalent Daily Dose, HDRS = Hamilton depression rating scale.

Results are represented as mean (SD), unless otherwise specified.

Cognitive performance was compared between the two groups. No significant difference was found between the PIGD and TD subgroups on the Mattis DRS: total score ($p = 0.155$). However, the PIGD subgroup performed worse on tests related to attention and working memory (Mattis DRS: Attention subscale, $p = 0.033$; WAIS-R backward digit, $p = 0.042$; Symbol digit modalities test, $p = 0.002$; Trail Making Test-A, $p = 0.023$), executive functions (Trail Making Test-B, $p = 0.002$; Stroop: interference index, $p = 0.031$; Stroop: errors, $p = 0.038$), memory (Mattis DRS: Memory subscale, $p = 0.027$), language (Boston naming test, $p = 0.016$) and visuospatial function (Mattis DRS: Construction subscale, $p = 0.013$). None of the assessed cognitive domains displayed higher scores in the PIGD subgroup compared to the TD subgroup. Details regarding the neuropsychological assessment can be found in Table 2.

Table 2. Neuropsychological characteristics

N = 81	PIGD (n = 54)	TD (n = 27)	P-value
Overall cognition			
Mattis DRS: Total score (1-144)	135.9 (6.2)	138.1 (6.8)	0.155
- Attention subscale (1-37)	35.6 (1.4)	36.3 (1.0)	0.033*
- Initiation/perseveration subscale (1-37)	34.5 (2.7)	35.3 (2.8)	0.349
- Construction subscale (1-6)	5.81 (0.4)	6.00 (0.0)	0.013*
- Conceptualization subscale (1-39)	37.6 (1.9)	36.9 (2.9)	0.324
- Memory subscale (1-25)	22.4 (2.6)	23.6 (2.0)	0.027*
Attention and working memory			
WAIS-R forward digit (0-14)	7.3 (2.5)	8.1 (2.3)	0.197
WAIS-R backward digit (0-14)	5.2 (1.9)	6.2 (1.8)	0.042*
SDMT: Number in 90sec	36.5 (12.0)	46.8 (11.3)	0.002*
Trail Making Test – A (sec)	58.6 (29.9)	42.7 (16.8)	0.023*
Executive functions			
Trail Making Test – B (sec)	157.8 (71.7)	102.4 (57.3)	0.002*
Stroop: interference index	2.0 (0.7)	1.7 (0.4)	0.031*
Stroop: errors	5.8 (10.0)	1.7 (3.0)	0.038*
Phonemic fluency (60 sec)	12.7 (4.5)	13.6 (5.7)	0.539
Alternating fluency (60 sec)	10.2 (4.8)	12.6 (5.5)	0.053
Memory			
HVLT Learn1 (/12)	6.0 (2.0)	6.6 (2.1)	0.308
HVLT Learn total (/36)	24.4 (4.6)	26.3 (5.3)	0.135
HVLT number of intrusions (/36)	1.8 (2.3)	0.9 (1.5)	0.107
HVLT delayed recall (/12)	8.8 (2.3)	8.8 (3.0)	0.728
HVLT recognition hits (/12)	11.3 (1.0)	11.2 (1.2)	0.957
Language			
Boston naming test (/15)	11.8 (2.7)	13.3 (1.7)	0.016*
Semantic fluency (animals in 60 sec)	17.7 (6.6)	20.7 (6.1)	0.086
Visuospatial functions			
Judgement of line orientation	10.7 (3.2)	12.2 (2.1)	0.084

MMSE = Mini-mental state examination; Mattis DRS = Mattis Dementia rating scale; WAIS-R = Wechsler for adults intelligence scale revised; SDMT = Symbol digit modalities test; HVLT = Hopkins verbal learning test.

Results are represented as mean (SD).

3.2 Resting-state fMRI dual regression analysis

For details regarding the selected independent components see Figure 1 (and Supplementary data, Table 3). The dual regression analysis showed a significant difference between the two motor subtypes for several independent components (p -value < 0.05). These independent components were located in the occipital pole (IC 1), intracalcarine cortex/lingual gyrus (IC 2), angular gyrus/supramarginal gyrus (IC 10), precentral gyrus (IC 11), precentral gyrus/postcentral gyrus (IC 13), middle temporal gyrus/angular gyrus (21) and inferior frontal gyrus (23). However, after correction for

multiple comparisons (p -value < 0.001), none of the results remained significant when comparing the TD and PIGD subgroups (Supplementary data, Table 3).



Figure 1. Spatial maps of the 24 resting-state components of interest obtained from the group independent component analysis (ICA). Spatial maps are thresholded at $3 < z < 15$. Images are shown in radiological convention (right side of the image corresponds to the left hemisphere).

3.3 Network analysis

Following the dual regression analysis, network analysis was performed with FSLnets. A network hierarchy of the 24 selected independent components, clustered based on their covariance structure, was created (Supplementary data, figure 1). Furthermore, a clustering method was used to group the independent components together based on these correlations. This network hierarchy confirms that components of the major larger resting-state brain networks were involved in our analysis.

When comparing the PIGD and TD subgroups, a significant higher functional connectivity was found between the lateral occipital cortex (IC 5) and the pre- and post-central gyrus (IC 13) in the PIGD group, compared to the TD group ($p = 0.034$). Since differences between study centre were mainly driven by three variables (years of formal education, PD side of onset and sex), the analysis was repeated including these variables as co-variates. With the inclusion of these co-variates, again the edge between the lateral occipital cortex and the pre- and post-central gyrus showed a significant difference (PIGD > TD, $p = 0.033$). However, after the introduction of LEDD as a covariate this result did not remain significant ($p = 0.068$).

3.4 Voxel-based morphometry analysis

The VBM analysis, performed both with and without the co-variates described above (LEDD, years of formal education, PD side of onset and sex), did not reveal any cortical brain areas with a significant difference in local grey matter volume between PIGD and TD patients (corrected p -value > 0.05).

4. Discussion

This is the first study performing a whole-brain, inter-network, resting-state fMRI analysis of PD motor subtypes. The main aim of this study was to investigate if PD patients with a PIGD subtype show different functional network characteristics compared to the TD subtype. A significantly higher connectivity was found between the lateral occipital cortex and the pre- and post-central gyrus in PIGD patients compared to the TD subgroup. However, after the correction for dopaminergic medication use, this result was not significant anymore. Moreover, no significant differences in grey matter volume between the two motor subgroups are found.

In addition, cognitive performance was compared between PIGD and TD patients. Our results show that PIGD patients did perform worse in nearly all cognitive domains, especially on tests for attention, working memory and executive function. These findings correspond with the results of several earlier studies, that showed that

cognitive dysfunction is more pronounced in PIGD patients compared to TD patients (7). Moreover, it has been shown earlier that lower cognitive scores predict fall risk after five years, suggesting that cognitive decline itself may among other things lead to the gait deficits in the PIGD subgroup (26).

However, with this study we were unable to confirm our initial hypothesis that the PIGD and TD subtypes would be characterized by changes in different network configurations which in turn could also explain cognitive differences between the subtypes. It has been suggested that different motor subtypes of PD may be characterized by alterations in subcortical grey matter nuclei rather than by differences in large brain networks (27). Furthermore, pathological studies suggest a different degeneration pattern of the substantia nigra and locus coeruleus in TD patients compared to PIGD patients (28). Future studies, using more sensitive ultra-high field MRI, may prove to be more efficacious in visualising these subcortical structures and could help to elucidate the underlying pathophysiology of PD motor subtypes.

These negative findings are in contrast with results from earlier studies that report a variety of alterations in cerebral connectivity between a wide number of brain areas, as recently reviewed by Boonstra et al. (29). Although several resting state fMRI studies have focused on differences on functional connectivity between motor subtypes, the results of these studies vary widely, are incomparable and do not allow for an overall conclusion with regard to specific changes in connectivity per subgroup. The substantial variability of these results may be partially explained by the relatively small number of participants in these studies. Study samples typically vary between 10 and 40 PD patients (29). Such small studies are more likely to produce less robust results compared to large samples, due to a high sampling variability, and tend to have an increased probability of reporting false positive results (30). In addition, these studies are not well comparable due to different definitions of subtypes. Whereas all studies define a TD subgroup, the definition of non-TD groups varies, with some studies defining a PIGD subgroup, an akinetic-rigid (AR) group, or both; other studies defined a 'mixed group' or simply group all non-TD patients together. The difficulties in defining PD subtypes were recently the focus of a Movement Disorder Society (MDS) task force that concluded that subtyping has substantial methodological shortcomings and questionable clinical applicability (4). Moreover, since PD is a heterogeneous disorder, involving a wide range of both motor and non-motor symptoms, subtyping based solely on motor symptoms is probably too simplistic. However, new classification methods have not yet been developed and validated. At present, the subtyping of patients into a TD, indeterminate and PIGD subtype is most commonly used (5, 6). It has also been shown that the TD, mixed and PIGD subtyping is more sensitive for the identification of non-motor abnormalities than the TD, mixed and AR classification (31). We therefore believe that, while awaiting

new classification methods, it is acceptable to use the PIGD and TD motor subtyping classification. The application of the same criteria by different studies, also ensures the possibility to compare results among different reports.

In this study patients were assessed after having received their usual antiparkinsonian medication ('ON' state). Previous studies have already demonstrated that dopaminergic medication influences brain connectivity patterns both in a linear and non-linear way, with a tendency to normalize abnormal brain connectivity (23). Therefore, the results of the current analysis were corrected for LEDD. However, some earlier studies did not include LEDD as a covariate (32). Other studies try to evade this problem by scanning patients in an 'OFF' medication state (33). Whereas this rules out the direct confounding effect of levodopa use, it also introduces new problems, since secondary alterations in dopaminergic transmission, such as receptor up- and downregulation take a longer time to restore and may still confound outcomes by exaggerating alterations in connectivity (34). Due to these pharmacological effects, different study methods with regard to medication use might partially explain the variability in results between studies. The impact of dopaminergic medication was clearly illustrated by our analyses. Even though LEDD did not significantly differ between the two subgroups, significant between-group findings disappeared after correction for LEDD. Therefore, in order to reproduce reliable results, fMRI studies in PD patients 'ON' medication should always be corrected for LEDD.

Given the number of patients included and the correction for a number of covariates, we think these negative results are valid. They show that network analyses in PD is more complex than anticipated and that research into changes in network connectivity in PD probably requires more advanced statistical methods, such as machine learning techniques, in much larger datasets⁴.

This study has strengths and limitations. A strength is the fact that this is the largest study so far comparing differences in functional connectivity between motor subtypes in PD. Another strength is that patients were comprehensively assessed with measures on motor symptoms and cognitive performance. Also, the statistical approach was corrected for multiple comparisons, for between group differences and for LEDD. A limitation is the fact that this study was not initially designed to compare motor subtypes. The relative proportion of these subtypes also varied between the two centres, which we could not explain. We corrected for differences between centres and, given the negative outcome of this study, do not believe the results were affected by this. Another limitation is the difficulty in defining subtypes, as mentioned before. In this study we focussed on the TD and PIGD motor subtypes of PD, aware of potential criticism to this division. Finally, although the MRI protocols performed at the two different locations

were matched and the same type of 3T MRI scanner was used (Philips Achieva), minor differences in MRI output cannot be ruled out.

In conclusion, although the PIGD and TD PD subgroups clearly differ in terms of motor and cognitive performance, we were not able to demonstrate any between group differences in functional network connectivity. The resting-state fMRI network analyses suggested that the connection between the visual and sensorimotor network might differentiate between PIGD and TD subgroups. However, these results did not remain significant after correcting for LEDD. Methodological challenges, substantial individual-level symptom heterogeneity and the many involved variables and confounders make analyses and hypothesis building with respect to PD subtypes highly complex. More sensitive visualisation methods, such as ultra-high field MRI in combination with machine learning approaches that are able to handle much more variables in much larger datasets may be more efficacious in the search for clinically reliable subtypes of PD.

5. References

1. Bloem BR, Okun MS, Klein C. Parkinson's disease. *Lancet*. 2021;397(10291):2284-303.
2. Berg D, Postuma RB, Bloem B, Chan P, Dubois B, Gasser T, et al. Time to redefine PD? Introductory statement of the MDS Task Force on the definition of Parkinson's disease. *Mov Disord*. 2014;29(4):454-62.
3. Sieber BA, Landis S, Koroshetz W, Bateman R, Siderowf A, Galpern WR, et al. Prioritized research recommendations from the National Institute of Neurological Disorders and Stroke Parkinson's Disease 2014 conference. *Ann Neurol*. 2014;76(4):469-72.
4. Mestre TA, Fereshtehnejad SM, Berg D, Bohnen NI, Dujardin K, Erro R, et al. Parkinson's Disease Subtypes: Critical Appraisal and Recommendations. *J Parkinsons Dis*. 2021;11(2):395-404.
5. Jankovic J, McDermott M, Carter J, Gauthier S, Goetz C, Golbe L, et al. Variable expression of Parkinson's disease: a base-line analysis of the DATATOP cohort. The Parkinson Study Group. *Neurology*. 1990;40(10):1529-34.
6. Stebbins GT, Goetz CG, Burn DJ, Jankovic J, Khoo TK, Tilley BC. How to identify tremor dominant and postural instability/gait difficulty groups with the movement disorder society unified Parkinson's disease rating scale: comparison with the unified Parkinson's disease rating scale. *Mov Disord*. 2013;28(5):668-70.
7. Thenganatt MA, Jankovic J. Parkinson disease subtypes. *JAMA Neurol*. 2014;71(4):499-504.
8. Hu X, Jiang Y, Jiang X, Zhang J, Liang M, Li J, et al. Altered Functional Connectivity Density in Subtypes of Parkinson's Disease. *Front Hum Neurosci*. 2017;11:458.
9. Zhu J, Zeng Q, Shi Q, Li J, Dong S, Lai C, et al. Altered Brain Functional Network in Subtypes of Parkinson's Disease: A Dynamic Perspective. *Front Aging Neurosci*. 2021;13:710735.
10. Karunanayaka PR, Lee EY, Lewis MM, Sen S, Eslinger PJ, Yang QX, et al. Default mode network differences between rigidity- and tremor-predominant Parkinson's disease. *Cortex*. 2016;81:239-50.
11. Filippi M, Sarasso E, Agosta F. Resting-state Functional MRI in Parkinsonian Syndromes. *Mov Disord Clin Pract*. 2019;6(2):104-17.
12. Dujardin K, Moonen AJ, Behal H, Defebvre L, Duhamel A, Duits AA, et al. Cognitive disorders in Parkinson's disease: Confirmation of a spectrum of severity. *Parkinsonism Relat Disord*. 2015;21(11):1299-305.
13. Lopes R, Delmaire C, Defebvre L, Moonen AJ, Duits AA, Hofman P, et al. Cognitive phenotypes in parkinson's disease differ in terms of brain-network organization and connectivity. *Hum Brain Mapp*. 2017;38(3):1604-21.
14. Hughes AJ, Daniel SE, Kilford L, Lees AJ. Accuracy of clinical diagnosis of idiopathic Parkinson's disease: a clinico-pathological study of 100 cases. *J Neurol Neurosurg Psychiatry*. 1992;55(3):181-4.
15. Morris JC. The Clinical Dementia Rating (CDR): current version and scoring rules. *Neurology*. 1993;43(11):2412-4.
16. Emre M, Aarsland D, Brown R, Burn DJ, Duyckaerts C, Mizuno Y, et al. Clinical diagnostic criteria for dementia associated with Parkinson's disease. *Mov Disord*. 2007;22(12):1689-707; quiz 837.
17. Tomlinson CL, Stowe R, Patel S, Rick C, Gray R, Clarke CE. Systematic review of levodopa dose equivalency reporting in Parkinson's disease. *Mov Disord*. 2010;25(15):2649-53.
18. Goetz CG, Tilley BC, Shaftman SR, Stebbins GT, Fahn S, Martinez-Martin P, et al. Movement Disorder Society-sponsored revision of the Unified Parkinson's Disease Rating Scale (MDS-

- UPDRS): scale presentation and clinimetric testing results. *Mov Disord.* 2008;23(15):2129-70.
19. Jenkinson M, Bannister P, Brady M, Smith S. Improved optimization for the robust and accurate linear registration and motion correction of brain images. *Neuroimage.* 2002;17(2):825-41.
 20. Greve DN, Fischl B. Accurate and robust brain image alignment using boundary-based registration. *Neuroimage.* 2009;48(1):63-72.
 21. Griffanti L, Douaud G, Bijsterbosch J, Evangelisti S, Alfaro-Almagro F, Glasser MF, et al. Hand classification of fMRI ICA noise components. *Neuroimage.* 2017;154:188-205.
 22. Nickerson LD, Smith SM, Öngür D, Beckmann CF. Using Dual Regression to Investigate Network Shape and Amplitude in Functional Connectivity Analyses. *Frontiers in neuroscience.* 2017;11:115.
 23. Cole DM, Beckmann CF, Oei NY, Both S, van Gerven JM, Rombouts SA. Differential and distributed effects of dopamine neuromodulations on resting-state network connectivity. *Neuroimage.* 2013;78:59-67.
 24. Smith SM, Jenkinson M, Woolrich MW, Beckmann CF, Behrens TE, Johansen-Berg H, et al. Advances in functional and structural MR image analysis and implementation as FSL. *Neuroimage.* 2004;23 Suppl 1:S208-19.
 25. Andersson JL, Jenkinson M, Smith S. Non-linear registration, aka Spatial normalisation FMRIB technical report TR07JA2. FMRIB Analysis Group of the University of Oxford. 2007;2(1):e21.
 26. Mirelman A, Herman T, Brozgal M, Dorfman M, Sprecher E, Schweiger A, et al. Executive function and falls in older adults: new findings from a five-year prospective study link fall risk to cognition. *PLoS One.* 2012;7(6):e40297.
 27. Sun D, Wu X, Xia Y, Wu F, Geng Y, Zhong W, et al. Differentiating Parkinson's disease motor subtypes: A radiomics analysis based on deep gray nuclear lesion and white matter. *Neurosci Lett.* 2021;760:136083.
 28. Paulus W, Jellinger K. The neuropathologic basis of different clinical subgroups of Parkinson's disease. *J Neuropathol Exp Neurol.* 1991;50(6):743-55.
 29. Boonstra JT, Michielse S, Temel Y, Hoogland G, Jahanshahi A. Neuroimaging Detectable Differences between Parkinson's Disease Motor Subtypes: A Systematic Review. *Mov Disord Clin Pract.* 2021;8(2):175-92.
 30. Szucs D, Ioannidis JP. Sample size evolution in neuroimaging research: An evaluation of highly-cited studies (1990-2012) and of latest practices (2017-2018) in high-impact journals. *Neuroimage.* 2020;221:117164.
 31. Choi SM, Kim BC, Cho BH, Kang KW, Choi KH, Kim JT, et al. Comparison of two motor subtype classifications in de novo Parkinson's disease. *Parkinsonism Relat Disord.* 2018;54:74-8.
 32. Shen B, Pan Y, Jiang X, Wu Z, Zhu J, Dong J, et al. Altered putamen and cerebellum connectivity among different subtypes of Parkinson's disease. *CNS Neurosci Ther.* 2020;26(2):207-14.
 33. Wang Z, Chen H, Ma H, Ma L, Wu T, Feng T. Resting-state functional connectivity of subthalamic nucleus in different Parkinson's disease phenotypes. *J Neurol Sci.* 2016;371:137-47.
 34. Politis M, Wilson H, Wu K, Brooks DJ, Piccini P. Chronic exposure to dopamine agonists affects the integrity of striatal D2 receptors in Parkinson's patients. *Neuroimage Clin.* 2017;16:455-60.

Supplementary data

Table 1. Demographic and clinical features (PIGD)

N = 54	Lille	Maastricht	P-value
N (%)	35 (64.81)	19 (35.19)	
Sex (% male)	48.57	78.95	0.030*
Age (y)	64.86 (8.35)	67.78 (7.50)	0.150
Handedness (% right)	85.71	84.21	0.372
Formal education (y)	10.26 (2.77)	14.21 (3.87)	0.000*
Disease duration (y)	9.26 (4.47)	10.37 (8.75)	0.828
MDS UPDRS III score	22.51 (11.68)	34.68 (9.76)	0.000*
Hoehn & Yahr stage	2.24 (0.40)	2.24 (0.52)	0.813
Side of onset (% right)	62.86	26.32	0.002*
LEDD (mg/day)	1015.79 (433.57)	804.29 (373.88)	0.079
MATTIS DRS	134.51 (5.98)	138.32 (6.13)	0.016*

PIGD = postural instability and gait disorder; MDS UPDRS III = Movement Disorders Society sponsored revision of the Unified Parkinson's disease Rating Scale-Part III (severity of motor symptoms); LEDD = Levodopa Equivalent Daily Dose; Mattis DRS = Mattis dementia rating scale.

Results are represented as mean (SD), unless otherwise specified.

Table 2. Demographic and clinical features (TD)

N = 27	Lille	Maastricht	P-value
N (%)	6 (22.22)	21 (77.78)	
Sex (% male)	83.33	76.19	0.711
Age (y)	64.63 (5.71)	62.85 (9.22)	0.660
Handedness (% right)	100.00	80.95	0.511
Formal education (y)	9.50 (1.98)	13.60 (4.06)	0.022*
Disease duration (y)	6.67 (4.59)	8.62 (6.31)	0.489
MDS UPDRS III score	33.17 (9.91)	31.10 (11.40)	0.408
Hoehn & Yahr stage	2.00 (0.85)	2.00 (0.50)	1.00
Side of onset (% right)	50.00	42.86	0.810
LEDD (mg/day)	824.13 (971.53)	648.09 (811.16)	0.887
MATTIS DRS	139.17 (3.37)	137.81 (7.52)	0.932

TD = tremor-dominant; MDS UPDRS III = Movement Disorders Society sponsored revision of the Unified Parkinson's disease Rating Scale-Part III (severity of motor symptoms); LEDD = Levodopa Equivalent Daily Dose; Mattis DRS = Mattis dementia rating scale.

Results are represented as mean (SD), unless otherwise specified.

Table 3. Independent components

IC	N voxels	MNI (X,Y,X)			Location
1*	1950	-18	-99	-3	Left occipital pole
2*	2683	6	-75	9	Right intracalcarine cortex; lingual gyrus
3	2524	3	-54	24	Right precuneous cortex; cingulate gyrus, posterior division
4	2366	54	6	15	Right precentral gyrus; Inferior frontal gyrus, pars opercularis
5	2717	33	-81	12	Right lateral occipital cortex
6	1420	6	-60	51	Right precuneous cortex
7	731	-21	-3	-36	Left parahippocampal gyrus, anterior division
8	2229	63	-30	33	Right supramarginal gyrus; Parietal operculum cortex
9	1268	18	-93	30	Right occipital pole
10*	1299	54	-51	48	Right angular gyrus; Supramarginal gyrus posterior division
11*	1767	6	-24	66	Right precentral gyrus
12	817	-39	-12	-33	Left temporal fusiform cortex; Inferior temporal gyrus
13*	1759	-54	-6	27	Left precentral gyrus; Postcentral gyrus
14	1742	12	36	-12	Right frontal medial cortex
15	1917	-27	21	60	Left superior frontal gyrus, Middle frontal gyrus
16	1433	42	-27	45	Right postcentral gyrus; Supramarginal gyrus
17	912	45	48	-12	Right frontal pole
18	626	12	18	-18	Right frontal orbital cortex; Subcallosal cortex
19	1096	12	33	57	Right superior frontal gyrus
20	735	-3	66	-12	Left frontal pole
21*	2557	54	-54	9	Right middle temporal gyrus, temporooccipital part; Angular gyrus
22	1219	27	6	-3	Right putamen
23*	1869	57	24	9	Right inferior frontal gyrus
24	1844	51	-3	33	Right precentral gyrus

*Independent components for which the dual regression analysis initially showed a significant difference between the two groups ($PIGD > TD$, p -value <0.05). After correction for multiple comparisons (p -value <0.001), none of the significant results remained. Peak coordinates (x,y,z) of the independent components are given in MNI (Montreal Neurological Institute standard) space.

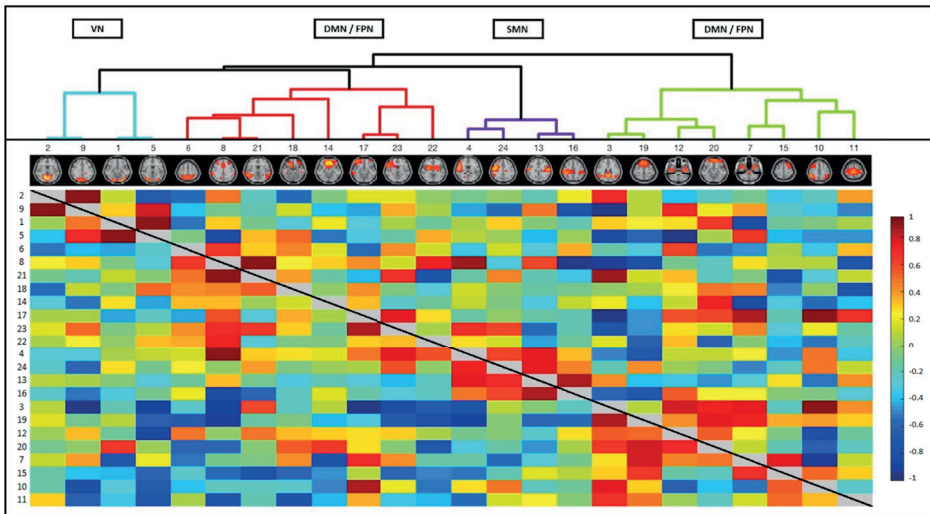


Figure 1. Correlation matrix of the 24 selected independent components for the whole group of participants. Each row or column represents a set of correlations between one specific independent component and all other components. Hot colours indicate a strong correlation, while cool colours indicate a weak correlation. Both full (lower triangle) and partial correlations (upper triangle) are displayed. The matrix of these components was arranged and clustered based on their covariance structure. VN = Visual network; DMN = Default mode network; FPN = Fronto-parietal network; SMN = Sensorimotor network.

CHAPTER 4



Grey matter abnormalities are associated only with severe cognitive decline in early stages of Parkinson's disease

Wolters AF, Moonen AJH, Lopes R, Leentjens AFG, Duits AA, Defebvre L, Delmaire C, Hofman PA, van Bussel FC, Dujardin K

Abstract

Cognitive impairment is common in Parkinson's disease (PD), yet with large heterogeneity in the range and course of deficits. In a cross-sectional study, 124 PD patients underwent extensive clinical and neuropsychological assessment as well as a 3T MRI scan of the brain. Our aim was to identify differences in grey matter volume and thickness, as well as cortical folding, across different cognitive profiles as defined through a data-driven exploratory cluster analysis of neuropsychological data. The identified cognitive groups ranged from cognitively intact patients to patients with severe deficits in all cognitive domains, whilst showing comparable levels of motor disability and disease duration. Each group was compared to the cognitively intact PD group using voxel- and vertex-based morphometry. Results revealed widespread age-related grey matter abnormalities associated with progressive worsening of cognitive functions in mild PD. When adjusted for age, significant differences were only seen between cognitively intact and severely affected PD patients and restricted to the right posterior cingulate and the right precuneus. Reduced cortical thickness occurs in the right inferior temporal gyrus and reduced folding in the right temporal region. As these differences were not associated with age, we assume that they are associated with underlying pathology of the cognitive decline. Given the limited involvement of grey matter differences, and the absence of differences in vascular changes across the groups, we hypothesize a more important role for white matter tract changes in cognitive decline in PD.

1. Introduction

Cognitive deficits are common in Parkinson's disease (PD) and are increasingly recognized as an integral part of the disease. Up to 40% of PD patients report mild cognitive deficits already at the time of diagnosis (1). Approximately 30% of patients convert to dementia during the course of the disease (2), which increases up to 80% within 20 years after diagnosis (3, 4). Yet, a substantial number of PD patients does not show any significant cognitive deficit, even years after being diagnosed (5, 6, 7). Recent studies support the large heterogeneity in the range of cognitive deficits in PD, and several studies have attempted to identify distinctive cognitive profiles (8). However, many studies investigated cognitive dysfunction using the diagnostic categories as defined by the Movement Disorders Society (MDS) criteria published by Litvan and colleagues (9). These include PD patients without cognitive impairment, patients with mild cognitive impairment (MCI), and patients with Parkinson's disease dementia (PDD). This approach does not allow the study of milder stages of cognitive decline, including cognitive deficits that do not reach the level for a diagnosis of MCI. In addition, although recent neuroimaging studies showed clear evidence for widespread cortical atrophy associated with MCI in PD and PD dementia (7, 10, 11, 12), using a classification approach may not only have masked neuroanatomical changes associated with more subtle cognitive deficits, but also obscure differences in possible sub-phenotypes that may correspond to different comorbid pathologies in more advanced stages of cognitive decline. This may be important, especially since a substantial number of PD patients appear to have neuropathological changes related to Alzheimer's disease in addition to diffuse Lewy body pathology (13, 14, 15).

In a prior study (16), we conducted a data-driven exploratory cluster analysis using retrospective neuropsychological test data from a large sample ($n=557$) of PD patients. We identified five cognitive phenotypes, that were replicated and confirmed in a more recent study by performing a model-based confirmatory cluster analysis on prospective neuropsychological data from an independent sample of mild PD patients ($n=156$) (17). The five phenotypes represent different stages of cognitive decline ranging from cognitively intact patients to patients with severe dysfunction in all cognitive domains. In the present study, we aimed at identifying the neuroanatomical correlates of each of the identified cognitive phenotypes using structural MRI. More specifically, we were looking for regional differences in the rate of grey matter volume, cortical thickness, and cortical folding between the different groups. Considering the heterogeneity of the clinical presentation and course of cognitive deficits in PD, we expect that different patterns of cerebral changes may underlie these different phenotypes. Detection of differences in grey matter may therefore increase our understanding of the underlying neurobiological changes that accompany the spectrum of cognitive disorders in PD.

Moreover, if we find alterations in patients with only slight cognitive deficits, this exploratory approach could reveal a group at risk of further cognitive decline, who may be considered for early treatment options. Thirdly, studying grey matter alterations in PD may shed light on possible sub-phenotypes in more advanced stages of cognitive decline other than PD dementia, such as phenotypes with comorbid pathologies, such as Alzheimer's disease (AD).

We hypothesized that all groups would show a decline in grey matter volume, thickness and cortical folding compared with the cognitively intact group, with a progressive severity gradient. We further hypothesized to see profound hippocampal or medial temporal lobe grey matter deviations in those patients with more profound memory deficits, possibly reflecting a sub-phenotype of PD patients with comorbid AD pathology. We followed an explorative whole brain approach, with post hoc region-of-interest analyses.

2. Materials and methods

In this section we report how we determined our sample size, all data exclusions, all inclusion/exclusion criteria, whether inclusion/exclusion criteria were established prior to data analysis, all manipulations, and all measures used in the study. The study was performed accordance with the Declaration of Helsinki, and was approved by the local institutional review boards (METC azM/UM, NL42701.068.12; CPP Nord-Ouest IV, 2012-A 01317-36) and registered in a clinical trial register (ClinicalTrials.gov Identifier: NCT01792843; <https://clinicaltrials.gov/ct2/show/NCT01792843?term=NCT01792843&rank=1>). Legal and ethical restrictions prevent us from archiving our data in a public repository. The study data were pseudonymised and cannot be fully anonymised. In order to comply with the EU General Data Protection Regulation, the transfer of clinical data to an external research team would require the performance of regulatory proceedings by the principal investigator's institution. A new informed consent form would have to be signed (especially for requests outside the European Economic Area) and a new submission to the competent ethics committee would be necessary in order to authorise such a transfer. Data access requests should be directed to the corresponding author. Data will be released for research purposes subject to the completion of a data transfer agreement between our institution and the research institution requesting the data. This agreement will include the description of the requested variables, the purpose of the research, and the duties of both entities under personal data protection regulations

2.1 Participants

One hundred fifty-six patients with idiopathic PD participated in this study (17). Patients were recruited from two independent European movement disorders clinics in Maastricht, the Netherlands (n=75) and Lille, France (n=81). The diagnosis of idiopathic

PD was established by means of the United Kingdom Brain Bank diagnostic criteria for PD (18). Patients with moderate and severe dementia (defined as a score >1 at the Clinical Dementia Rating (19) scale and following the MDS criteria (20), patients older than 80 years and patients with neurodegenerative disorders other than PD were excluded from the study. Patients treated with deep brain stimulation or those meeting contra-indications for MRI were excluded likewise. All patients were using stable doses of antiparkinson medication for at least 2 months and were tested in their “on” state. All patients gave informed consent prior to participation in the study.

2.2 Clinical assessment

All patients underwent a thorough neuropsychiatric examination (see also (17)) consisting of the MDS - Unified Parkinson’s disease Rating Scale (MDS-UPDRS, sections I-IV) (21) to measure severity and experiences of non-motor and motor symptoms, the Hoehn and Yahr staging scale to measure disease stage (Hoehn & Yahr score), the 17-item Hamilton Depression Rating Scale (HAMD) (22) to assess depressive symptoms, the Parkinson Anxiety Scale (PAS) (23) to measure anxiety symptoms, the Lille Apathy Rating Scale (LARS) (24) to measure levels of apathy, and the Lawton Instrumental Activities of Daily Living (IADL) (25) to score activities of daily living. In addition, we checked for the presence of several medical conditions such as high blood pressure, hypercholesterolemia, diabetes, history of myocardial infarction, history of lower limb arteriopathy, cerebrovascular disease, sleep apnea, and symptoms of Rapid Eye Movement (REM) sleep behavior disorders. Antiparkinson medication was checked and doses were converted to levodopa equivalent daily dose (LEDD) according to the algorithm by Tomlinson and colleagues (26).

2.3 Neuropsychological assessment

All patients also underwent an extensive neuropsychological test battery (see also (17)) measuring global cognition with the Mini Mental State Examination (MMSE) (27) and the Mattis dementia rating scale (MDRS) (28) as well as specific neuropsychological tests for multiple cognitive domains. Attention and working memory were assessed with the Digit span forward and backward and the Symbol Digit Modalities Test (SDMT) (29). Executive functioning was measured with the Trial Making Test (TMT, B/A ratio) (30), the interference index of the Stroop word color test, and the word generation task (i.e., single and alternating phonemic conditions). Verbal episodic memory was measured by means of the Hopkins Verbal Learning Test (HVLT) (31, 32). We used the Boston Naming test (33) and a categorical word generation task (i.e., animals) to assess language, and the short version of the Benton Judgment Line Orientation test (BJLO) (34) to measure visuospatial functioning.

2.4 Cognitive clusters

Model-based confirmatory cluster analysis based on the neuropsychological test scores from all 156 patients revealed the following five-cluster model that was statistically superior and clinically the most relevant (see (17) for a detailed description of the statistical procedure): 1) Cognitively intact patients with (above) average performance in all cognitive domains (25.6% of the total group), 2) Cognitively intact patients with slight mental slowing and mild deficit in verbal fluency (i.e., SDMT and Semantic Fluency for animals) (26.9%), 3) Patients showing mild cognitive deficits in attention, working memory, executive functioning, language and visuospatial functioning, as well as slight deficits in episodic verbal memory with intact recognition (37.2%), 4) Patients with impaired overall cognitive efficiency and severe deficits in all cognitive domains, particularly executive functioning (3.2%), and 5) Patients with impaired overall cognitive efficiency and severe deficits in all cognitive domains, particularly working memory and recall in verbal episodic memory (7.1%). However, due to the small number of patients in cluster 4 and 5, these groups were collapsed and considered as one cluster for further imaging analyses. Because the remaining four groups were not completely identical to the original clusters, we will use the term 'cognitive profile' rather than 'cluster'. The new groups, however, did not systematically differ from the original groups with respect to demographic, clinical and neuropsychological data.

2.5 MRI Data Acquisition and Analysis

Patients were scanned at two sites (Maastricht and Lille) using the same 3T whole-body scanner (Achieva TX, Philips Healthcare, Best, the Netherlands) with identical software versions, MR sequences and an eight-channel SENSE head coil. High-resolution 3-dimensional T1-weighted images were acquired in the sagittal plane (TR/TE/TI 7.2/3.3/900ms, 256 x 256 matrix, FOV 256 x 240 mm², 1.0mm³ isotropic voxel size after reconstruction), yielding 176 contiguous slices through the head.

2.6 Optimized Voxel-Based Morphometry

Images were processed using the voxel-based morphometry (VBM) toolbox version 8 (VBM8; <http://dbm.neuro.uni-jena.de/vbm/>) within SPM8 (Wellcome Trust Centre for Neuroimaging, London, UK; <http://fil.ion.ucl.ac.uk/spm/software/spm8/>) in MATLAB 7.14 (Math-works Inc., Natick, MA, USA). Default settings were used unless otherwise specified. Prior to image analyses, all images were screened for artifacts and large anatomical abnormalities, such as ischemic strokes. Subjects displaying ischemic strokes or significant artifacts were excluded from our analysis. The Fazekas scale was applied to quantify the amount of white matter lesions related to chronic small vessel ischemia, on the MRI images (36). Afterwards, images were and manually re-orientated in SPM8, such that they were centered on the anterior commissure. For spatial normalization, we applied the high-dimensional Dartzel normalization approach (VBM-Dartzel; (37)).

The next step involved modulated normalization followed by segmentation of images into grey matter, white matter and cerebrospinal fluid, in order to obtain regional grey matter values and account for individual differences in global brain size. After checking the homogeneity of the sample, the normalized modulated images were smoothed with a standard Gaussian kernel of 8 mm, full width at half maximum (FWHM).

2.7 Vertex-based morphometry

Structural T1 images were processed using the Freesurfer software version 5.3 (<http://surfer.nmr.mgh.harvard.edu/>, version 5.3). This included the preprocessing steps of non-uniform signal correction, signal and spatial normalizations, skull stripping and brain tissue segmentation (38). Triangulated surface models of the inner and outer cortical surfaces were obtained for each patient. Surface reconstruction was reviewed by an expert and corrected with minor manual intervention when appropriate. After inflation and parameterization, cortical surface models were registered to a common surface template (Freesurfer's fsaverage) using a multiscale non-rigid spherical registration procedure minimizing folding pattern differences across individuals (39).

The cortical thickness was obtained by reconstructing representations of inner and outer surfaces and then calculating the distance between those surfaces using the t-link method, defined as the Euclidean distance between linked vertices on inner and outer surfaces (40, 41). Cortical thickness maps were finally smoothed with a 20-mm FWHM Gaussian surface kernel.

The local gyrification index was measured on each vertex from the outer cortical surface. This index is a measurement of the degree of cortical folding that quantifies the amount of cortex buried within the sulcal folds in the surrounding circular region. A 3D approach was used to take into account the 3D nature of the cortical folds and with the ability to localize abnormalities in cortical folding. The local gyrification index ratio between the outer surface and outer hull at the centre of a 20-mm spherical region was computed to each vertex (42).

2.8 Statistical analysis

The smoothed, modulated, normalized grey matter VBM data were analyzed in SPM8. T-tests were conducted to identify differences in whole brain grey matter volume between the patient groups. An absolute threshold of 0.1 was used, by which only voxels with grey matter values >0.1 were counted. Correction for global volume change was not necessary, since we already applied this correction directly to the data as part of the (non-linear) modulation step (recommended by the VBM8 manual). We ran the analysis twice, once with center, gender and education entered as covariates into the

design matrix and once including age as an additional covariate to investigate age related effects on grey matter volume differences.

An exploratory whole brain analysis was performed with a threshold for statistical significance of $P < 0.001$ without correction for multiple comparisons. Clusters were considered significant using the family-wise error (FWE) threshold of $PFWE < 0.05$, corrected for multiple comparisons based on the random field theory. In addition, post-hoc regions of interest analyses were performed using mask images for these regions from the SPM8 Anatomy Toolbox. Significant group differences are reported at $PSCV < 0.05$ (small volume correction, i.e., family wise error correction within the search volume of 8mm). The x, y, and z coordinates of areas displaying significant whole brain or regions of interest group differences in grey matter volume were identified using the Brede Database (43), the Nonlinear Yale MNI to Talairach Conversion Algorithm (44), and the SPM Anatomy Toolbox.

Between-group differences in cortical thickness and cortical folding were investigated with the same approach as the VBM approach adapted for surface-based analysis. Statistical analyses were performed using Keith Worsley's SurfStat toolbox (<http://www.math.mcgill.ca/keith/surfstat/>). T-tests were performed to investigate between-group differences with center, gender and education level as covariates. Significant vertices were firstly obtained with a threshold of $P < 0.001$ without correction for multiple comparisons. Clusters were secondly considered significant using FWE threshold of $PFWE < 0.05$, corrected for multiple comparisons based on the random field theory. We repeated the analysis including age as an additional covariate in order to assess age related effects on cortical thickness and cortical folding.

Statistical analysis of the behavioural data was performed using the Statistical Package for Social Sciences version 22 (SPSS, Chicago). The numerical variables were described as means and standard deviations and the categorical variables as medians, frequencies and percentages. Group comparisons were performed for demographical and clinical variables, as well as for the cognitive variables, using an analysis of variance with generalized linear model with Tukey correction for multiple testing when data distribution was normal, and a Kruskal-Wallis test was used for non-normal distributions. Categorical variables were compared with Chi-square test. A P-value < 0.05 was considered significant. No part of the study analyses was pre-registered prior to the research being conducted.

3. Results

3.1 Demographics

Of the 156 included patients, 133 patients had an MRI scan. An extensive data quality check resulted in the exclusion of 9 patients (6 due to large motion artifacts and 3 due to large lesions). Table 1 shows the demographic and clinical characteristics of the patients over the 4 cognitive profiles. Patients in group 1 were significantly younger than those in the three other groups and received more years of formal education than patients in group 3 and 4. Patients from group 4 showed more disease-related speech abnormalities (i.e., hypophonia) than those in the other three groups and more frequent and more severe hallucinations than patients in group 1 and 2. Mild dementia (based on clinical interpretation of test scores and level of autonomy) was more frequent in group 4 than in the other groups. Group 3 showed more symptoms of persistent and avoidance anxiety and more symptoms of apathy than group 1.

Table 1. Demographic and clinical features of the four patient groups.

Group (n)	Group 1 (34)		Group 2 (33)		Group 3 (44)		Group 4 (13)		P-values	Post-hoc tests
	Mean	SD	Mean	SD	Mean	SD	Mean	SD		
Demographic										
Sex (% male)	70.6		75.8		61.4		69.2		0.5897	
Age	60.0	8.4	66.1	5.6	66.9	8.0	71.29	5.88	<0.0001	1<2,3,4
Formal education (y)	13.8	3.2	13.5	4.2	11.5	3.5	9.1	2.1	<0.0001	1>3,4; 2>3,4; 3>4
Clinical										
Disease duration(y)	8.1	5.2	8.9	7.4	8.8	4.9	9.4	4.2	0.8909	NA
MDS_UPDRS3 score	25.5	10.4	30.2	12.0	28.1	11.2	31.9	16.7	0.2741	NA
Hoehn & Yahr stage	1.9	0.4	2.1	0.6	2.2	0.6	2.3	0.5	0.0405	
Dyskinesia (%)	17.6		15.2		27.3		30.8		0.4595	
Postural instability (score MDS_UPDRS3_12)	0.4	0.6	0.6	0.7	0.7	0.9	0.9	1.1	0.2617	NA
Hypophonia (score MDS_UPDRS3_1)	0.9	0.6	0.9	0.7	1.0	0.7	1.6	0.9	0.0067	4<1,2,3
REM sleep behaviour disorder (%)	23.5		36.4		45.5		38.5		0.2594	NA
IADL (% with full autonomy)	76.5		66.7		34.1		0.0		<0.0001	NA
Dementia (%)	0.0		0.0		11.4		46.2		<0.0001	NA
Medication										
LED (mg/day)	721.3	675.1	732.6	487.3	874.94	543.6	861.6	285.4	0.5433	NA
Levodopa (%)	82.4		84.8		90.9		100.0		0.3290	NA
Dopamine agonist (%)	58.8		60.6		47.7		69.2		0.4689	NA
Antidepressant (%)	11.8		12.1		18.2		15.4		0.8388	NA
Benzodiazepine (%)	2.9		6.1		15.9		15.4		0.1953	NA
Neuropsychiatry										
Hamilton depression rating scale	6.0	4.4	5.2	5.5	6.4	4.2	5.4	4.5	0.7369	NA
Lille apathy rating scale	-27.2	6.1	-26.8	6.3	-23.1	6.9	-22.5	7.3	0.0096	1<3
PAS (score of persistent anxiety)	3.4	3.9	4.2	4.2	6.4	4.9	6.3	5.5	0.0181	1<3
PAS (score of episodic anxiety)	0.7	1.1	1.1	2.0	1.1	1.8	1.1	1.6	0.7286	NA

	0.5	1.5	1.0	2.0	1.6	1.7	1.2	1.3	0.0457	1<3
PAS (score of avoidance)										
Hallucinations (%)	5.9	6.1	18.2	30.8	0.0538					NA
Vascular risk factors										
High blood pressure (%)	20.6	27.3	22.7	38.5	0.6103					NA
Hypercholesterolemia (%)	17.6	24.2	25.0	15.4	0.7920					NA
Diabetes (%)	2.9	12.1	9.1	7.7	0.5722					NA
Sleep apnea syndrome (%)	11.8	18.2	18.2	15.4	0.8676					NA
History of heart infarct (%)	0.0	6.1	4.5	0.0	0.4468					NA
Lower limb arteriopathy (%)	8.8	12.1	0.0	0.0	0.0838					NA

MDS_UPDRS3=Movement Disorders Society Unified Parkinson's Disease Rating Scale-Part III (severity of motor symptoms); IADL= instrumental activities of daily living; LEDD=Levodopa Equivalent Daily Dose; PAS=Parkinson Anxiety Scale; NA= Not applicable. Due to low frequency of observations, we only mentioned qualitative results of overall group comparisons.

3.2 Neuropsychological data

Table 2 shows the neuropsychological test data of the four patient groups per cognitive domain. Patients from group 1 and 2 were cognitively intact, with average to high levels of performance in all cognitive domains in group 1, and only slight slowing of information processing speed and verbal fluency in group 2 (i.e., SDMT and Semantic Fluency for animals, respectively). Group 3 scored lower on global cognition (i.e., MMSE and MDRS) than the cognitively intact groups, yet still within the normal range. Patients in group 3 further scored lower on tests measuring attention, working memory, episodic verbal memory (except recognition), executive functions, language and visuospatial functions. Patients in group 4 showed impaired global cognition and severe deficits in all cognitive domains.

Table 2. Cognitive test performance (mean and standard deviation) of the four patient groups.

	Group 1		Group 2		Group 3		Group 4		P-values	Post-hoc tests
	Mean	SD	Mean	SD	Mean	SD	Mean	SD		
Number of subjects (%)	34 (27.4)		33 (26.6)		44 (35.5)		13 (10.5)			
Global Cognition										
MMSE score (/30)	28.9	1.1	28.5	1.6	27.1	2.3	24.6	3.5	<0.0001	1>3,4; 2>4; 3>4
MDRS score (/144)	140.9	3.11	139.9	3.3	134.6	5.55	125.5	9.1	<0.0001	1>3,4; 2>3,4; 3>4
Attention and working memory										
WAIS-R forward digit (/14)	8.8	1.7	7.8	1.9	6.8	2.5	6.9	2.5	0.0004	1>3,4
WAIS-R backward digit (/14)	6.7	1.5	6.3	1.5	4.7	1.6	3.9	1.4	<0.0001	1>3,4; 2>3,4
SDMT: number in 90sec	55.7	7.0	43.5	3.4	33.2	6.7	18.1	9.2	<0.0001	1>2,3,4; 2>3,4; 3>4
Executive functions										
Trail Making Test (time B/time A)	2.2	0.6	2.5	0.7	2.8	0.8	3.0	1.1	0.0005	1>3,4
Stroop: interference index	1.6	0.4	1.7	0.2	2.1	0.6	2.4	1.0	<0.0001	1>3,4; 2>3,4
Stroop: errors	0.5	1.9	0.9	1.2	4.1	4.3	18.9	15.0	<0.0001	1>3,4; 2>4; 3>4
Phonemic fluency: naming in 60 sec.	15.4	5.3	14.9	2.9	10.9	3.9	7.5	3.2	<0.0001	1>3,4; 2>3,4; 3>4
Alternating fluency: naming in 60 sec	14.7	4.1	13.1	3.6	8.5	3.5	6.3	3.3	<0.0001	1>3,4; 2>3,4
Episodic Memory										
HVLT Learn trial 1 (/12)	7.4	1.7	6.9	1.5	5.5	2.1	3.7	1.5	<0.0001	1>3,4; 2>3,4; 3>4
HVLT Learn total (/36)	28.3	4.0	27.1	3.2	23.3	4.1	16.9	4.6	<0.0001	1>3,4; 2>3,4; 3>4
HVLT delayed recall (/12)	10.0	1.7	9.9	1.8	8.0	2.3	4.6	3.0	<0.0001	1>3,4; 2>3,4; 3>4
HVLT recognition hits (/12)	11.6	0.7	11.6	0.8	11.1	1.1	9.6	2.1	0.0004	1>4; 2>4; 3>4
HVLT number of intrusions	0.5	1.0	1.1	1.8	1.5	2.3	2.2	1.4	0.0018	1>4;
Language										
Boston naming test (/15)	13.9	1.2	13.4	1.8	11.2	2.6	10.9	3.0	<0.0001	1>3,4; 2>3,4
Animal naming in 60 sec	25.7	4.9	19.8	3.4	15.1	4.0	10.7	5.5	<0.0001	1>2,3,4; 2>3,4; 3>4
Visuospatial functions										
Judgment of line orientation	12.7	2.0	12.5	3.4	10.7	2.9	7.9	2.7	<0.0001	1>3,4; 2>3,4; 3>4

MMSE= Mini Mental State Examination; MDRS= Mattis dementia rating scale; WAIS-R= Wechsler for adults intelligence scale revised; SDMT= Symbol digit modalities test; HVLT=Hopkins verbal learning test.

3.3 Grey matter volume

Our first analysis, using center, gender and education level as covariates showed reduced grey matter volume between several different groups in a significant number of brain regions, located both in the temporal, parietal and frontal lobe areas. We refer to the supplementary data for the information regarding the location and MNI coordinates of these regions. However, after including age as a covariate into the model as well, no differences in grey matter volume between any of the groups remained significant. A more liberal statistical threshold of $P < 0.005$ revealed reduced grey matter volume in group 4 compared with group 1 within the left medial temporal pole (BA 38), and a trend within the right posterior cingulate gyrus (BA 31) and right precuneus (BA 7) (PFWE=0.052). Fig. 1 demonstrates the areas as identified by the VBM analyses with correction for center, gender, age and level of education where group 4 showed differences in grey matter volume compared with group 1. See also table 3 for specific details about location and MNI coordinates.

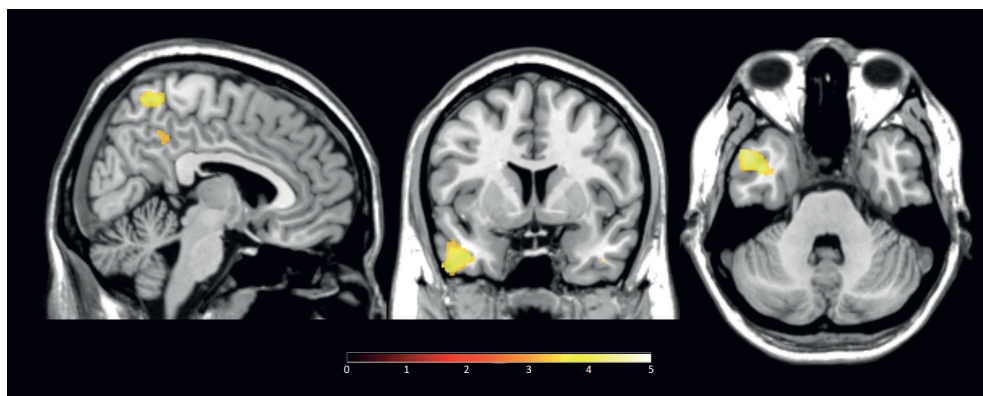


Figure 1. VBM group comparisons of grey matter volume with centre, gender, education level and age as covariates. The threshold was set at $PFWE < 0.05$, corrected for multiple comparisons based on the random field theory. A decreased grey matter volume was found in the left medial temporal pole in groups 4 versus group 1, and a trend within the right posterior cingulate gyrus and right precuneus. The color scale represents the T-value corresponding to the significant cluster.

Table 3. Location and MNI coordinates of significant clusters of grey matter volume loss after comparing all groups to the cognitively intact PD group (group 1).

Comparison	Location	Cluster size (k)	MNI Coordinates			T-value	P-value
			x	y	z		
Group 1 > 4	L medial temporal pole 38	1753	-48	12	-35	4.57	0.044
	L medial temporal pole 38		-40	3	-33	4.23	
	L medial temporal pole 38		-54	6	-41	4.04	
	R precuneus 7	1829	8	-54	64	4.24	0.052
	R posterior cingulate gyrus 31		14	-55	33	3.66	
	R posterior cingulate gyrus 31		16	-43	37	3.57	

Cluster size denotes the extent of the activation cluster by number of significant voxels (k). MNI coordinates refer to the location of the maximally activated voxel (peak) within an activation cluster. Results are considered significant at $PFWE < 0.05$ (FWE-corrected based on random field theory), corrected for center, gender, age and education. Numbers refer to Brodmann areas (location). L = left; R = right.

3.4 Cortical thickness and cortical folding

Fig. 2 shows the statistical comparisons for which cortical thickness were significantly reduced between two groups using center, gender, age and education level as covariates. At first, significantly reduced cortical thickness between groups was observed in several brain regions, most dominantly in the temporal regions. However, after including age as a covariate into the model as well, only reduced cortical thickness of group 4 compared with group 1 was observed in right inferior temporal gyrus (Fig. 4). See Table 4 for specific details about location and MNI coordinates of the significant age-adjusted results.

After including age, center, gender and education level as a covariate, the cortical folding was solely statistically reduced in group 4 compared with group 1. Group 4 showed less local gyrification index values in right temporal regions (Fig. 4). See Table 4 for specific details about location and MNI coordinates.

For the results of the cortical thickness and cortical folding analysis corrected for center, gender and education level, but not for a age, we refer to the supplementary data.

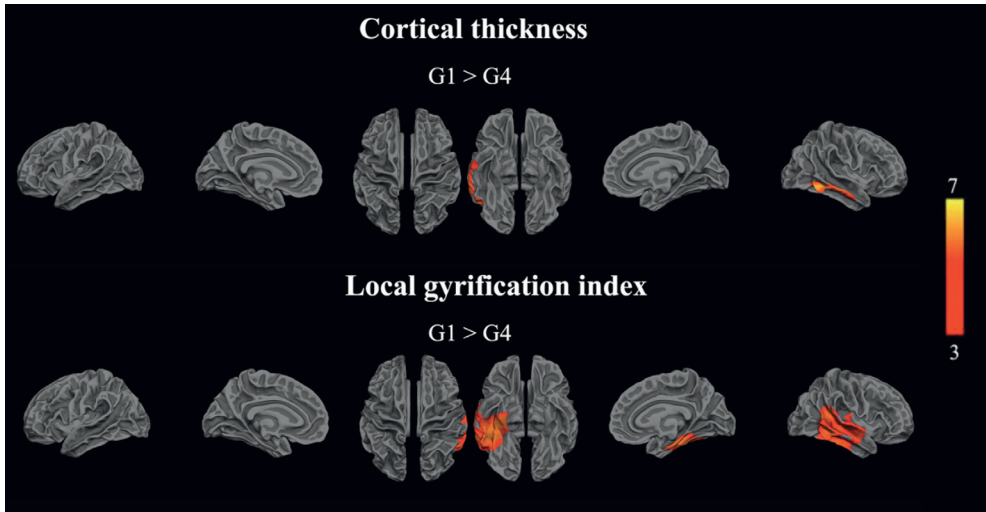


Figure 2. Between-group comparisons of cortical thickness and cortical folding values with center, gender, education level and age as covariates. The threshold was set at $PFWE < 0.05$, corrected for multiple comparisons based on the random field theory. The color scale represents the T-value corresponding to the significant vertices.

Table 4. Significant differences in cortical thickness and local gyrification index between patient groups.

Comparison	Location	Cluster size (# of vertices)	MNI coordinates			T-value	P-value
			x	y	z		
Cortical thickness							
Group 1 > 4	R inferior temporal gyrus	2616	58	-54	-11	5.92	0.016
	R middle temporal gyrus		67	-21	-11	4.64	
Local gyrification index							
Group 1 > 4	R medial occipitotemporal sulcus	18749	36	-25	-23	5.21	3.10-4
	R lateral occipitotemporal sulcus		45	-42	-19	4.73	
	R superior temporal sulcus		51	-45	15	4.46	
	R inferior temporal sulcus		58	-47	-9	4.46	
	R circular insula sulcus		38	-24	5	3.85	

Cluster size denotes the extent of the activation cluster by number of significant voxels (k). MNI coordinates refer to the location of the maximally activated vertex (peak) within an activation cluster. Results are considered significant at $PFWE < 0.05$ (FWE-corrected based on random field theory), corrected for center, gender, age and education. L = left; R = right.

3.5 Small vessel disease

The amount of white matter lesions related to chronic small vessel disease, was scored on all MRI images according to the Fazekas scale. All groups displayed a median Fazekas score of 1. Analysis using a Chi-Square test did not reveal a significant difference between groups ($p = 0.327$).

4. Discussion

The age-corrected results of this study show a significant difference in grey matter volume only between the group with severe cognitive decline (group 4) and the cognitively intact group (group 1). More specifically, group 4 showed a reduced grey matter volume within the right posterior cingulate gyrus (BA 31) and right precuneus (BA 7). Furthermore, our results gave no indication for a regional progressive severity gradient of reduced grey matter volume associated with more severe cognitive decline. In other words, we found no difference in the degree of grey matter volume in specific brain regions between patients with slight versus more severe cognitive deficits. Instead, we observed pathological changes in patients with more severe cognitive decline (group 4) compared to cognitively intact patients (group 1). In addition, a significant reduction in cortical thickness and cortical folding between group 4 and group 1 was predominantly seen in the right temporal regions. No significant results in cortical folding or cortical thickness were observed between the other groups when age was introduced as a covariate. Moreover, we did not find any significant differences in Fazekas scores between the groups.

Patients in all four groups were at relatively early motor stages, showing no significant differences in severity of motor disability, disease duration or medication use. Interestingly, patients in group 3 (comparable to 'PD-MCI') displayed significantly more severe symptoms of anxiety and apathy when compared to the cognitively intact groups. Therefore, this data-driven approach indicates that it is useful to also consider non-motor symptoms such as neuropsychiatric symptoms when classifying PD patients, as this probably provides a more representative classification.

The fourth group, characterized by global and severe cognitive decline in multiple cognitive domains (e.g., verbal episodic memory and visuospatial deficits), showed reduced cortical thickness and cortical folding in the medial temporal lobe. The involvement of medial temporal areas is in line with other VBM studies (7, 10) and possibly reflects more widespread Lewy body pathology as well as a marker for conversion to PDD. Within group 4, six patients already met the diagnostic criteria for mild PDD, while the remaining patients ($n=7$) could be classified as multiple domains

MCI (9). Another characteristic of this group was the high rate of visual hallucinations. The association between visual hallucinations and severe cognitive decline (45), as well as a higher risk for developing dementia (3), has been related to both Lewy body pathology in the temporal lobe (46) and to cholinergic deficits (47). Moreover, group 4 was the only group with a higher score of hypophonia, an axial sign which has also been associated with cognitive worsening (48).

Interestingly, autopsy studies revealed that a substantial number of PD patients appear to have neuropathological changes related to AD in addition to diffuse Lewy body pathology (13, 14, 15). As such, more advanced stages of cognitive decline in PD may reflect an interaction of different neurodegenerative processes such as comorbid AD-related neurodegenerative changes (49). Moreover, the combination of amyloid- and tau-related pathological changes and limbic and cortical Lewy body abnormalities appear to be the strongest correlate of dementia in PD (50). Other factors, such as neuroinflammation, synaptic pathological changes and neurotransmitters may be involved as well. In our sample, we did not find evidence for a contribution of vascular changes to cognitive decline.

Contrary to our expectations, grey matter changes were not widespread and only visible between the cognitive intact group and the group with the most severe cognitive decline. This may indicate that grey matter alternations may not be as important as previously thought, at least in the early stages of cognitive decline. Since we also did not find differences in vascular lesions between the groups, this may point in the direction that alterations in white matter tracts may play a role. This hypothesis is supported by results of previous studies, which investigated both white and grey matter alterations in a group of PD patients. These authors conclude that changes in white matter precede grey matter alterations (51, 52). Grey matter atrophy is an expression of neuronal cell death, a phenomenon that is seen in relatively late stages of PD dementia. In contrast to this, the earliest stages of cognitive impairment in PD are characterized by axonal and synaptic changes. Other MRI techniques, such as diffusion-weighted imaging, are able to detect alterations in white matter integrity related to axonal damage and might therefore be more useful in early stages of cognitive decline in PD (53).

Levy (2007) proposed a model for the relationship between PD and advanced aging, stating that advanced age is associated with a faster rate of motor progression, decreased levodopa responsiveness, more severe gait and postural impairments, reduced autonomy, more severe cognitive impairment and a higher risk for developing dementia in PD (54). The model further suggests a substantial role for aging in the pathogenesis of PD, by means of a biological interaction between the effects of the disease process and aging in non-dopaminergic structures, which may indeed denote

the involvement of monoaminergic and cholinergic structures in more advanced stages of PD. As such, it is not surprising that most of the between group differences in our study were no longer significant after the correction for age.

For this study two different methods to assess grey matter alterations were combined, VBM and surface-based cortical thickness approaches. We believe that both of the methods add complementary information. VBM is able to evident grey matter differences based on voxel values on the whole brain, while surface-based cortical thickness approaches are limited to the cortex and provide more subtle information about cortical thickness (55). Furthermore, VBM quantifies grey matter volume changes between groups, which is a combination of information about the cortical thickness and surface areas. Several previous studies showed the additional value of combining these methods, both in healthy subjects (56) and PD patients (57).

Our study has several limitations. First, due the research question and study design (data-driven approach in order to identify cognitive phenotypes in PD), we did not include a healthy control group. The cognitively intact PD patients (group 1) was considered our reference group. Consequently, we were not able to identify (early) differences in grey matter volume loss between this group and healthy controls. Also, we were not able to disentangle the absolute contribution of disease to cognitive decline independently of age. Age appeared to be an overpowering factor in the model, possibly masking other factors. Secondly, the number of patients in the original clusters 4 and 5 was low, because of the exclusion of patients with moderate or severe dementia to limit imaging artifacts and missing data due to misunderstanding of instructions. However, despite collapsing these two clusters, the remaining group 4 still remained very small (n=13). Results for this group after correction for age would probably have reached the level of significance without a more liberal threshold if the sample had been larger. Thirdly, patients were recruited from tertiary referral centers, making the sample possibly not representative for the general population. Fourthly, spatial normalization and image segmentation in VBM is fully automated, which may lead to difficulties in detecting subtle changes in areas that show high variability among elderly and diseased groups (e.g., the hippocampus) and may lead to misclassification of voxels due to reduced tissue contrast. However, the use of a strict threshold for significance reduced the possibility for such errors substantially. Moreover, the use of automated whole brain analysis methods for evaluating brain structure in diseased brains is less prone to subjectivity associated with regions-of-interest-based methods and is not restricted by a priori assumptions about specific regions of interest. Another important aspect concerns the use of a cross-sectional design, which limited us to merely describe the clinical characteristics and neural substrates of the separate cognitive profiles. A follow-up of the identified groups would be essential to explore differences in disease progression. Moreover, this may

reveal the extent to which neural substrates associated with early markers of cognitive impairment (e.g., slowed mental speed) can be used as a predictor of severe cognitive decline and conceivable conversion to dementia. An important strength of our study is the use of a data-driven approach. Groups were not previously defined based on diagnostic criteria for MCI and PDD. This allowed recognition of different phenotypes regarding cognitive functioning and other non-motor symptoms in early PD patients with similar motor disability. We believe that a data-driven approach to define groups can be very useful for identifying early markers of cognitive decline in PD.

In conclusion, our results revealed grey matter abnormalities associated only with severe cognitive decline in PD. Reduction of cortical volume occurs in the right posterior cingulate and precuneus, while reduced cortical thickness and folding occurs bilateral in the medial temporal regions. These seem to be attributable to processes of cognitive decline and not associated with age. The absence of cortical changes and vascular lesions point in the direction of a more prominent involvement of white matter tract alterations. Future studies should preferably be prospective and include a larger number of PD patients with more advanced cognitive decline. Studies may also benefit from more specific interest in white matter changes.

5. References

1. Yarnall AJ, Breen DP, Duncan GW, Khoo TK, Coleman SY, Firkbank MJ, et al. Characterizing mild cognitive impairment in incident Parkinson disease: the ICICLE-PD study. *Neurology*. 2014;82(4):308-16.
2. Svenningsson P, Westman E, Ballard C, Aarsland D. Cognitive impairment in patients with Parkinson's disease: diagnosis, biomarkers, and treatment. *Lancet Neurol*. 2012;11(8):697-707.
3. Aarsland D, Andersen K, Larsen JP, Lolk A, Kragh-Sorensen P. Prevalence and characteristics of dementia in Parkinson disease: an 8-year prospective study. *Arch Neurol*. 2003;60(3):387-92.
4. Hely MA, Reid WG, Adena MA, Halliday GM, Morris JG. The Sydney multicenter study of Parkinson's disease: the inevitability of dementia at 20 years. *Mov Disord*. 2008;23(6):837-44.
5. Janvin C, Aarsland D, Larsen JP, Hugdahl K. Neuropsychological profile of patients with Parkinson's disease without dementia. *Dement Geriatr Cogn Disord*. 2003;15(3):126-31.
6. Foltyniec T, Brayne CE, Robbins TW, Barker RA. The cognitive ability of an incident cohort of Parkinson's patients in the UK. The CamPaIGN study. *Brain*. 2004;127(Pt 3):550-60.
7. Weintraub D, Doshi J, Koka D, Davatzikos C, Siderowf AD, Duda JE, et al. Neurodegeneration across stages of cognitive decline in Parkinson disease. *Arch Neurol*. 2011;68(12):1562-8.
8. Kehagia AA, Barker RA, Robbins TW. Neuropsychological and clinical heterogeneity of cognitive impairment and dementia in patients with Parkinson's disease. *Lancet Neurol*. 2010;9(12):1200-13.
9. Litvan I, Goldman JG, Troster AI, Schmand BA, Weintraub D, Petersen RC, et al. Diagnostic criteria for mild cognitive impairment in Parkinson's disease: Movement Disorder Society Task Force guidelines. *Mov Disord*. 2012;27(3):349-56.
10. Burton EJ, McKeith IG, Burn DJ, Williams ED, O'Brien JT. Cerebral atrophy in Parkinson's disease with and without dementia: a comparison with Alzheimer's disease, dementia with Lewy bodies and controls. *Brain*. 2004;127(Pt 4):791-800.
11. Song SK, Lee JE, Park HJ, Sohn YH, Lee JD, Lee PH. The pattern of cortical atrophy in patients with Parkinson's disease according to cognitive status. *Mov Disord*. 2011;26(2):289-96.
12. Pereira JB, Svenningsson P, Weintraub D, Bronnick K, Lebedev A, Westman E, et al. Initial cognitive decline is associated with cortical thinning in early Parkinson disease. *Neurology*. 2014;82(22):2017-25.
13. Jellinger KA, Seppi K, Wenning GK, Poewe W. Impact of coexistent Alzheimer pathology on the natural history of Parkinson's disease. *J Neural Transm (Vienna)*. 2002;109(3):329-39.
14. Kurosinski P, Guggisberg M, Gotz J. Alzheimer's and Parkinson's disease--overlapping or synergistic pathologies? *Trends Mol Med*. 2002;8(1):3-5.
15. Kalaitzakis ME, Pearce RK. The morbid anatomy of dementia in Parkinson's disease. *Acta Neuropathol*. 2009;118(5):587-98.
16. Dujardin K, Leentjens AF, Langlois C, Moonen AJ, Duits AA, Carette AS, et al. The spectrum of cognitive disorders in Parkinson's disease: a data-driven approach. *Mov Disord*. 2013;28(2):183-9.
17. Dujardin K, Moonen AJ, Behal H, Defebvre L, Duhamel A, Duits AA, et al. Cognitive disorders in Parkinson's disease: Confirmation of a spectrum of severity. *Parkinsonism Relat Disord*. 2015;21(11):1299-305.
18. Gibb WR, Lees AJ. The relevance of the Lewy body to the pathogenesis of idiopathic Parkinson's disease. *J Neurol Neurosurg Psychiatry*. 1988;51(6):745-52.

19. Morris JC. The Clinical Dementia Rating (CDR): current version and scoring rules. *Neurology*. 1993;43(11):2412-4.
20. Emre M, Aarsland D, Brown R, Burn DJ, Duyckaerts C, Mizuno Y, et al. Clinical diagnostic criteria for dementia associated with Parkinson's disease. *Mov Disord*. 2007;22(12):1689-707; quiz 837.
21. Goetz CG, Tilley BC, Shaftman SR, Stebbins GT, Fahn S, Martinez-Martin P, et al. Movement Disorder Society-sponsored revision of the Unified Parkinson's Disease Rating Scale (MDS-UPDRS): scale presentation and clinimetric testing results. *Mov Disord*. 2008;23(15):2129-70.
22. Hamilton M. A rating scale for depression. *J Neurol Neurosurg Psychiatry*. 1960;23(1):56-62.
23. Leentjens AF, Dujardin K, Pontone GM, Starkstein SE, Weintraub D, Martinez-Martin P. The Parkinson Anxiety Scale (PAS): development and validation of a new anxiety scale. *Mov Disord*. 2014;29(8):1035-43.
24. Sockeel P, Dujardin K, Devos D, Deneve C, Destee A, Defebvre L. The Lille apathy rating scale (LARS), a new instrument for detecting and quantifying apathy: validation in Parkinson's disease. *J Neurol Neurosurg Psychiatry*. 2006;77(5):579-84.
25. Lawton MP, Brody EM. Assessment of older people: self-maintaining and instrumental activities of daily living. *Gerontologist*. 1969;9(3):179-86.
26. Tomlinson CL, Stowe R, Patel S, Rick C, Gray R, Clarke CE. Systematic review of levodopa dose equivalency reporting in Parkinson's disease. *Mov Disord*. 2010;25(15):2649-53.
27. Folstein MF, Folstein SE, McHugh PR. "Mini-mental state". A practical method for grading the cognitive state of patients for the clinician. *J Psychiatr Res*. 1975;12(3):189-98.
28. Mattis S. Mental status examination for organic mental syndrome in the elderly patient. *Geriatric psychiatry*. 1976.
29. Smith A. Symbol Digit Modalities Test (SDMT) Manual. Los Angeles, Western Psychological Services. 1982.
30. Reitan R. TMT, trail making test a & B. South Tucson, AR: Reitan Neuropsychology Laboratory. 1992.
31. Brandt J. Hopkins verbal learning test. *Clinical Neuropsychologist*. 2001.
32. Brandt J, Benedict R. Hopkins Verbal Learning Test-revised, Psychological Assessment Resources, Lutz. 2001.
33. Graves RE, Bezeau SC, Fogarty J, Blair R. Boston naming test short forms: a comparison of previous forms with new item response theory based forms. *J Clin Exp Neuropsychol*. 2004;26(7):891-902.
34. Benton AL, Varney NR, Hamsner KD. Visuospatial judgment. A clinical test. *Arch Neurol*. 1978;35(6):364-7.
35. Benton AL, Varney NR, Hamsner KS. Visuospatial judgment: A clinical test. *Archives of Neurology*. 1978;35(6):364-7.
36. Fazekas F, Chawluk JB, Alavi A, Hurtig HI, Zimmerman RA. MR signal abnormalities at 1.5 T in Alzheimer's dementia and normal aging. *AJR Am J Roentgenol*. 1987;149(2):351-6.
37. Ashburner J. A fast diffeomorphic image registration algorithm. *Neuroimage*. 2007;38(1):95-113.
38. Dale AM, Fischl B, Sereno MI. Cortical surface-based analysis. I. Segmentation and surface reconstruction. *Neuroimage*. 1999;9(2):179-94.
39. Fischl B, Sereno MI, Dale AM. Cortical surface-based analysis. II: Inflation, flattening, and a surface-based coordinate system. *Neuroimage*. 1999;9(2):195-207.
40. Lerch JP, Evans AC. Cortical thickness analysis examined through power analysis and a population simulation. *Neuroimage*. 2005;24(1):163-73.

41. Fischl B. FreeSurfer. *Neuroimage*. 2012;62(2):774-81.
42. Schaer M, Cuadra MB, Tamarit L, Lazeyras F, Eliez S, Thiran JP. A surface-based approach to quantify local cortical gyrification. *IEEE Trans Med Imaging*. 2008;27(2):161-70.
43. Nielsen FÅ. The Brede database: a small database for functional neuroimaging. *NeuroImage*. 2003;19(2):19-22.
44. Lacadie CM, Fulbright RK, Rajeevan N, Constable RT, Papademetris X. More accurate Talairach coordinates for neuroimaging using non-linear registration. *Neuroimage*. 2008;42(2):717-25.
45. Aarsland D, Andersen K, Larsen JP, Perry R, Wentzel-Larsen T, Lolk A, et al. The rate of cognitive decline in Parkinson disease. *Arch Neurol*. 2004;61(12):1906-11.
46. Harding AJ, Broe GA, Halliday GM. Visual hallucinations in Lewy body disease relate to Lewy bodies in the temporal lobe. *Brain*. 2002;125(Pt 2):391-403.
47. Perry EK, Marshall E, Kerwin J, Smith CJ, Jabeen S, Cheng AV, et al. Evidence of a monoaminergic-cholinergic imbalance related to visual hallucinations in Lewy body dementia. *J Neurochem*. 1990;55(4):1454-6.
48. Uc EY, McDermott MP, Marder KS, Anderson SW, Litvan I, Como PG, et al. Incidence of and risk factors for cognitive impairment in an early Parkinson disease clinical trial cohort. *Neurology*. 2009;73(18):1469-77.
49. Sabbagh MN, Adler CH, Lahti TJ, Connor DJ, Vedders L, Peterson LK, et al. Parkinson disease with dementia: comparing patients with and without Alzheimer pathology. *Alzheimer Dis Assoc Disord*. 2009;23(3):295-7.
50. Compta Y, Parkkinen L, O'Sullivan SS, Vandrovicova J, Holton JL, Collins C, et al. Lewy- and Alzheimer-type pathologies in Parkinson's disease dementia: which is more important? *Brain*. 2011;134(Pt 5):1493-505.
51. Rektor I, Svatkova A, Vojtisek L, Zikmundova I, Vanicek J, Kiraly A, et al. White matter alterations in Parkinson's disease with normal cognition precede grey matter atrophy. *PLoS One*. 2018;13(1):e0187939.
52. Duncan GW, Firbank MJ, Yarnall AJ, Khoo TK, Brooks DJ, Barker RA, et al. Gray and white matter imaging: A biomarker for cognitive impairment in early Parkinson's disease? *Mov Disord*. 2016;31(1):103-10.
53. Weil RS, Costantini AA, Schrag AE. Mild Cognitive Impairment in Parkinson's Disease-What Is It? *Curr Neurol Neurosci Rep*. 2018;18(4):17.
54. Levy G. The relationship of Parkinson disease with aging. *Arch Neurol*. 2007;64(9):1242-6.
55. Clarkson MJ, Cardoso MJ, Ridgway GR, Modat M, Leung KK, Rohrer JD, et al. A comparison of voxel and surface based cortical thickness estimation methods. *Neuroimage*. 2011;57(3):856-65.
56. Hutton C, Draganski B, Ashburner J, Weiskopf N. A comparison between voxel-based cortical thickness and voxel-based morphometry in normal aging. *Neuroimage*. 2009;48(2):371-80.
57. Gerrits NJ, van Loenhoud AC, van den Berg SF, Berendse HW, Foncke EM, Klein M, et al. Cortical Thickness, Surface Area and Subcortical Volume Differentially Contribute to Cognitive Heterogeneity in Parkinson's Disease. *PLoS One*. 2016;11(2):e0148852.

Supplementary material

Statistical details of the cluster analysis

Cluster analysis

The 19 variables derived from the neuropsychological tests were considered for the cluster analysis (CA). The CA was based on the k-means method in which similarity between individuals is measured using the usual Euclidian distance. We performed several analyses with different numbers of clusters and the optimal number was determined by consensus among three statistical properties: local peaks of the cubic cluster criterion (CCC), pseudo F and R^2 (ratio between the inter-cluster variation and the total variation). The number of subjects in each cluster and face validity as judged by experts (K.D., A.L., A.M., A.A.D) were also considered. All the patients were included in the CA.

Characterization of clusters

To compare the cluster on quantitative variables, an analysis of variance with generalized linear model with Tukey correction for multiple testing was performed when data distribution was normal and a Kruskal-Wallis test was used for non-normal distributions. Pairwise comparisons suggested by Elliott and Hynan were applied. Categorical variables were compared with Chi-square test or a Fisher's exact test when the expected cell frequency was <5 . A p-value <0.05 was considered significant.

Cluster comparisons were performed for the cognitive variables (the cluster variables) as well as for the clinical and demographical variables (the descriptive variables).

To evaluate the quality of clusters separation, a first factorial discriminant analysis was performed with the clusters as dependent and the cognitive features as independent variables. The correlations between these variables and the discriminant scores were computed to identify the variables contributing most to the separation of clusters. A second factorial discriminant analysis was performed on the clinical and demographical variables to illustrate the clusters profile.

This is an excerpt of the methods section of: Dujardin K, Moonen AJH, Behal H, Defebvre L, Duhamel A, Duits AA, Plomhause L, Tard C, Leentjens AFG. Cognitive disorders in Parkinson disease: confirmation of a spectrum of severity. *Park Rel Disord* 2015;21:1299-305. doi: 10.1016/j.parkreldis.2015.08.032

Supplementary table 1. Location and MNI coordinates of significant clusters of grey matter volume loss after comparing all groups to the cognitively intact PD group (group 1).

Comparison	Location	Cluster size (k)	MNI Coordinates			T-value	P-value
			x	y	z		
Group 1 > 2	L superior temporal gyrus 22	1782	-42	-45	21	5.27	0.001
	L inferior parietal lobe 40		-54	-40	27	4.85	
	L lateral inferior parietal lobule/ L supramarginal gyrus 40		-45	-39	30	4.74	
	L inferior frontal gyrus p. Orbitalis/ L middle orbital gyrus 47	818	-30	30	-9	4.79	0.038
	L temporal pole 38		-21	15	-17	3.98	
	L fronto-orbital gyrus 11		-32	12	-20	3.85	
	R inferior frontal gyrus 44	1543	58	-1	28	4.73	0.003
	R postcentral gyrus 3a/3b		51	-12	22	4.68	
	R inferior frontal gyrus 44		51	6	6	3.80	
	Group 1 > 3	posterior cingulate gyrus 31	744	0	-37	37	4.42
L inferior parietal lobule/ L supramarginal gyrus 40		1103	-50	-40	28	4.39	0.013
L superior temporal gyrus 22			-46	-43	16	4.14	
L anterior transverse temporal area 41			-40	-31	16	3.84	
R hippocampus		1557	36	-24	-15	4.28	0.003
R amygdala			20	2	-18	4.24	
R hippocampus (CA2)			33	-13	-15	4.20	
Group 1 > 4	R posterior Cingulate gyrus 31	979	16	-43	37	4.93	0.016
	R posterior Cingulate gyrus (ventral) 23		9	-42	30	4.56	
	R posterior Cingulate gyrus (ventral) 23		14	-54	31	4.13	
	L medial temporal pole 38	2141	-48	14	-35	4.91	0.000
	L middle temporal gyrus 21		-46	-10	-18	4.38	
	L parahippocampal gyrus 36		-27	-7	-42	4.34	
	R fusiform gyrus (posterior) 37	711	40	-42	-26	4.89	0.050
	R fusiform gyrus (posterior) 37		46	-46	-15	4.57	
	L medial temporal pole 38	1753	-48	12	-35	4.57	0.044*
	L medial temporal pole 38		-40	3	-33	4.23	
	L medial temporal pole 38		-54	6	-41	4.04	
	R precuneus 7	1829	8	-54	64	4.24	0.052*
	R posterior cingulate gyrus 31		14	-55	33	3.66	
R posterior cingulate gyrus 31		16	-43	37	3.57		

Cluster size denotes the extent of the activation cluster by number of significant voxels (k). MNI coordinates refer to the location of the maximally activated voxel (peak) within an activation cluster. Results are considered significant at $P_{FWE} < 0.05$ (FWE-corrected based on random field theory), corrected for center, gender, and education. Numbers refer to Brodmann areas (location). L = left; R = right. * P_{FWE} -value remains significant after correction for age.

Supplementary table 2. Significant differences in cortical thickness and local gyrification index between patient groups.

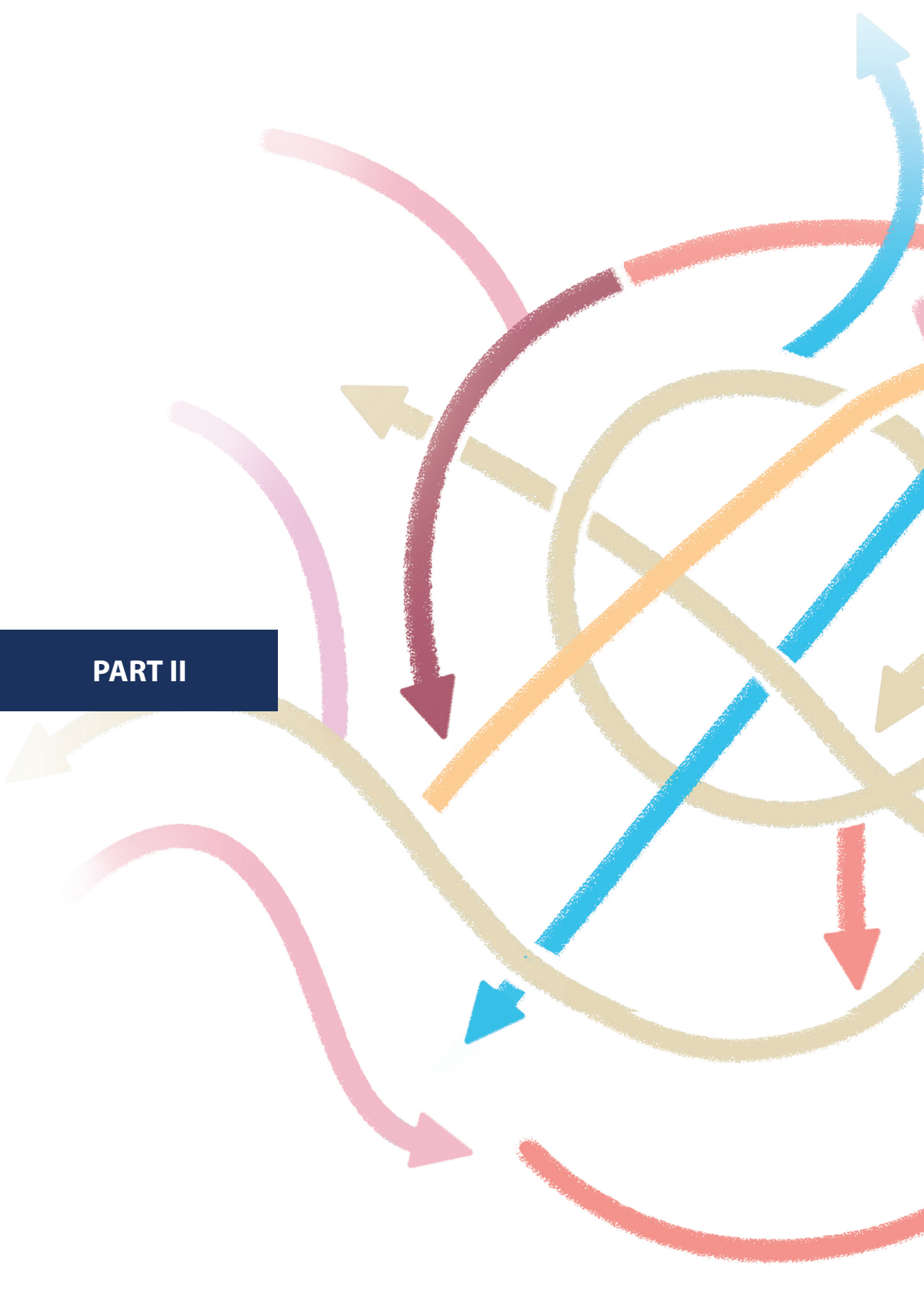
Comparison	Location	Cluster size (# of vertices)	MNI coordinates			T-value	P-value
			x	y	z		
Cortical thickness							
Group 1 > 4	R inferior temporal gyrus	10897	59	-56	-10	6.73	2.10-6
	R middle temporal gyrus		58	-58	9	5.90	
	R transverse collateral sulcus		40	-9	-32	4.83	
	L medial occipitotemporal sulcus	3791	-34	-43	-11	4.78	9.10-4
	L inferior occipital sulcus gyrus		-36	-80	-17	4.61	
	L transverse collateral sulcus		-40	-27	-25	4.57	
	L lateral fusiform gyrus		-43	-61	-23	4.32	
	L superior temporal sulcus	5307	-49	-33	-4	4.84	9.10-4
	L superior temporal gyrus		-66	-37	14	4.51	
	R medial occipitotemporal sulcus	2328	25	-55	-9	5.89	0.008
R lateral fusiform gyrus		25	-50	-17	4.41		
	R inferior temporal gyrus	2616	58	-54	-11	5.92	0.016*
	R middle temporal gyrus		67	-21	-11	4.64	
Group 2 > 4	L superior temporal sulcus	2539	-51	-19	-11	4.91	0.024
	L superior temporal gyrus		-68	-38	11	4.13	
Group 3 > 4	R superior temporal sulcus	2065	46	-54	21	5.24	0.025
	R middle temporal gyrus		61	-56	-2	3.83	
Group 1 > 3	L lateral fissure	5199	-40	-36	15	5.21	4.10-4
	L opercular part of inferior frontal gyrus		-41	8	4	4.66	
	L circular sulcus		-40	-4	15	4.57	
	L collateral sulcus	3100	-43	-21	-26	4.39	0.007
	L lateral occipitotemporal sulcus		-44	-41	-23	4.15	
	L inferior temporal sulcus		-53	-13	-27	3.96	
	R medial occipitotemporal sulcus	2428	26	-59	-8	5.19	0.017
	R middle temporal gyrus	2869	62	-12	-28	4.86	0.021
	L circular insula sulcus	1965	-33	15	-16	4.71	0.040
	L orbital sulcus		-29	33	-13	4.37	
	L long gyrus of insula		-37	3	-20	3.83	
	R anterior cingulate cortex	1773	12	38	20	4.40	0.043
	R superior temporal gyrus	2080	36	6	-24	4.71	0.047
R circular insula sulcus		43	-9	-13	4.70		
Local gyrification index							
Group 1 > 4	R precentral gyrus	39266	32	-13	66	6.02	4.10-6

Supplementary table 2. Continued

Comparison	Location	Cluster size (# of vertices)	MNI coordinates			T-value	P-value
			x	y	z		
	R superior temporal sulcus		54	-42	12	5.42	
	R inferior parietal gyrus		51	-28	24	4.68	
	R inferior temporal gyrus		51	-41	-26	4.07	
	R lateral fissure		39	-23	7	3.88	
	L superior temporal sulcus	35879	-59	-33	-1.42	5.22	2.10-5
	L rectus gyrus		-3	34	-29	4.90	
	L circular insula sulcus		-38	-9	14	4.67	
	L superior temporal gyrus		-45	-18	2	4.52	
	L subcentral gyrus		-56	-8	7	4.44	
	L inferior temporal gyrus		-60	-46	-16	4.09	
	R medial occipitotemporal sulcus	18749	36	-25	-23	5.21	3.10-4*
	R lateral occipitotemporal sulcus		45	-42	-19	4.73	
	R superior temporal sulcus		51	-45	15	4.46	
	R inferior temporal sulcus		58	-47	-9	4.46	
	R circular insula sulcus		38	-24	5	3.85	

Cluster size denotes the extent of the activation cluster by number of significant voxels (k). MNI coordinates refer to the location of the maximally activated vertex (peak) within an activation cluster. Results are considered significant at $PFWE < 0.05$ (FWE-corrected based on random field theory), corrected for center, gender, and education. L = left; R = right. * PFWE-value remains significant after correction for age.

PART II





Ultra-high field imaging as a biomarker in Parkinson's disease

CHAPTER 5



The TRACK-PD study: protocol of a longitudinal ultra-high field imaging study in Parkinson's disease

A.F. Wolters, M. Heijmans, S. Michielse, A.F.G Leentjens, A.A. Postma, J.F.A. Jansen, D. Ivanov, A.A. Duits, Y. Temel, M.L. Kuijf

Abstract

Background: The diagnosis of Parkinson's Disease (PD) remains a challenge and is currently based on the assessment of clinical symptoms. PD is also a heterogeneous disease with great variability in symptoms, disease course, and response to therapy. There is a general need for a better understanding of this heterogeneity and the interlinked long-term changes in brain function and structure in PD. Over the past years there is increasing interest in the value of new paradigms in Magnetic Resonance Imaging (MRI) and the potential of ultra-high field strength imaging in the diagnostic work-up of PD. With this multimodal 7T MRI study, our objectives are: 1) To identify distinctive MRI characteristics in PD patients and to create a diagnostic tool based on these differences. 2) To correlate MRI characteristics to clinical phenotype, genetics and progression of symptoms. 3) To detect future imaging biomarkers for disease progression that could be valuable for the evaluation of new therapies.

Methods: The TRACK-PD study is a longitudinal observational study in a cohort of 130 recently diagnosed (≤ 3 years after diagnosis) PD patients and 60 age-matched healthy controls (HC). A 7T MRI of the brain will be performed at baseline and repeated after two and four years. Complete assessment of motor, cognitive, neuropsychiatric and autonomic symptoms will be performed at baseline and follow-up visits with wearable sensors, validated questionnaires and rating scales. At baseline a blood DNA sample will also be collected.

Discussion: This is the first longitudinal, observational, 7T MRI study in PD patients. With this study, an important contribution can be made to the improvement of the current diagnostic process in PD. Moreover, this study will be able to provide valuable information related to the different clinical phenotypes of PD and their correlating MRI characteristics. The long-term aim of this study is to better understand PD and develop new biomarkers for disease progression which may help new therapy development. Eventually, this may lead to predictive models for individual PD patients and towards personalized medicine in the future.

Trial registration: Dutch Trial Register, NL7558. Registered March 11, 2019.

1. Background

Parkinson's disease (PD) is the second most common neurodegenerative disorder after Alzheimer's disease and is characterized by motor symptoms such as bradykinesia, rigidity and tremor (1-3). Patients with PD also experience a broad spectrum of non-motor symptoms such as anxiety, depression, pain and autonomic dysfunction, making the disease a typical example of a neuropsychiatric disorder. The diagnosis of PD is currently based on the assessment of clinical symptoms and their course over time. However, the early diagnosis of PD can be challenging since its presentation is heterogeneous and mild symptoms are often not immediately recognised. Clinico-pathological research shows that the error rate for a clinical diagnosis of PD can be as high as 24%, even in specialized centres (4).

Recently, clinical criteria have been revised for the diagnosis of PD (3) and several subtypes of PD are being recognised (5, 6). Currently a Movement Disorder Society (MDS) task force is mandated to review the evidence for these subtypes and propose a subtype classification system. The different subtypes of PD might be influenced by a combination of environmental and genetic factors (7). However, the underlying aetiology of the clinical heterogeneity in PD is not well understood (8). This is why the National Institutes of Health (NIH) pointed out that obtaining more insight in this heterogenous nature and defining the different PD subtypes, is one of the top three research priorities in PD (9).

In clinical practice, Magnetic Resonance Imaging (MRI) is currently used as a method to exclude other potential causes of parkinsonian symptoms. To date, it is impossible to diagnose a patient with PD based on MRI characteristics. However, over the past years it has become well-established that MRI may serve as a valuable method in the diagnostic work-up of PD (10). Early indicators, such as signal loss of the nigrosome-1 area on iron-sensitive MR Images and reduced volume and signal intensity of the substantia nigra on neuromelanin-sensitive images, have been described in PD (11-14). Additionally, functional MRI (fMRI) techniques can display changes related to specific symptoms in PD (15, 16). With the emergence of ultra-high-field scanners (7T and above) submillimetre anatomical information can be obtained. Compared with 3T MRI, ultra-high-field MRI at 7T provides an increased spatial resolution and a higher signal-to-noise ratio enabling a potential higher degree of diagnostic detail (10).

The primary objective of this study is to identify early and subtle MRI changes in PD patients which distinguish them from the healthy population and to create a reliable tool for the early diagnosis of PD based on these differences. Secondary objectives are to detect whether different clinical phenotypes of PD patients also show different

imaging characteristics and to design a prognostic tool for individual PD patients by correlating specific MRI characteristics to clinical phenotype, genetic characteristics and progression of symptoms. Moreover, this large longitudinal ultra-high field imaging study may eventually also find new imaging biomarkers for disease progression that could be valuable for the development and evaluation of new therapies in PD. In addition, the database will serve as a biobank for further related research.

2. Methods

This is a longitudinal observational study in PD patients and healthy controls (HC). The TRACK-PD study (www.trackpd.nl) will assess the structural and functional characteristics of PD patients on ultra-high field 7T MRI. The study has been registered at the Dutch Trial Register (www.trialregister.nl) with identification number NL7558.

2.1 Participants

In this study, 130 participants with PD will be recruited from the PD population visiting the movement disorder clinic of the Department of Neurology of the Maastricht University Medical Centre and other collaborating hospitals. In addition, we will use other media, such as websites, social media and patient meetings to recruit patients. 60 HC participants will be recruited through advertisements in the hospital and university.

2.2 Inclusion and exclusion criteria

Participants are eligible for participation in this study if they meet the following criteria: 1) All patients have to be diagnosed with PD by a neurologist, within the last 3 years before inclusion. 2) A score of ≥ 24 on the Montreal Cognitive Assessment (MoCA) at baseline. 3) Able to read and understand Dutch. 4) 18 years of age or older. 5) Providing written informed consent.

Participants with advanced cognitive impairment, defined as a score of <24 on the Montreal Cognitive Assessment (MoCA), or a diagnosis of dementia according to the fifth edition of the Diagnostic and Statistical Manual of Mental Disorders (DSM 5, (17)) criteria at baseline, will be excluded from participation. The presence of a clear diagnosis of neurodegenerative diseases other than PD is also an exclusion criterion. Lastly, potential participants cannot take part if there are any contra-indications for a 7T MRI scan, such as claustrophobia, permanent makeup or the presence of incompatible metallic devices in their body. These exclusion criteria are also in place for the HC group.

2.3 Study procedure

This is a longitudinal observational study in which all participants will be tracked for four years. All data will be collected in one academic hospital in the Netherlands (Maastricht University Medical Centre). A 7T brain MRI will be conducted at baseline, after two years and after four years. Basic clinical and demographic information, such as age, sex, handedness, disease duration, and the total levodopa equivalent daily dose (LEDD, (18)) will also be collected. Motor, cognitive, autonomic and neuropsychiatric symptoms will all be assessed by validated questionnaires and rating scales as summarized in Table 1. The assessments have been aligned with other national and international PD cohort studies, to permit future cross validation studies (19, 20). Wearable sensors measuring movement will be applied at each wrist and at the chest during the assessment days. In addition to the tests described above, a blood sample from all participants will be collected at baseline, which will be used for genetic and epigenetic testing on genes related to PD. Providing a blood sample is not mandatory for participation.

2.4 Clinical assessments

2.4.1 Motor assessment

Motor functions will be assessed with the unified Parkinson's Disease rating scale (MDS-UPDRS) and the Hoehn and Yahr scale (H&Y). The H&Y is the most commonly used scale to estimate the global disease stage of PD patients (21). The MDS-UPDRS consists of four parts, assessing both non-motor and motor disabilities in PD (22). All four parts will be assessed by trained and certified investigators. At baseline, the UPDRS part III will also be used to check whether patients meet the MDS clinical diagnostic criteria for parkinsonism (3). The motor evaluation is performed in medication 'ON' state.

Furthermore, wearable sensor data will be collected on all testing days. The wearables contain both an accelerometer and a gyroscope and are described in more detail elsewhere (23). During each testing day, the wearables will be put on after signing the informed consent form and will be removed while preparing the participant for the 7T MRI. The wearables will be applied to the wrists by using comfortable straps. A hanger will be used for the chest wearable.

Table 1. Overview of included study measures and scales in the TRACK-PD study

Method	Outcome	Scales	Visit 1 (Baseline)	Visit 2 (2 Years) [*]	Visit 3 (4 Years) [*]
Assessed by trial assessor	Motor functioning in 'ON' state	MDS-UPDRS III (including H&Y stage)	X*	X*	X*
		MDS-UPDRS IV	X*	X*	X*
	Neuropsychological symptoms	MoCA	X	X	X
		Phonemic and semantic fluency	X	X	X
		15 Words Test	X	X	X
		Benton Judgment of Line Orientation	X	X	X
		Letter Number Sequencing	X	X	X
		Symbol Digit Modalities Test	X	X	X
		MDS-UPDRS I	X*	X*	X*
	Demographics and lifestyle	Medical history	X	X	X
		Medication	X	X	X
	Biospecimen	EDTA Plasma (DNA)	X		
		Pax Gene (RNA)	X		
	Brain structure and function	Resting-state functional MRI	X	X	X
Structural MRI (T1, T2*, neuromelanin, DWI)		X	X	X	
Wearable sensors	Motor parameters	IMU including 3-axis accelerometer and 3-axis gyroscope	X	X	X
Self-reported patient questionnaires	Neuropsychiatric symptoms	BDI	X	X	X
		QUIP-RS	X	X	X
		PAS	X	X	X
	Quality of life	PDQ-8	X*	X*	X*
	Autonomic symptoms	SCOPA-AUT	X	X	X
	Sleep disorders	RBDQ	X	X	X
Various		MDS-UPDRS II	X*	X*	X*

BDI: Beck Depression Inventory, HC: healthy controls, H&Y: Hoehn and Yahr scale, IMU: Inertial Measurement Unit, MDS-UPDRS: Movement Disorders Society Unified Parkinson Disease Rating Scale, MoCA: Montreal Cognitive Assessment, NPA: Neuropsychological assessment, PAS: Parkinson Anxiety Scale, PD: Parkinson's disease patients, PDQ-8: Parkinson's Disease Questionnaire, QUIP-RS: Questionnaire for Impulsive-Compulsive Disorders in Parkinson's disease, RBDQ: REM-sleep behaviour disorder screening questionnaire, SCOPA-AUT: Scales for Outcomes in Parkinson's Disease - Autonomic dysfunction questionnaire.

^{*} ± 60 days; ^{*} Only for PD patients

2.4.2 Autonomic assessment

The Scales for Outcomes in Parkinson's Disease - Autonomic dysfunction (SCOPA-AUT) questionnaire will be applied to assess autonomic functions in all participants. This questionnaire consists of 25 items assessing several different autonomic symptoms in patients with PD. It is a reliable and valid questionnaire for the evaluation of autonomic dysfunction in PD (24).

2.4.3 Neuropsychological assessment

At baseline, global cognitive function is assessed with the MoCA, which is a 30 point screening tool, including several cognitive domains (25). If, at baseline the MoCA score is ≥ 24 , the participant can continue the study protocol and a full neuropsychological assessment will be performed. If the MoCA score drops below 24 during follow-up, participants will remain in the study. Neuropsychological assessment consists of the following standard tests: 1. The 'Phonemic and Semantic Fluency Test' for executive function (26); 2. The 'Auditory Verbal Learning Test' for memory (27); 3. The 'Benton Judgment of Line Orientation' for visuospatial function (28); 4. The 'Symbol Digit Modalities Test' for mental speed and attention (29); and 5. The 'Letter Number Sequencing Test' for working memory (30).

2.4.4 Neuropsychiatric assessment

In addition, several questionnaires will assess psychiatric symptoms. The 'Beck Depression Inventory' (BDI), a 21-item questionnaire, is used to assess depression (31). The Parkinson Anxiety Scale (PAS) (32) is used to assess anxiety. The 'Questionnaire for Impulsive-Compulsive Disorders' in Parkinson's disease (QUIP-RS) will assess impulsive and compulsive behaviours (33). The Parkinson's Disease Questionnaire (PDQ-8) assesses quality of life of PD patients (34). For each questionnaire the total sum score will be calculated.

2.4.5 REM-sleep behaviour disorders

Symptoms related to REM-sleep behaviour disorders will be assessed by using the 'REM-sleep behaviour disorder screening questionnaire' (RBDSQ). This questionnaire is a 13-item screening tool for the detection of REM sleep behaviour disorders (35). A total score will be calculated.

2.4.6 Genetic testing

Several contributing factors for PD risk, onset, and progression of symptoms have been associated with genetic variants. Especially in early-onset PD, strong penetrant mutations have been found. Possible new MRI correlates with known genetic variants could be valuable in further understanding the genetic basis and progression of PD. However, more than 20 mutations in genes have been associated with PD onset and

more than 90 independent risk-associated variants in genome-wide association studies have been reported (36). Blood samples of the participants will be tested on common genetic variants and stored in a database for further epigenetic testing, including the examination of DNA methylation patterns (37). Drawing of the blood samples will be performed only by researchers or research nurses who are certified to do this. From every participant two ethylenediamine tetra-acetic acid buffered (EDTA) tubes with a size of 4.5 ml each and two PAXgene® tubes with a size of 2.5ml each will be collected. These blood samples will be transferred to the BioBank of Maastricht University Medical Centre, where they will be stored at -80°C.

2.4.7 MRI acquisition

Participants will be scanned on a 7T MRI scanner (Magnetom, Siemens, Erlangen, Germany) equipped with a Nova Medical 32-channel head coil. Dielectric pads will be applied to enhance the signal in the temporal brain regions (38). In PD patients, the MRI will be carried out while they are in the ON-medication state in order to reduce the possibility of motion artefacts due to tremor and to reflect clinical practice. During the scan session participants will also watch a movie to reduce movements. Cardiac and respiratory physiological signals will be measured synchronized with the scan start.

A localizer sequence will be acquired for optimal planning. B0 and B1 mapping and shimming will be performed to correct for field inhomogeneities. The scan protocol consists of 1) a whole-brain MP2RAGE (Magnetization Prepared 2 Rapid Acquisition Gradient Echoes) scan with an acquisition time of 10:57 minutes, resulting in a T1-weighted image and a quantitative T1 map. This MP2RAGE is combined with a SA2RAGE (Saturation Prepared with 2 Rapid Gradient Echoes) scan of 2:40 minutes, to eliminate any B1-related biases from the results, which can reduce the accuracy of the measurements (39), 2) A multi-echo GRE, 4.8 cm coverage, acquisition time 7:42 minutes, used to provide susceptibility (T2*)-weighted images and T2* maps. In addition, quantitative susceptibility maps can be reconstructed from the same acquisition. This scan is sensitive for measuring variations in iron concentration (Field of View (FoV) is shown in Figure 1), 3) A magnetization transfer-weighted TFL (MTW TFL), 3 cm coverage, acquisition time 4:38 minutes, which can be used to visualise myelination or nuclei containing neuromelanin such as the substantia nigra and locus coeruleus (40) (FoV is shown in Figure 2), 4) A whole-brain diffusion weighted scan along 66 random directions with an average b-value of 2000s/mm² mixed with six B0-volumes and one additional B0-volume and five diffusion weighted volume recorded with opposite phase-encoding direction, acquisition time 9:48 minutes, 5) A whole brain resting-state fMRI scan with 280 volumes and an additional five volumes recorded with reverse phase-encoding direction. Acquisition time for the resting-state fMRI is 11:12 minutes. During the resting-state fMRI scan participants are instructed to focus on a crosshair

projected on a screen while letting their mind wander and not to think about anything in particular. In total the scan protocol takes a little less than 60 minutes and details can be found in Table 2.

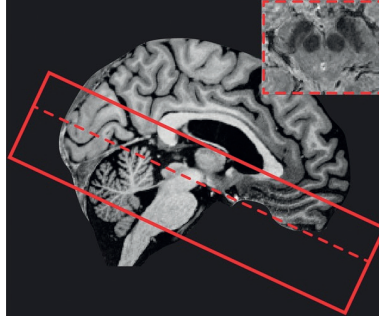


Figure 1. Visualisation of the multi-echo GRE field-of-view (FoV) with 4.8 cm coverage. The FoV is placed perpendicular to the brainstem. The inferior border of the FoV is positioned at the bottom of the 4th ventricle. Furthermore, an example of the multi-echo GRE transverse brain stem slice at the substantia nigra is displayed in the right corner.

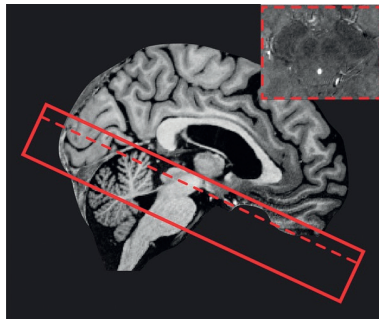


Figure 2. Visualisation of the magnetization transfer-weighted TFL (MTW TFL) field-of-view (FoV) with 3 cm coverage. The FoV is placed perpendicular to the brainstem. It covers the area between the upper part of the mesencephalon and the lateral recess of the 4th ventricle. Furthermore, an example of the MTW TFL transverse brain stem slice at the substantia nigra is displayed in the right corner.

Table 2. Technical details of the MRI protocol used for the TRACK-PD study

Weighting	Sequence	TE (ms)	TR (ms)	TI (ms)	Flip angle (°)	FoV (mm)	Resolution (mm ³) (x-y-z)	Slices	Orientation
T1	MP2RAGE	2.51	5000	900, 2750	5 and 3	208	0.65 x 0.65 x 0.65	240	Sagittal
	SA2RAGE	0.78	2400	58, 1800	4 and 10	256	2.0 x 2.0 x 2.0	88	Sagittal
T2*	GRE	2.49, 6.75, 13.50, 20.75	33	-	12	204	0.5 x 0.5 x 0.5	96	Axial
Neuromelanin	MTW TFL	4.08	538	-	8	192	0.4 x 0.4 x 0.5	60	Axial
Diffusion	EPI	60.6	7000	-	90	192	1.5 x 1.5 x 1.5	80	Axial
fMRI	BOLD	18.6	2000	-	70	200	1.25 x 1.25 x 1.25	92	Axial

MP2RAGE = Magnetization Prepared 2 Rapid Acquisition Gradient Echoes. SA2RAGE = Saturation Prepared with 2 Rapid Gradient Echoes), GRE = Gradient Echo, MTW TFL = Magnetization transfer weighted TFL, EPI = Echo Planar Imaging, BOLD = Blood oxygen level dependent, TE = Echo time, TR = Repetition time, TI = Inversion Time, FoV = Field of view.

2.5 Sample size calculation

Previous longitudinal MRI studies in PD have included a variety of sample sizes, but most studies contain about 15 to 25 patients and HC (41-43). One larger longitudinal 3T MRI study, the ICICLE-PD, recruited 105 PD patients and 37 matched HC and followed their participants for 18 months (44). So far, no longitudinal 7T studies nor 7T MRI studies combining multiple MRI sequences in PD patients have been published. However, several cross-sectional 7T MRI studies have been performed, all consisting of relatively small patient groups varying from 13 to 36 PD patients (45-49).

A sample size calculation was based on the effect size of a study that evaluated the dorsal nigral hyperintensity sign in PD and HC at T2* weighted 7T images (47). Our power analysis with a significance level of $\alpha = 0.05$ and power of 0.80 was performed with G*Power (version 3.1.9.4) (50). Based on this analysis a total sample size of 102 participants, 51 PD and 51 HC, is needed to detect a significant difference between these two groups. Due to an expected loss to follow-up of about ten percent for HC, we decided to include 60 HC patients instead of 51. For our secondary objectives we will also perform subgroup analysis for PD patients. To assure a sufficient amount of PD patients for this subgroup analysis, we decided to double the amount of PD patients to 102. Furthermore, the drop-out rate in the PD group is expected to be higher compared to the HCs, due to an increase in disease burden over time. With an expected loss to follow-up of twenty percent, the PD group should include 130 participants.

2.6 Patients and public involvement

This study has been designed in collaboration with the Dutch Parkinson society. This patient organisation has a scientific advisory board that comments on and contributes to research proposals from a patient's perspective. They will remain involved in the study

during the inclusion and follow-up period. Throughout the study, we aim to stay in close contact with all participants. They will be kept informed about the study progress with newsletters and updates on the study website. Moreover, when problems or questions occur, participants can easily contact the study team by e-mail or phone. In this way we intend to minimise the loss to follow-up.

2.7 Data collection and management

The data collected in this study will be stored in a pseudonymised manner. All patient data will be linked to a unique participant number. Two separate databases are in place. Source data of the participants will be kept in a password protected, secure database, which is only accessible by the research team, the health inspector, the data monitor (of the CTCM (Clinical Trial Centre Maastricht)) and members of the medical ethics committee. A second database will be used to store all experimental data and participant numbers. The anonymous data will only be used for research purposes and publications or communications. The handling of personal data will comply with the EU General Data Protection Regulation (GDPR) and the Dutch Act on Implementation of the GDPR. The final study dataset can be accessed only by the research team. Datasets will be made available for other investigators on reasonable request. All study information will be stored for 15 years. Patients who do not give consent to store their information for 15 years, cannot be included in the study.

2.8 Data analysis

In this study we will analyse both structural and functional MRI data. Raw MRI data will be converted to BIDS NIFTI format for further processing (51, 52). Functional and anatomical MRI images will be pre-processed using MATLAB (MathWorks, version R2018a), the FMRIB Software Library (FSL) (53) and FreeSurfer (www.freesurfer.net) (54). Further analysis will be carried out using FSL. All multi-echo GRE, neuromelanin, DWI and functional MRI images will be coregistered with anatomical T1 weighted structural images. Segmentation of the substantia nigra (SN) and locus coeruleus (LC) is manually performed. The subareas of the SN, the pars reticulata and pars compacta ventralis and dorsalis, will also be differentiated. Volumes and signal-to-noise ratio of the SN and LC will be calculated on iron and neuromelanin sensitive images. Both quantitative and qualitative evaluation of the iron sensitive sequences will be performed. For DWI images, diffusion tensor imaging (DTI) will be applied. Furthermore, the fractional anisotropy (FA), radial diffusivity, axial diffusivity and mean diffusivity will be extracted in the SN ROIs. A whole-brain analysis using independent component analysis will be carried out for the functional MRI data. Subsequently, a graph theoretical method is performed to evaluate the topological properties in the whole brain. Finally, predefined ROIs will be assessed. A specific interest exists for regions that are part of the default mode network and fronto-parietal network.

Careful visual inspection and quantification of movement will be assessed after each processing step. Both structural and functional MRI differences between HCs and PD patients will be investigated, as well as longitudinal MRI changes in the PD brain.

Clinical and demographic variables will be taken into account as covariates, including handedness, sex, age, disease progression, dopaminergic medication, genetic characteristics, and motor, neuropsychiatric, cognitive and autonomic scores. More specifically, since dopaminergic medication influences brain connectivity patterns both in a linear and non-linear way, the LEDD will be included as a covariate in all fMRI data analysis (55, 56). The numerical variables will be described as means, median, standard deviations and ranges. Categorical variables will be described as frequencies, percentiles, and percentages.

Demographic and disease related variables of the samples at baseline will be compared with Pearson's chi-squared test for categorical variables (non-parametric test) and with the student's t-test and one-way ANOVA for continuous variables. These variables will be included as covariates in the analyses where appropriate.

For our primary objective we will compare structural and functional MRI characteristics between PD patients and HC. This includes iron-sensitive, neuromelanin-sensitive, diffusion weighted and functional sequences. Structural and functional differences will be calculated by using a linear regression model for continuous variables and a logistic regression model for binary variables. Covariates will be included when needed. The false discovery rate (FDR) method for the correction of multiple comparisons will be applied where appropriate.

After performing the regression analyses for both structural and functional MRI data, we will use a receiver operating characteristics (ROC) method to compute the sensitivity and specificity of the differences found between PD and HC. Furthermore, internal validation will be carried out by using a bootstrap method. In this way we aim to detect the optimal cut-off values for structural and functional differences which distinguish PD patients from HC. Finally, the optimal combination of variables for disease prediction will be assessed by using a logistic regression model. By combining the most important variables, we aim to develop a reliable diagnostic tool with high sensitivity and specificity, that enables us to distinguish PD from HC.

For our secondary objectives, a data-driven cluster analysis will be performed based on the standardized scores of the different variables assessed in our study (motor, genetic, cognitive, autonomic, RBDSQ and neuropsychiatric variables). This enables us to identify different clinical subtypes of PD without a priori assumptions. Structural and functional

MRI characteristics will be compared between these different subgroups of PD patients in the same way as described above. Also, longitudinal changes in clinical motor and non-motor symptoms and MRI characteristics will be compared between subgroups by applying a multivariate linear regression model to detect the degree of change for each variable between the PD subgroups.

Furthermore, the longitudinal clinical data (motor, genetic, cognitive, autonomic, RBDSQ and neuropsychiatric variables) of both follow-up moments will be correlated with the MRI characteristics at baseline by using a linear regression model. In this way it can be investigated if the disease course of an individual patient can be predicted based on early MRI-characteristics.

2.9 Ethics, safety and dissemination

The study will be conducted according to the principles of the Declaration of Helsinki (Fortaleza, Brazil, 2013) and in accordance with the Medical Research Involving Human Subjects Act (WMO). All unwanted and harmful outcomes spontaneously reported by the participants, that may or not be related to this study, will be recorded. In case of a serious adverse event, the Ethics committee and relevant authorities will be notified immediately.

This study was approved by the Institutional Review Committee (IRB) of the Maastricht University Medical Centre and written informed consent will be obtained from all participants prior to inclusion. Also, participants are given the choice to provide additional consent for the use of study data and biological specimens in ancillary studies. Before consenting, all participants will be extensively informed about the study. During the study patients have the right to withdraw from the study without explanation at any time.

Monitoring of the study will be performed at random moments by employees of CTCM. Those employees are trained and certified in monitoring studies and are not in any way involved in the study.

The results of this study will be shared with clinicians and researchers through scientific conferences and publications in peer-reviewed journals. During the progress of the study preliminary analysis and data validation will be performed, new relevant findings may be published during the study. Furthermore, a summary of the results will also be shared with patients on our web page in an easily comprehensible manner.

3. Discussion

The current error-rate for a reliable diagnosis of PD is unacceptable and at this moment it is unclear to what extent changes on MR imaging in PD patients are associated with the clinical deterioration over time. Ultra-high field imaging has made significant progress in recent years and has a resolution that might replace the requirement for a histologically confirmed diagnosis of PD. This new longitudinal ultra-high field 7T MRI study in a PD cohort in which relevant clinical metrics will be obtained for 4 years, will likely improve and change our diagnostic uncertainty in PD.

Several cross-sectional and cohort studies have indicated correlations between MRI characteristics and the clinical symptoms in PD. Most convincingly, a positive correlation between the iron content of the substantia nigra pars compacta and the progression of motor symptoms in PD was demonstrated in several studies (11, 12, 41, 46). In addition, neuromelanin sensitive T1-weighted MRI sequences of the substantia nigra pars compacta may be useful for monitoring motor complications of PD (57). Also, functional MRI studies demonstrate an altered functional connectivity in PD compared to HC, which is most consistently found in the posterior part of the inferior parietal lobule (58). Given these developments, the use of multiple MRI modalities and post-processing techniques such as quantitative susceptibility mapping (QSM) at higher field strengths have the potential to increase diagnostic certainty in PD. However, this has not been tested in a large longitudinal cohort study yet. Furthermore, when high-field MRI research is able to detect whether clinical deterioration or certain PD subtypes are correlated with specific MRI changes, patients can be more accurately informed about their prognosis and treatment options can be adjusted to the individual patient.

In order to correlate MRI changes with clinical progression, monitoring PD symptoms in robust longitudinal clinimetric testing is mandatory (19, 59). Wearable sensors are increasingly used for this purpose (60). They show promise in detecting tremor (61), freezing of gait (62), bradykinesia, and dyskinesia (63, 64). Whether wearables will eventually replace commonly used clinical scoring instruments, such as the MDS-UPDRS remains to be seen (22). The Personalized Parkinson cohort study in The Netherlands is a parallel longitudinal study in which a wearable sensor will be worn for 24h a day during a two year follow-up period (19). A subgroup of these participants will also participate in the TRACK-PD study. In the TRACK-PD study, wearables are used at baseline and during follow-up visits in addition to classical MDS scoring scales to measure symptom severity. Data from both studies can potentially be combined in the future, providing an even more complete pallet of information to identify patient subgroups in PD.

A potential limitation of this study is the ability of PD patients to lie still in the scanner for one hour and the possibility of motion artefacts. However, previous studies have indicated that PD patients are capable and are willing to lie for one hour in the scanner for obtaining high quality images (65). Due to the longitudinal nature of this study there is also a risk of high dropout rates during the follow-up period. By including a significant number of participants, we intend to compensate for the expected loss to follow-up. Moreover, by informing them regularly about the study progress, we aim to stay in close contact with all participants and to reduce the amount of loss to follow-up.

4. Conclusion

This is the first longitudinal, observational, ultra-high field MRI study in PD patients. With the TRACK-PD study, an important contribution can be made for the improvement of the current diagnostic process in PD. Moreover, this study will be able to provide valuable information related to the different clinical phenotypes of PD and their correlating MRI characteristics. The long-term aim of this study is to better understand PD and develop new biomarkers for disease progression which may help future new therapy development. Eventually, this may lead to predictive models for individual PD patients and towards personalized medicine in the future.

5. List of abbreviations

BDI: Beck Depression Inventory, BOLD: Blood oxygen level dependent, CTCM: Clinical Trial Centre Maastricht, EDTA: ethylenediamine tetra-acetic acid, EPI: Echo Planar Imaging, fMRI: Functional MRI, GDPR: General Data Protection Regulation, GRE: Gradient Echo, FoV: Field of view, HC: healthy controls, H&Y: Hoehn and Yahr scale, IMU: Inertial Measurement Unit, LEDD: Levodopa equivalent dose, MDS-UPDRS: Movement Disorders Society Unified Parkinson Disease Rating Scale, MoCA: Montreal Cognitive Assessment, MP2RAGE: Magnetization Prepared 2 Rapid Acquisition Gradient Echoes, MRI: Magnetic Resonance Imaging, MTWTFL: Magnetization transfer weighted TFL, NPA: Neuropsychological assessment, PAS: Parkinson Anxiety Scale, PD: Parkinson's disease patients, PDQ-8: Parkinson's Disease Questionnaire, QSM: Quantitative susceptibility mapping, QUIP-RS: Questionnaire for Impulsive-Compulsive Disorders in Parkinson's disease, RBDSQ: REM-sleep behaviour disorder screening questionnaire, SA2RAGE: Saturation Prepared with 2 Rapid Gradient Echoes, SCOPA-AUT: Scales for Outcomes in Parkinson's Disease - Autonomic dysfunction questionnaire. TE: Echo time, TI: Inversion time, TR: Repetition time.

6. Declarations

6.1 Ethics approval and consent to participate

This study will be conducted according to the principles of the Declaration of Helsinki (Fortaleza, Brazil, 2013) and in accordance with the Medical Research Involving Human Subjects Act (WMO). The handling of personal data will comply with the EU General Data Protection Regulation (GDPR) and the Dutch Act on Implementation of the GDPR. This study was approved by the Institutional Review Committee (IRB) of the Maastricht University Medical Centre (METC18-027; NL67241.068.18), and registered in the Dutch Trial Register (Trial NL7558; <https://www.trialregister.nl/trial/7558>). Written informed consent is obtained from all participants prior to inclusion. Participants who are not able to provide informed consent due to limitations in their cognitive status, will be excluded from participation. During the study, patients have the right to withdraw from the study without explanation at any time.

6.2 Availability of data and materials

The datasets generated during this study will become available from the corresponding author on reasonable request.

6.3 Funding

This study is funded by a grant from the Weijerhorst Foundation (Stichting de Weijerhorst). This Dutch foundation supports and promotes activities in the public interest, in particular scientific research. The sponsor has no role in the design of the study and collection, analysis, and interpretation of data. Also, the sponsor was not involved in writing this manuscript.

7. References

1. Jankovic J. Parkinson's disease: clinical features and diagnosis. *J Neurol Neurosurg Psychiatry*. 2008;79(4):368-76.
2. Al-Radaideh AM, Rababah EM. The role of magnetic resonance imaging in the diagnosis of Parkinson's disease: a review. *Clin Imaging*. 2016;40(5):987-96.
3. Postuma RB, Berg D, Stern M, Poewe W, Olanow CW, Oertel W, et al. MDS clinical diagnostic criteria for Parkinson's disease. *Mov Disord*. 2015;30(12):1591-601.
4. Hughes AJ, Daniel SE, Ben-Shlomo Y, Lees AJ. The accuracy of diagnosis of parkinsonian syndromes in a specialist movement disorder service. *Brain*. 2002;125(Pt 4):861-70.
5. Konno T, Deuschlander A, Heckman MG, Ossi M, Vargas ER, Strongosky AJ, et al. Comparison of clinical features among Parkinson's disease subtypes: A large retrospective study in a single center. *J Neurol Sci*. 2018;386:39-45.
6. Fereshtehnejad SM, Zeighami Y, Dagher A, Postuma RB. Clinical criteria for subtyping Parkinson's disease: biomarkers and longitudinal progression. *Brain*. 2017;140(7):1959-76.
7. Iwaki H, Blauwendraat C, Leonard HL, Liu G, Maple-Grodem J, Corvol JC, et al. Genetic risk of Parkinson disease and progression:: An analysis of 13 longitudinal cohorts. *Neurol Genet*. 2019;5(4):e348.
8. Thenganatt MA, Jankovic J. Parkinson disease subtypes. *JAMA Neurol*. 2014;71(4):499-504.
9. Sieber BA, Landis S, Koroshetz W, Bateman R, Siderowf A, Galpern WR, et al. Prioritized research recommendations from the National Institute of Neurological Disorders and Stroke Parkinson's Disease 2014 conference. *Ann Neurol*. 2014;76(4):469-72.
10. Lehericy S, Vaillancourt DE, Seppi K, Monchi O, Rektorova I, Antonini A, et al. The role of high-field magnetic resonance imaging in parkinsonian disorders: Pushing the boundaries forward. *Mov Disord*. 2017;32(4):510-25.
11. Schwarz ST, Afzal M, Morgan PS, Bajaj N, Gowland PA, Auer DP. The 'swallow tail' appearance of the healthy nigrosome - a new accurate test of Parkinson's disease: a case-control and retrospective cross-sectional MRI study at 3T. *PLoS One*. 2014;9(4):e93814.
12. Reiter E, Mueller C, Pinter B, Krismer F, Scherfler C, Esterhammer R, et al. Dorsolateral nigral hyperintensity on 3.0T susceptibility-weighted imaging in neurodegenerative Parkinsonism. *Mov Disord*. 2015;30(8):1068-76.
13. Bae YJ, Kim JM, Kim E, Lee KM, Kang SY, Park HS, et al. Loss of Nigral Hyperintensity on 3 Tesla MRI of Parkinsonism: Comparison With (123) I-FP-CIT SPECT. *Mov Disord*. 2016;31(5):684-92.
14. Castellanos G, Fernandez-Seara MA, Lorenzo-Betancor O, Ortega-Cubero S, Puigvert M, Uranga J, et al. Automated neuromelanin imaging as a diagnostic biomarker for Parkinson's disease. *Mov Disord*. 2015;30(7):945-52.
15. Wolters AF, van de Weijer SCF, Leentjens AFG, Duits AA, Jacobs HIL, Kuijff ML. Resting-state fMRI in Parkinson's disease patients with cognitive impairment: A meta-analysis. *Parkinsonism Relat Disord*. 2019;62:16-27.
16. Filippi M, Elisabetta S, Piramide N, Agosta F. Functional MRI in Idiopathic Parkinson's Disease. *Int Rev Neurobiol*. 2018;141:439-67.
17. Association AP. Diagnostic and statistical manual of mental disorders (DSM-5®): American Psychiatric Pub; 2013.
18. Tomlinson CL, Stowe R, Patel S, Rick C, Gray R, Clarke CE. Systematic review of levodopa dose equivalency reporting in Parkinson's disease. *Mov Disord*. 2010;25(15):2649-53.

19. Bloem BR, Marks WJ, Jr., Silva de Lima AL, Kuijf ML, van Laar T, Jacobs BPF, et al. The Personalized Parkinson Project: examining disease progression through broad biomarkers in early Parkinson's disease. *BMC Neurol.* 2019;19(1):160.
20. Manniën J, Ledderhof, T., Verspaget, H.W., Snijder, R.R., Flikkenschild, E.F., van Scherrenburg, N.P.C., Stolk, R.P., Zielhuis, G.A. The Parelinoer Institute: A National Network of Standardized Clinical Biobanks in the Netherlands. *Open Journal of Bioresources.* 2017;4(1), 3.
21. Goetz CG, Poewe W, Rascol O, Sampaio C, Stebbins GT, Counsell C, et al. Movement Disorder Society Task Force report on the Hoehn and Yahr staging scale: status and recommendations. *Mov Disord.* 2004;19(9):1020-8.
22. Goetz CG, Tilley BC, Shaftman SR, Stebbins GT, Fahn S, Martinez-Martin P, et al. Movement Disorder Society-sponsored revision of the Unified Parkinson's Disease Rating Scale (MDS-UPDRS): scale presentation and clinimetric testing results. *Mov Disord.* 2008;23(15):2129-70.
23. Heijmans M, Habets JGV, Herff C, Aarts J, Stevens A, Kuijf ML, et al. Monitoring Parkinson's disease symptoms during daily life: a feasibility study. *NPJ Parkinsons Dis.* 2019;5:21-.
24. Visser M, Marinus J, Stiggelbout AM, Van Hilten JJ. Assessment of autonomic dysfunction in Parkinson's disease: the SCOPA-AUT. *Mov Disord.* 2004;19(11):1306-12.
25. Palavra NC, Naismith SL, Lewis SJ. Mild cognitive impairment in Parkinson's disease: a review of current concepts. *Neurol Res Int.* 2013;2013:576091.
26. Gladsjo JA, Schuman CC, Evans JD, Peavy GM, Miller SW, Heaton RK. Norms for letter and category fluency: demographic corrections for age, education, and ethnicity. *Assessment.* 1999;6(2):147-78.
27. Vakil E, Blachstein H. Rey Auditory-Verbal Learning Test: structure analysis. *J Clin Psychol.* 1993;49(6):883-90.
28. Benton AL, Varney NR, Hamsher KD. Visuospatial judgment. A clinical test. *Arch Neurol.* 1978;35(6):364-7.
29. Smith A. Symbol Digit Modalities Test (SDMT) Manual. Los Angeles, Western Psychological Services. 1982.
30. Wechsler D. Wechsler adult intelligence scale. San Antonio, TX: Psychological Corporation. 2008.
31. Visser M, Leentjens AF, Marinus J, Stiggelbout AM, van Hilten JJ. Reliability and validity of the Beck depression inventory in patients with Parkinson's disease. *Mov Disord.* 2006;21(5):668-72.
32. Leentjens AF, Dujardin K, Pontone GM, Starkstein SE, Weintraub D, Martinez-Martin P. The Parkinson Anxiety Scale (PAS): development and validation of a new anxiety scale. *Mov Disord.* 2014;29(8):1035-43.
33. Probst CC, Winter LM, Moller B, Weber H, Weintraub D, Witt K, et al. Validation of the questionnaire for impulsive-compulsive disorders in Parkinson's disease (QUIP) and the QUIP-rating scale in a German speaking sample. *J Neurol.* 2014;261(5):936-42.
34. Luo N, Tan LC, Zhao Y, Lau PN, Au WL, Li SC. Determination of the longitudinal validity and minimally important difference of the 8-item Parkinson's Disease Questionnaire (PDQ-8). *Mov Disord.* 2009;24(2):183-7.
35. Stiasny-Kolster K, Mayer G, Schafer S, Moller JC, Heinzel-Gutenbrunner M, Oertel WH. The REM sleep behavior disorder screening questionnaire--a new diagnostic instrument. *Mov Disord.* 2007;22(16):2386-93.
36. Blauwendraat C, Nalls MA, Singleton AB. The genetic architecture of Parkinson's disease. *Lancet Neurol.* 2020;19(2):170-8.

37. Jakubowski JL, Labrie V. Epigenetic Biomarkers for Parkinson's Disease: From Diagnostics to Therapeutics. *J Parkinsons Dis.* 2017;7(1):1-12.
38. Teeuwisse WM, Brink WM, Webb AG. Quantitative assessment of the effects of high-permittivity pads in 7 Tesla MRI of the brain. *Magn Reson Med.* 2012;67(5):1285-93.
39. Eggenschwiler F, Kober T, Magill AW, Gruetter R, Marques JP. SA2RAGE: a new sequence for fast B1+ -mapping. *Magn Reson Med.* 2012;67(6):1609-19.
40. Priovoulos N, Jacobs HIL, Ivanov D, Uludag K, Verhey FRJ, Poser BA. High-resolution in vivo imaging of human locus coeruleus by magnetization transfer MRI at 3T and 7T. *Neuroimage.* 2018;168:427-36.
41. Wieler M, Gee M, Martin WR. Longitudinal midbrain changes in early Parkinson's disease: iron content estimated from R2*/MRI. *Parkinsonism Relat Disord.* 2015;21(3):179-83.
42. Ofori E, Pasternak O, Planetta PJ, Li H, Burciu RG, Snyder AF, et al. Longitudinal changes in free-water within the substantia nigra of Parkinson's disease. *Brain.* 2015;138(Pt 8):2322-31.
43. Ulla M, Bonny JM, Ouchchane L, Rieu I, Claise B, Durif F. Is R2* a new MRI biomarker for the progression of Parkinson's disease? A longitudinal follow-up. *PLoS One.* 2013;8(3):e57904.
44. Mak E, Su L, Williams GB, Firbank MJ, Lawson RA, Yarnall AJ, et al. Baseline and longitudinal grey matter changes in newly diagnosed Parkinson's disease: ICICLE-PD study. *Brain.* 2015;138(Pt 10):2974-86.
45. Alkemade A, de Hollander G, Keuken MC, Schafer A, Ott DVM, Schwarz J, et al. Comparison of T2*-weighted and QSM contrasts in Parkinson's disease to visualize the STN with MRI. *PLoS One.* 2017;12(4):e0176130.
46. Kim JM, Jeong HJ, Bae YJ, Park SY, Kim E, Kang SY, et al. Loss of substantia nigra hyperintensity on 7 Tesla MRI of Parkinson's disease, multiple system atrophy, and progressive supranuclear palsy. *Parkinsonism Relat Disord.* 2016;26:47-54.
47. Pyatigorskaya N, Magnin B, Mongin M, Yahia-Cherif L, Valabregue R, Arnaldi D, et al. Comparative Study of MRI Biomarkers in the Substantia Nigra to Discriminate Idiopathic Parkinson Disease. *AJNR Am J Neuroradiol.* 2018;39(8):1460-7.
48. Cosottini M, Frosini D, Pesaresi I, Costagli M, Biagi L, Ceravolo R, et al. MR imaging of the substantia nigra at 7 T enables diagnosis of Parkinson disease. *Radiology.* 2014;271(3):831-8.
49. Schmidt MA, Engelhorn T, Marxreiter F, Winkler J, Lang S, Kloska S, et al. Ultra high-field SWI of the substantia nigra at 7T: reliability and consistency of the swallow-tail sign. *BMC Neurol.* 2017;17(1):194.
50. Faul F, Erdfelder E, Lang AG, Buchner A. G*Power 3: a flexible statistical power analysis program for the social, behavioral, and biomedical sciences. *Behav Res Methods.* 2007;39(2):175-91.
51. Gorgolewski KJ, Alfaro-Almagro F, Auer T, Bellec P, Capota M, Chakravarty MM, et al. BIDS apps: Improving ease of use, accessibility, and reproducibility of neuroimaging data analysis methods. *PLoS Comput Biol.* 2017;13(3):e1005209.
52. Li X, Morgan PS, Ashburner J, Smith J, Rorden C. The first step for neuroimaging data analysis: DICOM to NIfTI conversion. *J Neurosci Methods.* 2016;264:47-56.
53. Jenkinson M, Beckmann CF, Behrens TE, Woolrich MW, Smith SM. Fsl. *Neuroimage.* 2012;62(2):782-90.
54. Dale AM, Fischl B, Sereno MI. Cortical surface-based analysis. I. Segmentation and surface reconstruction. *Neuroimage.* 1999;9(2):179-94.
55. Cole DM, Beckmann CF, Oei NY, Both S, van Gerven JM, Rombouts SA. Differential and distributed effects of dopamine neuromodulations on resting-state network connectivity. *Neuroimage.* 2013;78:59-67.

56. Dang LC, O'Neil JP, Jagust WJ. Dopamine supports coupling of attention-related networks. *J Neurosci*. 2012;32(28):9582-7.
57. Hatano T, Okuzumi A, Kamagata K, Daida K, Taniguchi D, Hori M, et al. Neuromelanin MRI is useful for monitoring motor complications in Parkinson's and PARK2 disease. *J Neural Transm (Vienna)*. 2017;124(4):407-15.
58. Tahmasian M, Eickhoff SB, Giehl K, Schwartz F, Herz DM, Drzezga A, et al. Resting-state functional reorganization in Parkinson's disease: An activation likelihood estimation meta-analysis. *Cortex*. 2017;92:119-38.
59. Parkinson Progression Marker I. The Parkinson Progression Marker Initiative (PPMI). *Prog Neurobiol*. 2011;95(4):629-35.
60. Sanchez-Ferro A, Elshehabi M, Godinho C, Salkovic D, Hobert MA, Domingos J, et al. New methods for the assessment of Parkinson's disease (2005 to 2015): A systematic review. *Mov Disord*. 2016;31(9):1283-92.
61. Delrobaei M, Memar S, Pieterman M, Stratton TW, Mclsaac K, Jog M. Towards remote monitoring of Parkinson's disease tremor using wearable motion capture systems. *J Neurol Sci*. 2018;384:38-45.
62. Rodriguez-Martin D, Sama A, Perez-Lopez C, Catala A, Moreno Arostegui JM, Cabestany J, et al. Home detection of freezing of gait using support vector machines through a single waist-worn triaxial accelerometer. *PLoS One*. 2017;12(2):e0171764.
63. Griffiths RI, Kotschet K, Arfon S, Xu ZM, Johnson W, Drago J, et al. Automated assessment of bradykinesia and dyskinesia in Parkinson's disease. *J Parkinsons Dis*. 2012;2(1):47-55.
64. Delrobaei M, Baktash N, Gilmore G, Mclsaac K, Jog M. Using Wearable Technology to Generate Objective Parkinson's Disease Dyskinesia Severity Score: Possibilities for Home Monitoring. *IEEE Trans Neural Syst Rehabil Eng*. 2017;25(10):1853-63.
65. Plantinga BR, Temel Y, Duchin Y, Uludag K, Patriat R, Roebroek A, et al. Individualized parcellation of the subthalamic nucleus in patients with Parkinson's disease with 7T MRI. *Neuroimage*. 2018;168:403-11.

A large, stylized teal number '6' is centered on the page. A dark blue horizontal bar is positioned to the left of the number, partially overlapping its left side.

CHAPTER 6

Neuromelanin related ultra-high field signal intensity of the locus coeruleus differs between Parkinson's disease and controls

Wolters AF, Heijmans M, Priovoulos N, Jacobs HIL, Postma AA, Temel Y, Kuijf ML, Michielse S.

Abstract

Introduction: Neuromelanin related signal changes in catecholaminergic nuclei are considered as a promising MRI biomarker in Parkinson's disease (PD). Until now, most studies have investigated the substantia nigra (SN), while signal changes might be more prominent in the locus coeruleus (LC). Ultra-high field MRI improves the visualisation of these small brainstem regions and might support the development of imaging biomarkers in PD.

Objectives: To compare signal intensity of the SN and LC on Magnetization Transfer MRI between PD patients and healthy controls (HC) and to explore its association with cognitive performance in PD.

Methods: This study was conducted using data from the TRACK-PD study, a longitudinal 7T MRI study. A total of 78 early-stage PD patients and 36 HC were included. A mask for the SN and LC was automatically segmented and manually corrected. Neuromelanin related signal intensity of the SN and LC was compared between PD and HC.

Results: PD participants showed a lower contrast-to-noise ratio (CNR) in the right SN ($p=0.029$) and left LC ($p=0.027$). After adding age as a confounder, the CNR of the right SN did not significantly differ anymore between PD and HC ($p=0.055$). Additionally, a significant positive correlation was found between the SN CNR and memory function.

Discussion: This study confirms that neuromelanin related signal intensity of the LC differs between early-stage PD patients and HC. No significant difference was found in the SN. This supports the theory of bottom-up disease progression in PD. Furthermore, loss of SN integrity might influence working memory or learning capabilities in PD patients.

1. Introduction

Parkinson's disease (PD) is the second most common neurodegenerative disorder after Alzheimer's disease and its incidence is expected to grow exponentially in the coming years (1). It is characterized by motor symptoms, such as bradykinesia, rigidity and tremor, and non-motor symptoms, such as depression, cognitive impairment and autonomic dysfunction (2, 3). The diagnosis of PD is based on clinical observations and therefore remains challenging. Patients often experience a delay in diagnosis and about a quarter of the clinical diagnoses of parkinsonism are incorrect (4).

In clinical practice, Magnetic Resonance Imaging (MRI) is often used as a method to exclude other potential causes of parkinsonian symptoms. To date, it is impossible to diagnose a patient with PD solely based on MRI characteristics. However, in recent years a lot of effort has been put into the development of MRI techniques that could be of interest in search for a potential PD biomarker (5). Magnetization Transfer (MT) MRI, a magnetization exchange between short T2 water protons bound to macromolecules and freely moving intra- and extra-cellular protons, has been shown to measure neuromelanin related signal in small catecholaminergic nuclei (6). Moreover, ultra-high-field 7T MRI provides an increased spatial resolution and a higher signal-to-noise (SNR) ratio, thereby enabling the visualisation of these small brainstem nuclei (7). This new imaging techniques and higher field strength are therefore of specific interest in the diagnostic work-up of PD.

The visualisation of neuromelanin related signal on anatomical MRI is considered one of the most promising radiological biomarkers in PD. The insoluble pigment neuromelanin is a by-product of the oxidative metabolism of dopamine and noradrenaline and is predominantly situated in the substantia nigra (SN) and locus coeruleus (LC) (7, 8). Although the biological source of the neuromelanin contrast on neuromelanin sensitive MRI sequences is not entirely clear, it is most likely indirectly related to neuromelanin cell density (9, 10). In PD, MRI studies consistently show lower neuromelanin related signal intensity and volume in the SN compared to healthy controls (HC) (11, 12, 13). Longitudinal changes in SN signal intensity on MRI might even be able to serve as a biomarker for disease progression (14, 15). However, until now this has mainly been investigated with 3T MRI, while it might be more reliable to visualize these small nuclei with 7T MRI (7). Furthermore, the vast majority of 3T MRI studies have focussed on the SN, while previous research suggests that in most PD patients neuromelanin related signal alterations may be more prominent in the LC (16). This is in line with the progression of neuropathology according to the Braak hypothesis, which states that the propagation of pathology goes via the brainstem upwards (17). However, recent evidence suggests

two different spreading routes for the pathologic process in PD, which could explain why most, but not all patients display more prominent alterations in the LC (18).

Furthermore, noradrenergic neurons in the LC are important for cognitive performance (19). This is underlined by the fact that LC alterations have extensively been reported in Alzheimer's disease (20). Moreover, in a previous 3T MRI study a lower signal in the LC was found in PD patients with cognitive impairment compared to HC participants (21). It is therefore suggested that alterations in LC functioning might contribute to cognitive decline in PD, possibly due to noradrenergic dysfunction (22).

Based on the considerations described above, the aim of this ultra-high-field MRI study is to compare 7T MRI neuromelanin related signal intensity between PD patients and HC in both the SN and LC. We also aim to explore the association between the signal intensity in the SN and LC and cognitive performance in PD patients. While previous studies are hampered both by inadequate resolution and a potential bias stemming from manual segmentation. This is the first ultra-high field MRI study investigating NM related changes in a relatively large cohort of PD patients and HC. In addition, automated techniques for the determination of the SN and LC regions-of-interest are applied. The development of automated analysis techniques is important as it generates more objective results, facilitates easier replication of study methods, and enhances translatability to clinical practice.

2. Materials and methods

This study was conducted using baseline data from the TRACK-PD study, a longitudinal, observational 7T MRI study in PD patients. The study protocol, including details related to the MRI acquisition and neuropsychological assessment, was extensively described elsewhere (23).

2.1 Participants

Early-stage PD patients and age and sex-matched HC participants were recruited from the Maastricht University Medical Hospital and the community between July 2019 and December 2021. All PD patients had to be diagnosed with idiopathic PD (according to the UK Parkinson's Disease Brain Bank criteria) within the last three years before inclusion (24). Participants with advanced cognitive impairment, defined as a score of <24 on the Montreal Cognitive Assessment (MoCA), a diagnosis of dementia according to the fifth edition of the Diagnostic and Statistical Manual of Mental Disorders (DSM 5 (25)) criteria or other neurodegenerative diseases, were excluded from participation. Potential participants were also excluded if they had any contra-indications for 7T MRI

acquisition, such as claustrophobia or ferromagnetic implants. These exclusion criteria were also in place for the HC group.

Written informed consent was obtained from all participants prior to study participation. The study was approved by the local institutional review board (METC AZM/UM 18-027) and performed in accordance with the principles of the Declaration of Helsinki.

2.2 Clinical and neurological examination

Demographic and disease related characteristics were documented, including the levodopa equivalent daily dose (LEDD) (26). Motor functions in PD patients were assessed with the Unified Parkinson's Disease rating scale (MDS-UPDRS) (27) and Hoehn and Yahr scale (28), by certified clinicians. For PD patients, all tests were performed while in the medication "ON" state.

For the neuropsychological assessment a screening test battery was composed which assesses the most important cognitive domains. This test battery was also largely aligned with the neuropsychological test battery of other PD studies (29, 30), which enables potential future validation studies or data exchange. Overall cognitive functions were evaluated with the Montreal Cognitive Assessment (MoCA) (31). This was followed by a neuropsychological assessment battery, consisting of the following standard tests: 1. The 'Phonemic and Semantic Fluency Test' for executive function (32); 2. The 'Auditory Verbal Learning Test' for memory (15 Words Test) (33); 3. The 'Benton Judgment of Line Orientation' for visuospatial function (34); 4. The 'Symbol Digit Modalities Test' (SDMT) for mental speed and attention (35); and 5. The 'Letter Number Sequencing Test' for working memory (36).

Previous studies suggest an association between degeneration of the LC and REM-sleep behaviour disorders (RBD) in PD (37). For this reason we assessed RBD symptoms of all participants with the 'REM-sleep behaviour disorder screening questionnaire' (RBDSQ). This self-reporting questionnaire is a validated 13-item screening tool for the detection of REM sleep behaviour disorders (38). A total score of five points or more is considered as a positive test result (38).

2.3 MR Imaging Acquisition

Participants were scanned on a 7T MRI scanner (Magnetom, Siemens, Erlangen, Germany) equipped with a Nova Medical 32-channel head coil. Dielectric pads were applied to improve the signal in the temporal brain regions (39). In PD patients, the MRI was carried out while in the "ON" medication state to reduce motion artefacts due to tremor and to reflect clinical practice.

The 7T protocol included a localizer sequence, which was acquired for optimal planning. B0 and B1 mapping and shimming were performed to correct for field inhomogeneities. Secondly, a whole-brain MP2RAGE (Magnetization Prepared 2 Rapid Acquisition Gradient Echoes) scan was performed, with the following parameters: Repetition Time (TR) 5000ms; Echo Time (TE) 2.51ms; flip angle (FA) 5 and 3°; Field-of-view (FoV) 208 x 208mm²; Voxel size 0.65 x 0.65 x 0.65 mm³; 240 sagittal slices; resulting in an anatomical T1-weighted image. This MP2RAGE was combined with a sagittal SA2RAGE (Saturation Prepared with 2 Rapid Gradient Echoes) scan: TR/TE, 2400/0.78ms; FA 4 and 10°; FoV 256 x 256mm²; Voxel size 2.0 x 2.0 x 2.0 mm³; 88 sagittal slices. This scan was used to eliminate any B1-related biases (40). Furthermore, a magnetization transfer-weighted turbo flash (MT-TFL) (6) was performed, with 3 cm coverage of the brainstem region, used to visualise the SN and LC. The following parameters were used for this scan: TR/TE, 538/4.08ms; FA 8°; FoV 192 x 192mm²; Voxel size 0.4 x 0.4 x 0.5 mm³; 60 axial slices (6). The orientation of the MT-TFL slices was set perpendicular to the brainstem and it covered the part between the upper border of the mesencephalon and the lateral recess of the 4th ventricle (23).

2.4 MRI quality control and pre-processing

First, raw DICOM images were converted to nifti format. Then, MRI quality control was performed by visual inspection of all images. Participants with distorted brain images, including ghosting, motion or pulsation artefacts affecting the SN or LC region were excluded from analysis. This also applied to participants of whom the SN or LC region was localised outside the FoV of the MT-TFL images. In total, 150 participants provided MRI data. Eight participants were excluded because either the SN or LC region was located outside the FoV of the MT-TFL images. Furthermore, 28 participants were excluded because of motion or pulsation artefacts in the SN or LC region. In total, 27 PD and nine HC participants were excluded from analysis.

Structural T1-weighted images of the remaining participants were pre-processed using FreeSurfer (v6.0) software (<http://surfer.nmr.mgh.harvard.edu/>). This included the processing steps of non-uniform signal correction, signal and spatial normalizations, skull stripping and brain tissue segmentation.

MT-TFL images were skull stripped with the Brain Extraction Tool (BET) in FSL (v6.0) (41). Next, for all individual participants the MT-TFL images were linearly registered to the anatomical T1-weighted structural images using the boundary-based registration (BBR) in FreeSurfer and the FLIRT toolbox in FSL (42, 43, 44). All registrations were visually checked and a manual correction was applied if necessary with ITK-SNAP 4.0 software (45).

2.5 MRI analysis

The probability maps of the 'Atlas of the Basal Ganglia' (ATAG) were used for the creation of the SN region-of-interest (ROI). This atlas has been created using ultra-high resolution 7T MRI data of 30 young, 14 middle-aged and 10 elderly participants(46). For this study, the elderly atlas of the SN probability maps was used. Within these maps a separate mask of the left and right SN was drawn at the lowest level on which the SN could be well visualised. These masks were then converted to a voxel size of $0.65 \times 0.65 \times 0.65 \text{ mm}^3$ and registered to the anatomical T1-weighted images of the individual participants through a linear transformation with the FLIRT toolbox in FSL(43, 44). All masks were visually checked and if necessary minor manual corrections were applied with FSLeyes nudge. Corrected masks were then resampled with FSL FLIRT. Two reference masks (left and right) were drawn at the same level as the SN ROI in the cerebral peduncle (CP) and tegmentum (TEG). These reference masks were converted to a $0.65 \times 0.65 \times 0.65 \text{ mm}^3$ voxel size and registered to the anatomical T1-weighted images alike the SN ROI (Figure 1).

Because of the small size of the LC it was chosen not to manipulate the MT-TFL sequence and to, unlike the SN analysis, directly use these images as the target for the LC analysis. In this manner, interpolation artefacts were avoided while preserving the original signal(47). The raw MT-TFL data were used to create a template for the whole dataset utilizing "buildtemplateparallel", which is part of the Advanced Normalization Tools (ANTs). Within this template a mask was drawn manually for both the left and right LC. Next, within the centre of this LC mask, a 1×2 voxel mask ($0.4 \times 0.8 \text{ mm}^2$) centred over the highest intensity voxels of three consecutive slices, was defined as the LC ROI. At the same level a reference mask was drawn in the pontine tegmentum (PT), equidistant from both LC masks and with the apex of the 4th ventricle as a dorsal limit, with a total size of $2.4 \times 2.4 \times 1.5 \text{ mm}^3$ (Figure 1).

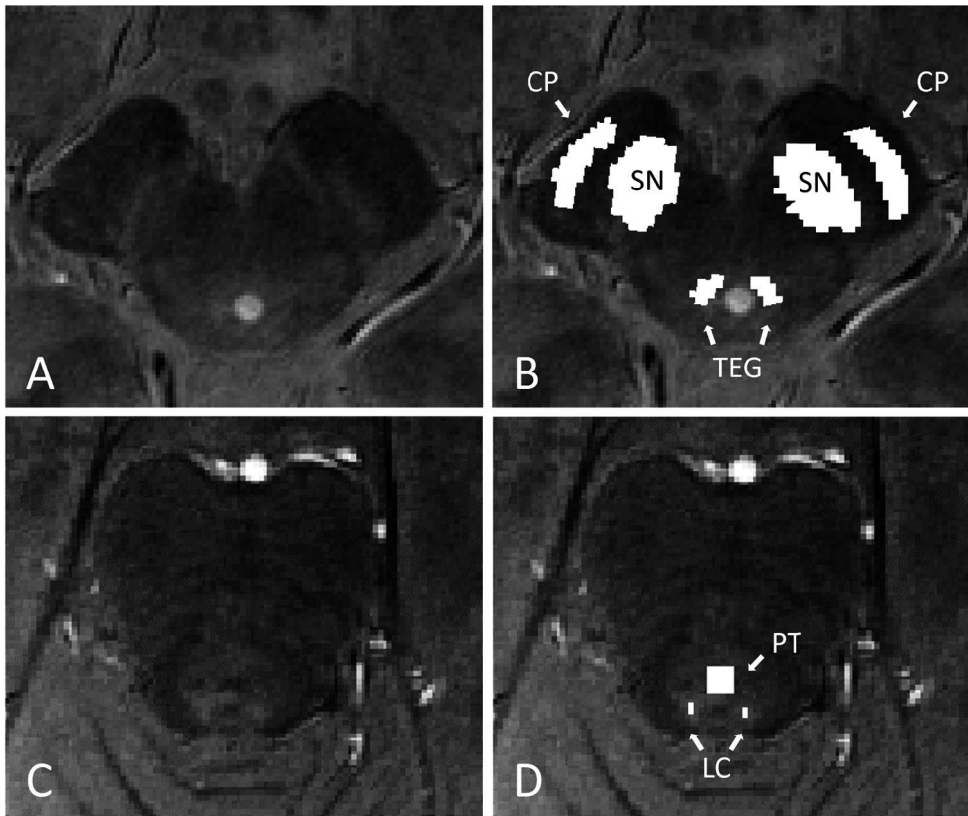


Figure 1. Visualisation of the region-of-interest and reference masks. (A) Axial MT-TFL brainstem slice at the level of the mesencephalon; (B) ROI masks in the bilateral substantia nigra (SN) region and reference masks in the bilateral cerebral peduncle (CP) and tegmentum (TEG). (C) Axial brain stem slice at the pontine level; (D) ROI masks in the bilateral locus coeruleus (LC) region and a reference mask in the pontine tegmentum (PT).

Mean signal intensity of the SN and LC was calculated and normalized to the mean signal intensity values of the surrounding reference ROIs (CP and TEG for the SN and PT for the LC). The contrast-to-noise ratio (CNR) of the SN and LC signal intensity was calculated using the following formula:

$$CNR = (S_{roi} - S_{ref}) / S_{ref}$$

Where S_{roi} is the signal intensity measured in the SN or LC ROI and S_{ref} is the reference signal intensity in respectively the cerebral peduncle and tegmentum region or pontine tegmentum.

2.6 Statistical analysis

Data were statistically analysed using IBM SPSS version 25 (IBM Corp. Released 2017. IBM SPSS Statistics for Windows, Version 25.0. Armonk, NY: IBM Corp). Demographic and disease-related variables between PD and HC were compared with Pearson's chi-squared test for categorical variables (non-parametric test), the Mann-Whitney U Test for ordinal variables and non-normally distributed continuous variables and the student's t-test for normally distributed continuous variables. The Shapiro-Wilk test was used to assess the normality of the data. The statistical significance threshold was set at $p < 0.05$.

Potential differences in CNR ratios of the SN and LC between PD and HC participants were assessed with the student's t-test for normally distributed variables and the Mann-Whitney U Test for non-normally distributed variables. In addition, since age is known to influence signal intensity on neuromelanin-sensitive MRI sequences (48), an analysis of covariance (ANCOVA) was performed including age as a covariate. A p-value < 0.05 was considered to be statistically significant.

Correlation analysis was performed using Spearman's correlation. For the whole group of participants, correlations were investigated between CNR values of the SN and LC and cognitive test scores and age. For the PD participants specifically, correlations were assessed between the SN and LC CNR values and both the total MDS-UPDRS III motor score and right- and left lateralized MDS-UPDRS III motor scores. The lateralized MDS-UPDRS III scores were calculated by adding together the right- and left-sided items of tremor, rigidity and bradykinesia (items 20-25 and 32-34) (27). Bonferroni correction was applied to correct for multiple comparisons, resulting in a significance value of $p < 0.004$ for the correlation analyses.

3. Results

3.1 Demographic and clinical characteristics

A group of 78 early-stage PD patients and 36 HC participants were included. As presented in Table 1, no significant differences in demographic characteristics were found between PD patients and HC. Although no significant difference was found between PD and HC regarding the overall cognitive performance assessed with the MoCA test ($p = 0.583$), PD participants performed worse on the SDMT ($p = 0.001$), which evaluated mental speed and attention. None of the other cognitive tests showed a significant difference between the two groups. To correct for age, sex and education, Z-scores were calculated for each cognitive test using Dutch normative values (Supplementary data, Table 1). In addition, RBDSQ scores of the PD participants did not significantly differ from the HC

group ($p = 0.087$). However, when a RBDSQ test score of five or higher is regarded as positive, it can be concluded that 32 (41.0%) of the PD patients have RBD, whereas 8 (22.2%) of the HC subjects demonstrate the same.

Table 1. Demographic and clinical features

	PD (n = 78)	HC (n = 36)	P-value
Sex (n (%) male)	57 (73.1)	25 (69.4)	0.688
Age (years)	62.6 (7.9)	61.1 (8.6)	0.431
Handedness (n (%) right)	68 (87.2)	33 (92.7)	0.484
Level of education completed (n (%))			0.556
Primary	0.0 (0.0)	0.0 (0.0)	
Secondary	18 (23.1)	10 (27.7)	
Lower tertiary	44 (56.4)	14 (38.9)	
Higher tertiary	16 (20.5)	12 (33.3)	
Time since diagnosis (months)	17.6 (8.9)		
MDS UPDRS III score	19.0 (8.0)		
Hoehn & Yahr stage (1/2/3/4/5)	27/48/3/0/0		
Side of onset (left/right/unknown)	41/34/3		
LEDD (mg/day)	370.0 (206.4)		
RBDSQ	3.4 (4.1)	1.9 (3.3)	0.087
MoCA	27.9 (1.6)	27.8 (1.6)	0.583
Phonemic fluency	39.7 (11.1)	38.5 (8.6)	0.587
Semantic fluency	39.1 (8.7)	40.5 (7.1)	0.294
15 Words Test			
Total score (0-75)	37.3 (10.0)	39.1 (9.3)	0.387
Maximum immediate recall (0-15)	10.2 (2.5)	10.5 (2.3)	0.519
Retention score (MRET1PC) (%)	92.6 (30.8)	106.1 (52.8)	0.161
Retention score (MRET2PC) (%)	71.8 (21.9)	77.3 (20.7)	0.122
BJOL	26.9 (3.3)	26.9 (3.0)	0.900
LNST	18.8 (2.3)	18.9 (2.2)	0.517
SDMT	44.9 (10.5)	52.8 (11.7)	0.001*

MDS UPDRS III = Movement Disorders Society sponsored revision of the Unified Parkinson's disease Rating Scale-Part III (severity of motor symptoms); LEDD = Levodopa Equivalent Daily Dose; RBDSQ = REM-sleep behaviour disorder screening questionnaire; MoCA = Montreal Cognitive Assessment; BJOL = Benton Judgment of Line Orientation; LNST = Letter Number Sequencing Test; SDMT = Symbol Digit Modalities Test.

Results are represented as mean (SD), unless otherwise specified.

3.2 Signal intensity analysis in the LC and SN

Compared with HC, PD participants showed significantly lower CNR values in the right SN region (HC: mean = -0.049, std = 0.082, PD: mean = -0.090, std = 0.102; $p = 0.029$) and left LC (HC: mean = 0.127, std = 0.043, PD: mean = 0.108, std = 0.043; $p = 0.027$). No differences in CNR values were found between PD and HC participants in the left SN

region (HC: mean = -0.051, std = 0.069, PD: mean = -0.066, std = 0.089; $p = 0.446$) and right LC (HC: mean = 0.106, std = 0.048, PD: mean = 0.104, std = 0.048; $p = 0.826$) (Figure 2). Also, no group differences were found when averaging the left and right SN (HC: mean = -0.058, std = 0.087, PD: mean = -0.084, std = 0.094; $p = 0.109$) or the left and right LC (HC: mean = 0.117, std = 0.041, PD: mean = 0.106, std = 0.038; $p = 0.165$).

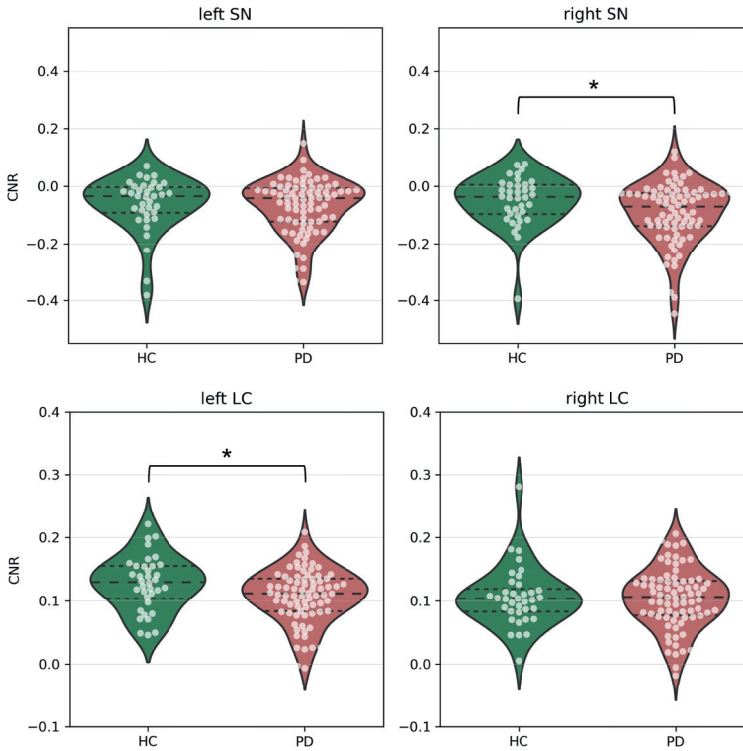


Figure 2. Comparison of SN and LC CNR values between PD and HC groups. Dashed lines represent the quartiles of the distribution. A significant difference in CNR values between PD and HC was found in the right SN (HC: mean = -0.049, std = 0.082, PD: mean = -0.090, std = 0.102; $p = 0.029$) and left LC (HC: mean = 0.127, std = 0.043, PD: mean = 0.108, std = 0.043; $p = 0.027$).

The ANCOVA, correcting for age effects, showed a significant different CNR value between PD and HC in the left LC ($p = 0.017$). However, by adding age as a confounder, the CNR values of the right SN did not differ anymore between PD and HC ($p = 0.055$).

3.3 Correlation analysis

For the PD and HC participants combined, a positive correlation was found between the CNR of the right SN and the second 15-WT retention score (MRET2PC, $p = 0.001$, $r_s = 0.297$). There was also a trend towards a positive correlation between the CNR of the

right SN and the first 15-WT retention score (MRET1PC, $p = 0.007$, $r_s = 0.251$) and the MoCA total score ($p = 0.009$, $r_s = 0.243$). No significant correlation was found between the CNR of the left SN and any of the cognitive scores. In addition, a positive correlation between the mean CNR of the bilateral SN and the second 15-WT retention score (MRET2PC, $p = 0.002$, $r_s = 0.287$) was found. There was also a trend towards a positive correlation between the mean CNR of the bilateral SN and the first 15-WT retention score (MRET1PC, $p = 0.004$, $r_s = 0.265$) (Figure 3). Both retention scores are assessing delayed recall. No statistically different correlation was found between the CNR of the LC and any of the cognitive outcome measures.

In addition, both groups were separately compared regarding associations with motor and cognitive scores. For the HC group, no significant correlations were found between the CNR of the SN or LC and any of the cognitive measures. For the PD group, a positive correlation was found between the CNR of the right SN and the maximum immediate recall score of the 15-WT ($p = 0.003$, $r_s = 0.336$) and a trend for a positive correlation between the CNR of the right SN and the 15-WT total score ($p = 0.009$, $r_s = 0.295$) (Supplementary material, Figure 1 and 2).

Another correlation analysis was performed assessing the association between LC and SN CNR and lateralized MDS-UPDRS III motor scores. While there seemed to be a positive correlation between the right LC CNR and right-lateralized motor score and a negative correlation between the right LC CNR and left-lateralized motor scores visually, this relationship was not found to be statistically significant ($p = 0.014$, $r_s = 0.277$ and $p = 0.016$, $r_s = -0.273$, respectively). Also the left LC CNR and left and right SN CNR did not show a significant correlation with the lateralized motor scores (Supplementary material, Figure 3).

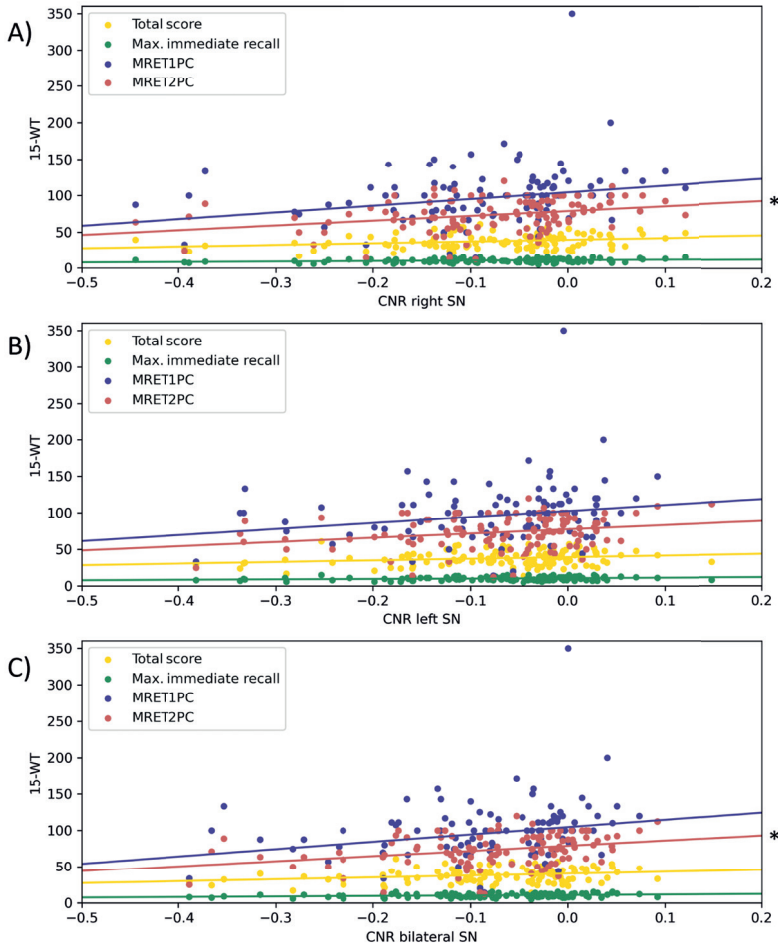


Figure 3. Correlation between SN CNR values and 15 words test scores for the whole group of participants. (A) Correlation between the CNR of the right SN and 15 words test scores. There was a significant positive correlation between the right SN CNR and the MRET2PC score ($p = 0.001$, $r_s = 0.297$). (B) Correlation between the CNR of the left SN and 15 words test scores. No significant correlations were found for the left SN CNR. (C) Correlation between mean CNR of the bilateral SN and 15 words test scores. There was a significant positive correlation between the CNR of the bilateral SN and the MRET2PC score ($p = 0.002$, $r_s = 0.287$).

4. Discussion

In this ultra-high-field 7T MRI study neuromelanin related signal intensity of the SN and LC was compared between a large group of early-stage PD patients and controls. PD participants showed lower CNR values in the right SN and left LC. However, the finding in the SN did not survive age-correction. Upon examining the associations with

cognitive scores, we found that lower CNR in the SN was associated with worse memory performance in the whole group as well as in the PD patients separately.

The SN and LC modulate various cognitive and behavioural functions and have a proposed role in the pathophysiology of several neurodegenerative diseases. For this reason, they make an interesting target for studies searching for imaging biomarkers. In addition to PD, lower signals on neuromelanin-sensitive MRI sequences in these nuclei have been reported in several other neuropsychiatric diseases, such as Alzheimer's disease or depressive disorders (49). Until now, only two 7T MRI studies have been published comparing neuromelanin related signal changes in the LC between PD and HC. Both found a lower signal intensity in the LC of PD patients compared to HC, but only in the caudal portion. There were no differences between PD and HC when assessing the LC as a whole (50, 51). Despite being not able to visualize the caudal part of the LC with our current MRI protocol, we were able to demonstrate that alterations between early-stage PD and HC can also be found in the central portion of the LC.

Lateralized results were also reported by one of the previous 7T MRI studies, with signal changes in PD patients found in the right, but not in the left, caudal LC (51). The exact role of the LC in motor control and its association with ipsi- and contralateral motor symptoms is not fully clarified. Previous studies have yielded contrasting results. Some report an association between LC integrity and ipsilateral motor symptoms (51), while others have observed a more significant decrease in LC signal intensity contralateral to the clinically most affected side (52). In the current analysis we searched for a correlation between LC CNR and lateralized motor scores. However, no significant correlation was found between the LC CNR and lateralized motor symptoms (Supplementary data, Figure 3). The exact relation between LC integrity and motor symptoms therefore remains unclear.

This is the first 7T MRI study comparing neuromelanin related signal changes in the SN between PD and HC. However, no differences were demonstrated between groups in this region. These results imply that the LC is affected more early in the disease course compared to the SN, which is in line with the bottom-up progression of disease theory based on the pathological studies by Braak and colleagues (17). Although this theory seems to be applicable to a significant proportion of PD patients, recent evidence suggest that some PD cases display an alternative route of disease progression, starting in the olfactory bulb. In this group of patients PD pathology mainly affects the amygdala region, with limited or no brainstem involvement (18).

In contrast, various 3T MRI studies have been performed assessing neuromelanin-sensitive signal intensity in the SN or LC. Several studies have reported a decrease

in neuromelanin related signal intensity in PD patients compared to HC (53, 54, 55). Previous research comparing 3T and 7T MRI modalities determined that 7T MRI is superior in terms of localizing small brain structures (56). It is therefore remarkable that we did not find signal changes in the SN, while previous 3T MRI studies did report differences in PD patients in this region. A possible explanation for this could be related to Specific Absorption Rate (SAR) restrictions at 7T MRI. While SNR greatly increases with 7T MRI, the SAR restrictions cause the CNR of the MT-TFL sequence to be slightly decreased compared to 3T MRI (6). It might therefore be harder to demonstrate group differences. However, since registration is critical when assessing small brain stem nuclei, the increased spatial resolution and contrast of 7T MRI allow for a more reliable localization and more valid analysis compared to 3T MRI.

We found a positive correlation between the SN CNR and performance on the 15 words test in PD patients. None of the other cognitive test scores displayed a correlation with either LC or SN integrity. Although we believe that the inclusion of an early-stage PD group, which did not show evident signs of cognitive impairment in comparison to the age-matched HC population, can explain this lack of correlation, it is still striking that a correlation was found with the 15-WT. For the PD group this mainly concerned immediate recall and not delayed recall function. This corresponds with the belief that memory disorders in PD are related to retrieval rather than to consolidation failure (57). Liu et al. reported a similar result as they found a relationship between SN integrity and working memory deficits in PD (58). In addition, another paper reported an association between iron concentration in the SN and working memory in HC (59). It could therefore be possible that SN integrity is associated with memory function. However, studies on the involvement of the basal ganglia in cognitive functioning suggest a central role in learning, rather than it being associated with deficits in specific cognitive domains (60). Besides assessing memory function, the 15-WT evaluates an individual's learning abilities, as they are presented with the same words in five repeated trials. It could therefore be hypothesized that the loss of SN integrity is not necessarily associated with impaired memory function but with an impaired learning function in general, which could explain why only a correlation with this specific neuropsychological test is found. The correlation analysis in the current study is exploratory and results should be interpreted with caution. To further establish the relationship between the SN integrity, memory function and learning capabilities, future longitudinal studies are necessary.

Results in this study were corrected for age, since this is known to influence signal intensity on neuromelanin-sensitive MRI sequences (48). In addition to age, previous literature suggests a correlation between several clinical symptoms and degeneration of the locus coeruleus. This includes cognitive impairment, RBD and psychiatric complaints (21, 51, 61, 62, 63). The RBD questionnaire included in this study, did not

significantly differ between PD and HC. As for the cognitive evaluation, only the results of the SDMT differed significantly between PD and HC. Other cognitive tests did not show a difference between groups. Also, no correlation was found between the individual cognitive test scores and the neuromelanin related signal intensity in the LC. We believe that this might be caused by the fact that an early-stage PD group was included in this study, which did not show evident signs of cognitive impairment in comparison to the age-matched HC population. The study of Li et al. also showed that altered CNR values in the LC are less apparent in early PD without cognitive impairment compared to PD with cognitive complaints (21). It would therefore be interesting to repeat the current analysis on longitudinal data, too see whether the development of cognitive impairment over time is correlated with a decrease of neuromelanin related signal intensity in the LC. However, for this current analysis we believe that neither RBD symptoms nor cognitive complaints have had a confounding effect on the study results.

This study has several limitations. First of all, due to technical restrictions the FoV for the NM sensitive MRI sequence was relatively small. Since we aimed to examine signal intensity in both the SN and LC, we had to exclude several participants because either the SN or LC was located outside the FoV. Furthermore, since the cranial part of the SN and the caudal part of the LC was often positioned outside the FoV, volumetry measurements or spatial pattern analysis could not be performed. This is unfortunate since recent studies suggest a spatial pattern of LC and SN degeneration(64, 65). Future ultra-high field studies focussing on the spatial organisation of the LC and SN are therefore necessary. Another limitation relates to (involuntary) motion artefacts, as these are one of the biggest challenges in high-resolution imaging (66). This is especially true for visualising parts of the brainstem, since there is a close relation to surrounding vascular structures and cerebrospinal fluid compartments. In this study several participants displayed artefacts in either the SN or LC and have therefore been excluded from analysis. The reasons described above resulted in a relatively large exclusion rate for this study. Future ultra-high-field MRI studies, specifically aiming to incorporate both the midbrain and the pontine catecholaminergic nuclei, should use a more extensive MRI protocol with a larger FoV, so that all relevant nuclei can be fully visualised.

In addition, this current study only consists of PD patients and HC. In order to investigate if NM related signal intensity in the LC can also differentiate PD from patients with other neurodegenerative diseases, such as atypical parkinsonism, future studies should include a control group with other neurodegenerative diseases. This would help to differentiate between PD related alterations and changes which occur due to aging or other neurodegenerative processes.

Lastly, this study focusses on neuromelanin related signal intensity, which is a very specific potential MRI biomarker. There probably is no single method with the potential to serve as the perfect PD biomarker and different biomarker techniques are likely to complement each other (67). However, we believe that in order to determine an ideal set of combined biomarkers for PD, it is important to first adequately study the individual markers and to develop optimal methods for analysis. In this way the most promising biomarkers can be determined, which can then be combined in future studies. Besides MRI, nuclear imaging techniques visualizing the noradrenergic and dopaminergic system, could also serve a valuable role in this. Eventually, a combination of different biochemical and imaging techniques is expected to have the best results for both the diagnosis and monitoring of PD.

In conclusion, the results of this study confirm that early-stage PD patients exhibit lower signal intensity in the LC compared to HC. No differences between groups were found in signal intensity of the bilateral SN. In addition, loss of SN integrity might influence working memory or learning capabilities in PD patients. Although 7T MRI yields advantages in terms of increased spatial resolution and better localisation of small brain stem nuclei, group comparisons might be influenced by a small decrease in CNR. Future studies should preferably investigate longitudinal signal changes in the LC and SN to further elucidate the pathophysiological mechanisms of PD.

5. References

1. Dorsey ER, Sherer T, Okun MS, Bloem BR. The Emerging Evidence of the Parkinson Pandemic. *J Parkinsons Dis.* 2018;8(s1):S3-S8.
2. Jankovic J. Parkinson's disease: clinical features and diagnosis. *J Neurol Neurosurg Psychiatry.* 2008;79(4):368-76.
3. Postuma RB, Berg D, Stern M, Poewe W, Olanow CW, Oertel W, et al. MDS clinical diagnostic criteria for Parkinson's disease. *Mov Disord.* 2015;30(12):1591-601.
4. Joutsa J, Gardberg M, Rötttä M, Kaasinen V. Diagnostic accuracy of parkinsonism syndromes by general neurologists. *Parkinsonism Relat Disord.* 2014;20(8):840-4.
5. Lehericy S, Vaillancourt DE, Seppi K, Monchi O, Rektorova I, Antonini A, et al. The role of high-field magnetic resonance imaging in parkinsonian disorders: Pushing the boundaries forward. *Mov Disord.* 2017;32(4):510-25.
6. Priovoulos N, Jacobs HIL, Ivanov D, Uludag K, Verhey FRJ, Poser BA. High-resolution in vivo imaging of human locus coeruleus by magnetization transfer MRI at 3T and 7T. *Neuroimage.* 2018;168:427-36.
7. Prange S, Metereau E, Thobois S. Structural Imaging in Parkinson's Disease: New Developments. *Curr Neurol Neurosci Rep.* 2019;19(8):50.
8. Rispoli V, Schreglmann SR, Bhatia KP. Neuroimaging advances in Parkinson's disease. *Curr Opin Neurol.* 2018;31(4):415-24.
9. Watanabe T, Tan Z, Wang X, Martinez-Hernandez A, Frahm J. Magnetic resonance imaging of noradrenergic neurons. *Brain Struct Funct.* 2019;224(4):1609-25.
10. Priovoulos N, van Boxel SCJ, Jacobs HIL, Poser BA, Uludag K, Verhey FRJ, et al. Unraveling the contributions to the neuromelanin-MRI contrast. *Brain Struct Funct.* 2020;225(9):2757-74.
11. Castellanos G, Fernandez-Seara MA, Lorenzo-Betancor O, Ortega-Cubero S, Puigvert M, Uranga J, et al. Automated neuromelanin imaging as a diagnostic biomarker for Parkinson's disease. *Mov Disord.* 2015;30(7):945-52.
12. Schwarz ST, Rittman T, Gontu V, Morgan PS, Bajaj N, Auer DP. T1-weighted MRI shows stage-dependent substantia nigra signal loss in Parkinson's disease. *Mov Disord.* 2011;26(9):1633-8.
13. Reimao S, Pita Lobo P, Neutel D, Correia Guedes L, Coelho M, Rosa MM, et al. Substantia nigra neuromelanin magnetic resonance imaging in de novo Parkinson's disease patients. *Eur J Neurol.* 2015;22(3):540-6.
14. Matsuura K, Maeda M, Tabei KI, Umino M, Kajikawa H, Satoh M, et al. A longitudinal study of neuromelanin-sensitive magnetic resonance imaging in Parkinson's disease. *Neurosci Lett.* 2016;633:112-7.
15. Pavese N, Tai YF. Nigrosome Imaging and Neuromelanin Sensitive MRI in Diagnostic Evaluation of Parkinsonism. *Mov Disord Clin Pract.* 2018;5(2):131-40.
16. Isaias IU, Trujillo P, Summers P, Marotta G, Mainardi L, Pezzoli G, et al. Neuromelanin Imaging and Dopaminergic Loss in Parkinson's Disease. *Front Aging Neurosci.* 2016;8:196.
17. Braak H, Del Tredici K, Bratzke H, Hamm-Clement J, Sandmann-Keil D, Rub U. Staging of the intracerebral inclusion body pathology associated with idiopathic Parkinson's disease (preclinical and clinical stages). *J Neurol.* 2002;249 Suppl 3:III/1-5.
18. Borghammer P, Just MK, Horsager J, Skjaerbaek C, Raunio A, Kok EH, et al. A postmortem study suggests a revision of the dual-hit hypothesis of Parkinson's disease. *NPJ Parkinsons Dis.* 2022;8(1):166.
19. Mather M, Harley CW. The Locus Coeruleus: Essential for Maintaining Cognitive Function and the Aging Brain. *Trends Cogn Sci.* 2016;20(3):214-26.

20. Theofilas P, Ehrenberg AJ, Dunlop S, Di Lorenzo Alho AT, Nguy A, Leite REP, et al. Locus coeruleus volume and cell population changes during Alzheimer's disease progression: A stereological study in human postmortem brains with potential implication for early-stage biomarker discovery. *Alzheimers Dement.* 2017;13(3):236-46.
21. Li Y, Wang C, Wang J, Zhou Y, Ye F, Zhang Y, et al. Mild cognitive impairment in de novo Parkinson's disease: A neuromelanin MRI study in locus coeruleus. *Mov Disord.* 2019;34(6):884-92.
22. Sommerauer M, Fedorova TD, Hansen AK, Knudsen K, Otto M, Jeppesen J, et al. Evaluation of the noradrenergic system in Parkinson's disease: an 11C-MeNER PET and neuromelanin MRI study. *Brain.* 2018;141(2):496-504.
23. Wolters AF, Heijmans M, Michielse S, Leentjens AFG, Postma AA, Jansen JFA, et al. The TRACK-PD study: protocol of a longitudinal ultra-high field imaging study in Parkinson's disease. *BMC Neurol.* 2020;20(1):292.
24. Hughes AJ, Daniel SE, Kilford L, Lees AJ. Accuracy of clinical diagnosis of idiopathic Parkinson's disease: a clinico-pathological study of 100 cases. *J Neurol Neurosurg Psychiatry.* 1992;55(3):181-4.
25. Association AP. Diagnostic and statistical manual of mental disorders (DSM-5®): American Psychiatric Pub; 2013.
26. Tomlinson CL, Stowe R, Patel S, Rick C, Gray R, Clarke CE. Systematic review of levodopa dose equivalency reporting in Parkinson's disease. *Mov Disord.* 2010;25(15):2649-53.
27. Goetz CG, Tilley BC, Shaftman SR, Stebbins GT, Fahn S, Martinez-Martin P, et al. Movement Disorder Society-sponsored revision of the Unified Parkinson's Disease Rating Scale (MDS-UPDRS): scale presentation and clinimetric testing results. *Mov Disord.* 2008;23(15):2129-70.
28. Goetz CG, Poewe W, Rascol O, Sampaio C, Stebbins GT, Counsell C, et al. Movement Disorder Society Task Force report on the Hoehn and Yahr staging scale: status and recommendations. *Mov Disord.* 2004;19(9):1020-8.
29. Fereshtehnejad SM, Zeighami Y, Dagher A, Postuma RB. Clinical criteria for subtyping Parkinson's disease: biomarkers and longitudinal progression. *Brain.* 2017;140(7):1959-76.
30. Bloem BR, Marks WJ, Jr., Silva de Lima AL, Kuijf ML, van Laar T, Jacobs BPF, et al. The Personalized Parkinson Project: examining disease progression through broad biomarkers in early Parkinson's disease. *BMC Neurol.* 2019;19(1):160.
31. Nasreddine ZS, Phillips NA, Bédirian V, Charbonneau S, Whitehead V, Collin I, et al. The Montreal Cognitive Assessment, MoCA: a brief screening tool for mild cognitive impairment. *J Am Geriatr Soc.* 2005;53(4):695-9.
32. Gladsjo JA, Schuman CC, Evans JD, Peavy GM, Miller SW, Heaton RK. Norms for letter and category fluency: demographic corrections for age, education, and ethnicity. *Assessment.* 1999;6(2):147-78.
33. Vakil E, Blachstein H. Rey Auditory-Verbal Learning Test: structure analysis. *J Clin Psychol.* 1993;49(6):883-90.
34. Benton AL, Varney NR, Hamsher KD. Visuospatial judgment. A clinical test. *Arch Neurol.* 1978;35(6):364-7.
35. Smith A. Symbol Digit Modalities Test (SDMT) Manual. Los Angeles, Western Psychological Services. 1982.
36. Wechsler D. Wechsler adult intelligence scale. San Antonio, TX: Psychological Corporation. 2008.

37. García-Lorenzo D, Longo-Dos Santos C, Ewencyk C, Leu-Semenescu S, Gallea C, Quattrocchi G, et al. The coeruleus/subcoeruleus complex in rapid eye movement sleep behaviour disorders in Parkinson's disease. *Brain*. 2013;136(Pt 7):2120-9.
38. Stiasny-Kolster K, Mayer G, Schafer S, Moller JC, Heinzel-Gutenbrunner M, Oertel WH. The REM sleep behavior disorder screening questionnaire--a new diagnostic instrument. *Mov Disord*. 2007;22(16):2386-93.
39. Teeuwisse WM, Brink WM, Webb AG. Quantitative assessment of the effects of high-permittivity pads in 7 Tesla MRI of the brain. *Magn Reson Med*. 2012;67(5):1285-93.
40. Eggenschwiler F, Kober T, Magill AW, Gruetter R, Marques JP. SA2RAGE: a new sequence for fast B1+ -mapping. *Magn Reson Med*. 2012;67(6):1609-19.
41. Smith SM. Fast robust automated brain extraction. *Human Brain Mapping*. 2002;17(3):143-55.
42. Greve DN, Fischl B. Accurate and robust brain image alignment using boundary-based registration. *Neuroimage*. 2009;48(1):63-72.
43. Jenkinson M, Bannister P, Brady M, Smith S. Improved optimization for the robust and accurate linear registration and motion correction of brain images. *Neuroimage*. 2002;17(2):825-41.
44. Jenkinson M, Smith S. A global optimisation method for robust affine registration of brain images. *Med Image Anal*. 2001;5(2):143-56.
45. Yushkevich PA, Piven J, Hazlett HC, Smith RG, Ho S, Gee JC, et al. User-guided 3D active contour segmentation of anatomical structures: significantly improved efficiency and reliability. *Neuroimage*. 2006;31(3):1116-28.
46. Keuken MC, Bazin PL, Backhouse K, Beekhuizen S, Himmer L, Kandola A, et al. Effects of aging on T(1), T(2)*, and QSM MRI values in the subcortex. *Brain Struct Funct*. 2017;222(6):2487-505.
47. Guinea-Izquierdo A, Gimenez M, Martinez-Zalacain I, Del Cerro I, Canal-Noguer P, Blasco G, et al. Lower Locus Coeruleus MRI intensity in patients with late-life major depression. *PeerJ*. 2021;9:e10828.
48. Shibata E, Sasaki M, Tohyama K, Kanbara Y, Otsuka K, Ehara S, et al. Age-related changes in locus ceruleus on neuromelanin magnetic resonance imaging at 3 Tesla. *Magn Reson Med Sci*. 2006;5(4):197-200.
49. Liu KY, Marijatta F, Hammerer D, Acosta-Cabronero J, Duzel E, Howard RJ. Magnetic resonance imaging of the human locus coeruleus: A systematic review. *Neurosci Biobehav Rev*. 2017;83:325-55.
50. O'Callaghan C, Hezemans FH, Ye R, Rua C, Jones PS, Murley AG, et al. Locus coeruleus integrity and the effect of atomoxetine on response inhibition in Parkinson's disease. *Brain*. 2021;144(8):2513-26.
51. Ye R, O'Callaghan C, Rua C, Hezemans FH, Holland N, Malpetti M, et al. Locus Coeruleus Integrity from 7 T MRI Relates to Apathy and Cognition in Parkinsonian Disorders. *Mov Disord*. 2022;37(8):1663-72.
52. Doppler CEJ, Kinnerup MB, Brune C, Farrher E, Betts M, Fedorova TD, et al. Regional locus coeruleus degeneration is uncoupled from noradrenergic terminal loss in Parkinson's disease. *Brain*. 2021;144(9):2732-44.
53. Gaurav R, Yahia-Cherif L, Pyatigorskaya N, Mangone G, Biondetti E, Valabregue R, et al. Longitudinal Changes in Neuromelanin MRI Signal in Parkinson's Disease: A Progression Marker. *Mov Disord*. 2021;36(7):1592-602.
54. Wang L, Yan Y, Zhang L, Liu Y, Luo R, Chang Y. Substantia nigra neuromelanin magnetic resonance imaging in patients with different subtypes of Parkinson disease. *J Neural Transm (Vienna)*. 2021;128(2):171-9.

55. Wang J, Li Y, Huang Z, Wan W, Zhang Y, Wang C, et al. Neuromelanin-sensitive magnetic resonance imaging features of the substantia nigra and locus coeruleus in de novo Parkinson's disease and its phenotypes. *Eur J Neurol*. 2018;25(7):949-e73.
56. Isaacs BR, Mulder MJ, Groot JM, van Berendonk N, Lute N, Bazin PL, et al. 3 versus 7 Tesla magnetic resonance imaging for parcellations of subcortical brain structures in clinical settings. *PLoS One*. 2020;15(11):e0236208.
57. Costa A, Monaco M, Zabberoni S, Peppe A, Perri R, Fadda L, et al. Free and cued recall memory in Parkinson's disease associated with amnesic mild cognitive impairment. *PLoS One*. 2014;9(1):e86233.
58. Liu W, Wang C, He T, Su M, Lu Y, Zhang G, et al. Substantia nigra integrity correlates with sequential working memory in Parkinson's disease. *J Neurosci*. 2021.
59. Xu J, Guan X, Wen J, Wang T, Zhang M, Xu X. Substantia nigra iron affects functional connectivity networks modifying working memory performance in younger adults. *Eur J Neurosci*. 2021;54(11):7959-73.
60. Foerde K, Shohamy D. The role of the basal ganglia in learning and memory: insight from Parkinson's disease. *Neurobiol Learn Mem*. 2011;96(4):624-36.
61. Prasuhn J, Prasuhn M, Fellbrich A, Strautz R, Lemmer F, Dreischmeier S, et al. Association of Locus Coeruleus and Substantia Nigra Pathology With Cognitive and Motor Functions in Patients With Parkinson Disease. *Neurology*. 2021;97(10):e1007-e16.
62. Del Tredici K, Braak H. Dysfunction of the locus coeruleus-norepinephrine system and related circuitry in Parkinson's disease-related dementia. *J Neurol Neurosurg Psychiatry*. 2013;84(7):774-83.
63. Nobileau A, Gaurav R, Chougar L, Faucher A, Valabrègue R, Mangone G, et al. Neuromelanin-Sensitive Magnetic Resonance Imaging Changes in the Locus Coeruleus/Subcoeruleus Complex in Patients with Typical and Atypical Parkinsonism. *Mov Disord*. 2023;38(3):479-84.
64. Madelung CF, Meder D, Fuglsang SA, Marques MM, Boer VO, Madsen KH, et al. Locus Coeruleus Shows a Spatial Pattern of Structural Disintegration in Parkinson's Disease. *Mov Disord*. 2022;37(3):479-89.
65. Biondetti E, Gaurav R, Yahia-Cherif L, Mangone G, Pyatigorskaya N, Valabrègue R, et al. Spatiotemporal changes in substantia nigra neuromelanin content in Parkinson's disease. *Brain*. 2020;143(9):2757-70.
66. Ladd ME, Bachert P, Meyerspeer M, Moser E, Nagel AM, Norris DG, et al. Pros and cons of ultra-high-field MRI/MRS for human application. *Prog Nucl Magn Reson Spectrosc*. 2018;109:1-50.
67. Weingarten CP, Sundman MH, Hickey P, Chen NK. Neuroimaging of Parkinson's disease: Expanding views. *Neurosci Biobehav Rev*. 2015;59:16-52.

Supplementary data

Table 1. Neuropsychological test scores (z-scores)

	PD (n = 78)	HC (n = 36)	P-value
Phonemic fluency	-0.01 (1.1)	-0.14 (0.8)	0.465
Semantic fluency			
Animals	-0.45 (0.8)	-0.25 (0.6)	0.216
Professions	-0.41 (0.8)	-0.35 (0.6)	0.704
15 Words Test			
Total score	-0.90 (1.0)	-0.73 (1.1)	0.459
Immediate recall	-0.66 (1.2)	-0.40 (1.1)	0.259
Retention score	-0.31 (1.2)	0.01 (1.1)	0.185
BJOL	0.59 (0.7)	0.61 (0.7)	0.908
LNST	0.16 (0.9)	0.01 (1.1)	0.786
SDMT	0.46 (1.0)	1.3 (1.2)	0.001*

BJOL = Benton Judgment of Line Orientation; LNST = Letter Number Sequencing Test; SDMT = Symbol Digit Modalities Test.

Results are represented as mean z-scores (SD), unless otherwise specified.

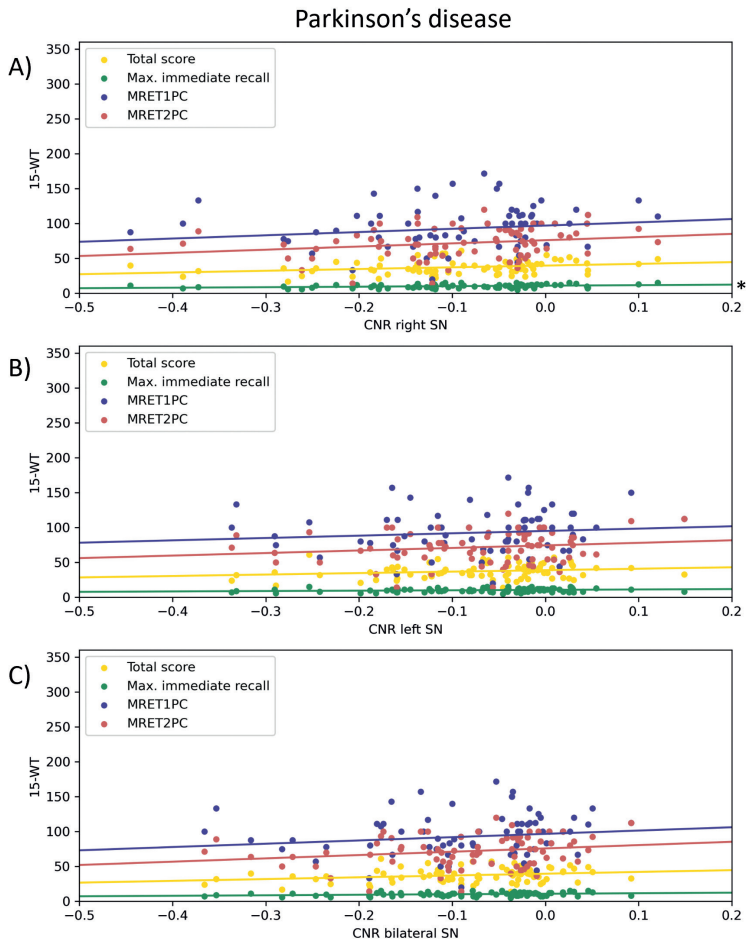


Figure 1. Correlation between SN CNR values and 15 words test scores for the PD group. (A) Correlation between right SN CNR and 15 words test scores. A positive correlation was found between the CNR of the right SN and the maximum immediate recall score ($p = 0.003$, $r_s = 0.336$). (B) Correlation between the CNR of the left SN and 15 words test scores. No significant correlations were found for the left SN CNR. (C) Correlation between mean CNR of the bilateral SN and 15 words test scores. No significant correlations were found for the CNR of the bilateral SN.

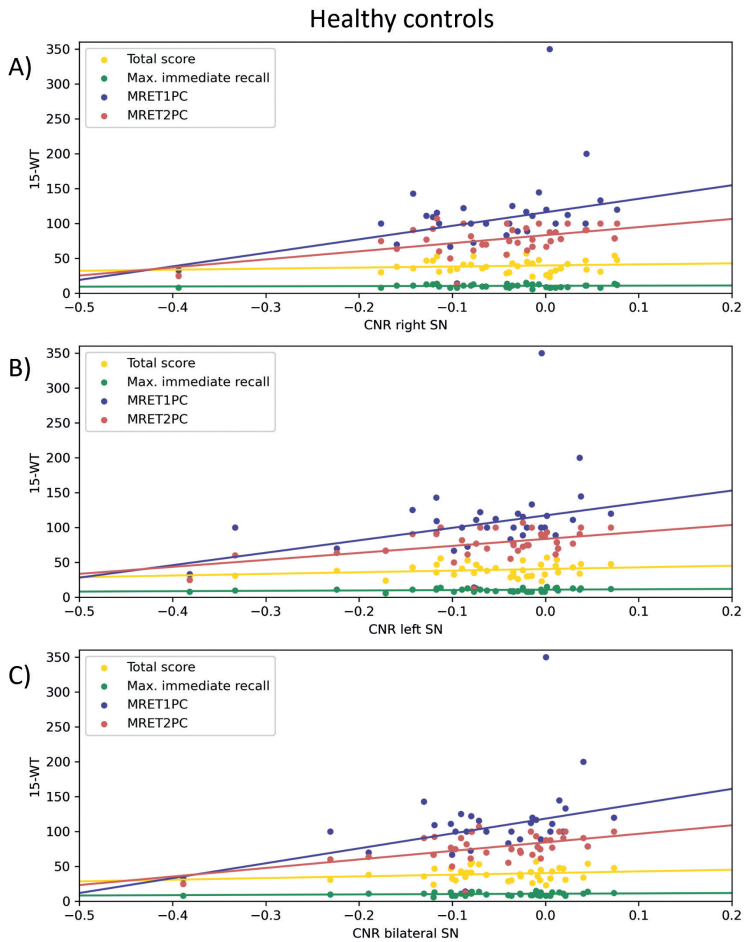


Figure 2. Correlation between SN CNR values and 15 words test scores for the HC group. (A) Correlation between the CNR of the right SN and 15 words test scores. No significant correlations were found for the right SN CNR. (B) Correlation between the CNR of the left SN and 15 words test scores. No significant correlations were found for the left SN CNR. (C) Correlation between mean CNR of the bilateral SN and 15 words test scores. No significant correlations were found for the bilateral SN CNR.

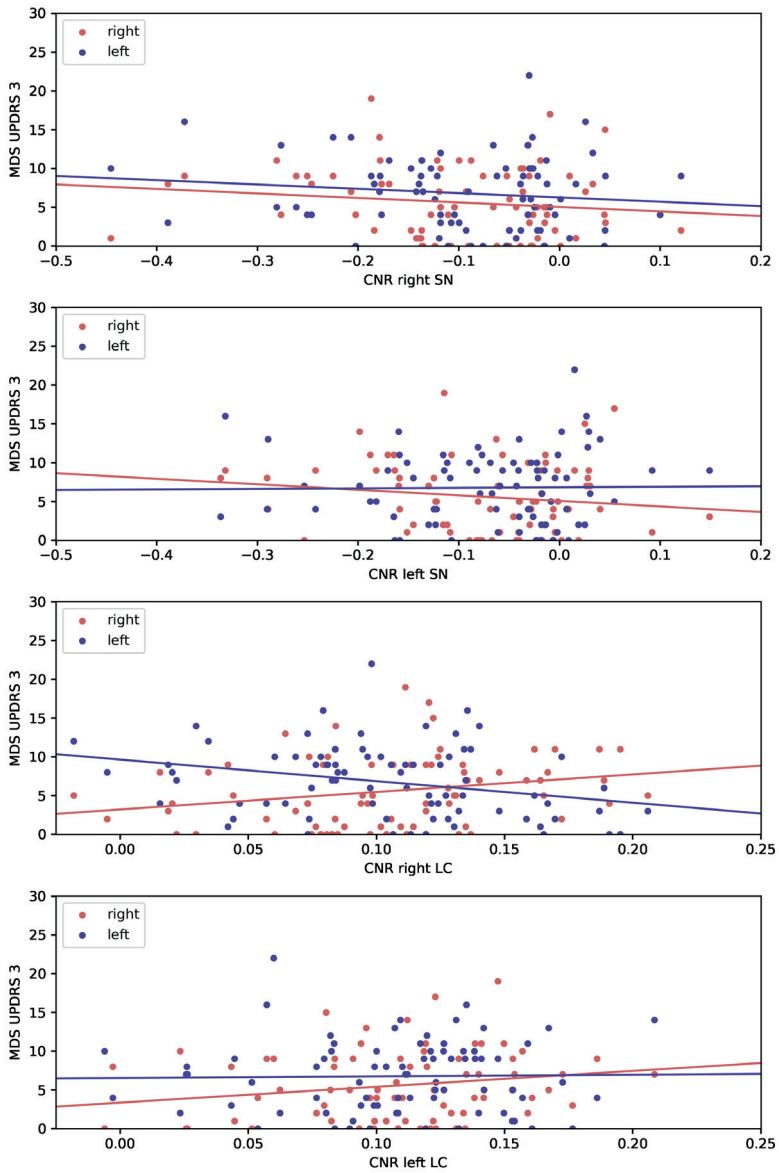


Figure 3. Correlation between LC and SN CNR values and right- and left-lateralized MDS-UPDRS III motor scores. No significant correlation was found between any of these measures.

CHAPTER 7



Comparison of Olfactory Tract Diffusion Measures Between Early Stage Parkinson's Disease Patients and Healthy Controls Using Ultra-High Field MRI

Heijmans M, **Wolters AF**, Temel Y, Kuijf ML, Michielse S.

Abstract

Background: MRI is a valuable method to assist in the diagnostic work-up of Parkinson's Disease (PD). The olfactory tract (OT) has been proposed as a potential MRI biomarker for distinguishing PD patients from healthy controls.

Objective: This study aims to further investigate whether diffusion measures of the OT differ between early stage PD patients and healthy controls.

Methods: Twenty hyposmic/anosmic PD patients, 65 normosmic PD patients and 36 normosmic healthy controls were evaluated and a 7T diffusion weighted image scan was acquired. Manual seed regions of interest were drawn in the OT region. Tractography of the OT was performed using a deterministic streamlines algorithm. Diffusion measures (fractional anisotropy and mean- radial- and axial diffusivity) of the generated streamlines were compared between groups.

Results: Diffusion measures did not differ between PD patients compared to healthy controls and between hyposmic/anosmic PD patients, normosmic PD patients, and normosmic healthy controls. A positive correlation was found between age and mean- and axial diffusivity within the hyposmic/anosmic PD subgroup, but not in the normosmic groups. A positive correlation was found between MDS-UPDRSIII scores and fractional anisotropy.

Conclusion: This study showed that fibre tracking of the OT was feasible in both early stage PD and healthy controls using 7T diffusion weighted imaging data. However, 7T MRI diffusion measures of the OT are not useful as an early clinical biomarker for PD. Future work is needed to clarify the role of other OT measurements as a biomarker for PD and its different subgroups.

1. Introduction

Parkinson's disease (PD) is a neurodegenerative disorder, often recognized by clinicians when motor symptoms like bradykinesia, rigidity and tremor become apparent. In current clinical practice, the diagnosis PD is based on the assessment of symptoms and their course over time according to clinical criteria (1). However, discriminating PD from other parkinsonian syndromes can be difficult as is illustrated by the error rate of 24% for a clinical diagnosis of PD, even in specialized movement disorders centres (2). The diagnostic challenge is in part due to PD being a heterogeneous disease with variation in clinical course, treatment response, genetic background and the influence of environmental factors. The gold standard for diagnosis remains a neuropathological confirmation of dopaminergic neuronal cell loss. Interestingly, recent advances in neuroimaging have led to the development of several new MRI technologies and to optimism for new useful non-invasive biomarkers for diagnosing PD.

MRI is a valuable method to assist in the diagnostic work-up of PD. Most prominently described in recent years as potential biomarkers to discriminate PD patients from healthy controls (HC) are the signal loss of the nigrosome-1 area on iron sensitive images and reduced signal intensity of the substantia nigra on neuromelanin sensitive images (3, 4, 5, 6). However, limitations of previous studies that investigated these potential MRI biomarkers are small sample sizes, low imaging resolution and the inclusion of already advanced-staged PD patients in cohort studies. Moreover, most research utilized MRI scanners with a field strength below 7T, with 3T being commonly applied in studies. With the application of various 7T MRI sequences, like iron sensitive scans, neuromelanin sensitive scans and diffusion weighted imaging (DWI) scans, diagnostic confidence may improve due to increased spatial resolution and a higher signal to noise ratio as a result of ultra-high field imaging (5, 7).

DWI is a MRI technique which enables the measurement of the random Brownian motion of water molecules within the brain (8). This movement can be quantified via Diffusion Tensor Imaging (DTI), which helps to better understand the underlying white matter neurobiology on the macroscopic level. Commonly used measures are the fractional anisotropy (FA), which quantifies the preferred diffusion direction of water molecules and fibre mixture, the mean diffusivity (MD), which represents the diffusion magnitude, the radial diffusivity (RD), which is perpendicular to the aligned axons and reflects myelination, and the axial diffusivity (AD), which is parallel to axons and reflects organization (9, 10). DTI can be used for the reconstruction of fibre tracts, which allows to perform a virtual dissection of white matter on the voxel level.

The decreased ability to smell and to detect odours is one of the classical early symptoms of PD. The pathological mechanism is poorly understood but possibly involves neurodegeneration of the olfactory tract (OT) (1). In fact, from a neuropathological point of view, the OT and olfactory bulb are often recognized as one of the first structures affected, according to the well accepted Braak stadia of PD pathology (11). Previously, a meta-analysis highlighted that the OT could potentially serve as a biomarker for PD (12). However, previous work studying diffusion measures of the OT or olfactory areas showed varying results. Based on DTI subregion analyses in PD patients and HC, lower FA was reported in the anterior olfactory regions of the PD patients without overlapping distributions between groups (13). Furthermore, the MD of the OT was higher in PD patients compared to HC and correlated positively with OFF-medication motor scores (14). In addition, AD was lower in the white matter adjacent to the olfactory sulcus, which can be attributed to potential axonal degeneration (15). When comparing PD patients with HC, it was shown that both FA and tract volume of the OT were decreased in PD (16).

When comparing hyposmic/anosmic PD patients with normosmic HC, results can be interpreted along two axis; Hyposmic versus normosmic, and PD versus HC. This study therefore includes three groups to determine whether DWI measures of the OT may be able to serve as an early biomarker for PD; hyposmic/anosmic early stage PD patients (HA-PD), normosmic early stage PD patients (N-PD) and normosmic HC (N-HC).

This report is part of the TRACK-PD study, an observational ultra-high field imaging study aiming to provide more information on diagnosing PD and its subtypes (7). We hypothesize that diffusion measures will differ between groups. More specific, we hypothesize that FA values in the OT will be decreased in HA-PD compared to N-HC, while MD values will be increased in HA-PD. Additionally, the association between age and diffusion measures of the OT and PD symptom scores and diffusion measures of the OT will be explored.

2. Materials and Methods

2.1 Participants

Data collection was performed between July 2019 and December 2021 as part of the TRACK-PD study. The inclusion procedure, in- and exclusion criteria, and the study procedure are described elsewhere (7). In short, patients were diagnosed with PD maximally three years before the first testing day and were excluded when diagnosed with neurodegenerative diseases other than PD. Overall, participants were excluded

when they scored <24 points on the Montreal Cognitive Assessment (MoCA (17)) or when they had any MRI contraindications (claustrophobia or ferromagnetic implants). During the testing day, patients took their prescribed PD medication. The TRACK-PD study was approved by the Institutional Review Committee (IRB) of the Maastricht University Medical Centre and written informed consent was obtained from all participants.

2.2 Clinical assessments

During the testing day motor functions were assessed by trained and certified investigators using the unified Parkinson's Disease rating scale (MDS-UPDRS) and the Hoehn an Yahr scale. The MDS-UPDRS consists of four parts, including a motor evaluation (MDS-UPDRS III) (18). The Hoehn and Yahr scale is used to estimate the global disease stage of PD patients (19). In addition, participants were asked to complete the Self-Reported Mini Olfactory Questionnaire (Self-MOQ) at home (20). According to previous work, a cut-off score of 3.5 was used to distinguish normosmic versus hyposmic/anosmic participants (20).

2.3 MRI acquisition

Participants were scanned in a 7T MRI scanner (Magnetom, Siemens, Erlangen, Germany) equipped with a Nova Medical 32-channel head coil. PD patients were scanned in the ON-medication state for practical reasons such as a lower chance of motion artifacts by OFF-related tremors (if present). In addition, previous work shows that diffusion measures are not affected by antiparkinsonian medication (21). When possible, dielectric pads were applied to enhance the signal in especially the temporal brain regions (22). During the scan session, participants had the possibility to watch a movie projected on a screen, which was visible via a mirror.

The MRI protocol of the TRACK-PD study was described elsewhere (7). First a localizer sequence was acquired for optimal planning, and B0 and B1 mapping and shimming were used to correct for field inhomogeneities. A whole brain DWI scan was acquired using an echo-planar imaging (EPI) sequence, along 66 random directions with an average B-value of 2000s/mm² mixed with six B0-volumes. One B0-volume and five DWI volumes were acquired with an opposite phase encoding direction. Technical details of the DWI scan included; TE = 60.6 ms, TR = 7000 ms, flip angle = 90 degrees, FOV = 192x192 mm, resolution = 1.5 mm isotropic, number of slices = 80, orientation = interleaved axial, GeneRALized Autocalibrating Partial Parallel Acquisition (GRAPPA) (23) acceleration factor = 3, and acquisition time = 9:48 minutes.

2.4 MRI preprocessing

After conversion of the raw DICOM data to nifti format (24), DWI scans were denoised and potential Gibbs ringing artifacts were removed using MRtrix version 3 (25, 26, 27). Following this, the DWI scans were corrected for susceptibility induced distortions using topup, for eddy currents and subject motion (28, 29, 30), and b-matrix reorientation was performed using software from the FMRIB software library of FSL 5.0 (<http://www.fmrib.ox.ac.uk/fsl>). After this the generated mask was manually enlarged to include the area covering the OT. Data quality control was performed by visual inspection and quantification of the mean displacement values per volume based on the eddy current correction routine (31).

2.5 OT tractography

Seed regions of interest (ROI) were manually drawn by two raters (MH and AW) blinded to the clinical status of the participants. For each dataset, the average image of movement corrected B0 volumes was visualized. Next, an empty mask was created and seed ROIs were drawn for each participant according to the following guidelines; 1) Two axial slices of the average B0 image were selected in which the OT was best visible (Figure 1A). 2) Within these slices, five conjoined squares of 2x2 voxels were drawn for both the left and right OT, resulting in 40 voxels per slice and 80 voxels in total (Figure 1B).

Tractography of the OT was performed using MRtrix3. First, the response function was estimated with the constrained spherical deconvolution algorithm (32) and the fibre orientation distribution was estimated (33). Next, streamline tractography was performed utilizing the drawn seed ROI as seed and with the deterministic streamlines algorithm based on spherical deconvolution (34) (angle threshold = 30 degree, minimum track length = 5 mm, seeding direction = anterior-posterior). An example of the tractography results are shown in Figure 1C. Finally, tensors were fitted (35) and metrics were calculated in MRtrix3 to generate FA, MD, AD and RD maps. The total number of tracts, mean FA, MD, AD and RD values of the generated streamlines were calculated. The average diffusion measures of both raters were used for further analysis.

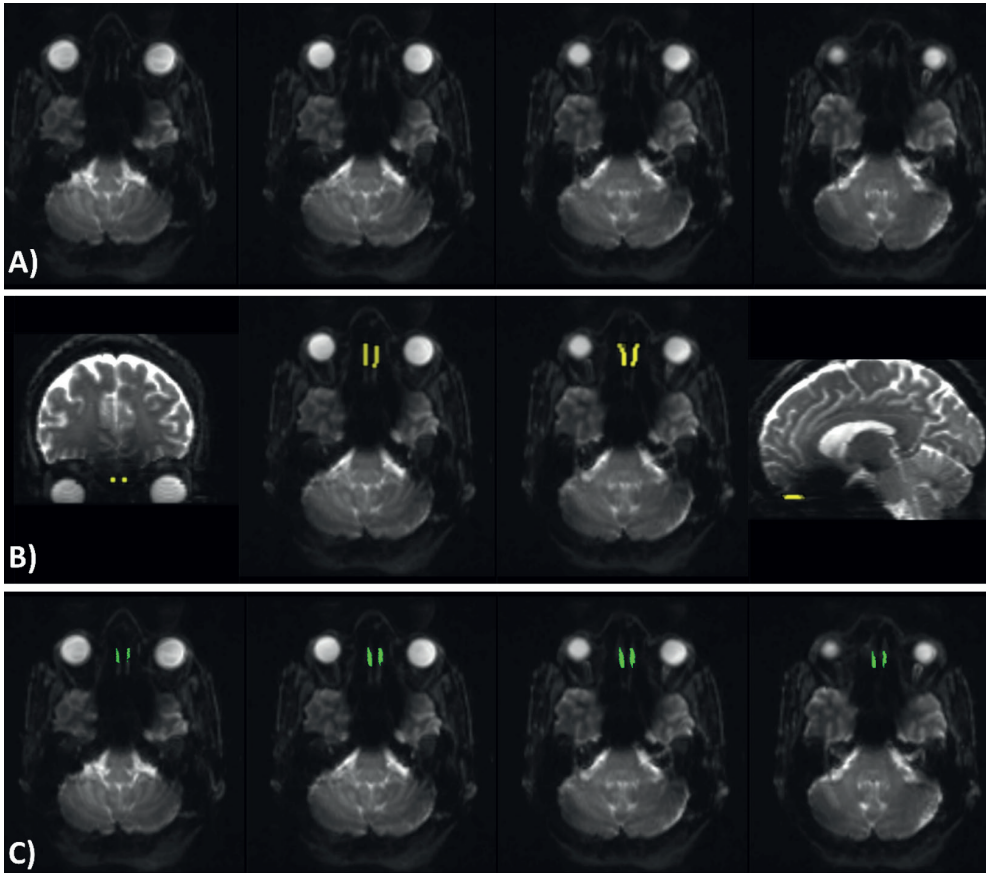


Figure 1. A) Four axial slices of the average corrected B_0 volumes. The two middle images were selected as the ones having the best visible olfactory tract. B) Coronal, axial, and sagittal view of the seed ROI representing the olfactory tract area. C) The same four axial slices as shown in A, showing the olfactory tract tractography results. Images are in radiological orientation.

2.6 Statistical analyses

Statistical analyses were performed using Rstudio version 1.4.1103. Demographic variables were compared between groups with Pearson's chi-squared test for categorical variables and student's t-test or one-way ANOVA for continuous variables. Any differences in diffusion measures of the OT between the PD and HC groups were tested utilizing student's t-test. Any differences in diffusion measures of the OT between the HA-PD, N-PD and N-HC groups were tested utilizing the one-way ANOVA. The Shapiro-Wilk test was used to assess the normality of the data. Non-parametric tests were used in case the assumption of normality was violated. The inter-rater reliability of the two ROI raters was assessed using the Intraclass Correlation Coefficient (ICC) (36). Correlations between diffusion measures of the OT and age and correlations between

diffusion measures of the OT and PD symptom scores (MDS-UPDRSIII score and PD disease duration) were assessed using Spearman correlation. Bonferroni corrections were applied to correct for multiple comparisons, leading to a significance level of 0.0125 for the correlation analyses.

3. Results

3.1 MRI quality control

Data quality control resulted in the exclusion of 11 datasets, resulting in a total of 123 participants. Four datasets were excluded since they contained multiple volumes which had a mean displacement larger than the voxel size (1.5 mm). Six datasets were excluded since the field of view did not cover the OT area. One dataset was excluded since the OT region showed an unacceptable amount of noise.

3.2 Demographics

In addition to the exclusions based on MRI quality control, one HC was excluded because of being classified as hyposmic (Self-MOQ > 3.5). Further, one PD patient was excluded because this participant was classified as outlier based on age. The resulting participant characteristics (n=121) are shown in Table 1.

No significant association was found between sex and group ($\chi^2(2) = 1.273$, $p = 0.529$), indicating an equal sex distribution between groups. No significant differences were found for age and MoCA scores between the groups ($p = 0.090$ and $p = 0.994$ respectively). Self-MOQ scores differed between groups ($p < 0.001$). Post-hoc tests showed that Self-MOQ scores differed between HA-PD and N-PD ($p < 0.001$) and between HA-PD patients and N-HC ($p < 0.001$), but not between N-PD and N-HC ($p = 0.090$). Time since PD diagnosis, LEDD and MDS-UPDRSIII scores did not differ between the PD groups ($p = 0.430$, $p = 0.083$, and $p = 0.686$ respectively). No significant association was found between Hoehn and Yahr score and PD groups ($p = 0.644$), indicating an equal Hoehn and Yahr distribution between groups.

Table 1. Demographic characteristics

	HA-PD (n=20)	N-PD (n=65)	N-HC (n=36)	P value
Male/female, n	15/5	45/20	22/14	0.529
Age, year	65.1 (7.7)	62.6 (8.0)	60.0 (8.4)	0.090
MoCA	27.7 (1.9)	27.7 (1.5)	27.7 (1.5)	0.994
Self-MOQ	4.8 (0.4)	0.7 (1.0)	0.3 (0.8)	<0.001
Time since PD diagnosis, months	18.2 (8.9)	19.9 (9.3)	-	0.430
Levodopa Equivalent Daily Dose	354.0 (229.8)	417.4 (223.7)	-	0.083
MDS-UPDRSIII	18.0 (7.3)	18.9 (7.5)	-	0.686
Hoehn and Yahr stage, n	Stage 1: 8 Stage 2: 12 Stage 3: 0 Stage 4: 0	Stage 1: 20 Stage 2: 42 Stage 3: 3 Stage 4: 0	-	0.644

Data are presented as mean (std). HA-PD: hyposmic/anosmic Parkinson's disease patients, N-PD: normosmic Parkinson's disease patients, N-HC: normosmic healthy controls, MoCA: Montreal Cognitive Assessment score, Self-MOQ: Self-Reported Mini Olfactory Questionnaire, MDS-UPDRS III: Movement Disorders Society Unified Parkinson Disease Rating Scale

3.3 Inter-rater reliability

The diffusion measures extracted from the tracts of the two ROI raters showed a good (FA ICC = 0.89, MD ICC = 0.90, RD ICC = 0.89) and excellent (AD ICC = 0.916) inter-rater reliability.

3.4 Group comparison of diffusion measures of the OT – PD vs. HC

The number of tracts did not significantly differ between PD (mean = 381.2, std = 79.3) and HC (mean = 406.1, std = 111.1). There was no significant difference in FA ($p = 0.211$), MD ($p = 0.505$), RD ($p = 0.735$), and AD values ($p = 0.220$) between PD and HC (Figure 2).

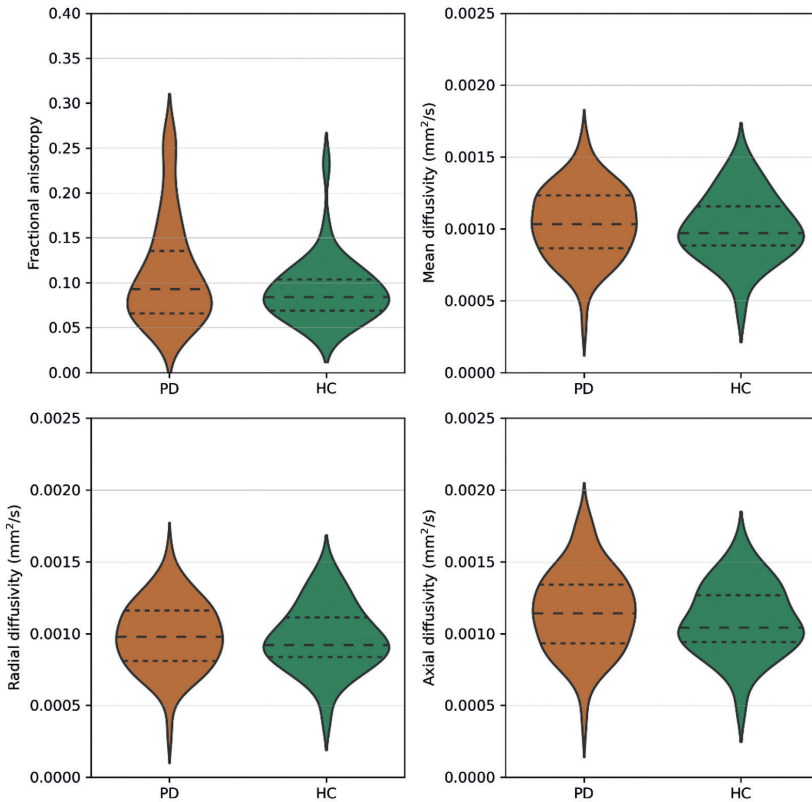


Figure 2. Fractional anisotropy, mean diffusivity, radial diffusivity and axial diffusivity values of the olfactory tract of Parkinson's disease patients (PD) and healthy controls (HC). Dashed lines represent the quartiles of the distribution. A significant difference in fractional anisotropy was found between PD (mean = 0.1116, std = 0.0581) and HC [(mean = 0.0911, std = 0.0350), $p=0.019$].

3.5 Group comparison of diffusion measures of the OT – HA-PD vs N-PD vs. N-HC

The number of tracts did not significantly differ between HA-PD (mean = 374.6, std = 76.2), N-PD (mean = 383.2, std = 80.7), and N-HC (mean = 406.1, std = 111.1). There was no significant difference in FA ($p=0.313$), MD ($p=0.750$), RD ($p=0.825$), and AD values ($p=0.509$) between the HA-PD, N-PD, and N-HC groups (Figure 3, Table 2).

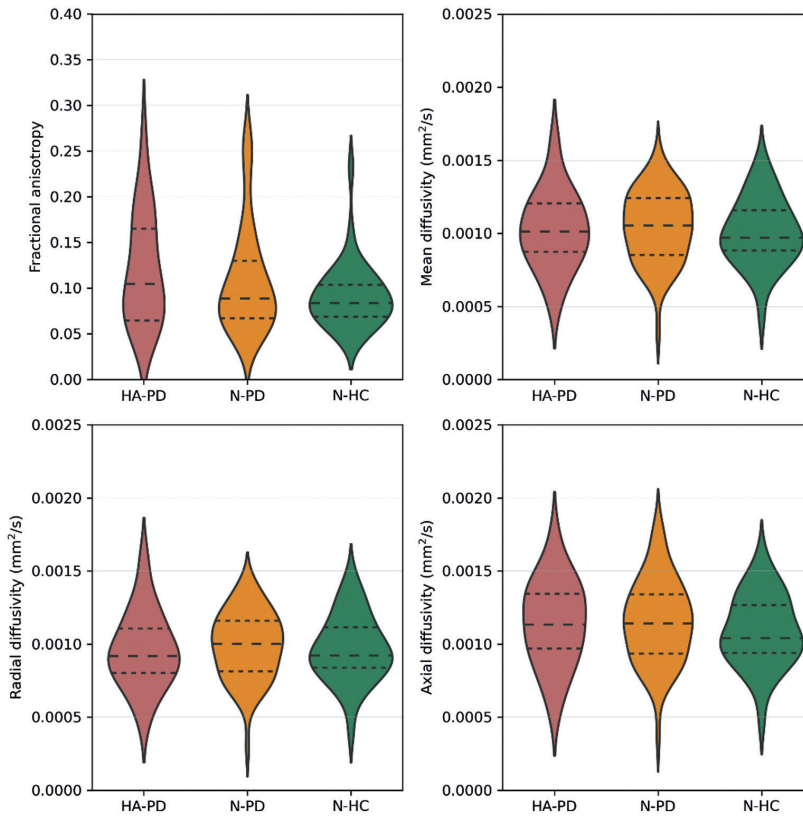


Figure 3. Fractional anisotropy, mean diffusivity, radial diffusivity and axial diffusivity values of the olfactory tract of hyposmic/anosmic Parkinson's disease patients (HA-PD), normosmic Parkinson's disease patients (N-PD), and normosmic healthy controls (N-HC). Dashed lines represent the quartiles of the distribution.

Table 2. Diffusion measures of the olfactory tract

	HA-PD (n=20)	N-PD (n=65)	N-HC (n=36)	P value
FA	0.1212 (0.0600)	0.1087 (0.0577)	0.0911 (0.0350)	0.313
MD (mm²/s)	0.0010 (0.0003)	0.0010 (0.0002)	0.0010 (0.0002)	0.750
RD (mm²/s)	0.0010 (0.0003)	0.0010 (0.0002)	0.0010 (0.0002)	0.825
AD (mm²/s)	0.0011 (0.0003)	0.0012 (0.0003)	0.0011 (0.0002)	0.509

Data are presented as mean (std). HA-PD: hyposmic/anosmic Parkinson's disease patients, N-PD: normosmic Parkinson's disease patients, N-HC: normosmic healthy controls, FA: fractional anisotropy, MD: mean diffusivity, RD: radial diffusivity, AD: axial diffusivity

3.6 Clinical correlations of diffusion measures of the OT

For the total group, significant positive correlations were found between MD and age ($r=0.283, p=0.006$), RD and age ($r=0.246, p=0.007$) and AD and age ($r=0.317, p<0.001$), but

not between FA and age ($r=-0.072$, $p=0.434$). When groups were compared separately regarding the association of MD, RD, and AD with age, significant positive correlations were found between MD and age ($r=0.576$, $p=0.008$) and AD and age ($r=0.667$, $p=0.001$) for only the HA-PD group (Figure 4). In contrast, no significant correlations were found between MD and age (N-PD $r=0.191$, $p=0.128$; N-HC $r=0.265$, $p=0.119$) and AD and age (N-PD $r=0.212$, $p=0.089$; N-HC $r=0.270$, $p=0.111$) for the N-PD and N-HC groups. No significant correlations were found between RD and age for the separate groups (HA-PD $r=0.538$, $p=0.015$; N-PD $r=0.157$, $p=0.210$; N-HC $r=0.270$, $p=0.111$).

In the PD group, a significant positive correlation was found between MDS-UPDRSIII (ON-medication) and FA ($r=0.304$, $p=0.005$). When PD groups were compared separately, no significant correlations were found for both the HA-PD ($r=0.359$, $p=0.120$) and the N-PD group ($r=0.302$, $p=0.015$). No significant correlations were found for PD duration and OT diffusion measures (FA $r=-0.056$, $p=0.608$; MD $r=0.091$, $p=0.407$; RD $r=0.097$, $p=0.377$; AD $r=0.076$, $p=0.489$).

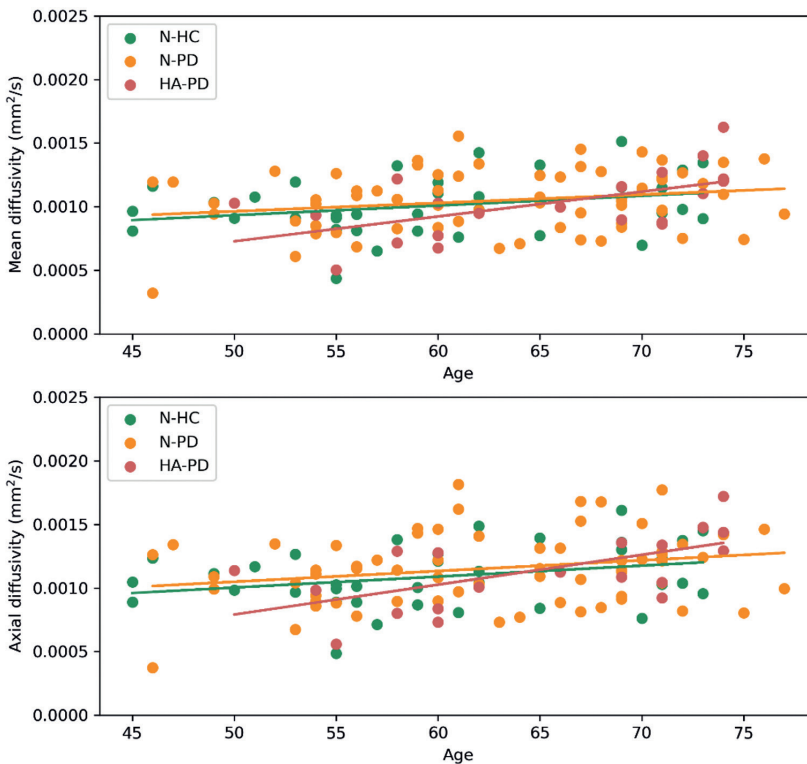


Figure 4. Correlation between mean diffusivity and age per group, and correlation between axial diffusivity and age per group. For the hyposmic/anosmic Parkinson's disease patients (HA-PD) significant correlations were found between age and mean diffusivity ($r=0.576$, $p=0.008$) and between age and axial diffusivity ($r=0.667$, $p=0.001$).

4. Discussion

This is the first study which shows feasible and reliable fibre tracking of the OT in both early stage PD and HC using 7T DWI data. We showed that diffusion measures of the OT did not differ between PD and HC and between HA-PD, N-PD, and N-HC. A positive correlation was found for age with MD, RD and AD. More specific, a correlation was found for age with MD and AD within the HA-PD group, but not within the N-PD and N-HC group. A significant positive correlation between MDS-UPDRSIII (ON-medication state) and FA was found, but not for the other diffusion measures. No significant correlations were found between disease duration and diffusion measures of the OT.

The positive correlation found in this study between MDS-UPDRSIII (ON-medication) and FA of the OT paradoxically suggests that OT integrity increases with PD severity. However, due to the presence of many crossing fibres in the white matter, FA can also increase as a result of disproportionate degradation of one or more of these fibre bundles, even despite an actual decrease in local fibre density and myelination (10, 37). This would indicate that the white matter fibres in the OT are less complex as PD severity increases, while myelin and axons are preserved. FA results should therefore be interpreted carefully. Recent work also emphasizes that MD measures are far more robust and interpretable compared to FA, AD, and RD (37). A previous study found a positive correlation between MD and MDS-UPDRSIII (OFF-medication), which is in the expected direction (14). These previous results should however be interpreted with caution, since the sample size in this study was small (n=16). The question therefore remains in which direction diffusion measures change in relation to neurodegenerative processes in different brain regions.

The positive correlation found in this study between age and MD supports the idea that aging plays an important role in OT alternations (38, 39). Since the positive correlation of MD with age was found only within the HA-PD subgroup, and an increase in MD can be related to higher axonal degeneration (9, 10), we suggest that aging is accelerated within the HA-PD group compared to the normosmic group. Another recent tractography study showed a negative correlation between FA values of the OT and age for only the HC group and not for the hyposmic PD group (16). It was suggested that hyposmic PD patients show a more constant and already early degenerated OT, while the OT degenerates with age in the HC group (16). This would infer that when comparing hyposmic PD with HC of a relatively low mean age, differences in OT degeneration should already be present. Future work comparing PD and HC groups of varying ages should be performed to replicate findings and to unravel how these correlations between FA and MD of the OT and age should be interpreted.

Results from previous studies (13, 14, 15, 16) can be interpreted along two axis; hyposmic versus normosmic, and PD versus HC. By using three subgroups, this study ruled out this interpretation along two axis. Our results did however not show any differences in diffusion measures between HA-PD, N-PD, and N-HC. Our methods most resemble the recent study by Nigro et al., 2020, which also used OT tractography of DWI images of a recently diagnosed PD group and a HC group. PD and HC groups were comparable to the groups in our study regarding age and disease duration. The main difference between the study performed by Nigro et al., 2020 and our study is the difference in MRI field strength (3T versus 7T). The fact that we did not replicate differences in diffusion measures of the OT between groups may be caused by the higher field strength used in this study. Although the use of 7T DWI may result in more precise targeting of the OT, DWI is one of the techniques for which the actual gain of using 7T may be limited (40), especially since the OT is anatomically close to air-filled sinuses which make this region more prone to susceptibility artifacts. Current results should be replicated using another 7T dataset.

There are several limitations of our study. First of all we used a questionnaire, the Self-MOQ, to assess smell capabilities, while previous work used olfactory testing. The Self-MOQ was previously tested extensively and has a good internal reliability and validity (20). By taking the cut-off score of 3.5 points, normosmic and hyposmic/anosmic participants were classified with an area under the curve of 0.85 (20). Although the Self-MOQ has been shown to be able to screen olfactory dysfunction, it cannot replace olfactory testing. It should also be taken into account that the incidence of hyposmic/anosmic PD patients in this study according to the Self-MOQ was 24%, while previous work reports percentages of over 60% (41). Second, we did not have any knowledge about potential COVID-19 infections at the time the Self-MOQ questionnaire was completed by the participants. It might be that a COVID-19 infection was the reason participants were classified as (temporarily) hyposmic/anosmic. Last, we used a fairly standard 7T MRI sequence in the TRACK-PD study, which was not optimized to measure the OT, and maybe multi-shell DWI is more sensitive. Extensive quality control of the diffusion data was however performed and we were able to reliably trace the OT for all participants.

In conclusion, this study showed that fibre tracking of the OT was feasible in both early stage PD and HC using 7T DWI data. In order to serve as a clinically relevant biomarker, the diffusion measures of the OT should differ between N-PD and N-HC. We therefore conclude, based on the presented results, that 7T diffusion measures of the OT are not useful as an early clinical biomarker for PD. Future work is needed to clarify the role of other OT measurements as a biomarker for PD.

5. References

1. Postuma RB, Berg D, Stern M, Poewe W, Olanow CW, Oertel W, et al. MDS clinical diagnostic criteria for Parkinson's disease. *Mov Disord*. 2015;30(12):1591-601.
2. Hughes AJ, Daniel SE, Ben-Shlomo Y, Lees AJ. The accuracy of diagnosis of parkinsonian syndromes in a specialist movement disorder service. *Brain*. 2002;125(Pt 4):861-70.
3. Isaias IU, Trujillo P, Summers P, Marotta G, Mainardi L, Pezzoli G, et al. Neuromelanin Imaging and Dopaminergic Loss in Parkinson's Disease. *Front Aging Neurosci*. 2016;8:196.
4. Lehericy S, Vaillancourt DE, Seppi K, Monchi O, Rektorova I, Antonini A, et al. The role of high-field magnetic resonance imaging in parkinsonian disorders: Pushing the boundaries forward. *Mov Disord*. 2017;32(4):510-25.
5. Prange S, Metereau E, Thobois S. Structural Imaging in Parkinson's Disease: New Developments. *Curr Neurol Neurosci Rep*. 2019;19(8):50.
6. Schwarz ST, Afzal M, Morgan PS, Bajaj N, Gowland PA, Auer DP. The 'swallow tail' appearance of the healthy nigrosome - a new accurate test of Parkinson's disease: a case-control and retrospective cross-sectional MRI study at 3T. *PLoS One*. 2014;9(4):e93814.
7. Wolters AF, Heijmans M, Michielse S, Leentjens AFG, Postma AA, Jansen JFA, et al. The TRACK-PD study: protocol of a longitudinal ultra-high field imaging study in Parkinson's disease. *BMC Neurol*. 2020;20(1):292.
8. Basser PJ, Mattiello J, LeBihan D. MR diffusion tensor spectroscopy and imaging. *Biophys J*. 1994;66(1):259-67.
9. Alexander AL, Lee JE, Lazar M, Field AS. Diffusion tensor imaging of the brain. *Neurotherapeutics*. 2007;4(3):316-29.
10. Mori S, Zhang J. Principles of diffusion tensor imaging and its applications to basic neuroscience research. *Neuron*. 2006;51(5):527-39.
11. Braak H, Ghebremedhin E, Rub U, Bratzke H, Del Tredici K. Stages in the development of Parkinson's disease-related pathology. *Cell Tissue Res*. 2004;318(1):121-34.
12. Atkinson-Clement C, Pinto S, Eusebio A, Coulon O. Diffusion tensor imaging in Parkinson's disease: Review and meta-analysis. *Neuroimage Clin*. 2017;16:98-110.
13. Rolheiser TM, Fulton HG, Good KP, Fisk JD, McKelvey JR, Scherfler C, et al. Diffusion tensor imaging and olfactory identification testing in early-stage Parkinson's disease. *J Neurol*. 2011;258(7):1254-60.
14. Scherfler C, Esterhammer R, Nocker M, Mahlknecht P, Stockner H, Warwitz B, et al. Correlation of dopaminergic terminal dysfunction and microstructural abnormalities of the basal ganglia and the olfactory tract in Parkinson's disease. *Brain*. 2013;136(Pt 10):3028-37.
15. Georgiopoulos C, Warntjes M, Dizdar N, Zachrisson H, Engstrom M, Haller S, et al. Olfactory Impairment in Parkinson's Disease Studied with Diffusion Tensor and Magnetization Transfer Imaging. *J Parkinsons Dis*. 2017;7(2):301-11.
16. Nigro P, Chiappiniello A, Simoni S, Paolini Paoletti F, Cappelletti G, Chiarini P, et al. Changes of olfactory tract in Parkinson's disease: a DTI tractography study. *Neuroradiology*. 2021;63(2):235-42.
17. Nasreddine ZS, Phillips NA, Bédirian V, Charbonneau S, Whitehead V, Collin I, et al. The Montreal Cognitive Assessment, MoCA: a brief screening tool for mild cognitive impairment. *J Am Geriatr Soc*. 2005;53(4):695-9.
18. Goetz CG, Tilley BC, Shaftman SR, Stebbins GT, Fahn S, Martinez-Martin P, et al. Movement Disorder Society-sponsored revision of the Unified Parkinson's Disease Rating Scale (MDS-UPDRS): scale presentation and clinimetric testing results. *Mov Disord*. 2008;23(15):2129-70.

19. Goetz CG, Poewe W, Rascol O, Sampaio C, Stebbins GT, Counsell C, et al. Movement Disorder Society Task Force report on the Hoehn and Yahr staging scale: status and recommendations. *Mov Disord*. 2004;19(9):1020-8.
20. Zou LQ, Linden L, Cuevas M, Metasch ML, Welge-Lussen A, Hahner A, et al. Self-reported mini olfactory questionnaire (Self-MOQ): A simple and useful measurement for the screening of olfactory dysfunction. *Laryngoscope*. 2020;130(12):E786-E90.
21. Chung JW, Burciu RG, Ofori E, Shukla P, Okun MS, Hess CW, et al. Parkinson's disease diffusion MRI is not affected by acute antiparkinsonian medication. *Neuroimage Clin*. 2017;14:417-21.
22. Teeuwisse WM, Brink WM, Webb AG. Quantitative assessment of the effects of high-permittivity pads in 7 Tesla MRI of the brain. *Magn Reson Med*. 2012;67(5):1285-93.
23. Griswold MA, Jakob PM, Heidemann RM, Nittka M, Jellus V, Wang J, et al. Generalized autocalibrating partially parallel acquisitions (GRAPPA). *Magn Reson Med*. 2002;47(6):1202-10.
24. Li X, Morgan PS, Ashburner J, Smith J, Rorden C. The first step for neuroimaging data analysis: DICOM to NIFTI conversion. *J Neurosci Methods*. 2016;264:47-56.
25. Kellner E, Dhital B, Kiselev VG, Reiser M. Gibbs-ringing artifact removal based on local subvoxel-shifts. *Magn Reson Med*. 2016;76(5):1574-81.
26. Veraart J, Fieremans E, Novikov DS. Diffusion MRI noise mapping using random matrix theory. *Magn Reson Med*. 2016;76(5):1582-93.
27. Veraart J, Novikov DS, Christiaens D, Ades-Aron B, Sijbers J, Fieremans E. Denoising of diffusion MRI using random matrix theory. *Neuroimage*. 2016;142:394-406.
28. Andersson JL, Skare S, Ashburner J. How to correct susceptibility distortions in spin-echo echo-planar images: application to diffusion tensor imaging. *Neuroimage*. 2003;20(2):870-88.
29. Andersson JLR, Sotiropoulos SN. An integrated approach to correction for off-resonance effects and subject movement in diffusion MR imaging. *Neuroimage*. 2016;125:1063-78.
30. Smith SM, Jenkinson M, Woolrich MW, Beckmann CF, Behrens TE, Johansen-Berg H, et al. Advances in functional and structural MR image analysis and implementation as FSL. *Neuroimage*. 2004;23 Suppl 1:S208-19.
31. Bastiani M, Cottaar M, Fitzgibbon SP, Suri S, Alfaro-Almagro F, Sotiropoulos SN, et al. Automated quality control for within and between studies diffusion MRI data using a non-parametric framework for movement and distortion correction. *Neuroimage*. 2019;184:801-12.
32. Tournier JD, Calamante F, Connelly A. Determination of the appropriate b value and number of gradient directions for high-angular-resolution diffusion-weighted imaging. *NMR Biomed*. 2013;26(12):1775-86.
33. Tournier JD, Calamante F, Connelly A. Robust determination of the fibre orientation distribution in diffusion MRI: non-negativity constrained super-resolved spherical deconvolution. *Neuroimage*. 2007;35(4):1459-72.
34. Tournier J-D, Calamante F, Connelly A. MRtrix: Diffusion tractography in crossing fiber regions. *International Journal of Imaging Systems and Technology*. 2012;22(1):53-66.
35. Basser PJ, Mattiello J, LeBihan D. Estimation of the effective self-diffusion tensor from the NMR spin echo. *J Magn Reson B*. 1994;103(3):247-54.
36. Bartko JJ. The intraclass correlation coefficient as a measure of reliability. *Psychol Rep*. 1966;19(1):3-11.
37. Figley CR, Uddin MN, Wong K, Kornelsen J, Puig J, Figley TD. Potential Pitfalls of Using Fractional Anisotropy, Axial Diffusivity, and Radial Diffusivity as Biomarkers of Cerebral White Matter Microstructure. *Frontiers in neuroscience*. 2021;15:799576.

38. Felix C, Chahine LM, Hengenius J, Chen H, Rosso AL, Zhu X, et al. Diffusion Tensor Imaging of the Olfactory System in Older Adults With and Without Hyposmia. *Front Aging Neurosci.* 2021;13:648598.
39. Kondo K, Kikuta S, Ueha R, Suzukawa K, Yamasoba T. Age-Related Olfactory Dysfunction: Epidemiology, Pathophysiology, and Clinical Management. *Front Aging Neurosci.* 2020;12:208.
40. Polders DL, Leemans A, Hendrikse J, Donahue MJ, Luijten PR, Hoogduin JM. Signal to noise ratio and uncertainty in diffusion tensor imaging at 1.5, 3.0, and 7.0 Tesla. *J Magn Reson Imaging.* 2011;33(6):1456-63.
41. Kanavou S, Pitz V, Lawton MA, Malek N, Grosset KA, Morris HR, et al. Comparison between four published definitions of hyposmia in Parkinson's disease. *Brain Behav.* 2021;11(8):e2258.

CHAPTER 8



General discussion

Parkinson's disease (PD) is a common neurodegenerative disorder, characterized by bradykinesia, rigidity and resting tremor, which greatly affects the quality of life of patients and their caregivers. Despite the strongly rising incidence of the disease, the underlying pathophysiology is still not fully clarified. Patients often experience a delay in diagnosis and have visited multiple healthcare providers such as an orthopedic surgeon, rheumatologist or psychiatrist, before getting diagnosed with PD. Fortunately, with the introduction of new diagnostic criteria, there has been a noticeable improvement in clinical diagnostic accuracy in recent years (1). However, it is important to note that at present, there are no treatment options that can cure or slow down the disease. The aim of the studies presented in this thesis is to identify magnetic resonance imaging (MRI) biomarkers for PD, with a specific focus on cognitive impairment associated with PD. Furthermore, by investigating structural and functional MRI changes in relation to different PD symptoms, this thesis aims to contribute to the elucidation of the PD pathophysiology and the neurodegenerative processes which underline cognitive impairment in PD. In this chapter we will further discuss the results of these studies, the advantages and limitations of MRI biomarkers in the assessment of cognitive decline and their use for the diagnosis and monitoring of PD. We conclude with future directions for MRI research in PD.

1. The role of MRI in assessing cognitive impairment in Parkinson's disease

Already in the earliest phases of the disease mild cognitive impairment can be found in up to 42.5% of the PD patients (2). Eventually, in the advanced stages of the disease, 80% of the patients develop Parkinson's disease dementia (PDD) (3). Therefore, recognizing cognitive impairment in PD and elucidating the underlying pathophysiology is of great importance. In our meta-analysis in chapter 2, we intend to provide an overview and synthesis of the network disruptions associated with cognitive impairment in PD. It underlines the important role of the default mode network in cognitive decline and shows that differences in functional connectivity in this network differentiate between PD patients with cognitive impairment and PD patients without cognitive impairment. The importance of network changes in the early phases of cognitive impairment is confirmed by the results of the study presented in chapter 3. The observation that differences in cortical thickness, cortical folding and grey matter are only evident in PD patients with severe cognitive impairment, rather than those with milder forms of cognitive decline, suggests that white matter tracts might play a more prominent role in the early stages of cognitive impairment, as opposed to grey matter structures. Based on these results it can be hypothesized that white matter changes precede grey matter alterations. An alternative explanation could be that the methods used in our study

were not able to detect subtle grey matter changes. However, other studies which have analyzed white and grey matter simultaneously by combining structural and diffusion-weighted MRI techniques, also point towards changes in white matter preceding grey matter alterations in cognitively impaired PD patients (4, 5). It therefore does not appear likely that our results are caused by methodological shortcomings. By all means, assessing white matter tracts or cerebral network connectivity is more promising as an early biomarker for the identification of PD patients at risk for cognitive decline than measurements of cortical thickness, cortical folding or grey matter volume. These findings also offer a more comprehensive understanding of the initial pathophysiology underlying cognitive impairment in Parkinson's disease.

The detection of cognitive impairment in PD and the discovering of its underlying pathophysiology is very important, not only to provide treatment and support for the cognitive complaints, but also because deficits in specific cognitive domains (such as executive functions and attention) predict fall risk in older individuals after five years (6). A possible explanation for the latter may be that people with well-developed executive functions have better strategies for dealing with difficult walking conditions that require higher-level cognitive control. Fall risk in cognitively impaired PD patients might be even more increased, since these patients already have PD related gait difficulties. In line with this, cross-sectional studies show that PD patients with prominent postural instability and gait disorders perform worse in cognitive tests compared to patients with a tremor-dominant phenotype (7). Future longitudinal studies are necessary to assess the temporal relationship between cognition and fall risk in PD. However, including executive function and attention tests to screening batteries evaluating fall risk in PD is important. And conversely, gait analysis might be important in patients with cognitive impairment. Several studies have already indicated that motor-cognitive dual-task training contributes to a reduction of fall risk in the elderly (8). This might also elucidate the reason behind the positive effect that the acetylcholinesterase inhibitor rivastigmine has on gait stability and the risk of falling in PD (9). We therefore propose early cognitive screening and the application of targeted motor-cognitive dual-task training in PD patients with cognitive decline to reduce fall risk.

At this moment there are no proven disease modifying therapies for cognitive impairment in PD. However, many pharmacological and non-pharmacological treatment strategies are being investigated (10, 11). Providing better insight into the underlying pathophysiology of cognitive dysfunction might aid in the development of these future therapeutic interventions. Furthermore, radiological biomarkers could be an objective tool to monitor future therapeutic strategies in research settings. Of course, cognitive performance can be monitored clinically with a neuropsychological assessment. But these tests provide a snapshot in time, which can be influenced by several varying

factors such as fatigue, mood and motivation. This complicates the development of new therapeutic strategies. MRI parameters might be able to provide a more objective monitoring tool, potentially being able to detect smaller changes compared to clinical tests. However, no MRI modality has yet been discovered that alone is able to fulfill this monitoring function. For this reason, there is a need for the development of future multi-modal MRI approaches (12). Determining reliable monitoring biomarkers can also aid in the selection of promising therapeutic strategies in early phase studies, which can subsequently be investigated further in clinical practice.

When therapeutic strategies become available, a next step would be to investigate whether functional connectivity alterations in the default mode network can already be detected before clinical manifestation of cognitive impairment appear. When patients at risk for cognitive decline can be identified in a prodromal stage, patients might benefit from early treatment to prevent further cognitive deterioration. We therefore believe that there is a need for future longitudinal MRI studies, following large patient groups over an extended period of time, which evaluate the temporal relationship between cognition and default mode network connectivity in PD.

2. Heterogeneity in Parkinson's disease and subtyping approaches

At this moment subtyping in PD still has substantial methodological shortcomings and questionable clinical applicability (13). Patients are often divided into a tremor-dominant (TD), indeterminate and postural instability and gait disorders (PIGD) subtype (14). However, since PD consists of a wide variety of both motor and non-motor symptoms, subtyping patients based on motor symptoms alone is most likely too simplistic. Unfortunately, other proposed data-driven subtype classifications have so far not proven to be reproducible or stable over time (15). Improved knowledge about PD subtypes and different pathophysiological processes would create the possibility to develop new therapies and to apply personalized medicine. For this reason, determining consistent and reproducible PD subtypes, with unique pathological characteristics, is currently one of the biggest challenges in PD research. To advance this field of research, it may be necessary to conduct extensive multimodal studies in a data driven approach (not hypothesis driven). These studies should combine clinical, genetic, radiological, and biochemical parameters while implementing machine learning techniques.

Over the past years, knowledge has been acquired about molecular pathways that are implicated in the PD pathogenesis by studying patients with familial PD. This includes aggregation of α -synuclein, neuroinflammation, oxidative stress and mitochondrial and

lysosomal dysfunction (16). However, the question remains whether this information can also be applied to idiopathic PD and whether the heterogeneity of PD represents a disease spectrum with different clinical subtypes, or rather separate diseases with a distinct molecular profile (15). Genetic studies have also redefined our understanding of the clinical entity of Parkinson's disease. Evaluation of monogenetic patients taught us that PD is a phenotypically diverse illness and that there is greater overlap with atypical parkinsonism than previously thought. Patients with a disease-causing mutation in the LRRK2 gene can present with a typical levodopa responsive PD, but a minority of these cases display a progressive supranuclear palsy phenotype (17). Moreover, most LRRK2 PD patients display indistinguishable pathological features from patients with sporadic PD. However, there is a subset of LRRK2 PD patients who do not have Lewy-body pathology and lack alpha synuclein aggregates in their cerebrospinal fluid (18, 19). While the classic PD motor symptoms can manifest without Lewy-body pathology, several non-motor symptoms, such as anxiety and cognitive decline, are associated with the presence of Lewy-bodies (20). Patients with other genetic mutations, such as in the GBA, SNCA or VPS13C genes, can manifest with a levodopa responsive PD, but more often they develop progressive cognitive impairment resembling Lewy body dementia (17). Apart from the fact that different kinds of pathogenic mutations in the same gene can cause different disease manifestations, the pathophysiological process is also likely to be influenced by environmental factors. This causes the phenotype of an individual patient to be the result of an interaction between genetics and environmental exposures (21). Studying these familial patient groups may provide more information regarding the pathways involved in the development of parkinsonism and may help to discover targets for therapy.

The substantial symptom heterogeneity at the level of individual patients and the many involved variables and confounders make analyses and hypothesis building with respect to PD subtypes highly complex. Advances in MRI methods and analytical techniques create the possibility to investigate changes within the nigrostriatal system, as well as in other brain regions associated with motor and non-motor symptoms of PD. Neuroimaging can therefore aid in the search for biomarkers associated with different PD subtypes and distinct pathophysiological processes. Extensive and detailed phenotyping in longitudinal cohort studies that combine different MRI techniques with other biomarkers such as genetics and cerebrospinal fluid biomarkers, would allow to further define specific MRI correlates underlying various phenotypes of the disease. The longitudinal ultra-high field study described in chapter 4 aims to help in the elucidation of these research questions. In the next two paragraphs, two first attempts will be discussed that aimed to detect imaging biomarkers for PD using baseline data from this ultra-high field study.

3. Imaging of the olfactory tract

Hyposmia is a frequent non-motor symptom in prodromal and early PD. It can be detected in 73% of the early-PD patients, compared to 29% of the healthy population (22). For this reason, imaging characteristic of the olfactory tract have been a topic of interest in the search for early biomarkers. Several studies have investigated diffusion measures of the olfactory tract. Results between studies vary, but indicate that alterations in mean diffusivity and fractional anisotropy of the olfactory tract could be a biomarker for PD (23). In chapter 5 we demonstrated that fiber tracking of the olfactory tract is feasible on ultra-high field 7T MRI. However, no differences in diffusion measures were found between normosmic healthy controls and PD patients with and without hyposmia. The results therefore indicate that 7T diffusion measures of the olfactory tract are not useful as an early clinical biomarker in PD. However, it should be noted that the olfactory function in this study was assessed by a self-reporting questionnaire and not by a specific olfactory test, which might have influenced the study results. Nonetheless, the study in chapter 5 also possesses certain advantages in comparison to previous studies (24, 25). These include a significantly larger sample size of early-stage PD patients and the application of ultra-high field MRI technology. Although compared to other MRI techniques, the actual gain of using 7T MRI for diffusion tensor imaging may be more limited (26).

Variability in study results and lack of distinctiveness between PD and HC in our study, might be partially explained by recent findings suggesting a revision of the dual-hit hypothesis in PD. Originally, a dual-hit hypothesis was suggested by Braak and colleagues, proposing that PD pathophysiology enters the brain via two different entry points, namely via the nasal area and the autonomic nerve system (27). That being said, recent data suggests that a single-hit hypothesis in PD might be more appropriate. This theory suggests that in some patients the PD pathology enters the brain through the autonomic nervous system and lower brainstem without involvement of the olfactory bulb in early disease stages, while in other patients it enters the brain through the olfactory tract, predominantly affecting the olfactory bulb and amygdala region, without early involvement of the autonomic nervous system (28). Based on this hypothesis some PD patients are expected to display alterations in the olfactory tract early in the disease course, while this is not the case in another subgroup of patients. Results of studies investigating olfactory tract changes in unselected groups of PD patients could substantially be affected by this. Furthermore, it is yet another example of how heterogeneity in PD complicates the search for early biomarkers.

Based on this theory more distinctive results might be expected when a specific subgroup of early PD patients with hyposmia is compared to HC. This requires strict

selection, identifying only patients with obvious olfactory disturbances early in the disease course. Based on the results in chapter 5, a self-reporting questionnaire might be too subjective and insensitive for a proper selection and it is suggested that olfactory testing is a more appropriate method to select these patients.

4. Neuromelanin imaging

The visualization of neuromelanin related signal on structural MRI is considered to be one of the most promising radiological biomarkers in PD. The insoluble pigment neuromelanin is a by-product of the oxidative metabolism of dopamine and noradrenaline and is predominantly situated in the substantia nigra (SN) and locus coeruleus (LC) (29). Neuromelanin related signal intensity decreases with age in the normal population, but this process is accelerated in PD patients. Several 3T MRI studies have consistently shown a reduced neuromelanin related signal intensity of the SN in PD compared to HC subjects (30). The study described in chapter 6 aimed to replicate these findings with ultra-high field 7T MRI in a relatively large group of early PD patients. In addition, 7T MRI facilitates the visualisation of smaller brain stem nuclei such as the LC. The results of this study show that neuromelanin related signal in the LC differentiates between early PD and HC. However, no differences in signal intensity of the SN were found between groups. This supports the theory of bottom-up disease progression proposed by Braak and colleagues (31). Although this theory seems to be applicable to a subgroup of PD patients, the recent single-hit hypothesis described in the previous paragraph suggests that some PD cases display an alternative route of disease progression (28). When we elaborate on the single-hit hypothesis, differences in NM related signal intensity of the LC and SN between PD patients and HC might be more obvious when a subgroup of PD patients is selected with early autonomic symptoms, suggesting an entry of the PD pathology to the brain through the autonomic nervous system and lower brainstem. Although intriguing, this remains very speculative and future studies are first required to confirm the single-hit hypothesis.

Neuromelanin related signal changes in the LC and SN appear to have a regional distribution. Although our study confirmed that signal intensity alterations can also be found in the mid-portion of the LC, recent research indicates that signal changes are even more pronounced in the caudal parts of the LC (32). In addition, neuromelanin related signal decrease in the dorsal pars compacta of the SN (SNc) may be more apparent compared to the ventral pars reticulata (SNr) (33). More detailed ultra-high field MRI analyses, focussing on different subregions of the LC and SN, are needed to find out more about this regional distribution of signal alterations and the way it can be used as a imaging biomarker for PD.

Research focussing on neuromelanin related signal changes in the brain is complicated by the use of several different analytical methods. In addition, it often requires manual outlining of the LC and SN. This makes it difficult to replicate study results and compare outcomes. On top of that it is a labour intensive process, making it hard to translate these methods to clinical practice. For these reasons, the study described in this thesis used largely automated methods for the segmentation of the SN and LC. Future studies should focus on the further development of automated segmentation and quantification approaches.

5. The role of MRI in identifying biomarkers for Parkinson's disease

One of the biggest problems related to neurodegenerative diseases, including PD, is the current lack of disease-modifying interventions. Early and accurate diagnosis and monitoring indicators are necessary to develop new treatment methods. Many different biomarkers such as clinical assessments, genetic testing, biochemical markers and several different imaging methods are investigated (34). MRI is a non-invasive imaging method with no harmful effects for the patient. By combining different techniques, such as functional MRI, tractography and structural imaging, it enables us to assess and monitor both regional changes and network alterations. This is important, since symptoms in PD are presumably not solely driven by degeneration of one brain area but rather by multifocal involvement of multiple regions causing broader network dysfunction (35). MRI therefore serves as a promising biomarker for both motor and non-motor symptoms in PD.

Defining MRI biomarkers in PD might serve several goals. First of all, by comparing structural and functional MRI characteristics between PD and HC, information can be acquired regarding the underlying pathophysiology of PD. Also, imaging of several different brain areas involved in the PD pathophysiology may help to explain the heterogeneity between patients and support in the definition of PD subgroups. Additionally, structural and functional MRI biomarkers could distinguish PD patients from HC in early stages of their disease and are therefore able to facilitate the clinical diagnosis of PD. These MRI characteristics can also improve patient selection for clinical trials. Finally, MRI biomarkers assessing disease progression can be used to monitor treatment effect in studies investigating disease-modifying therapies. Especially in phase 1 studies, neuroimaging outcome measures provide a more objective way to select promising intervention strategies compared to clinical measures (36).

As mentioned above, one can distinguish between biomarkers that can be useful in the diagnosis of PD and biomarkers that can be used as a monitoring tool for disease progression. Some MRI characteristics might differentiate between PD and healthy controls but might not be correlated with disease progression and are therefore not suited to be used as a monitoring tool. However, MRI has the potential to be used for both diagnostic and monitoring purposes, with some imaging techniques being more suitable as a diagnostic while others serve better as a monitoring biomarker. For example, structural changes of the SN in early-stage PD patients start within the Nigrosome 1 (N1) area. The loss of dopaminergic neurons in the N1 is thought to reach a lower limit early in the disease course. Signal changes in this area can therefore serve as a diagnostic biomarker, but are not able to monitor disease progression and are therefore not very helpful as a disease marker in therapeutic intervention studies (30). In addition, fMRI can be influenced by several external factors such as the use of (dopaminergic) medication and current state of mind (37). For this reason, fMRI is less usable as a disease monitoring tool. On the other hand, evidence suggests that neuromelanin related signal changes in PD are associated with disease progression and might therefore be able to serve as a monitoring biomarker (38). For studies evaluating new therapeutic interventions it is very important to consider these differences when selecting the outcome measures that are used to evaluate treatment effects.

Recently, many advances in MRI techniques have been made. With the emergence of ultra-high-field scanners (7T and above) submillimetric anatomical information can be obtained. Ultra-high field MRI provides higher spatial resolution and an increased signal-to-noise ratio enabling a higher degree of diagnostic detail compared to traditional MRI techniques (1.5 or 3T) (39). This improves the visualization of small brain stem nuclei which are important in the PD pathophysiology. However, some limitations also emerge regarding the use of 7T MRI. One of these limitations is related to Specific Absorption Rate (SAR) restrictions at 7T MRI. While signal-to-noise ratio greatly improves with 7T MRI, the SAR restrictions cause the contrast-to-noise ratio of the MT-TFL sequence to be slightly less than that in 3T MRI (40). Furthermore, scanning at a higher field strength can be subject to increased inhomogeneity of the radio frequency field (B1 inhomogeneity). This can introduce artefacts resulting from varying signal intensity and tissue contrast in the acquired image (41). However, ongoing technological advancements are expected to further improve the reliability and quality of the 7T MRI in the upcoming years, making it a promising technique to detect subtle structural and functional abnormalities.

An important limitation for MRI studies is the fact that many different methods are used for the analysis and processing of images. This makes it harder to compare findings across studies and causes varying and sometimes contradicting results. Variability in results is also induced by the relatively small number of participants in many MRI studies.

Moreover, many methods that are currently applied in clinical studies require manual outlining of subcortical nuclei or specific brain regions. This process is time consuming and introduces variability due to inter-rater differences. To be able to apply research findings in clinical practice, there is a need for the development of automated analysis methods. Another limitation specifically related to fMRI, is that results are heavily influenced by dopaminergic medication. Previous studies have already demonstrated that dopaminergic medication influences brain connectivity patterns both in a linear and non-linear way, with a tendency to normalize abnormal brain connectivity (37). Hence it is very important to always correct for the levodopa equivalent daily dose in fMRI studies or to make sure that participants are scanned in 'OFF' medication state. However, whereas scanning in 'OFF' state rules out the direct confounding effect of levodopa use, there are still some challenges. Secondary alterations in dopaminergic transmission, such as receptor up- and downregulation take a longer time to restore and may still confound outcomes by exaggerating alterations in connectivity (42).

6. The relation between MRI and other biomarkers

Besides MRI, several other promising imaging and biochemical techniques have been investigated as a biomarker for PD. It has been demonstrated that α -synuclein seed amplification assays in the cerebrospinal fluid might be able to detect prodromal individuals at-risk for PD before diagnosis. In addition, α -synuclein seed amplification assays are able to differentiate PD patients from healthy controls with high accuracy (sensitivity 87,7%, specificity 96,3%) (43). Novel techniques designed to detect α -synuclein in serum also show promising results in differentiating between PD patients and healthy individuals (44). This makes α -synuclein detection in cerebrospinal fluid and serum an interesting diagnostic biomarker for PD and a valuable tool for study population selection in intervention studies. However, a certain amount of heterogeneity within the PD population has been detected. LRRK2 variant carriers and individuals with preserved olfactory function are for example more likely to have a negative α -synuclein seed amplification assay result (43). Another promising serum biomarker is neurofilament light chain, which might be able to differentiate PD from atypical forms of parkinsonism (45). Furthermore, it has yet to be determined whether α -synuclein and neurofilament light chain levels also correlate with clinical symptoms and disease progression. This will determine its utility as a monitoring biomarker in PD.

In addition, single photon emission computed tomography (SPECT) and positron emission tomography (PET) nuclear imaging techniques, able to detect minor alterations in the molecular organization of the brain, have proven to be a valuable biomarker method in PD (46). Dopamine transporter (DAT)-SPECT scans, measuring the

presynaptic striatal dopamine transporter function, offer a reliable way to distinguish between patients with parkinsonism, healthy controls, and Parkinson mimics such as drug-induced parkinsonism (47). Furthermore, abnormal dopaminergic imaging characteristics can already be detected in prodromal subjects, years before the onset of motor symptoms (48). However, DAT-SPECT cannot discriminate between PD and atypical parkinsonism (49). Although FDG-PET might be able to contribute to the differentiation between different forms of parkinsonism, the use of FDG-PET for this purpose is not yet standardized (46). Additionally, several SPECT and PET tracers for non-dopaminergic neurotransmitter receptors and specific enzymes have been developed. This creates the opportunity to study for example noradrenergic and serotonergic transmission in relation to non-motor symptoms in PD (46). Moreover, nuclear tracers are currently being developed for the imaging of α -synuclein (50). These advances might be able to provide novel interesting nuclear imaging biomarkers in the near future.

The most commonly used biomarker methods for PD all have their own advantages and shortcomings. Compared to other modalities, MRI is a non-invasive imaging technique that does not cause any discomfort or harmful effects for the patient. It is therefore a safe method for repeated imaging and very well suited to be used in longitudinal research. Furthermore, its technique is already widely embedded in clinical practice. The diverse spectrum of motor and non-motor symptoms in PD are probably related to both structural and functional alterations in several different brain areas. MRI provides the opportunity to easily combine different techniques, such as functional MRI, tractography and various types of anatomical sequences, which provide detailed information regarding specific regions or networks. This wide applicability is a great advantage compared to other biomarker techniques. MRI is therefore particularly useful to study the underlying pathophysiology of individual PD symptoms. Moreover, as described in the subsection above, certain MRI characteristics such as neuromelanin related signal changes are associated with disease progression and might therefore be able to serve as a monitoring tool for PD.

Although the temporal ordering of biomarker alterations in PD still has to be determined, recent studies suggest that abnormalities in α -synuclein seed amplification assays might be present earlier in the disease process compared to physiological markers (43). Data suggests a premotor phase of PD years before the development of nigrostriatal dysfunction as detected by neuropathological studies or nuclear imaging techniques (51). Based on these results it seems likely that biochemical alterations precede structural changes, as assessed by anatomical MRI techniques, with several years. Measurements of α -synuclein are therefore better suited to serve as a prodromal diagnostic biomarker compared to MRI techniques.

In conclusion, there probably is no single method with the potential to serve as the perfect PD biomarker and different biomarker techniques are likely to complement each other (52). A combination of different biochemical and imaging techniques is therefore expected to have the best results for both the diagnosis and monitoring of PD.

7. Future directions

Although by using several advanced MRI techniques it has become possible to identify promising biomarkers for early PD, there might not be one single imaging target that could serve as the perfect MRI biomarker (52). Also for the distinction of PD from atypical parkinsonism, there is not one early radiological sign which can reliably differentiate between these conditions. Atypical parkinsonism might display more widespread degenerative tissue alterations compared to PD. In line with this, promising results have been published from an earlier study which investigated machine learning approaches with automated volumetry methods for the differentiation between PD and atypical parkinsonism (53). In addition, multimodal imaging combining several different MRI parameters enables the distinction of PD from atypical parkinsonism with far better accuracy compared to studies focusing on one single MRI biomarker (54). Future studies should therefore have a multimodal character, combining the most promising biomarkers, and implement observer-independent machine learning approaches and automated techniques.

While PD was previously seen as one disease entity, it is now considered more and more as a spectrum of disease, consisting of several subtypes with a different disease course and response to therapy. In the search for reliable and consistent PD subtypes, genetics will play an increasingly important role in the upcoming years. Additional genetic forms of PD might be identified. But more importantly, better understanding of the complex interaction between genetics and environmental or lifestyle factors needs to be acquired (55). This will enable the usage of polygenic risk scores or machine-learning approaches, also incorporating lifestyle factors, which can differentiate between PD, healthy controls and atypical parkinsonism. These approaches could also aid in the definition of PD subgroups and might be able to predict the disease course of individual patients (17). Longitudinal studies following PD patients over a longer time course, can also provide valuable information regarding the individual disease progression. This also enables the retrospective identification of baseline biomarkers which could predict the disease course of an individual patient. The ultra-high field MRI study described in this thesis will create the possibility to investigate these longitudinal changes in PD. In the near future individual patient characteristics, such as genetics, lifestyle factors,

clinical symptoms and imaging biomarkers may lead to personalized treatment options and will greatly improve patient education regarding their disease course.

With the ongoing search for disease-modifying therapies there is also an urgent need for biomarkers which can reliably monitor disease progression from a pathological perspective in order to evaluate therapy effect. Furthermore, when interventions become available, the identification of individuals with a prodromal stage of PD will be of great importance for the application of these treatments. Selection of these individuals must be based on reliable biomarkers and will most probably consist out of a combination of different features, including MRI characteristics. In this way, the diagnosis of PD will evolve from a purely clinical one towards a biomarkers-supported diagnosis with an increased diagnostic accuracy.

While current research mostly focuses on tracers that are able to capture the neurodegenerative process in PD, future studies should also focus on features which can image the cause of neurodegeneration during the asymptomatic phase of the disease in order to unravel the PD pathophysiology. Although this is a great challenge, studies in large prodromal PD patient populations, possibly with the application of machine-learning approaches, could provide valuable insights.

8. Conclusion

This thesis has provided a deeper insight into the role of MRI in the identification of biomarkers for both motor and non-motor symptoms of PD. It addresses the advantages and limitations of MRI research and provides some valuable insights for future studies. Specifically the use of ultra-high field MRI in PD is explored and the longitudinal 7T MRI study described in this thesis will create the possibility to more extensively investigate its role as a PD biomarker in the upcoming years. It was also shown that white matter tract alterations and decreased default mode network connectivity is important in the pathophysiology of cognitive impairment in PD. Furthermore, the visualization of neuromelanin related signal decrease in the LC might be a valuable biomarker for early PD, while diffusion measures of the olfactory tract did not prove to be a reliable imaging target to distinguish PD from HC. Future studies focusing on multimodal imaging methods, automated analysis methods and the application of machine-learning approaches will continue to contribute to the elucidation of PD pathophysiology, the identification of reliable subgroups and the validation of biomarkers for monitoring and diagnosing PD.

9. References

1. Virameteekul S, Revesz T, Jaunmuktane Z, Warner TT, De Pablo-Fernández E. Clinical Diagnostic Accuracy of Parkinson's Disease: Where Do We Stand? *Mov Disord.* 2023;38(4):558-66.
2. Yarnall AJ, Breen DP, Duncan GW, Khoo TK, Coleman SY, Firbank MJ, et al. Characterizing mild cognitive impairment in incident Parkinson disease: the ICICLE-PD study. *Neurology.* 2014;82(4):308-16.
3. Hely MA, Reid WG, Adena MA, Halliday GM, Morris JG. The Sydney multicenter study of Parkinson's disease: the inevitability of dementia at 20 years. *Mov Disord.* 2008;23(6):837-44.
4. Duncan GW, Firbank MJ, Yarnall AJ, Khoo TK, Brooks DJ, Barker RA, et al. Gray and white matter imaging: A biomarker for cognitive impairment in early Parkinson's disease? *Mov Disord.* 2016;31(1):103-10.
5. Rektor I, Svatkova A, Vojtisek L, Zikmundova I, Vanicek J, Kiraly A, et al. White matter alterations in Parkinson's disease with normal cognition precede grey matter atrophy. *PLoS One.* 2018;13(1):e0187939.
6. Mirelman A, Herman T, Brozgol M, Dorfman M, Sprecher E, Schweiger A, et al. Executive function and falls in older adults: new findings from a five-year prospective study link fall risk to cognition. *PLoS One.* 2012;7(6):e40297.
7. Thenganatt MA, Jankovic J. Parkinson disease subtypes. *JAMA Neurol.* 2014;71(4):499-504.
8. Khan MJ, Kannan P, Wong TW, Fong KNK, Winser SJ. A Systematic Review Exploring the Theories Underlying the Improvement of Balance and Reduction in Falls Following Dual-Task Training among Older Adults. *Int J Environ Res Public Health.* 2022;19(24).
9. Henderson EJ, Lord SR, Brodie MA, Gaunt DM, Lawrence AD, Close JC, et al. Rivastigmine for gait stability in patients with Parkinson's disease (ReSPonD): a randomised, double-blind, placebo-controlled, phase 2 trial. *Lancet Neurol.* 2016;15(3):249-58.
10. Weintraub D, Aarsland D, Biundo R, Dobkin R, Goldman J, Lewis S. Management of psychiatric and cognitive complications in Parkinson's disease. *Bmj.* 2022;379:e068718.
11. van de Weijer SCF, Duits AA, Bloem BR, de Vries NM, Kessels RPC, Köhler S, et al. Feasibility of a Cognitive Training Game in Parkinson's Disease: The Randomized Parkin'Play Study. *Eur Neurol.* 2020;83(4):426-32.
12. Hou Y, Shang H. Magnetic Resonance Imaging Markers for Cognitive Impairment in Parkinson's Disease: Current View. *Front Aging Neurosci.* 2022;14:788846.
13. Mestre TA, Fereshtehnejad SM, Berg D, Bohnen NI, Dujardin K, Erro R, et al. Parkinson's Disease Subtypes: Critical Appraisal and Recommendations. *J Parkinsons Dis.* 2021;11(2):395-404.
14. Stebbins GT, Goetz CG, Burn DJ, Jankovic J, Khoo TK, Tilley BC. How to identify tremor dominant and postural instability/gait difficulty groups with the movement disorder society unified Parkinson's disease rating scale: comparison with the unified Parkinson's disease rating scale. *Mov Disord.* 2013;28(5):668-70.
15. Espay AJ, Kalia LV, Gan-Or Z, Williams-Gray CH, Bedard PL, Rowe SM, et al. Disease modification and biomarker development in Parkinson disease: Revision or reconstruction? *Neurology.* 2020;94(11):481-94.
16. Dong-Chen X, Yong C, Yang X, Chen-Yu S, Li-Hua P. Signaling pathways in Parkinson's disease: molecular mechanisms and therapeutic interventions. *Signal Transduct Target Ther.* 2023;8(1):73.
17. Tolosa E, Garrido A, Scholz SW, Poewe W. Challenges in the diagnosis of Parkinson's disease. *Lancet Neurol.* 2021;20(5):385-97.

18. O'Hara DM, Pawar G, Kalia SK, Kalia LV. LRRK2 and α -Synuclein: Distinct or Synergistic Players in Parkinson's Disease? *Frontiers in neuroscience*. 2020;14:577.
19. Garrido A, Fairfoul G, Tolosa ES, Martí MJ, Green A. α -synuclein RT-QuIC in cerebrospinal fluid of LRRK2-linked Parkinson's disease. *Ann Clin Transl Neurol*. 2019;6(6):1024-32.
20. Kalia LV, Lang AE, Hazrati LN, Fujioka S, Wszolek ZK, Dickson DW, et al. Clinical correlations with Lewy body pathology in LRRK2-related Parkinson disease. *JAMA Neurol*. 2015;72(1):100-5.
21. Ball N, Teo WP, Chandra S, Chapman J. Parkinson's Disease and the Environment. *Front Neurol*. 2019;10:218.
22. Pont-Sunyer C, Hotter A, Gaig C, Seppi K, Compta Y, Katzenschlager R, et al. The onset of nonmotor symptoms in Parkinson's disease (the ONSET PD study). *Mov Disord*. 2015;30(2):229-37.
23. Atkinson-Clement C, Pinto S, Eusebio A, Coulon O. Diffusion tensor imaging in Parkinson's disease: Review and meta-analysis. *Neuroimage Clin*. 2017;16:98-110.
24. Scherfler C, Esterhammer R, Nocker M, Mahlknecht P, Stockner H, Warwitz B, et al. Correlation of dopaminergic terminal dysfunction and microstructural abnormalities of the basal ganglia and the olfactory tract in Parkinson's disease. *Brain*. 2013;136(Pt 10):3028-37.
25. Nigro P, Chiappiniello A, Simoni S, Paolini Paoletti F, Cappelletti G, Chiarini P, et al. Changes of olfactory tract in Parkinson's disease: a DTI tractography study. *Neuroradiology*. 2021;63(2):235-42.
26. Polders DL, Leemans A, Hendrikse J, Donahue MJ, Luijten PR, Hoogduin JM. Signal to noise ratio and uncertainty in diffusion tensor imaging at 1.5, 3.0, and 7.0 Tesla. *J Magn Reson Imaging*. 2011;33(6):1456-63.
27. Braak H, Del Tredici K, Rüb U, de Vos RA, Jansen Steur EN, Braak E. Staging of brain pathology related to sporadic Parkinson's disease. *Neurobiol Aging*. 2003;24(2):197-211.
28. Borghammer P, Just MK, Horsager J, Skjærbæk C, Raunio A, Kok EH, et al. A postmortem study suggests a revision of the dual-hit hypothesis of Parkinson's disease. *NPJ Parkinsons Dis*. 2022;8(1):166.
29. Rispoli V, Schreglmann SR, Bhatia KP. Neuroimaging advances in Parkinson's disease. *Curr Opin Neurol*. 2018;31(4):415-24.
30. Ryman SG, Poston KL. MRI biomarkers of motor and non-motor symptoms in Parkinson's disease. *Parkinsonism Relat Disord*. 2020;73:85-93.
31. Braak H, Del Tredici K, Bratzke H, Hamm-Clement J, Sandmann-Keil D, Rub U. Staging of the intracerebral inclusion body pathology associated with idiopathic Parkinson's disease (preclinical and clinical stages). *J Neurol*. 2002;249 Suppl 3:III/1-5.
32. Ye R, O'Callaghan C, Rua C, Hezemans FH, Holland N, Malpetti M, et al. Locus Coeruleus Integrity from 7 T MRI Relates to Apathy and Cognition in Parkinsonian Disorders. *Mov Disord*. 2022;37(8):1663-72.
33. Lehericy S, Bardinet E, Poupon C, Vidailhet M, Francois C. 7 Tesla magnetic resonance imaging: a closer look at substantia nigra anatomy in Parkinson's disease. *Mov Disord*. 2014;29(13):1574-81.
34. Gwinn K, David KK, Swanson-Fischer C, Albin R, Hillaire-Clarke CS, Sieber BA, et al. Parkinson's disease biomarkers: perspective from the NINDS Parkinson's Disease Biomarkers Program. *Biomark Med*. 2017;11(6):451-73.
35. Jellinger KA. Neuropathology of sporadic Parkinson's disease: evaluation and changes of concepts. *Mov Disord*. 2012;27(1):8-30.
36. Vijiaratnam N, Simuni T, Bandmann O, Morris HR, Foltynie T. Progress towards therapies for disease modification in Parkinson's disease. *Lancet Neurol*. 2021;20(7):559-72.

37. Cole DM, Beckmann CF, Oei NY, Both S, van Gerven JM, Rombouts SA. Differential and distributed effects of dopamine neuromodulations on resting-state network connectivity. *Neuroimage*. 2013;78:59-67.
38. Matsuura K, Maeda M, Tabei KI, Umino M, Kajikawa H, Satoh M, et al. A longitudinal study of neuromelanin-sensitive magnetic resonance imaging in Parkinson's disease. *Neurosci Lett*. 2016;633:112-7.
39. Lehericy S, Vaillancourt DE, Seppi K, Monchi O, Rektorova I, Antonini A, et al. The role of high-field magnetic resonance imaging in parkinsonian disorders: Pushing the boundaries forward. *Mov Disord*. 2017;32(4):510-25.
40. Priovoulos N, Jacobs HIL, Ivanov D, Uludag K, Verhey FRJ, Poser BA. High-resolution in vivo imaging of human locus coeruleus by magnetization transfer MRI at 3T and 7T. *Neuroimage*. 2018;168:427-36.
41. Verma G, Balchandani P. Ultrahigh field MR Neuroimaging. *Top Magn Reson Imaging*. 2019;28(3):137-44.
42. Politis M, Wilson H, Wu K, Brooks DJ, Piccini P. Chronic exposure to dopamine agonists affects the integrity of striatal D(2) receptors in Parkinson's patients. *Neuroimage Clin*. 2017;16:455-60.
43. Siderowf A, Concha-Marambio L, Lafontant DE, Farris CM, Ma Y, Urenia PA, et al. Assessment of heterogeneity among participants in the Parkinson's Progression Markers Initiative cohort using α -synuclein seed amplification: a cross-sectional study. *Lancet Neurol*. 2023;22(5):407-17.
44. Okuzumi A, Hatano T, Matsumoto G, Nojiri S, Ueno SI, Imamichi-Tatano Y, et al. Propagative α -synuclein seeds as serum biomarkers for synucleinopathies. *Nat Med*. 2023;29(6):1448-55.
45. Marques TM, van Rumund A, Oeckl P, Kuiperij HB, Esselink RAJ, Bloem BR, et al. Serum NFL discriminates Parkinson disease from atypical parkinsonisms. *Neurology*. 2019;92(13):e1479-e86.
46. Bidesi NSR, Vang Andersen I, Windhorst AD, Shalgunov V, Herth MM. The role of neuroimaging in Parkinson's disease. *J Neurochem*. 2021;159(4):660-89.
47. Scherfner C, Schwarz J, Antonini A, Grosset D, Valldeoriola F, Marek K, et al. Role of DAT-SPECT in the diagnostic work up of parkinsonism. *Mov Disord*. 2007;22(9):1229-38.
48. Jennings D, Siderowf A, Stern M, Seibyl J, Eberly S, Oakes D, et al. Imaging prodromal Parkinson disease: the Parkinson Associated Risk Syndrome Study. *Neurology*. 2014;83(19):1739-46.
49. Matesan M, Gaddikeri S, Longfellow K, Miyaoka R, Elojeimy S, Elman S, et al. I-123 DaTscan SPECT Brain Imaging in Parkinsonian Syndromes: Utility of the Putamen-to-Caudate Ratio. *J Neuroimaging*. 2018;28(6):629-34.
50. Kuebler L, Buss S, Leonov A, Ryazanov S, Schmidt F, Maurer A, et al. [(11C)MODAG-001-towards a PET tracer targeting α -synuclein aggregates. *Eur J Nucl Med Mol Imaging*. 2021;48(6):1759-72.
51. Savica R, Rocca WA, Ahlskog JE. When does Parkinson disease start? *Arch Neurol*. 2010;67(7):798-801.
52. Weingarten CP, Sundman MH, Hickey P, Chen NK. Neuroimaging of Parkinson's disease: Expanding views. *Neurosci Biobehav Rev*. 2015;59:16-52.
53. Scherfner C, Göbel G, Müller C, Nocker M, Wenning GK, Schocke M, et al. Diagnostic potential of automated subcortical volume segmentation in atypical parkinsonism. *Neurology*. 2016;86(13):1242-9.

54. Péran P, Barbagallo G, Nemmi F, Sierra M, Galitzky M, Traon AP, et al. MRI supervised and unsupervised classification of Parkinson's disease and multiple system atrophy. *Mov Disord.* 2018;33(4):600-8.
55. Nalls MA, Blauwendraat C, Vallerga CL, Heilbron K, Bandres-Ciga S, Chang D, et al. Identification of novel risk loci, causal insights, and heritable risk for Parkinson's disease: a meta-analysis of genome-wide association studies. *Lancet Neurol.* 2019;18(12):1091-102.

Summary

The studies presented in this thesis investigated the role of magnetic resonance imaging (MRI) as a biomarker for Parkinson's disease (PD). In part I we focused on cognitive impairment and explored structural and functional alterations related to cognitive decline in PD patients. Part II specifically investigates the use of ultra-high field 7T MRI as an early biomarker for PD.

1. Part I

Chapter 2 is a meta-analysis of resting-state functional MRI (fMRI) studies in PD patients with cognitive impairment. For this meta-analysis an extensive search was performed to select all existing studies focusing on resting-state fMRI characteristics of PD patients with cognitive impairment compared to either cognitively unimpaired PD patients or healthy controls (HC). Seventeen studies were included in the meta-analysis, consisting of 222 PD patients with mild cognitive impairment, 68 patients with PD dementia, 289 cognitively unimpaired PD patients and 353 HC. A voxel-based meta-analysis was performed using the anisotropic effect-size version of the signed differential mapping method. Results showed that PD patients with cognitive impairment predominantly display a reduced connectivity in brain areas that are part of the default mode network. The default mode network is believed to serve an important role in several cognitive functions. Alterations in this network have also been described in other neurodegenerative disorders, such as Alzheimer's disease and frontotemporal dementia. Although results of this meta-analysis might be influenced by methodological heterogeneity and variations in patient characteristics across individual studies, it provides a more definite step in the differentiation of network disruptions associated with cognitive impairment in PD. It suggests an important role for the default mode network in the pathophysiology of cognitive decline and indicates that functional connectivity alterations of the default mode network might be able to serve as a biomarker for cognitive impairment in PD.

In **chapter 3** functional brain network characteristics and cognitive performance is compared between different motor subtypes of PD. For this study, data of a cross-sectional resting-state 3T MRI study was used. Based on a numerical ratio derived from the mean tremor score and mean-postural instability and gait disorder score at the MDS-UPDRS III, two subgroups were defined, namely a tremor-dominant (TD) and postural instability and gait disorder (PIGD) subgroup. Differences in functional connectivity were investigated using dual regression analysis and inter-network connectivity analysis. Also, cognitive performance was investigated between subgroups. The PIGD

subgroup performed worse compared to the TD subgroup across all cognitive domains. Resting-state fMRI network analyses suggested the connection between the visual and sensorimotor network to be a potential differentiator between PIGD and TD subgroups. However, after correcting for dopaminergic medication use these results were not significant anymore. So based on this study, no reliable connectivity differences between PIGD and TD motor subgroups could be established.

Chapter 4 compares grey matter alterations between clusters of PD with mild, moderate and severe stages of cognitive impairment. In this cross-sectional study, 124 PD patients underwent extensive clinical and neuropsychological assessments as well as a 3T MRI scan of the brain. Four groups were identified ranging from cognitively intact patients to patients with severe deficits in all cognitive domains, whilst showing comparable levels of motor disability and disease duration. Each group was compared to the cognitively intact PD group using voxel- and vertex-based morphometry. After correcting for age, significant differences in grey matter volume, cortical thickness and cortical folding were only seen between cognitively unimpaired PD patients and PD patients with severe cognitive deficits. Volume alterations were restricted to the right posterior cingulate and the right precuneus. Reduced cortical thickness was seen in the right inferior temporal gyrus and reduced folding in the right temporal region. As these differences were not associated with age, we assume that they are associated with underlying pathology of the cognitive decline. However, given the limited involvement of grey matter differences between groups, we hypothesize a more important role for white matter tract alterations in early stages of cognitive impairment in PD.

2. Part II

Chapter 5 provides the detailed protocol of the TRACK-PD study, which is the first and largest longitudinal ultra-high field 7T MRI study in PD patients to date. In this study an extensive 7T MRI protocol of the brain is performed at baseline and repeated after 2 and 4 years. Extensive assessment of motor, cognitive, neuropsychiatric and autonomic symptoms are performed at baseline and follow-up visits with wearable sensors, validated questionnaires and rating scales. At baseline a blood DNA sample is also collected. This study will provide a relatively large, longitudinal database of PD with extensive information related to motor and non-motor symptoms. Due to the use of ultra-high field 7T MRI it creates the opportunity to investigate the brain in even more detail than the MRI techniques with lower field strengths (1.5 or 3T) used clinically. Aim of this study is to improve our understanding of PD and its pathophysiology by establishing MRI characteristics that can distinguish between PD patients and healthy control subjects. In addition, we aim to detect new imaging biomarkers for disease

progression that could be valuable for the evaluation of future therapies. Lastly, correlating MRI characteristics to clinical phenotype and genetics might help us to further define PD subtypes.

Chapter 6 describes an ultra-high field imaging study comparing neuromelanin related signal intensity in the substantia nigra (SN) and locus coeruleus (LC) between early-stage PD patients and HC. In addition, the association of neuromelanin related signal intensity in the SN and LC with cognitive performance was explored. The study was conducted using data from the TRACK-PD study described in chapter 5. Masks for the SN and LC were automatically segmented and manually corrected. Mean signal intensity of the SN and LC was calculated and normalized to the mean signal intensity values of pre-selected reference regions. PD participants displayed a lower contrast-to-noise ratio (CNR) in the right SN and left LC. After adding age as a confounder, the CNR of the right SN did not significantly differ anymore between PD and HC. Additionally, a significant positive correlation was found between the SN CNR and the 15 Words Test. These results confirm that neuromelanin related signal intensity of the LC differs between early-stage PD patients and HC. No significant differences were found in the SN. These result are in favour of the theory of bottom-up disease progression in PD. Furthermore, it suggests that loss of SN integrity might influence working memory or learning capabilities in PD patients.

In **chapter 7** we visualized the olfactory tract with DWI techniques on ultra-high field MRI and evaluated if previous findings, showing distinctive diffusion measures of the olfactory tract between PD and HC, could be replicated on 7T MRI. The study was conducted using data from the TRACK-PD study described in chapter 5. Manual seed regions of interest were drawn in the olfactory tract region. Tractography of the olfactory tract was performed using a deterministic streamlines algorithm. Diffusion measures (fractional anisotropy and mean- radial- and axial diffusivity) of the generated streamlines were compared between groups. Diffusion measures did not differ between hyposmic PD patients, anosmic PD patients and normosmic HC. The study showed that fiber tracking of the olfactory tract was feasible in early-stage PD patients using 7T DWI data. However, based on these results 7T diffusion measures of the olfactory tract are not useful as an early clinical biomarker for PD. Using olfactory testing instead of a self-reporting questionnaire might be better suited to objectively identify hyposmic participants and define olfactory subgroups in future studies.

Chapter 8 provides a general discussion in which the most relevant findings of this thesis are discussed and put into perspective. Also, advantages and limitations of MRI biomarkers are highlighted and potential future research directions are described.

Nederlandse samenvatting

De studies in dit proefschrift onderzoeken of er met behulp van magnetic resonance imaging (MRI) scans biomarkers kunnen worden gevonden voor zowel motore als niet-motore klachten van de ziekte van Parkinson (PD). Deel I van dit proefschrift is met name gefocust op cognitieve stoornissen. Hierin wordt gezocht naar structurele en functionele MRI veranderingen gerelateerd aan cognitieve achteruitgang bij PD. Deel II richt zich op het gebruik van hoge veldsterkte (7T) MRI en onderzoekt of hiermee vroege biomarkers voor PD kunnen worden gevonden.

Deel I

Hoofdstuk 2 beschrijft een meta-analyse waarin de resultaten van eerdere studies gericht op resting-state functionele MRI (fMRI) bij PD patiënten met cognitieve problemen zijn samengevoegd. Voor deze meta-analyse is er uitgebreid gezocht in verschillende medische databases. Alle eerdere onderzoeken welke zich focussen op fMRI veranderingen bij PD patiënten met cognitieve problemen in vergelijking met PD patiënten zonder cognitieve klachten of met gezonde proefpersonen (HC) zijn geselecteerd. Zeventien studies werden geïnccludeerd, bestaande uit 222 PD patiënten met milde cognitieve stoornissen, 68 patiënten met PD dementie, 289 PD patiënten zonder cognitieve klachten en 353 gezonde proefpersonen. Een voxel-based meta-analyse werd uitgevoerd met behulp van een signed differential mapping (SDM) methode, welke ook rekening houdt met effectgrootte (ES-SDM). De resultaten tonen aan dat PD patiënten met cognitieve problemen met name een verlaagde connectiviteit hebben in hersengebieden welke onderdeel zijn van het default mode netwerk. Veranderingen in dit netwerk zijn ook beschreven bij andere neurodegeneratieve aandoeningen, zoals de ziekte van Alzheimer en fronto-temporale dementie. Alhoewel niet is uitgesloten dat de resultaten enigszins beïnvloed worden door heterogeniteit in de gebruikte methodes en patiëntkarakteristieken van de verschillende studies, levert dit onderzoek belangrijke informatie over de netwerkveranderingen bij PD patiënten met cognitieve achteruitgang. De resultaten wijzen erop dat veranderingen in het default mode netwerk een belangrijke rol te spelen in de pathofysiologie van deze cognitieve klachten. Mogelijk kan deze verlaagde connectiviteit in het default mode netwerk in de toekomst ook fungeren als biomarker voor cognitieve stoornissen bij PD.

In **hoofdstuk 3** worden cognitieve prestaties en functionele hersenactiviteit vergeleken tussen verschillende motorische subgroepen van PD. Er is hierbij gebruik gemaakt van resting-state 3T fMRI data. Met behulp van de MDS-UPDRS III score werd voor iedere

proefpersoon de verhouding berekend tussen een gemiddelde tremorscore en een gemiddelde score voor posturele instabiliteit en loopproblemen. Op basis hiervan werden de deelnemers ingedeeld als een tremor-dominant (TD) subtype of als een subtype met posturele instabiliteit en loopproblemen (PIGD). Met behulp van een duale regressieanalyse en een inter-netwerk connectiviteitsanalyse werd verschillen in functionele connectiviteit tussen de twee groepen onderzocht. Ook werden de cognitieve prestaties tussen de groepen vergeleken. De PIGD subgroep scoorde op alle cognitieve domeinen slechter dan de TD subgroep. De resting-state fMRI netwerkanalyse leek aan te tonen dat veranderingen in de banen tussen het visuele en sensomotore netwerk mogelijk onderscheidend zijn tussen PD patiënten met een PIGD en TD subtype. Echter, na correctie voor het gebruik van dopaminerge medicatie waren deze resultaten niet meer significant. Op basis van deze studie konden er dus geen betrouwbare verschillen in netwerk connectiviteit tussen PIGD en TD PD patiënten worden vastgesteld.

Hoofdstuk 4 vergelijkt grijze stof veranderingen tussen PD patiënten met milde, gemiddelde en ernstige cognitieve klachten. Als onderdeel van deze cross-sectionele studie werd bij 124 PD patiënten een uitgebreid neuropsychologisch onderzoek, verschillende klinische testen en een 3T MRI van de hersenen uitgevoerd. Er werden vier groepen geïdentificeerd, variërend van cognitief intacte patiënten tot patiënten met ernstige problemen in alle cognitieve domeinen. De groepen hadden een vergelijkbare ziekteduur en mate van motorische beperkingen. Voor elke groep werden er uitgebreide analyses gedaan van de grijze stof en deze kenmerken werden vergeleken met de groep PD patiënten zonder cognitieve problemen. Na correctie van de resultaten voor leeftijd, werden er alleen significante verschillen in grijze stof volume, corticale dikte en mate van corticale windingen gezien tussen PD patiënten zonder cognitieve klachten en de PD patiënten met de meest ernstige cognitieve stoornissen. Dit betrof volumeveranderingen in de rechter posterieure gyrus cinguli en de rechter precuneus. Een afname van corticale dikte in de rechter inferieure temporale gyrus en verminderde corticale winding in de rechter temporale regio. Aangezien deze verschillen niet verklaard werden door leeftijd, kan worden aangenomen dat het een uiting is van de pathologische veranderingen gerelateerd aan cognitieve problemen bij PD. Aangezien deze grijze stof veranderingen alleen worden gezien bij patiënten met ernstige cognitieve klachten, lijkt het waarschijnlijk dat in de vroegere fases van cognitieve achteruitgang bij PD, met name witte stof veranderingen een belangrijke rol spelen.

Deel II

Hoofdstuk 5 geeft een gedetailleerde omschrijving van de TRACK-PD studie. Dit is de eerste en grootste longitudinale hoge veldsterkte 7T MRI studie in PD patiënten tot nu toe. In deze studie ondergaan proefpersonen een uitgebreid 7T MRI protocol van de hersenen bij baseline, na 2 jaar en na 4 jaar. Tevens worden bij ieder meetmoment cognitieve, psychologische, motorische en autonome klachten uitgebreid in kaart gebracht door middel van een neuropsychologisch onderzoek, verschillende vragenlijsten en draagbare bewegingssensoren. Ook wordt er bij baseline eenmaal bloed afgenomen ten behoeve van genetische diagnostiek. Op basis van deze studie kan een uitgebreide database worden opgericht bestaande uit longitudinale informatie over zowel motorische als niet-motorische symptomen gerelateerd aan PD. Door het gebruik van hoge veldsterkte MRI (7T) kan het brein bovendien in meer detail worden bekeken dan bij eerdere 1.5 of 3T MRI studies. Middels deze studie willen we meer duidelijkheid krijgen over de pathofysiologische veranderingen bij PD. Daarnaast gaan we op zoek naar MRI karakteristieken welke PD patiënten kunnen onderscheiden van HC. Ook zal er worden gezocht naar MRI veranderingen welke gerelateerd zijn aan ziekteprogressie en mogelijk kunnen dienen als biomarker bij de evaluatie van toekomstige therapieën. Ten slotte is het doel om MRI veranderingen te correleren met klinische symptomen en op die manier een bijdrage te leveren aan de subtypering van PD.

Hoofdstuk 6 beschrijft een hoge veldsterkte MRI studie welke de neuromelanine gerelateerde signaalintensiteit in de substantia nigra (SN) en locus coeruleus (LC) vergelijkt tussen recent gediagnosticeerde PD patiënten en HC. Ook wordt de associatie tussen neuromelanine gerelateerde signaalintensiteit in de SN en LC en cognitieve prestaties onderzocht. De studie is verricht met data van de TRACK-PD studie, welke in hoofdstuk 5 is beschreven. De doelregio's in de SN en LC werden automatisch gesegmenteerd en zo nodig met de hand gecorrigeerd. De gemiddelde signaalintensiteit in de SN en LC werd berekend en genormaliseerd met behulp van de gemiddelde signaalintensiteit in vooraf bepaalde referentieregio's. PD patiënten hadden een lagere contrast-to-noise ratio (CNR) in de rechter SN en linker LC in vergelijking met HC. Na het corrigeren van de resultaten voor leeftijd, verviel echter de significante bevinding in de rechter SN. Daarnaast werd er een positieve correlatie gevonden tussen de CNR in de SN en de 15-woorden test. Deze test meet geheugenprestaties, maar ook het lerend vermogen. De resultaten van dit onderzoek bevestigen dat neuromelanine gerelateerde signalen in de LC verschillen tussen recent gediagnosticeerde PD patiënten en HC. Er werden geen significante verschillen in de SN aangetoond. Deze uitkomsten ondersteunen de theorie dat pathologische veranderingen bij PD zich vanuit de hersenstam omhoog verspreiden naar de rest van het brein. Daarnaast is de SN mogelijk belangrijk voor het geheugen dan wel het leervermogen.

In **hoofdstuk 7** hebben we de tractus olfactorius in beeld gebracht met behulp van diffusie-gewogen beeldvorming (DWI) op de hoge veldsterkte MRI. Er werd onderzocht of bevindingen uit eerdere studies, welke een verschil in diffusie parameters tussen PD patiënten en HC aantoonde, gerepliceerd konden worden op de 7T MRI. Deze studie werd uitgevoerd met data van de TRACK-PD studie, welke in hoofdstuk 5 is beschreven. De doelregio's in het gebied van de tractus olfactorius werden handmatig ingetekend. Op deze regio's werd een deterministisch tractografie algoritme toegepast. Verschillende diffusie parameters (fractionele anisotropie en gemiddelde, radiale en axiale diffusiviteit) van de geïdentificeerde banen werden vergeleken tussen de groepen. Deze diffusie parameters toonde geen significant verschil tussen PD patiënten met reukproblemen, PD patiënten zonder reukproblemen en HC zonder reukproblemen. De studie toonde aan dat het identificeren van de witte stofbanen van de tractus olfactorius op de 7T MRI mogelijk is in recent gediagnosticeerde PD patiënten. Echter op basis van deze resultaten lijken deze diffusie maten niet bruikbaar als vroege biomarker voor PD. Voor toekomstige studies is het wellicht aan te raden om specifieke reuktesten te gebruiken in plaats van vragenlijsten, zodat reukproblemen objectiever kunnen worden vastgesteld en er een meer betrouwbare subgroep indeling kan plaatsvinden.

De algemene discussie in **hoofdstuk 8** beschrijft de belangrijkste bevindingen in dit proefschrift en zet deze af tegen eerdere literatuur en de klinische praktijk. Tevens worden de voor- en nadelen van MRI onderzoek bij PD besproken en worden er suggesties gegeven voor toekomstig onderzoek.

Impact paragraph

Parkinson's disease (PD) is a progressive neurological disorder characterized by slowness of movements (bradykinesia), stiffness (rigidity) and resting tremor. In later stages of the disease, PD patients often suffer from postural instability and gait problems. Also, a broad spectrum of non-motor symptoms, such as cognitive impairment, depression, autonomic failure and sleep disorders can occur. In less than two centuries PD has become a common disorder, affecting 6.2 million people worldwide in 2015 (1). Moreover, in about 20 years the PD population is expected to reach more than 12 million patients globally (2). Due to the progressive character, wide variety of symptoms and the long-lasting disease course PD greatly affect the quality of life of patients and their caregivers. Moreover, non-motor symptoms seem to have an even greater effect on the quality of life than motor manifestations (3). However, the underlying cause of the non-motor symptoms is not very well understood. Although dopaminergic medication is used to improve PD motor symptoms and reduce physical disability, there are currently no treatment options which can cure PD or slow down the disease process. Because of the increasing patient numbers and the great impact on society, patients and caregivers, urgent calls are made to search for ways to prevent and treat PD. Accurate diagnostic markers and monitoring indicators are highly necessary for the development of new therapeutic strategies. This thesis aims to contribute to the elucidation of the PD pathophysiology by investigating structural and functional changes in the PD brain with magnetic resonance imaging (MRI) techniques and to search for radiological biomarkers.

The main findings of these thesis are that disruptions in the default mode network serve an important role in the pathophysiology of cognitive impairment in PD. In line with this, white matter tract alterations are probably more important in the early stages of cognitive decline in PD compared to grey matter alterations. Also, we confirmed that cognitive impairment is more prevalent in PD patients with a postural instability and gait disorder subtype, compared to patients with a tremor-dominant subtype. Furthermore, a comprehensive description of the study protocol of the TRACK-PD study is provided. This is the first and largest longitudinal ultra-high field 7T MRI study in PD patients to date. Based on the data of this study, we confirmed that neuromelanin related signal intensity in the locus coeruleus differs between PD and healthy controls (HC). No differences between PD and HC could be established in diffusion measures of the olfactory tract.

1. Contribution to science

The findings of this thesis provide several interesting insights into the PD pathophysiology of both motor and non-motor symptoms. Acquiring knowledge about the neurodegenerative disease process is essential for the development of new therapeutic strategies. Also, specific functional and structural MRI alterations might be able to serve as radiological biomarkers that can aid in the diagnostic process of PD. Furthermore, the identification of biomarkers which are correlated with clinical symptoms or disease progression is crucial for the development of monitoring biomarkers that can be used in future disease modifying therapy studies.

The TRACK-PD study, of which the study protocol is described in chapter 5 of this thesis and published in BMC Neurology, will provide an unique database consisting of longitudinal clinical, genetic and radiological information of a relatively large group of PD patients and HC. It is the biggest longitudinal 7T MRI study so far and thereby functions as a biobank for ongoing and future research. Within our research group, several other analysis are currently being performed with this data. This for example includes the search for neuroanatomical correlates of anxiety in PD and functional connectivity patterns in relation to cognitive impairment. In addition, the data is available for other researchers on reasonable request and can therefore be used by other research groups globally. In this way it will be possible to answer many more future research questions with data of the TRACK-PD study.

Furthermore, the outcomes in this thesis related to cognitive impairment in PD might have implications for future studies. Based on our results it is indicated that white matter tract alterations are more important in the early phases of cognitive decline compared to grey matter disruptions. This is an important outcome, which may guide future studies investigating the pathophysiology of cognitive impairment in PD. It can also provide guidance for the development of new therapies. For example, other researchers have recently indicated that the white matter disruptions might be induced by a demyelination process (4). This offers a new perspective on the pathophysiology of cognitive decline in PD and creates a novel target for future intervention studies searching for disease modifying therapies.

Lastly, based in the studies described in this thesis several suggestions for future studies are given in the general discussion. This includes the application of multimodal imaging techniques, automated analysis methods and the use of machine-learning approaches. In addition, it seems beneficial to combine different biochemical and imaging techniques for the diagnosis and monitoring of PD, since different techniques are likely to complement each other. Moreover, longitudinal analysis are essential to

determine the temporal relationship between imaging alterations, PD symptoms and disease progression in general. Other research groups may be encouraged to develop new studies and research questions based on these suggestions.

2. Contribution to society

As described above, PD is a highly prevalent disease worldwide with an enormous impact on both society and the life of patients and caregivers. The most important goal of PD research is to develop new disease-modifying strategies which are able to cure the disease or at least slow down disease progression. Understanding the PD pathophysiology enables researchers to determine the most promising targets for future medication strategies and is therefore an essential step in the development of new therapies. Furthermore, in order to develop and test new treatment options valid biomarkers are necessary to monitor and evaluate therapy effect. The TRACK-PD study aims to contribute in the search for these new biomarkers, which can potentially be used in intervention studies. For example, the neuromelanin related alterations in PD, which have also been established in the study in chapter 6 of this thesis, has recently led to the development of new therapeutic strategies focusing on neuromelanin accumulation in PD (5). In addition, gene therapies are being researched for monogenetic forms of PD (6). Future analysis incorporating the genetic information collected by the TRACK-PD study can provide insights in the clinical and radiological phenotype of genetic-linked PD, which can be used for the development of new interventions. Studies investigating iron chelation therapy in PD have not yet led to satisfactory results (7). However, future analysis on iron-sensitive sequences of the TRACK-PD study, might provide information that can be useful for the development of novel iron-related treatment strategies.

Moreover, quality of life in PD patients is influenced to a greater extent by non-motor than motor symptoms. In the past, the majority of studies have however focused on motor symptoms. In the first part of this thesis structural and functional cerebral alterations related to cognitive impairment in PD are explored. These studies provide valuable information regarding the neurodegenerative process underlying this important non-motor symptom. From the patient point of view it is essential to improve our knowledge about these and other non-motor symptoms, in order to create more effective management options.

The diagnosis of PD is complicated by the heterogenous nature of the disease and the fact that it is a clinical diagnosis. Patients often experience a delay in diagnosis and have visited multiple healthcare providers, before getting diagnosed with PD. Furthermore, the disease course of different patients is highly variable and at this moment we are

not able to predict this for the individual patient. Studies have shown that a correct explanation about the disease and diagnosis had a long-lasting impact on the quality of life of PD patients (8). This emphasizes the importance of a correct clinical diagnosis and preferably also an accurate prediction of what the patient can expect for the upcoming years. By studying specific PD symptoms in relation to MRI alterations this thesis aims to contribute to an improved diagnostic process. Furthermore, the longitudinal nature of the TRACK-PD study enables us to study symptoms over time and will create the possibility to correlate clinical symptoms with specific MRI changes. It might therefore help to better predict the disease course of an individual patient based on MRI characteristics.

The fact that this kind of biomarker research is important to patients is underlined even further by the overwhelming number of participants which have voluntarily registered themselves for participation in the TRACK-PD study. It was truly inspirational to meet so many PD patients, each with their own story and distinct experience of the disease. Since the study outcomes are relevant to these patients, we attach great importance to communicating the results with the participants by sending them a comprehensible Dutch summary of all study results.

3. References

1. Collaborators GBDN. Global, regional, and national burden of neurological disorders, 1990-2016: a systematic analysis for the Global Burden of Disease Study 2016. *Lancet Neurol.* 2019;18(5):459-80.
2. Dorsey ER, Bloem BR. The Parkinson Pandemic-A Call to Action. *JAMA Neurol.* 2018;75(1):9-10.
3. Santos-García D, de la Fuente-Fernandez R. Impact of non-motor symptoms on the quality of life of patients with Parkinson's disease: some questions beyond research findings. *J Neurol Sci.* 2013;335(1-2):239.
4. Kan H, Uchida Y, Ueki Y, Arai N, Tsubokura S, Kunitomo H, et al. R2* relaxometry analysis for mapping of white matter alteration in Parkinson's disease with mild cognitive impairment. *NeuroImage: Clinical.* 2022;33:102938.
5. Gonzalez-Sepulveda M, Compte J, Cuadros T, Nicolau A, Guillard-Sirieix C, Peñuelas N, et al. In vivo reduction of age-dependent neuromelanin accumulation mitigates features of Parkinson's disease. *Brain.* 2023;146(3):1040-52.
6. McFarthing K, Buff S, Rafaloff G, Fiske B, Mursaleen L, Fuest R, et al. Parkinson's Disease Drug Therapies in the Clinical Trial Pipeline: 2023 Update. *J Parkinsons Dis.* 2023;13(4):427-39.
7. Levi S, Volonté MA. Iron chelation in early Parkinson's disease. *The Lancet Neurology.* 2023;22(4):290-1.
8. Global Parkinson's Disease Survey Steering C. Factors impacting on quality of life in Parkinson's disease: results from an international survey. *Mov Disord.* 2002;17(1):60-7.

Dankwoord

Het is zover, mijn boekje is af, de datum is geprikt en ik sta op het punt om mijn promotietraject af te ronden. Dit kan ik natuurlijk niet doen zonder een aantal mensen te bedanken, welke allemaal op hun eigen manier in meer of minder mate hebben bijgedragen aan dit proefschrift.

Om te beginnen wil ik alle deelnemers aan de TRACK-PD studie ontzettend bedanken voor hun inzet, enthousiasme en de moeite die zij hebben gedaan om af te reizen naar Maastricht voor de testdagen. Het was ontzettend inspirerend om jullie allen te ontmoeten. Zonder jullie geen onderzoek en zonder onderzoek geen vooruitgang. Duizend maal dank voor jullie inspanningen!

Natuurlijk wil ik ook graag mijn promotieteam bedanken. Om te beginnen Mark, mijn copromotor en begeleider vanaf het eerste uur. Als student kwam ik voor mijn onderzoeksstage bij jou terecht. Binnen de neurologie wist jij direct jouw enthousiasme voor de bewegingsstoornissen op mij over te brengen. Al hoewel je mij de kans gunde om verder te kijken, wist ik zelf eigenlijk meteen dat ik mijn promotietraject binnen de bewegingsstoornissen wilde voortzetten. Mijn onderzoeksstage vormde dan ook de basis voor dit proefschrift. Je rustige, vriendelijke en enthousiaste begeleiding, met soms een tikje warrigheid, heb ik altijd als heel prettig ervaren. Ook op persoonlijk vlak ben je altijd geïnteresseerd en ik heb gedurende het hele traject het gevoel gehad dat ik volledig op jouw support kon rekenen. Bedankt voor de hele fijne samenwerking!

Albert, ik was heel blij toen jij je bij mijn promotieteam voegde als promotor. Ik heb veel respect voor de manier waarop jij met oneindig veel geduld, tomeloze inzet en een positieve kritische blik je werk doet. Als ik een artikel naar jou doorstuurde, wist ik altijd zeker dat ik niet alleen snel, maar ook hele nuttige en uitgebreide feedback terug zou krijgen. Dat is de kwaliteit van dit proefschrift zeker ten goede gekomen, waarvoor mijn grote dank!

En uiteraard mijn promotor, Yasin. Ondanks dat je mij op dat moment eigenlijk nog niet of nauwelijks kende, heb je mij vanaf het begin het vertrouwen gegund om onder jouw hoede mijn promotietraject uit te voeren. Hierin gaf je mij altijd de volledig vrijheid, waarbij ik zo nodig op je kon terugvallen. In onze gesprekken wist je me altijd te stimuleren om out-of-the-box te denken en tot nieuwe inzichten te brengen.

Tevens wil ik hier ook Stijn bedanken. Ook al was je officieel geen lid van mijn promotieteam, zonder jouw begeleiding en supervisie op het gebied van MRI en de

analyses hiervan, was het niet mogelijk geweest om dit boekje in zijn huidige vorm af te maken. Heel erg bedankt voor je duidelijke uitleg, oneindige geduld, het meedenken en natuurlijk je inzet voor de TRACK-PD studie.

Mijn dank gaat ook uit naar de leden van de beoordelingscommissie voor het lezen en beoordelen van dit proefschrift: prof. dr. D.E.J. Linden, prof.dr. S.A. Kotz, prof.dr. V.A. Coenen en dr. R.C.G. Helmich.

Daarnaast natuurlijk mijn paranimfen. Margot, vanaf het moment dat we begonnen met de TRACK-PD studie voegde jij je bij ons studieteam. Tijdens de jaren erna hebben we een super fijne samenwerking opgebouwd, waarin ik altijd op je kon rekenen. Zonder jou was het nooit gelukt om de studie zo goed te laten lopen. Je bent super betrouwbaar, georganiseerd en hebt je steeds volledig ingezet voor de studie en de proefpersonen. Ook buiten het werk was het heel gezellig, met etentjes, vlaaimomenten, Funda zoektochten, een reisje naar Tsjechië en het uitstippelen van mooie hikes. Ik vond het een eer dat ik ook jouw paranimf mocht zijn en ik ben blij dat we elkaar nog steeds regelmatig spreken!

Josselien, studiegenootjes, dispuutsgenootjes en daarna ook collega's in het ziekenhuis. Eerst allebei in de kliniek en later samen in het onderzoek. Naast alle leuke momenten buiten werk, hebben we in het ziekenhuis ontelbare koffiemomentjes gehad, waarbij er over en weer carrière switches en adviezen werden besproken, maar het natuurlijk ook heel vaak gewoon over wintersport, verbouwingsperikelen, interieurveranderingen en kroketten ging. Ik bewonder je inzet en doorzettingsvermogen, maar ook zeker de verbouwingsskills die je ondertussen hebt opgebouwd. Ik ben blij dat jij tijdens de ceremonie naast mij staat!

Tevens wil ik graag de andere coauteurs van de hoofdstukken in mijn proefschrift bedanken. Anja, Annelien, Christine, Dimo, Frank, Heidi, Jaap, Kathy, Linda, Luc, Nikos, Paul, Renaud en Sjors, heel erg bedankt voor al jullie hulp en alle nuttige feedback. Dit proefschrift is mede door jullie inzet tot stand gekomen. Bedankt voor de prettige samenwerking!

Daarnaast zijn er ook een aantal studenten betrokken geweest bij de uitvoering en data verzameling van de TRACK-PD studie. Elle, Meriek, Niels en Sjoerd, heel erg bedankt voor al jullie inzet en de fijne samenwerking!

Uiteraard wil ik ook alle andere leden van de neurochirurgie research groep bedanken. In het bijzonder mijn kantoorgenootjes Jana en Sylvana. Samen met Margot hebben we gedurende het grootste deel van mijn promotietraject een onderzoekskamer gedeeld.

Heel erg bedankt voor alle gezelligheid, zowel op werk als ook daarbuiten. We waren helaas niet heel goed in het in leven houden van onze kantoorplanten, maar verder had ik mij geen betere kantoorgenoottjes kunnen wensen.

Met het einde van mijn promotietraject is er ook een einde gekomen aan mijn opleiding neurologie in het MUMC+. Ik wil de vakgroep neurologie en alle fijne collega AIOS heel erg bedanken voor de mooie jaren in het zuiden! Ik heb met ieder van jullie met heel veel plezier samengewerkt en we gaan elkaar zeker nog tegenkomen op de Biemond. In het bijzonder natuurlijk Kimberley en Nandi, mijn jaargenootjes (Blumenfeld forever). Kimberley, we begonnen samen als broekies direct vanuit de geneeskunde opleiding en ik kan me nog goed herinneren hoe blij we waren toen we toegelaten werden als AIOS. Gelukkig konden we altijd op elkaar terugvallen en hebben we samen deze beginperiode doorstaan. Ik heb heel veel respect voor hoe jij de opleiding combineert met het gezinsleven thuis! Nandi, kamergenootje, Bob, top collega, team KNF, vele persoonsverwisselingen en linzenstukjes later ben ik heel blij dat jij mijn collega was. Ondertussen hebben we allebei een mooie nieuwe baan gevonden, maar we blijven elkaar zeker zien!

Natuurlijk wil ik ook mijn nieuwe collega's in Eindhoven bedanken voor de hele warme ontvangst en het feit dat jullie me direct weer thuis lieten voelen in het 'Cathrien'. Ik kijk uit naar een fijne samenwerking in de komende jaren.

Er zijn daarnaast nog een aantal andere mensen die misschien niet direct, maar toch zeker indirect van positieve invloed zijn geweest op mijn proefschrift. Zonder compleet te zijn, wil ik hiervan een aantal mensen noemen. Marissa en Irene (S), ik ben blij met onze hechte vriendschap en het feit dat we altijd op elkaar kunnen terugvallen. Ik weet zeker dat er nog veel meer weekendjes, festivals en gokavonturen gaan volgen. Irene (M), hoe leuk is het dat we beide in de neurologie terecht zijn gekomen. Ook al zaten we helaas nooit lang op dezelfde plek, toch vind ik het heel gezellig dat we niet alleen jaarclubgenootjes maar ook collega's zijn geweest. Natuurlijk ook Sanne, Elke en Natasja bedankt voor alle leuke etentjes, activiteiten en weekendjes. Ik had geen beter introductiegroepje kunnen treffen. Nico, heel erg bedankt voor je luisterend oor en interesse rondom mijn promotieperikelen. Daarnaast duizendmaal dank voor alle katten en otterplaatjes. Elise, ik kan niet wachten om samen een volgend avontuur te beleven en hoop dat we snel een canyoning tripje kunnen plannen. Romy en Marleen, bedankt voor de gezelligheid en afleiding tijdens alle mooie festivals is de afgelopen jaren. Merle en Danique, we kennen elkaar ondertussen al heel lang en ook al zien we elkaar maar een paar keer per jaar, voelt het toch altijd direct weer vertrouwd. Ik ben blij dat onze vriendschap nog steeds stand houdt!

Lieve schoonfamilie, Marijon, Connie, Maartje, Iris, Simon en Lotte, ik kan me geen betere tweede familie wensen! Heel erg bedankt voor de interesse die jullie altijd hebben gehad in mijn onderzoek!

Opa en oma, ook al is het afgelopen jaar een zwaarder jaar geweest, toch blijven jullie altijd positief en vol energie. Het is niet altijd eenvoudig om bij te houden waar we allemaal mee bezig zijn, maar jullie zijn altijd geïnteresseerd in mijn werkzaamheden en activiteiten. Heel erg bedankt hiervoor!

Lieve Nine, het van dichtbij meemaken van jouw afkeer tegen je eigen promotietraject werkte niet direct motiverend. Maar ik ben ontzettend trots dat je het hebt volbracht en gelukkig ben je volgens mij ondertussen ook wel trots op jezelf. Al hoewel we zeker op elkaar lijken, zijn we in sommigen opzichten ook erg verschillend. Van jou leer ik om dingen op een ander manier te bekijken en te waarderen. Ondanks dat we wat verder uit elkaar wonen, ben ik blij dat ik jou, Yvonne en Noa regelmatig zie!

Papa en mama, heel erg bedankt voor jullie onvoorwaardelijke support. Jullie hebben me altijd gestimuleerd om overal het maximale uit te halen en mijn doelen na te streven. Door jullie ben ik de persoon geworden die ik nu ben. Ik weet dat ik altijd bij jullie terecht kan en daarvoor ben ik jullie ontzettend dankbaar.

Lieve Coen, ik zou bijna niet weten hoe ik jou zou kunnen bedanken. Je staat altijd voor mij klaar, moedigt me aan en ondersteunt me in alles wat ik doe, je hebt altijd het volste vertrouwen in mij en zorgt bovendien dat ik het werk allemaal even aan de kant kan zetten als dat nodig is. Thuiskomen bij jou verveelt nooit en ik kan niet wachten op de rest van ons leven samen.

Curriculum Vitae

Amée (Fleur) Wolters was born on August 18th 1992 in Vught, the Netherlands. In 2010 she graduated cum laude from pre-university education Gymnasium at the Maurick College in Vught. She moved to Maastricht to study Medicine at the Faculty of Health, Medicine and Life Sciences at the Maastricht University in 2010. At the end of her medical studies she completed a research internship focused on magnetic resonance imaging and cognitive impairment in Parkinson's disease, which set the beginning of this thesis. In August 2016 she received her medical doctor degree. After graduation she worked as a resident (not in training) at the neurology department of the Maastricht University Medical Center for three months. She began her specialist training in neurology at the same department in January 2017. In January 2018 she started a part-time PhD project under the supervision of prof. Yasin Temel, prof. Albert Leentjens and dr. Mark Kuijf at Maastricht University. Throughout her residency she continued and completed the research described in this thesis. During her final years of training she worked at the Radboudumc Centre for Rare and Genetic Movement Disorders in Nijmegen for six months. She graduated as a neurologist in October 2023.

Amée started working as a neurologist in the Catharina hospital in Eindhoven in November 2023, where she will continue her medical and scientific career.

List of publications

Wolters AF, Snijders AH, Bloem BR. Video case: A new phenotype within the spectrum of functional orofacial movement disorders. *J Neurol*. 2023 Aug 24.

Wolters AF, Heijmans M, Priovoulos N, Jacobs HIL, Postma AA, Temel Y, Kuijf ML, Michielse S. Neuromelanin related ultra-high field signal intensity of the locus coeruleus differs between Parkinson's disease and controls. *Neuroimage Clin*. 2023 Jul 22;39:103479.

Wolters AF, Michielse S, Kuijf ML, Defebvre L, Lopes R, Dujardin K, Leentjens AFG. Brain network characteristics and cognitive performance in motor subtypes of Parkinson's disease: A resting state fMRI study. *Parkinsonism Relat Disord*. 2022 Oct 28;105:32-38.

Heijmans M, **Wolters AF**, Temel Y, Kuijf ML, Michielse S. Comparison of Olfactory Tract Diffusion Measures Between Early Stage Parkinson's Disease Patients and Healthy Controls Using Ultra-High Field MRI. *J Parkinsons Dis*. 2022;12(7):2161-2170.

Wolters AF, Heijmans M, Michielse S, Leentjens AFG, Postma AA, Jansen JFA, Ivanov D, Duits AA, Temel Y, Kuijf ML. The TRACK-PD study: protocol of a longitudinal ultra-high field imaging study in Parkinson's disease. *BMC Neurol*. 2020 Aug 5;20(1):292.

Wolters AF, Moonen AJH, Lopes R, et al. Grey matter abnormalities are associated only with severe cognitive decline in early stages of Parkinson's disease. *Cortex*. 2020;123:1-11.

Wolters AF, van Nuenen BFL. Restless legs syndrome and its variants: a case report. *Neurol Sci*. 2020 Apr;41(4):967-968.

Wolters AF, van de Weijer SCF, Leentjens AFG, Duits AA, Jacobs HIL, Kuijf ML. "Resting-state fMRI in Parkinson's disease patients with cognitive impairment: A meta-analysis": Answer to Wang and colleagues. *Parkinsonism Relat Disord*. 2019;66:253-254.

Wolters AF, van de Weijer SCF, Leentjens AFG, Duits AA, Jacobs HIL, Kuijf ML. Resting-state fMRI in Parkinson's disease patients with cognitive impairment: A meta-analysis. *Parkinsonism Relat Disord*. 2019;62:16-27.

